

# UC San Diego

## Research Theses and Dissertations

**Title**

Antiviral Natural Products from Marine Sources

**Permalink**

<https://escholarship.org/uc/item/7wk515wr>

**Author**

Rowley, David C.

**Publication Date**

2001

Peer reviewed

## **INFORMATION TO USERS**

**This manuscript has been reproduced from the microfilm master. UMI films the text directly from the original or copy submitted. Thus, some thesis and dissertation copies are in typewriter face, while others may be from any type of computer printer.**

**The quality of this reproduction is dependent upon the quality of the copy submitted. Broken or indistinct print, colored or poor quality illustrations and photographs, print bleedthrough, substandard margins, and improper alignment can adversely affect reproduction.**

**In the unlikely event that the author did not send UMI a complete manuscript and there are missing pages, these will be noted. Also, if unauthorized copyright material had to be removed, a note will indicate the deletion.**

**Oversize materials (e.g., maps, drawings, charts) are reproduced by sectioning the original, beginning at the upper left-hand corner and continuing from left to right in equal sections with small overlaps.**

**Photographs included in the original manuscript have been reproduced xerographically in this copy. Higher quality 6" x 9" black and white photographic prints are available for any photographs or illustrations appearing in this copy for an additional charge. Contact UMI directly to order.**

**ProQuest Information and Learning  
300 North Zeeb Road, Ann Arbor, MI 48106-1346 USA  
800-521-0600**

**UMI<sup>®</sup>**



**UNIVERSITY OF CALIFORNIA, SAN DIEGO**

**Antiviral Natural Products from Marine Sources**

**A dissertation submitted in partial satisfaction of the  
requirements for the degree Doctor of Philosophy in  
Oceanography**

**by**

**David Chapman Rowley**

**Committee in charge:**

**Professor William H. Fenical, Chair  
Professor D. John Faulkner  
Professor Farooq Azam  
Professor Frederic Bushman  
Professor Murray Goodman**

**2001**

**UMI Number: 3035894**

**UMI<sup>®</sup>**

---

**UMI Microform 3035894**

**Copyright 2002 by ProQuest Information and Learning Company.  
All rights reserved. This microform edition is protected against  
unauthorized copying under Title 17, United States Code.**

---

**ProQuest Information and Learning Company  
300 North Zeeb Road  
P.O. Box 1346  
Ann Arbor, MI 48106-1346**

**Copyright**

**David Chapman Rowley, 2001**

**All rights reserved.**

The dissertation of David Chapman Rowley is approved, and it  
is acceptable in quality and form for publication on microfilm:

D. John Faulkner

10

Fanny Kamm

Murray Goodman

William Pericol

Chair

University of California, San Diego

2001

**To my Family.**



## TABLE OF CONTENTS

Signature Page .....	iii
Dedication.....	iv
Table of Contents .....	v
List of Figures.....	vii
List of Tables.....	x
Acknowledgments .....	xi
Vita and Publications.....	xvi
Abstract.....	xviii

### Chapter

1. Introduction .....	1
2. Marine Microorganisms as a Resource for Antiviral Drug Discovery.....	9
2.1 Introduction .....	9
2.1.1 Marine Microorganisms in Drug Discovery.....	10
2.1.2 The Discovery of Novel Antivirals Produced by Non- Marine Microorganisms .....	16
2.1.3 Precedent for Discovering Antivirals from Marine Microorganisms.....	21
2.1.4 Evidence for Microbial Mediation of Viral Inactivation in the Ocean.....	23
2.2 General Strategies and Methodologies for the Discovery of Bioactive Metabolites Produced by Marine Microorganisms.....	26
3. Discovery of Crude Extracts Produced by Marine Microorganisms Active Against the Herpes Simplex Virus-1 .....	46
3.1 The Herpes Simplex Virus .....	47
3.1.1 Biological Background.....	47
3.1.2 Replication of HSV-1 .....	49
3.1.3 Clinically Used Antiviral Agents Against HSV Infections....	51
3.2 Screening Program for Identification of Anti-HSV Agents.....	57
3.2.1 Choice of Assay Design .....	57
3.2.2 Production and Titer of Viral Stocks.....	59
3.2.3 Standard Assay Protocol for Screening Extract Library .....	63
3.2.4 Strategy for the Discovery of Antivirals .....	65
3.2.5 Screening Results .....	66
3.2.6 Description of Extracts Used in this Study.....	69
3.2.7 Summary and Discussion .....	69
4. Halovirs A-F, Novel Antiviral Agents from a Marine Fungus .....	74
4.1 Isolation and Structural Characterization of Halovirs A-C .....	74

4.2	Secondary Structure of Halovir A .....	89
4.3	Discovery of Halovirs D-F by LC/MS Analysis .....	98
4.4	Biological Properties of the Halovir Peptides .....	105
4.5	Discussion.....	116
4.6	Experimental.....	123
5.	Synthesis and Structure-Activity Relationships of the Halovirs .....	133
5.1	Introduction .....	133
5.2	Synthesis and Biological Activities of Halovir Analogs .....	135
5.3	Discussion.....	151
5.4	Materials and Methods .....	154
6.	New Marine-Derived Inhibitors of HIV cDNA Integration.....	175
6.1	Introduction .....	176
6.2	Thalassiolins A-C: Inhibitors of HIV cDNA Integration .....	180
6.2.1	Isolation and Structural Characterization .....	181
6.2.2	Biological Properties .....	186
6.2.3	Possible Binding Sites on Integrase .....	191
6.2.4	Discussion.....	193
6.2.5	Experimental.....	198
7.	Discovery of Marine-Derived Inhibitors of Molluscum Contagiosum Virus Topoisomerase.....	206
7.1	Introduction .....	206
7.2	Sansalvamide A, a Novel Inhibitor of MCV Topoisomerase.....	208

## LIST OF FIGURES

### Figure

1. Two-dimensional proton detected NMR experiments .....	30
2. Bioassay-guided fractionation of extract CNL240 used in the purification of halovirs A-C .....	76
3. The structures of the halovir peptides A, B, and C. ....	79
4. Fragment ions generated during an MS <sup>4</sup> experiment involving halovir A. ....	82
5. Negative-mode electrospray MS <sup>3</sup> analysis of halovir A. ....	83
6. Negative-mode electrospray MS <sup>3</sup> analysis of halovir B. ....	85
7. Negative-mode electrospray MS <sup>3</sup> analysis of halovir C. ....	86
8. Mosher's ester diagram of (R)- and (S)-MTPA esters of halovir A. ....	88
9. <sup>1</sup> H NMR chemical shift temperature dependence of the backbone amide protons of halovir A measured in DMSO- <i>d</i> <sub>6</sub> . ....	91
10. Solvent dependence of NH chemical shifts of halovir A as a function of DMSO- <i>d</i> <sub>6</sub> concentration in CDCl <sub>3</sub> . ....	93
11. Proposed 3 <sub>10</sub> -helical hydrogen-bonding scheme and observed ROESY correlations relevant to the helical nature of halovir A. ....	96
12. Three-dimensional space filling model of halovir A in a 3 <sub>10</sub> -helix formation....	97
13. LC/MS chromatogram of a CNL240 fraction containing the halovirs D-F .....	100
14. Mass chromatogram showing molecular ions and fragmentation peaks for halovir D during an LC/MS experiment. ....	101
15. The structures of the halovir peptides D, E, and proposed F. ....	102
16. Comparative antiviral activities of halovirs A, D, and E against HSV-1 in pre-infected Vero cells. ....	106
17. Inactivation study of halovir A versus HSV-1. ....	107
18. Time and concentration dependent inactivation of HSV-1 by halovir A. ....	110

19. Comparison of virucidal activities of halovirs A, B, and C. ....	111
20. Time and dependent inactivation of HSV-1 by incubation with halovir A with subsequent drug removal.....	112
21. Pre-incubation of halovir A with Vero cells prior to infection with HSV-1.....	114
22. Plaque assay of halovir A against herpes simplex viruses 1 and 2. ....	115
23. Structure of Aib and TOAC residues. ....	119
24. Synthesis of halovir A peptide fragment.....	136
25. Completion of synthesis of halovir A. ....	137
26. <sup>1</sup> H NMR of natural and synthetic halovir A in DMSO- <i>d</i> <sub>6</sub> . ....	138
27. Anti-HSV-1 activity of halovir A versus the Leu-OMe and <i>N</i> <sup>α</sup> -acetyl analogs.....	140
28. Synthesis of <i>N</i> -acetyl halovir analog.....	141
29. Synthesis of halovir analogs with different lipophilic chain lengths. ....	142
30. Anti-HSV-1 activities of halovir A methyl ester analogs with various lipophilic chain lengths. ....	143
31. The effects of unsaturation in the lipophilic chain on the anti-HSV-1 activities of halovir A methyl ester analogs. ....	145
32. Synthesis of a halovir analog with an L-Ala substitution for the Aib residue...	146
33. Synthesis of a halovir peptide analog incorporating a sarcosine substitution at the proline residue. ....	148
34. The effects of amino acid substitutions on the anti-HSV-1 activities of halovir A methyl ester analogs.....	149
35. Integration events catalyzed by HIV integrase. ....	178
36. Proton NMR spectrum (300 MHz) of thalassiolin B in DMSO- <i>d</i> <sub>6</sub> . ....	184
37. Carbon NMR spectrum (100 MHz) of thalassiolin B in DMSO- <i>d</i> <sub>6</sub> . ....	185

<b>38. Partial HMBC analysis of thalassiolin B.....</b>	<b>186</b>
<b>39. Inhibition of integration <i>in vitro</i> by thalassiolin A.....</b>	<b>187</b>
<b>40. Dose dependent antiviral activity of thalassiolins A versus HIV-1. ....</b>	<b>188</b>
<b>41. Docking of thalassiolin A to the catalytic core domain of HIV-1 integrase .....</b>	<b>192</b>

## LIST OF TABLES

### Table

1. Marine Fungal Metabolites .....	11
2. Marine Bacterial Metabolites .....	13
3. Initial Screening Results for Crude Extract Antiviral Activity Versus HSV-1...66	
4. Crude Marine Microbial Extracts Exhibiting Anti-HSV Activity .....	68
5. <sup>1</sup> H and <sup>13</sup> C NMR Assignments for Halovirs A-C in pyridine- <i>d</i> <sub>5</sub> . ....	80
6. Temperature Dependence of Amide Backbone Protons of Halovir A.....	92
7. <sup>1</sup> H and <sup>13</sup> C NMR Assignments for Halovir D in DMSO- <i>d</i> <sub>6</sub> .....	103
8. <sup>1</sup> H and <sup>13</sup> C NMR Assignments for Halovir E in DMSO- <i>d</i> <sub>6</sub> . ....	104
9. Summary of Biological Activities for the Synthetic Halovir Analogs.....	150
10. <sup>1</sup> H and <sup>13</sup> C NMR Assignments for Thalassiolins A-C in DMSO- <i>d</i> <sub>6</sub> .....	183
11. IC <sub>50</sub> Inhibitory Activities of the Thalassiolins. ....	189

## **ACKNOWLEDGEMENTS**

**Bill Fenical gave me the chance of a lifetime. These last six years have been like living a dream. Bill has been, and I hope will continue to be, and incredible mentor. He provided me with the tools and guidance essential for success and the independence required for self-discovery. Thanks for believing in me, Bill.**

**My doctoral committee comprising professors John Faulkner, Farooq Azam, Rick Bushman, and Murray Goodman also significantly contributed to my success at SIO. Dr. John Faulkner frequently provided exceptional insight into our scientific discussions, and I have benefited greatly from our interactions. I will miss his tutelage and (occasionally unusual) sense of humor. The marine natural products students at SIO and scientific community at large are lucky to have him. Dr. Farooq Azam changed the ways in which I think about the ocean. His classes on marine microbial ecology directly influenced the course of my graduate research, and enabled me to “think” like a bacterium. Rick Bushman provided me the opportunity for a first-class collaboration with a highly respected virology laboratory. My interactions with his group were scientifically productive and extremely educational. I thank Dr. Murray Goodman for his generosity in helping mediate my progression through this graduate program.**

**My graduate studies at the Scripps Institution of Oceanography have provided me with some of the most memorable occasions in my life. I will never be able to thank Bill Fenical enough for enabling me to travel the world’s oceans in search of scientific discovery and personal adventure. Whether onboard the R/V Seward**

Johnson in the Bahamas, chewing beetlenut with the locals in Papua New Guinea, half sinking in the Philippines aboard the Malena, or yachting with the Golden Crew in the South Pacific and Caribbean, I have traveled these last six years. How can I ever forget table dancing in the Billabong, thunderstorm drum circles in PNG, outrageous 4<sup>th</sup> of July parties, or shark diving off Moorea? The two-week journey from San Diego to La Paz aboard the Osprey added salt to my veins and lines to my face. (This is the end....) I have lived enough for many lifetimes. These journeys have also endeared to me many close friends, especially Chris Kauffman, Paul Jensen, Chris Blackburn, Christine Salomon, Tegan Eve, Alan Spyere, Stephanie Lewis, Helena Vervoort, and Tracey Mincer. I am especially indebted to Chris Kauffman for saving my life on numerous occasions, and also for helping me to get into situations where I would need my life saved.

My scientific endeavors at SIO would not have been possible without the friendship, guidance, and assistance of my colleagues in the Fenical laboratory. Stephanie Lewis was instrumental, usually daily, in seemingly every undertaking. This was to such a degree that I couldn't imagine a professional career without her. How much will it take to get you to Rhode Island? Paul Jensen, Chris Kauffman, and Sy Teisan enabled the microbial fermentation aspects of my research. I am indebted to them for their patience, assistance, and for allowing me to think that I could change everything. Sara Kelley took over responsibility for conducting the antiviral assays and her commitment to this program significantly facilitated my research. I feel like I owe her lunch for the rest of her life. Tegan Eve provided an endless source of amusement as well as unparalleled technical expertise with instrumentation. Again,



how much to get you to Rhode Island? Matt Woolery, king of the LC/MS and general hard rockin' hero, was indispensable for his technical support and quick wit. Helene Vervoort taught me NMR, and I appreciate the many years that we shared a laboratory and exchanged scientific ideas. Tracey Mincer pried open my eyes to the microbial world, was always available to attend scientific lectures, and frequently energized my enthusiasm for research. My fellow graduate students Allan Spyere, Akkharawit Kanjana-Opas, and Monica Puyana have influenced my awareness of many aspects of marine and biomedical research. I also had the tremendous fortune to interact with many other gifted scientists who have contributed to my development as a natural products chemist. I must especially acknowledge Kelley Jenkins, Dean Wilson, Ingo Hardt, Matt Renner, Steve Toske, Mercedes Cueto, Felix Flachsmann, Gil Belofsky, Julia Kubanek, and Robert Feling. I thank all of you for your friendship and guidance.

The best science is frequently accomplished via collaboration between scientists from diverse disciplines. During the course of my graduate studies, I've had the pleasure to collaborate with many intelligent and dedicated scientists that have made significant contributions to the quality of my research. I must especially acknowledge the efforts of Ms. Denise Rhodes, Dr. Mark Hansen, and Dr. Young Hwang at the Salk Institute for Biological Studies toward establishing the biological activities of the several of the molecules described in this dissertation. I always felt welcome in their laboratory, and thank you for your patience in enlightening this chemist. I was also fortunate to collaborate with members of the laboratory of Dr. J. Andrew McCammon in the Department of Chemistry and Biochemistry at UCSD. Dr. Christoph Sotriffer and Dr. Haihong Ni, both post-doctoral researchers, conducted

molecular modeling studies on potential binding interactions between the thalassiolins and the catalytic core domain of HIV integrase. I sincerely enjoyed working with all of you.

Despite being viewed as the enemy, I've developed special professional and personal friendships with members of the Faulkner laboratory. Chris Blackburn and Christine Salomon have caused significant disruption of my life in many positive ways. My closest colleagues and confidants, I'm happy that we started and ended this thing together. Eric Schmidt provided many stinging guitar licks to the otherwise quiet Scripps campus, and frequently engaged me in intriguing scientific discussions. I look forward to our professional interactions in the future. I wish Christian Ridley, Melissa Lerch, and Joel Sandler the best of luck in the future.

To my numerous other friends at SIO, you know who you are, and I thank you all for the memorable times we have had.

My early development as a chemist was greatly influenced by Dr. Won Pyo Hong at DuPont and by Dr. J. Edward Semple at Corvas International. Won Pyo started me at square one (TLC) and then worked me up to drunken billiards. Ed Semple developed my ability as a synthetic chemist, gave me the freedom to pursue independent ideas, and became a close friend in the process. I owe quite a lot of my professional success to Ed's tutelage and continued support. I would also like to thank John Crawford for his friendship, our summer backpacking adventures in the Sierra Nevada mountains, and countless letters of recommendation.

Lastly, my completion of this degree would not have been possible without the endless support and encouragement from my family. Gloria Sun, my partner and my

inspiration, makes everything in my life possible. You are an incredible person, mother, wife, and physician. Thank you for your love and understanding. My parents deserve special acknowledgement. My mother, Carol Rowley, taught me fairness and compassion. My father, David Rowley, instilled in me at an early age the scientific curiosity that influenced my academic inclinations. Thanks mom and dad, this one is for you.

\* \* \*

Chapter 7, in part, is a reprint of material as in appears in *Molecular Pharmacology*, 1999, 55, 1049-1053. The dissertation author was a secondary author and the co-authors listed in this publication directed and supervised the research which forms the basis for this chapter. This work is reprinted with permission of the American Society for Pharmacology and Experimental Therapeutics.

## VITA

- December 29, 1966 Born, David Chapman Rowley, New London, CT
- 1990 B. S. in Polymer Science, The Pennsylvania State University
- 1990-1991 U. S. Patent and Trademark Office, Arlington, VA
- 1991-1993 E. I. DuPont de Nemours & Company, Newark, DE
- 1993-1995 Corvas International, Inc., San Diego, CA
- 2001 Ph.D. Scripps Institution of Oceanography,  
University of California, San Diego

## PUBLICATIONS

**“Thalassiolins: New Inhibitors of HIV cDNA Integration Active Against Virus.”**  
**David Rowley, Mark Hansen, Denise Rhodes, Frederic Bushman, and William**  
**Fenical. (manuscript in preparation)**

**“Halovirs A-C, New Mechanistically-Novel Antiviral Agents From a Marine Fungus.”**  
**David Rowley, Paul R. Jensen, and William Fenical. (manuscript in preparation)**

**“Saprospirols A-E, Neoverrucosane Diterpenes Produced by the Marine Gliding**  
**Bacterium *Saprosira grandis*.” Allan Spyere, David Rowley, Paul Jensen, and**  
**William Fenical. (manuscript in preparation)**

**“Mechanism of inhibition of a poxvirus topoisomerase by the marine natural product**  
**sansalvamide A.” Young Hwang, David Rowley, Denise Rhodes, Jeff Gertsch,**  
**William Fenical, and Frederic Bushman. *Molecular Pharm.* 1999, 55, 1049-1053.**

**“Potent and Selective Thrombin Inhibitors Featuring Hydrophobic, Basic P3-P4-**  
**aminoalkyl lactam Moieties.” J. Edward Semple, David C. Rowley, Timothy Owens,**  
**Theresa H. Uong, and Terence K. Brunck. *Bioorg. Med. Chem. Lett.* 1998, 8, 3525-**  
**3530.**

**“Synthesis and Biological Activity of P2-P4 Azapeptidomimetic P1-Argininal and P1-**  
**Ketoargininamide Derivatives: A Novel Class of Serine Protease Inhibitors.” J.**  
**Edward Semple, David C. Rowley, Terence K. Brunck, and William C. Ripka. *Bioorg.***  
***Med. Chem. Lett.* 1996, 6, 315-320.**

**“Design, Synthesis, and Evolution of a Novel, Selective, and Orally Bioavailable Class of Thrombin Inhibitors: P1-Argininal Derivatives Incorporating P3-P4 Lactam Sulfonamide Moieties.”** J. Edward Semple, David C. Rowley, Terence K. Brunck, Theresa Ha-Uong, Nathaniel K. Minami, Timothy D. Owens, Susan Y. Tamura, Erick A. Goldman, Daniel V. Siev, Robert J. Ardecky, Stephen H. Carpenter, Yu Ge, Brigitte M. Richard, Kjell Hakanson, Al Tulinsky, Ruth F. Nutt and W. C. Ripka. *J. Med. Chem.* 1996, 39, 4531.

**“Discovery and Development of Potent, Selective, and Orally Bioavailable Thrombin Inhibitors.”** Ruth F. Nutt, J. Edward Semple, Odile E. Levy, Thomas G. Nolan, Susan Y. Tamura, Robert J. Ardecky, David C. Rowley, Michael L. Lim, Theresa Ha-Uong, Brigitte M. Richard, Peter W. Bergum, and William C. Ripka. In *Peptides 1996. Proc. 24th Eur. Pept. Symp.*; Ramage, R. Ed.; Mayflower Scientific, 1997.

## **ABSTRACT OF THE DISSERTATION**

### **Antiviral Natural Products from Marine Sources**

**By**

**David Chapman Rowley**

**Doctor of Philosophy in Oceanography**

**University of California, San Diego, 2001**

**Professor William H. Fenical, Chair**

Viruses have probably afflicted mankind for millennia, but modern factors such as the booming human population, fast and widespread global travel, and increased ecosystem perturbations have assured viral disease of an even brighter spotlight in the near future. The examples are frightening. HIV infection is still spreading around the globe. Deadly outbreaks of viruses such as Ebola and Lassa fever continue to occur ever more closely to heavily populated regions. Drug resistant strains of familiar pathogens such as herpes simplex virus are beginning to emerge. Clearly, our science is challenged to find new treatments for these diseases.

How will the next generation of antiviral medicines be discovered? A crucial component should continue to be the proven strategy of screening natural products. In the past, structurally diverse metabolites produced by terrestrial microorganisms and plants have shown inhibitory activities against various viral diseases. Unlike their

terrestrial counterparts, however, the antiviral potential of secondary metabolites produced by marine organisms is virtually unexplored.

This dissertation describes the discovery of novel antiviral agents produced by marine organisms. Studies involving several important viral targets are presented, and included are chemical investigations that have identified lead compounds for antiviral drug discovery. A series of linear, lipophilic peptides produced by a marine fungus are presented as novel inhibitors of the herpes simplex virus. Evidence suggests that these peptides directly inactivate the virus. Synthetic analogs of the natural substrates were prepared, leading to the development of structure-activity relationships outlining the biological importance of key structural features, and perhaps a greater insight into the possible mechanism of action. The thalassiolins, metabolites isolated from a sea grass *Thalassia testudinum*, were identified as inhibitors of the HIV enzyme integrase, and also the replication of HIV in cell culture. The marine cyclic peptide sansalvamide is presented as the first natural product inhibitor of the topoisomerase enzyme of the Molluscum contagiosum virus. I believe that the molecules described in this dissertation extend our knowledge and comprehension of viral inactivating agents, and further serve to support the recognition of the marine environment as a future resource for the continued discovery of novel antiviral medicines.

## **Chapter 1. Introduction**

Viruses have probably afflicted mankind for millennia, but modern factors such as the booming human population, fast and widespread global travel, and increased ecosystem perturbations have assured viral disease of an even brighter spotlight in the near future. The examples are frightening. HIV infection is still spreading around the globe. Deadly outbreaks of viruses such as Ebola and Lassa fever continue to occur ever more closely to heavily populated regions. Drug resistant strains of familiar pathogens such as herpes simplex virus are beginning to emerge. Clearly, our science is challenged to find new treatments for these diseases.

The recent breakthroughs in developing drugs against HIV have proven that viral disease can be successfully treated with chemotherapy. "Cocktails" consisting of protease and reverse-transcriptase enzyme inhibitors have proven effective in lowering the viral load in some patients to below detectable levels. Multi-drug therapy is necessary because the HIV genome rapidly mutates and thus quickly develops resistance to any single drug. However, these drugs are not without serious side effects<sup>1</sup> and most are prohibitively expensive for much of the world's infected population. New drugs are still needed, especially ones with novel modes of action to help prevent the evolution of HIV drug resistance.

The immunocompromised states of advanced AIDS victims, organ transplant recipients, and cancer patients undergoing chemotherapy have focused attention on devastating "opportunistic" infections caused by such pathogens as herpes simplex (HSV) and molluscum contagiosum (MCV) viruses. Taking advantage of the body's



decreased ability to mount an immune response, these infections tend to be massive and prolonged versus those observed in immunocompetent hosts. For some of these infections there are no effective medicines currently available.

Herpesviruses are the leading viral cause of morbidity and mortality in AIDS victims. HSV ulcers in these individuals progress to cover extensive surface areas and deeper tissues. This painful destruction of mucosal and skin integrity then further predisposes the patient to bacterial and fungal superinfections.<sup>2</sup> Traditional drug treatment of HSV has relied heavily on the uses of acyclovir and foscarnet. Now, strains of HSV resistant to these drugs have emerged.<sup>3</sup> Future attention is therefore cast on developing antivirals with novel modes of action for treatment of this debilitating disease.

How will the next generation of antiviral medicines be discovered? A crucial component should continue to be the proven strategy of screening natural products. In the past, structurally diverse compounds produced by terrestrial microorganisms and plants have shown inhibitory activities against various viral diseases.<sup>4,5</sup> Unlike their terrestrial counterparts, however, the antiviral potential of secondary metabolites produced by marine organisms has not been extensively explored.

The discovery of Ara-T, 1- $\beta$ -D-arabinofuranosylthymine, first brought attention to the marine environment as a frontier resource for the discovery of novel antiviral agents. This nucleoside-like compound isolated from a sponge by Bergmann and Feeney<sup>6</sup> in the late 1950's was subsequently identified to possess potent and selective inhibition of the herpes simplex virus.<sup>7,8</sup> Ara-T also demonstrated remarkable *in vivo* efficacy in the treatment of experimental HSV-1 encephalitis in

mice.<sup>9</sup> Since that time, other investigations have uncovered antiviral properties associated with secondary metabolites from other diverse marine organisms, including ascidians,<sup>10,11</sup> macroalgae,<sup>12</sup> microalgae,<sup>13</sup> cyanobacteria,<sup>14</sup> and bacteria.<sup>15,16</sup> However, with marine species estimated to account for at least half of the global biodiversity,<sup>17</sup> the oceans remain relatively unexplored with respect to antiviral drug discovery.

Marine ecosystems may represent the most logical of all environments for screening programs designed to identify naturally occurring antiviral agents. Viruses are the most abundant biological entities in the ocean, with typical concentrations of ten million viral particles per milliliter of seawater.<sup>18</sup> Within the past decade, viral pathogens have been identified for many marine organisms, including plants,<sup>19</sup> mammals,<sup>20</sup> fish,<sup>21</sup> invertebrates,<sup>22</sup> dinoflagellates,<sup>23</sup> and, especially, bacteria.<sup>18,24</sup> It has become increasingly evident that marine viruses play important roles in many ecological processes. For example, viruses are estimated to cause lysis of 20% of marine bacteria daily, and it is proposed that natural virus populations control marine microbial community structures.<sup>18</sup> Although the field of marine natural products has been successful in elucidating the structures of thousands of novel compounds from wide ranging organisms, slow progress has been made in assigning ecological roles for most of these molecules. Given the environmental pressure of viral parasitism, it may be reasonable to hypothesize that marine organisms have evolved survival strategies involving the selection of biosynthetic pathways leading to antiviral chemical defenses.

This thesis describes an investigation into the discovery of novel antiviral agents produced by marine organisms. Studies involving several important viral

targets are presented, and included are chemical investigations that have lead to the identification of novel lead compounds for antiviral drug discovery. A significant portion of this investigation has focused on the chemistry produced by marine bacteria and fungi. Prior to this study, there have been no published reports describing programs specifically targeting marine microorganisms for their ability to produce antiviral agents. Chapter two introduces strong evidence as to why marine microorganisms represent a particularly attractive resource, and describes the strategies and methods involved in assessing the biomedical potential of marine microbial natural products. Chapter three presents a screening program that evaluated the abilities of over 7000 crude extracts derived from the saline fermentation of marine bacteria and fungi to ameliorate the cytopathic effects of the herpes simplex virus. A cell-based assay involving infectious HSV-1 was developed for this survey, and several promising chemical leads were identified. Chapter four presents a detailed summary of the chemical investigation of the top ranked lead from this screening program. A series of linear, lipophilic peptides named the halovirs were discovered as novel inhibitors of HSV. I present evidence that these peptides directly inactivate the herpes simplex virus, a mechanism of action that would make these compounds candidates for topical microbicides. Chapter five describes a synthetic effort aimed at elucidating the structural features of the halovir peptides most critical to their antiviral activities. Synthetic analogs of the natural substrates were prepared, leading to the development of structure-activity relationships outlining the biological importance of key structural features, and perhaps a greater insight into the possible mode of action.

The remaining two chapters of this thesis summarize projects carried out in collaboration with the laboratory of Dr. Frederic Bushman at the Salk Institute for Biological Studies. Chapter six presents the efforts involved in finding agents active against the HIV integrase enzyme, and describes a series of marine plant metabolites dubbed the thalassiolins that are not only potent inhibitors of this important enzyme target, but are also active against HIV in cell culture. HIV integrase represents an attractive target for antiviral drug development, but no clinically useful inhibitors have been identified to date. Chapter seven discusses the screening for inhibitors of the topoisomerase enzyme of the molluscum contagiosum virus (MCV) using a unique assay developed in the Bushman laboratory. MCV is a disfiguring poxvirus found primarily in immunocompromised patients, but unfortunately no clinical therapeutics are currently available to treat this viral pathogen. The marine cyclic peptide sansalvamide is presented as the very first natural product inhibitor of this target.

I believe that the discussion and data presented in this thesis further demonstrates that the marine environment, and the microbial component in particular, represents a resource worth exploring for the discovery of novel antiviral agents. Although the so-called "hit rates" in the chosen assays were not startling, this initial probe was able to identify molecules with intriguing potential against important viral targets. In the end, the value of natural products in drug discovery lies not only in the identification of molecules that can be utilized as medicines directly, but also those that provide novel molecular scaffolds for optimization in medicinal chemistry programs and others that serve as new biomedical tools to help improve our understanding of disease progression. I believe that the molecules described in this

thesis have extended our knowledge and comprehension of viral inactivating agents, and further serve to support the recognition of the marine environment as a future resource for the continued discovery of novel antiviral medicines.

### References

1. Sahai, J. (1996). Risks and synergies from drug interactions. *Aids* **10**, S21-S25.
2. Wood, M.J. (1996). Antivirals in the context of HIV disease. *J. Antimicrob. Chemother.* **37**, 97-112.
3. Field, A.K. & Biron, K.K. (1994). The end of innocence revisited - Resistance of herpesviruses to antiviral drugs. *Clin. Microbiol. Rev.* **7**, 1-13.
4. Harnden, M.R. (1985). Approaches to antiviral agents. Distribution for USA and Canada VCH Publishers, Deerfield Beach FL USA. xii, 326 pp.
5. El Sayed, K.A. (2000). Natural Products as antiviral agents. *in* Studies in natural products chemistry. Vol. 24. Atta-ur Rahman, editor. Elsevier Science B. V. 473-572.
6. Bergmann, W. & Feeney, R.J. (1950). The isolation of a new thymine pentoside from sponges. *J. Am. Chem. Soc.* **72**, 2809-2810.
7. Gentry, G.A. & Aswell, J.F. (1975). Inhibition of herpes simplex virus replication by Ara-T. *Virology* **65**, 294-296.
8. Miller, R.L., Iltis, J.P. & Rapp, F. (1977). Differential effect of arabinofuranosylthymine of the replication of human herpesviruses. *J. Virol.* **23**, 679-684.
9. Machida, H., Ichikawa, M., Kuninaka, A., Saneyoshi, M. & Yoshino, H. (1980). Effect of treatment with 1-beta-D-arabinofuranosylthymine of experimental encephalitis induced by herpes simplex virus in mice. *Antimicrob. Agents Chemother.* **17**, 109-114.
10. Rinehart, K.L., Jr., Gloer, J.B., Hughes, R.G., Jr., Renis, H.E., McGovren, J.P., Swynenberg, E.B., Stringfellow, D.A., Kuentzel, S.L. & Li, L.H. (1981). Didemnins: antiviral and antitumor depsipeptides from a caribbean tunicate. *Science* **212**, 933-5.
11. Rinehart, K.L., Jr., Kobayashi, J., Harbour, G.C., Gilmore, J., Mascal, M., Holt, T.G., Shield, L.S. & Lafargue, F. (1987). Eudistomins A-Q,  $\beta$ -carboline from

- the antiviral Caribbean tunicate *Eudistoma olivaceum*. *J. Am. Chem. Soc.* **109**, 3378-3387.
12. Carlucci, M.J., Ciancia, M., Matulewicz, M.C., Cerezo, A.S. & Damonte, E.B. (1999). Antiherpetic activity and mode of action of natural carrageenans of diverse structural types. *Antiviral Res.* **43**, 93-102.
  13. Ohta, S., Ono, F., Shiomi, Y., Nakao, T., Aozasa, O., Nagate, T., Kitamura, K., Yamaguchi, S., Nishi, M. & Miyata, H. (1998). Anti-herpes simplex virus substances produced by the marine green alga, *Dunaliella primolecta*. *J. App. Phycol.* **10**, 349-355.
  14. Patterson, G.M.L., Baker, K.K., Baldwin, C.L., Bolis, C.M., Caplan, F.R., Larsen, L.K., Levine, I.A., Moore, R.E., Nelson, C.S., Tschappat, K.D., Tuang, G.D., Boyd, M.R., Cardellina, J.H., Collins, R.P., Gustafson, K., Snader, K.M., Weislow, O.S. & Lewin, R.A. (1993). Antiviral activity of cultured blue-green algae (*Cyanophyta*). *J. Phycol.* **29**, 125-130.
  15. Gustafson, K., Roman, M. & Fenical, W. (1989). The macrolactins, a novel class of antiviral and cytotoxic macrolides from a deep-sea marine bacterium. *J. Am. Chem. Soc.* **111**, 7519-7524.
  16. Davidson, B.S. & Schumacher, R.W. (1993). Isolation and synthesis of caprolactins A and B, new caprolactams from a marine bacterium. *Tetrahedron* **49**, 6569-6574.
  17. De Vries, D.J. & Hall, M.R. (1994). Marine biodiversity as a source of chemical diversity. *Drug Dev. Res.* **33**, 161-173.
  18. Fuhrman, J.A. (1999). Marine viruses and their biogeochemical and ecological effects. *Nature* **399**, 541-548.
  19. Kapp, M. (1998). Viruses infecting marine brown algae. *Virus Genes* **16**, 111-117.
  20. Kennedy, S. (1998). Morbillivirus infections in aquatic mammals. *J. Comp. Path.* **119**, 201-225.
  21. Munday, B.L. & Owens, L. (1998). Viral diseases of fish and shellfish in Australian mariculture. *Fish. Path.* **33**, 193-200.
  22. Morales-Covarrubias, M.S., Nunan, L.M., Lightner, D.V., Mota-Urbina, J.C., Garza-Aguirre, M.C. & Chavez-Sanchez, M.C. (1999). Prevalence of infectious hypodermal and hematopoietic necrosis virus (IHHNV) in wild adult blue shrimp *Penaeus stylirostris* from the Northern Gulf of California, Mexico. *J. Aquat. Anim. Health* **11**, 296-301.

23. Tarutani, K., Nagasaki, K., Itakura, S. & Yamaguchi, M. (2001). Isolation of a virus infecting the novel shellfish-killing dinoflagellate *Heterocapsa circularisquama*. *Aquat. Microb. Ecol.* **23**, 103-111.
24. Bratbak, G., Thingstad, F. & Heldal, M. (1994). Viruses and the microbial loop. *Microb. Ecol.* **28**, 209-221.

## **Chapter 2. Marine Microorganisms as a Resource For Antiviral Drug Discovery**

### **2.1 Introduction**

A significant portion of this thesis deals with the investigation and evaluation of marine bacteria and fungi as a resource for the discovery of novel antiviral agents. Prior to this study, there were no published reports describing programs specifically aimed at this purpose. Interestingly, however, the rationale for screening marine microorganisms for their ability to produce antiviral agents is supported by several factors. First, marine bacteria and fungi have been proven to be a unique resource for the identification of secondary metabolites with diverse and significant biomedical potential. Second, potent and selective antiviral inhibitors against human pathogens have been identified through the chemical investigation of terrestrial microbes. And lastly, evidence supports the concept that marine bacteria are capable of producing inactivating agents against a wide range of viruses. With compelling factors such as these, why have marine microbes not yet been investigated for their production of antiviral metabolites? Possible reasons include that marine microbial natural products chemistry is still a developing scientific area, that the few researchers involved in the field have committed their resources to other areas of research (i.e. anticancer), and that the identification of genuinely selective antiviral compounds is notoriously difficult. This latter point must be emphasized since viral replication invariably relies upon numerous processes that are linked to normal cellular metabolism.



### **2.1.1 Marine Microorganisms in Natural Product Drug Discovery**

The chemical investigation of varied marine microbial taxa under laboratory fermentation conditions has resulted in the discovery of structurally diverse secondary metabolites.<sup>1-7</sup> Many of these molecular entities, never before encountered by scientists, have demonstrated potent biological activities in wide-ranging human disease models.<sup>8</sup> Should we be surprised to discover compounds with significant drug potential produced by marine microbes? The answer is definitely not, since investigations of terrestrial microbial flora over the last six decades have yielded over 120 of today's clinically used medicines. Indeed, bacteria and fungi from land have given us such life saving chemotherapeutic agents as penicillin and streptomycin for bacterial infections, the immunosuppressant drug cyclosporin used in organ transplant operations, adriamycin for cancer chemotherapy, and even the cholesterol reducing agent lovastatin for treatment of excessive arterial plaque formation. In recent years, however, the repeated isolation and cultivation of the same microbial species from terrestrial environments has lead to unacceptable levels of projects resulting in isolation of previously identified compounds. Frontier resources for the discovery of novel bioactive compounds are therefore highly desirable in order to meet the genuine need for new medicines. Marine microbial communities represent such a source since their unique adaptation to varied marine environments has promoted the evolution of exceptional biosynthetic capabilities.

Tables 1 and 2 list marine microbial secondary metabolites that have been demonstrated to possess inhibitory properties against human disease models. Most of the biological activities identified involve either cytotoxicity against cancer cells or

antibacterial properties. To far lesser extents, antifungal, antiviral, and anti-inflammatory activities have been reported. This does not so much represent a limitation of the resource in identifying novel agents against wide ranging disease states, but rather reflects a bias, often based upon the availability of research funding, toward certain assays employed by individual research programs. A weakness in the current paradigm for drug discovery is that compounds are not screened broadly enough to fully evaluate their biological potential. Indeed, many newly discovered natural products are reported without any biological activities at all. To meet the future need for finding cures to both existing and emerging diseases, as well as to fully evaluate newly identified resources for drug discovery, programs targeting diverse human health issues require development.

Table 1. Marine Fungal Metabolites

Isolate	Compound(s)	Source	Reference
<b>Anticancer</b>			
<i>Aspergillus fumigatus</i>	fumiquinazolines	fish	9
<i>Aspergillus fumigatus</i>	tryprostatins	sediment	10
<i>Aspergillus niger</i>	asperazine	sponge	11
<i>Aspergillus</i> sp.	aspergillamide	sediment	12
<i>Aspergillus versicolor</i>	sesquiterpenoids		13
<i>Fusarium</i> sp.	neomangicols	wood	14
<i>Gymnasella dankaliensis</i>	gymnastatins	sponge	15,16
<i>Gymnasella dankaliensis</i>	gymnasterones	sponge	17
<i>Leptosphaeria</i> sp.	leptosins	alga	18
<i>Penicillium fellutanum</i>	fellutamides	fish	19
<i>Penicillium</i> sp.	cummunesins	alga	20
<i>Penicillium</i> sp.	penochalasin	alga	21
<i>Penicillium</i> sp.	penostatins	alga	22
<i>Penicillium waksmanii</i>	pyrenocines	alga	23
<i>Penicillium</i> sp.	penostatins	alga	24

<i>Periconia</i> sp.	pericosines	sea hare	25
<i>Phomopsis</i> sp.	phomopsidin	coral reef	26
<i>Trichoderma harzianum</i>	trichodenones, harzialactones	sponge	27
unidentified	spiroxins	soft coral	28
<i>Penicillium</i> sp.	epidithiodioxopiperazines		29
<i>Gymnascella</i> sp.	dankasterone	sponge	30
<i>Fusarium</i> sp.	sansalvamide	seagrass	31
<i>Fusarium</i> sp.	<i>N</i> -methylsansalvamide	green alga	32
<i>Acremonium</i> sp.	verrol 4-acetate	wood	33
Hyphomycete	kasarin	zooanthid	34
<i>Microsphaeropsis</i>	betaenone derivatives	sponge	35
<i>Acremonium striatisporum</i>	virescenosides M and N	sea cucumber	36
<i>Myrothecium roridum</i>	deoxyroridin E	wood	37
<b>Antibiotic</b>			
<i>Aspergillus</i> sp.	mactanamide	alga	38
<i>Coniothyrium</i> sp.	dihydroxyphenylbutanone	sponge	39
<i>Microsphaeropsis</i> sp.	microsphaeropsisin	sponge	39
<i>Corollospora pulchella</i>	melinacidins, gancidin	sand	40
<i>Hypoxylon oceanicum</i>	15G256y	wood	41
<i>Preussia aurantiaca</i>	urantins	mangrove	42
unidentified	secocurvularin	sponge	43
unidentified	hirsutanols	sponge	44
<i>Corollospora maritima</i>	collosporine		45
<i>Hypoxylon croceum</i>	hypoxysordarin	driftwood	46
unidentified	seragakinone	alga	47
<i>Emericella unguis</i>	guisinol	mollusc, medusa	48
<i>Aspergillus niger</i>	yanuthones	ascidian	49
<i>Ascochyta salicorniae</i>	ascosalipyrrolidinone	alga	50
<b>Anti-inflammatory</b>			
<i>Acremonium</i> sp.	oxepinamides	tunicate	51
<b>Enzyme Inhibitors</b>			
<i>Corollospora pulchella</i>	pulchellalactam	drift wood	52
<i>Microascus longirostris</i>	epoxysuccinates	sponge	53
<i>Gliocladium roseum</i>	roselipins		54
<i>Ulocladium botrytis</i>	ulocladol	sponge	39
<b>Other Targets</b>			
<i>Penicillium</i> sp.	epolactaene	sediment	55
<i>Phoma</i> sp.	phomactins	crab shell	56,57

The potential for marine microorganisms as a resource for the discovery of new medicines is underscored by recent insight into the extensive diversity of marine microbes, the development of new saline culturing techniques to provide better access this diversity, and the identification of novel drug targets in the wake of the genomics and proteomics revolution. Over the last decade, the sequencing of environmental samples of small-subunit (16S or 18S) ribosomal RNA coupled with molecular phylogeny has revealed that a major portion of the marine microbial biota has remained invisible to traditional cultivation practices.<sup>58-61</sup> In fact, most planktonic bacteria are likely new species yet unrecognized by bacteriologists.<sup>61</sup>

Table 2. Marine Bacterial Metabolites

Isolate	Compound(s)	Source	Reference
<b>Anticancer</b>			
<i>Altermonas haloplanktis</i>	bisucaberin	deep-sea sediment	62,63
<i>Altermonas</i> sp.	alteramide	sponge	64
<i>Bacillus cereus</i>	homocereulide	snail	65
<i>Bacillus</i> sp.	halobacillin	deep-sea sediment	66
<i>Bacillus</i> sp.	isocoumarin	sediment	67
<i>Chaina purpurigena</i>	SS-228Y	sediment	68,69
<i>Micromonospora</i> sp.	thiocoraline	soft coral	70,71
<i>Pelagiobacter</i> sp.	pelagiomicins	alga	72
<i>Streptomyces hygroscopicus</i>	halichomycin	fish gut	73
<i>Streptomyces sioyaensis</i>	altemicidin	sediment	74,75
<i>Streptomyces</i> sp.	octalacins	gorgonian	76
<i>Streptomyces</i> sp.	indomycinones	sediment	77,78
<i>Vibrio</i> sp.	kailuins	driftwood	79
<i>Agrobacterium</i>	agrochelin		80
<i>Bacillus pumilus</i>	depsiptides	sponge	81
<i>Micromonospora</i>	macrolide		82,83
<i>Micromonospora</i>	staurosporines	sponge	84
Actinomycete	neomarinone	sediment	85
<i>Streptomyces</i> sp.	aburatubolactam	mollusc	86,87

<b>Antibiotic</b>			
<b>Actinomycete</b>	marinone	sediment	88
<i>Bacillus</i> sp.	loloatins	worm	89,90
<i>Aalteromonas rava</i>	thiomarinol	seawater	91-93
<i>Chromobacterium</i> sp.	pyrrole	seawater	94
<b>Maduromycete</b>	maduralide	sediment	95
<b>Pseudomonad</b>	quinolinol	sea water	96
<i>Pseudoalteromonas</i>	korormicin	green alga	97
<i>Pseudomonas aeruginosa</i>	diketopiperazine	sponge	98
<i>Pseudomonas bromoutilis</i>	pentabromopseudilin	seagrass	99
<i>Pseudomonas flourescens</i>	andrimid, noiramides	ascidian	100
<i>Pseudomonas</i> sp.	massetolides	red alga	101
<i>Streptomyces griseus</i>	aplasmomycins	sediment	102-105
<i>Streptomyces tenjimariensis</i>	istamycins	sediment	106,107
<i>Streptomyces</i> sp.	phenazines	sediment	108
<i>Streptomyces</i> sp.	urauchimycins	sponge	109
<i>Streptomyces</i> sp.	bioxalomycins	intertidal sediment	110
<b>Streptomycete</b>	wailupemycins	sediment	111
<i>Thermococcus</i> sp.	cyclic polysulfides	hydrothermal vent	112
<i>Vibrio gazogenes</i>	magnesidins	sediment	113-115
<i>Vibrio</i> sp.	O-aminophenol	sponge	116
<i>Vibrio</i> sp.	trisindoline	sponge	117
<i>Streptomyces</i> sp.	phospholipid	sediment	118
<b>Streptomycete</b>	lorneamides	beach sand	119
<i>Bacillus laterosporus</i>	bogorol A	tube worm tissue	120
<i>Bacillus</i> sp.	macrolactins	sediments	121
<b>Antiviral</b>			
unidentified Gram positive	macrolactins	deep-sea sediment	122
unidentified Gram positive	caprolactams	deep-sea sediment	123
<b>Antiinflammatory</b>			
<b>Actinomycete</b>	salinamides	jelly-fish	124,125
<b>Actinomycete</b>	cyclomarins		126
<b>Actinomycete</b>	lobophorins	alga	127
<b>Enzyme inhibitors</b>			
<i>Agrobacterium aurantiacum</i>	hydroxyakalone		128
<i>Blastobacter</i> sp.	B-90063	seawater	129
<i>Flavobacterium</i> sp.	flavocristamides	bivalve	130
<i>Streptomyces</i> sp.	pyrostatins	sediment	131
unidentified	B-5354a-c	seawater	132,133

As the boundaries of the microbial world continue to expand, access to this newly identified diversity will likely depend upon the development of new culture methods. Scientists in the past have achieved limited success by borrowing techniques used in the cultivation of terrestrial bacteria and fungi. However, recent studies have revealed what should have been predicted: That marine microorganisms have unique adaptations to their natural environment and therefore require specialized isolation and culture methods. Jensen and coworkers demonstrated this point by improving the numbers of bacteria isolated from marine algal surfaces by using low-nutrient media.<sup>134</sup> Their findings further revealed that traditional media components such as yeast extract inhibit the growth of many marine microorganisms. The importance of incorporating “marine nutrients” at appropriate concentrations into medium formulations is therefore stressed. Further investigation of the physical and chemical parameters defining marine microhabitats will certainly provide insight for the design of novel isolation techniques.

Due to recent advances in the fields of genomics and proteomics, future acquisitions of novel molecular entities will coincide with an escalating number of potential drug targets. The completion of the human genome project, along with the sequencing of the entire genomes of many human pathogens, continues to expand our comprehension of disease progression. DNA microarrays now allow for the simultaneous analysis of all transcriptional events occurring in both healthy and diseased cells. Such tools are revolutionizing our ability to identify gene regulation events that represent novel targets for therapeutic development. The coupling of

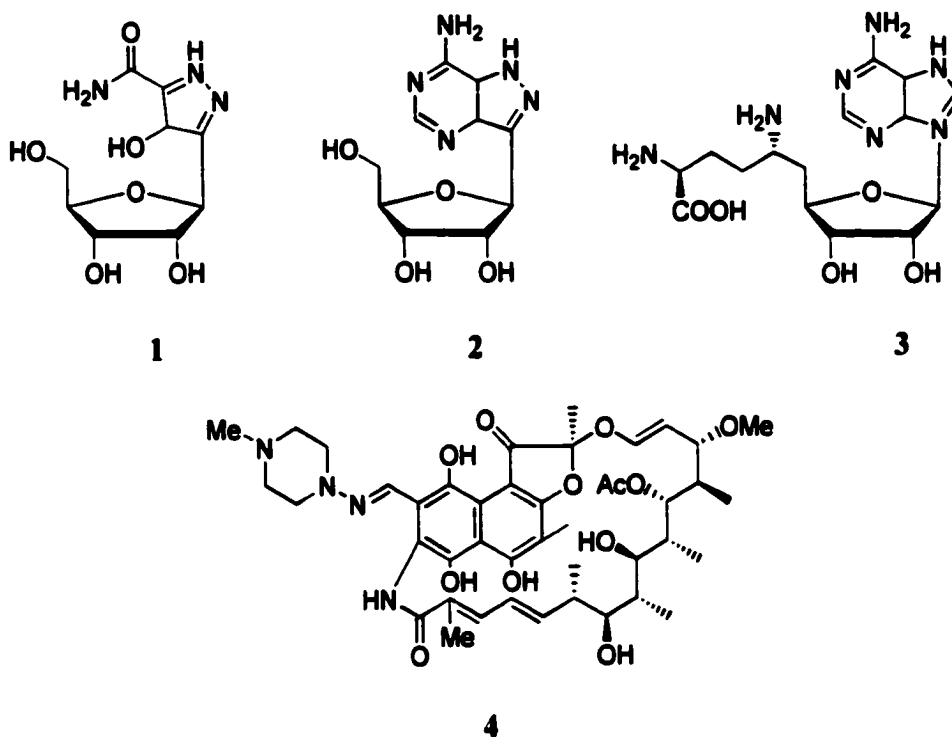
natural products chemistry with high throughput assays built upon these new technologies will provide a powerful platform for future drug discovery.

### **2.1.2 The Discovery of Antivirals Produced by Non-Marine Microorganisms**

In the past, structurally diverse compounds produced by laboratory culture of terrestrial bacteria and fungi have shown inhibitory activities in various viral disease models.<sup>135,136</sup> Although none of these natural products has yet found utility in treating clinical disease, the success of finding antiviral agents produced by terrestrial and freshwater microorganisms at least partly forms the foundation for targeting marine microorganisms. The following is not a comprehensive review, but rather highlights the structural and biological diversity of microbial derived antiviral agents. It should be noted that many of the producing organisms discussed below belong to taxa from which marine isolates have also been described.

The study of secondary metabolites produced by actinomycetes has yielded a large array of compounds with interesting antiviral properties. Pyrazofurin (1), a C-nucleoside isolated from the fermentation broth of *Streptomyces candidus*, has an extremely broad spectrum of activity against both DNA (herpes simplex, vaccinia) and RNA viruses (polio, influenza, measles, and yellow fever amongst others).<sup>137</sup> Pyrazofurin inhibits the replication of some of these viruses *in vitro* at IC<sub>50</sub>'s as low as 0.01 µg/mL, while DNA, RNA, and protein synthesis are unaffected at 1000-fold higher concentrations. Unfortunately, *in vivo* toxicity in mammals halted development of 1 as an antiviral therapeutic.<sup>138</sup> Other notable antiviral nucleoside analogs isolated from streptomycete fermentations include formycin (3)<sup>139</sup> and sinefungin (2).<sup>140</sup> The

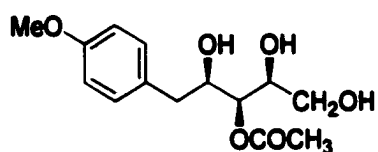
antitubercular drug rifampicin (4) produced by *Streptomyces mediterranei* was shown to inhibit the replication of poxviruses and adenoviruses.<sup>141</sup> The activity in these studies, however, was only observed at modestly high test concentrations of 50-60  $\mu\text{g/mL}$ .



A strain of *Pseudomonas fluorescens/putida* was discovered which produces the antiviral agent karalycin (5) that displays inhibitory activity against the herpes simplex viruses types 1 and 2, vaccinia virus, and poliovirus.<sup>142</sup> In the case of HSV-1, addition of the compound up to 10 hours after cell infection still resulted in 90% inhibition of virus production. At the same test concentration, RNA was found to accumulate in HSV-1 infected cells, but not in uninfected cells. This type of

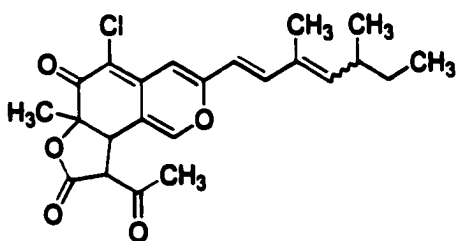


phenomenon has been observed with other antibiotics that inhibit protein biosynthesis. A contact time of one hour between HSV-1 infected cells and karalycin decreased virus production by more than 50%, demonstrating good cellular uptake of the compound.<sup>142</sup>

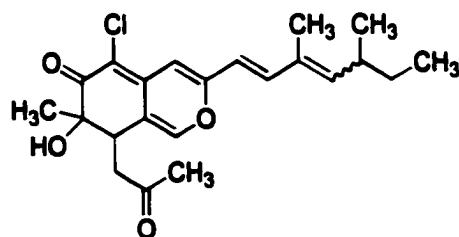


5

The isochromophilones 1 (6) and 2 (7) were the first anti-HIV agents of microbial origin that specifically inhibited binding of the viral gp120 envelope protein to the CD4 receptor of host cells.<sup>143</sup> These compounds were isolated from the culture broth of a soil fungus identified as *Penicillium multicolor* as mixtures of *E,Z*-isomers in the side chain. Isochromophilone 2 inhibited gp120-CD4 binding at 3.9  $\mu\text{M}$  and HIV replication in peripheral human lymphocytes at 25  $\mu\text{M}$ .

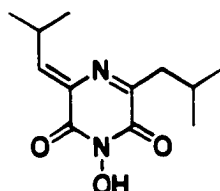


6

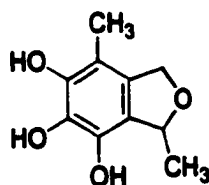


7

The influenza virus inhibitor flutidine (**8**) was isolated from the fermentation of a fungal species reported as *Delitschia confertaspora*.<sup>144</sup> This substituted 2,6-diketopiperazine was identified as a specific inhibitor of the viral transcriptase ( $IC_{50} = 5.5 \mu\text{M}$ ) and was later proven to inhibit the replication of influenza viruses in cell culture. Discovered as part of a random screening program involving extracts, flutidine is the first natural product with this mechanism of action and represents a novel scaffold for further drug design.

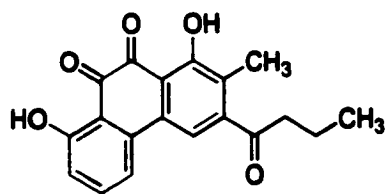
**8**

Another inhibitor of the influenza virus is the hydroxyl benzaldehyde compound FR198248 (**9**).<sup>145</sup> A fungal metabolite of an *Aspergillus terreus* isolate, this molecule may block virus adsorption. FR198248 was active in a murine *in vivo* model of influenza at 2 mg/kg.

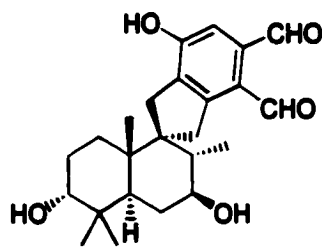
**9**

One of the most interesting discoveries involves the virucidal protein cyanovirin-N (CV-N). This unique 101-amino acid, disulfide bridged polypeptide was isolated from cultures of the cyanobacterium *Nostoc ellipsosporum*.<sup>146</sup> CV-N irreversibly inactivates diverse strains of HIV and simian immunodeficiency virus at low nanomolar concentrations. In addition, CV-N aborts cell-to-cell fusion and transmission of HIV-1 infection. The antiviral activity of CV-N is due to high-affinity interactions with the viral surface envelope glycoprotein gp120. Due to its potent virucidal activity and high therapeutic index, CV-N is a promising candidate for development as a topical microbicide to prevent sexual transmission of HIV infection.<sup>147</sup>

Chemical investigations of microbial fermentations have also yielded novel lead compounds active against enzymes crucial to viral replication. Since biochemical assays involving purified enzymes generally target replication steps unexploited by existing chemotherapies, these types of discoveries may eventually lead to drugs possessing new mechanisms of action. One example is Sch 65676 (**10**), a fungal metabolite that was found to inhibit the serine protease of human cytomegalovirus.<sup>148</sup> This enzyme is involved in the specific cleavage of virus-encoded polypeptides necessary for encapsulation of the viral genomic DNA and maturation of the viral capsid. Compound **10** is a member of the stachybatrydial family of compounds, and was the first in this class to be identified as a CMV protease inhibitor. Another example is Sch 68631 (**11**), an inhibitor of a hepatitis C virus serine protease produced by a soil streptomycete.<sup>149</sup>



10



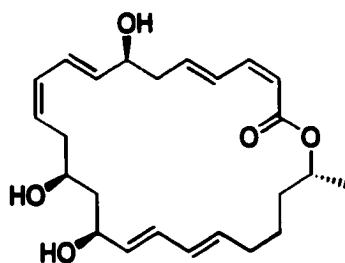
11

### 2.1.3 Precedent for Discovering Antivirals From Marine Microorganisms

Unlike their terrestrial counterparts, the antiviral potential of secondary metabolites produced by marine microorganisms remains virtually unexplored. In fact, there have only been two published reports to date describing antiviral molecules of marine microbial origin that are active against biomedical targets. In both of these cases, the antiviral activities were likely identified once the molecules were obtained in a pure state, rather than as a result of a targeted screening program.

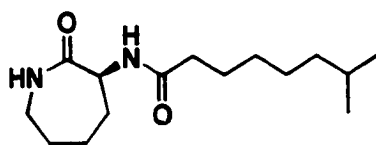
The macrolactins are 24-membered ring lactones of an unprecedented C24 linear acetogenin biosynthetic origin.<sup>122</sup> These molecules were isolated from the culture broth of a taxonomically unclassifiable marine bacterium obtained from a deep-sea sediment core. Macrolactin A (12) exhibited potent activity against HSV-1 and HSV-2 with  $IC_{50}$  values of 5.0 and 8.3  $\mu\text{g/mL}$ , respectively. When compared with the cytotoxicity against the cell lines used in the assays, 12 showed a therapeutic index range of 10-100. Further, HIV replication in human T-lymphoblast cells was controlled at 10  $\mu\text{g/ml}$ . Macrolactin A was also found to possess significant antibacterial and cancer cell cytotoxicity properties. The bacteria *Bacillus subtilis* and *Staphylococcus aureus* were inhibited at concentrations of 5 and 20  $\mu\text{g/disk}$  using a

standard disk diffusion assay. B16-F10 murine melanoma cell replication was inhibited in vitro with an  $IC_{50}$  of 3.5  $\mu\text{g/mL}$ . Recently, several macrolactin congeners have been discovered from the laboratory culture of a marine *Bacillus* sp. isolated from sediments off the coast of Thailand.<sup>121</sup>

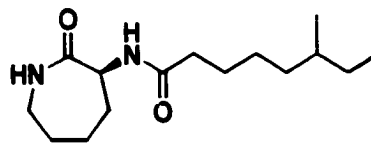


12

Davidson and coworkers isolated the caprolactins A (13) and B (14) from the fermentation of an unidentified deep-sea sediment bacterium.<sup>123</sup> These compounds showed very modest inhibition of HSV-2 at a concentration of 100  $\mu\text{g/mL}$ . Additionally, the caprolactins displayed mild cytotoxicity against human colorectal adenocarcinoma and human epidermoid carcinoma cells at low micromolar concentrations. Both the caprolactins and the macrolactins were obtained by extracting whole-cell culture suspensions with ethyl acetate so it is unclear to what degree these compounds are extracellular.



13



14

#### **2.1.4 Evidence for Microbial Mediation of Viral Inactivation in the Ocean**

Within the past decade, it has become increasingly evident that marine viruses play important roles in many ecological processes. Most striking has been the proposition that natural virus populations can control marine microbial community structure.<sup>150-152</sup> Indeed, it is estimated that viruses are on average responsible for lysing 20% of marine bacteria daily.<sup>150</sup> This has implications for affecting food web dynamics, element cycling, horizontal gene transfer, and microbial diversity.<sup>153</sup>

Viral abundance in marine environments parallels that of bacteria both spatially and temporally, decreasing from nearshore to offshore and from surface to deeper waters. Direct counts using epifluorescence and transmission electron microscopy have shown that viruses are generally present in the range of  $10^4$ - $10^7$  mL<sup>-1</sup> and are usually 5-10 fold more abundant than bacteria.<sup>154</sup> The strength of this relationship, coupled with the fact that bacteria are the most naturally abundant viral hosts, is highly suggestive that most marine viruses are bacteriophages.

Direct counting methods estimate the total viral population and do not differentiate between infective and non-infective viruses. UV radiation has been implicated as a primary mechanism in causing decay of viral infectivity. Sunlight in near surface and shallow coastal waters can destroy the infectivity of most of the viral community in a few hours. Other mechanisms of viral inactivation in marine environments have been proposed, including adhesion to particulates, grazing by protozoans, and biological processes that may include chemical interactions.<sup>155</sup>

One might hypothesize that chemical mediation of viral infectivity in the ocean is linked with the production of organic molecules of microbial origin. Already

presented is evidence that marine microorganisms are capable of producing structurally diverse secondary metabolites possessing significant biological activities. For the most part, however, the ecological roles of microbial natural products in the natural environment remain a mystery. Perhaps microbial communities have evolved survival strategies involving the selection of biosynthetic pathways leading to antiviral chemical defenses to mediate the environmental pressure of viral parasitism. Chemical defense by marine microbes against viral infection has not been specifically addressed in the literature. However, there is building evidence that marine bacteria manufacture and exude antiviral compounds.

Extracellular bacterial metabolites have been shown to inactivate certain fish and human enteric viruses in the water column. The fates of sewageborne human enteric viruses such as polio, Coxsackie, and ECHO have been studied in detail due to the potential for disease transmission after their release into the ocean. In most marine waters, these viruses remain infectious for a period of hours to several days. Several studies have implicated the role of microbiological processes in inactivating enteroviruses. Girones and coworkers isolated a marine bacterium tentatively classified as *Moraxella* with antiviral properties toward poliovirus.<sup>156</sup> They reported that the inactivating components could not be separated from the viable bacteria, indicating that the active agents either remain associated with the bacteria, have a short lifetime, or both. Toranzo and coworkers investigated bacteria belonging to the genera *Pseudomonas* and *Vibrio* that produced extracellular products with potent activity against poliovirus under laboratory cultivation conditions. The inactivation mechanism apparently involved substantial alterations to the viral capsid.

Other investigators have focused on the microbial mediation of fish virus inactivation. Waterborne transmission is one of the most common routes for infectious diseases in aquaculture. Kamei and coworkers evaluated 748 bacterial isolates from estuarine and marine environments in Japan for antiviral activity against infectious hematopoietic virus (IHN), a chum salmon pathogen.<sup>157</sup> The bacteria cultures were filtered through a Millex-HA filter and reacted with an equal volume of a diluted virus suspension. Fresh medium was used as a control. The suspensions were then plaque assayed to assess viral infectivity. Nearly 52% of the cell-free extracts caused at least a fifty percent plaque reduction, while 11% exhibited a ninety percent plaque reduction. Most of the bacteria showing antiviral activity were identified as belonging to the genera *Pseudomonas*, *Achromobacter*, and *Vibrio*.

Kimura and coworkers isolated and partially characterized an antiviral compound exuded by an aquatic bacterium tentatively identified as *Pseudomonas fluorescens*.<sup>158</sup> The culture broth from this organism was found to strongly inhibit the infectivity of IHN and *Oncorhynchus masou* virus (OMV) in rainbow trout gonad cell lines. Preliminary evidence suggested that the isolated antiviral compound prevented adsorption of virus particles to host cells by changing the virus morphology or by coating the virus surface. The molecular properties were consistent with an *N*-terminal blocked peptide with a molecular weight of 1126, but a complete structural characterization was not reported. In a similar investigation, Myouga *et al.* isolated a potent antiviral agent of high molecular weight and low cytotoxicity from the culture supernatant of a marine *Alteromonas* sp..<sup>159</sup> The 52 kDa polypeptide was active at



concentrations ranging from 0.09 to 2.51  $\mu\text{g/ml}$  against six fish viruses that included one herpesvirus and five rhabdoviruses.

Although studies involving human enteroviruses and fish viral pathogens do not directly address a hypothesis regarding bacterial chemical defense against viral infection, the above results begin to answer basic issues such as whether bacteria produce extracellular compounds with antiviral potential. Evidence does support the hypothesis that marine microorganisms are capable of producing metabolites possessing significant antiviral activity.

## **2.2 General Strategies and Methodologies for the Discovery of Bioactive Metabolites Produced by Marine Microorganisms**

The discovery of biologically active metabolites produced by marine microorganisms involves a multi-disciplinary scientific approach incorporating aspects of ecology, microbiology, natural products chemistry, and pharmacology. Collaboration is often a key component of such endeavors since it is unlikely that a single investigator will have expertise in all these areas.

A successful screening program necessarily begins with a diverse collection of organisms. In the course of my graduate studies, it has been my privilege to participate in numerous field expeditions to collect microorganisms. Since almost all bacteria and fungi cannot be visualized in their natural habitats by unaided eye, we rely primarily on sampling from as many different microhabitats as possible to attempt to diversify the collection. Therefore, one must be competent to identify the various marine biota, distinguish between healthy and diseased states, and recognize

ecological processes that might indicate microbial interaction. Samples are typically harvested into small sterile bags and returned to the laboratory where they are plated onto agar nutrient dishes for microbial isolation. Prior to plating, the samples can be treated in numerous ways in order to select for different types of organisms (e.g. heat shocking, cold stamping, drying, addition of selective antibiotics, etc.). Likewise, agar plates containing various nutrients and trace metals can be prepared to also help select for particular microbes. Again, the importance in varying and developing isolation techniques for increased access to microbial diversity cannot be overemphasized.

Once bacteria and fungi are observed to grow on agar, they are then carefully “picked” with a sterile loop and transferred to individual secondary isolation plates. A pure isolate is achieved if uniform growth is visualized on this secondary plate by both the unaided eye and also by microscopy. Small portions of the growing organism are stored at  $-80^{\circ}\text{C}$  and retained for further study. Laboratory cultures can be started from these samples, typically starting at 10 or 100 mL scale in various media designed to optimize growth. These smaller cultures can be used to inoculate larger volumes of media for large-scale fermentation.

Laboratory fermentation conditions play a decisive factor in the spectrum of metabolites that a microorganism will produce. For example, the fermentation of fungal isolate CNL240, the producer of the halovirs presented in chapter 4, was undertaken in several diverse media, but only two conditions resulted in the production of the halovir antiviral molecules. Fungi can be grown under either shake or static conditions, and the development of novel growth media using wide-ranging concentrations and types of nutrients is an art. Indeed, outstanding concoctions that

promote secondary metabolism become trade secrets. To attempt to fully access a microorganism's potential for secondary metabolism, a successful program must involve multiple fermentation strategies.

Biochemical studies of microbial fermentations generally begin with the extraction of metabolites followed by compound purification. Extractions are achieved using organic solvents (ethyl acetate, dichloromethane, methanol) or solid-phase resins (e.g. HP-20). Whole cultures can be extracted, or else cell matter can be separated from culture broth and each extracted individually. The extracts obtained are then screened for the biological activity of interest, and those displaying activity are further investigated. Separations of crude mixtures of compounds are achieved using such techniques as high-performance liquid chromatography (HPLC), high-speed counter current chromatography (HSCCC), and size-exclusion open column chromatography. The fractions are biologically evaluated, and active fractions are pursued in similar fashion until pure compounds demonstrating the desired function are achieved.

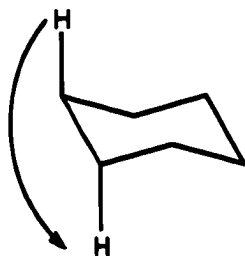
The determination of the absolute structure of an active molecule is undertaken using various spectral and chemical analyses. Mass spectrometry (MS) provides a measure of the molecular weight of an unknown compound, and high-resolution variations can provide a molecular formula determination. Qualitative information regarding structural components of the molecule in question can be gleaned using ultraviolet (UV) and infrared (IR) spectroscopies. By far the most useful techniques for structure determination, however, involve one- and two-dimensional nuclear magnetic resonance (NMR) spectrometry. Figure one shows a diagram indicating the

information that can be obtained from various two-dimensional NMR experiments. The Heteronuclear Multiple Quantum Coherence (HMQC) experiment provides correlations between protons and the carbons to which they are directly attached, whereas the Heteronuclear Multiple Bond Coherence (HMBC) experiment shows correlations between protons and carbon atoms either two or three bonds away. COrrrelation SpectroscopY (COSY) and TOtal Correlation SpectroscopY (TOCSY) experiments provide useful information pertaining to protons coupled to one another. TOCSY is especially useful in the structure elucidation of peptides since the entire spin systems of individual amino acids are revealed. Information regarding protons situated near one another through space is gained through Nuclear Overhauser Enhancement SpectroscopY experiments (NOESY). This data can prove critical for determining the relative configurations of chiral molecules, and also for gaining insight into the three dimensional arrangement of the molecule in solution. The structure determination of a compound is not complete until its absolute configuration has been established. Chemical degradation or derivatization techniques are often necessary to accomplish this goal. Mosher's ester analysis of secondary alcohols and chiral gas chromatography of peptide hydrolysates are two examples discussed in chapter four.

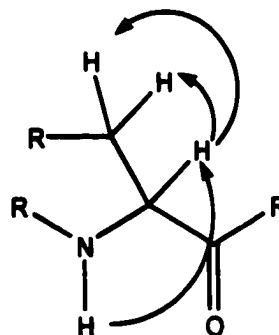
A biologically active molecule of determined structure becomes a tool for further study. New questions are raised regarding the origin of the pharmacological properties. Investigations into the mechanism of action, biological specificity, and the structural features most critical to the desired function may be warranted. Biosynthetic studies might be pursued with structurally unusual molecules, perhaps

leading to insights into fermentation optimization. Always there are speculations as to what natural roles the newly discovered molecule might play. Truly, the fun might be just beginning.

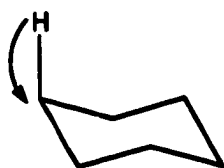
**COSY**  
COupled SpectroscopY



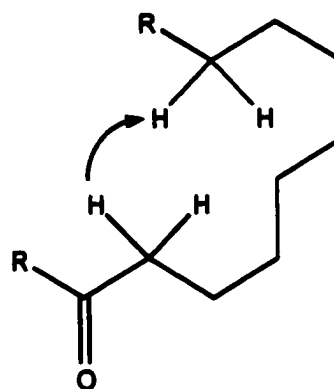
**TOCSY**  
TOfal Coupled SpectroscopY



**HMQC**  
Heteronuclear Multiple  
Quantum Coherence



**NOESY**  
Nuclear Overhauser  
Enhancement Spectroscopy



**HMBC**  
Heteronuclear Multiple  
Buantum Coherence

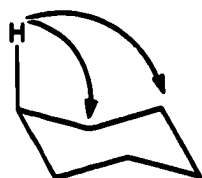


**Figure 1. Two-dimensional proton detected NMR experiments.**

## References

1. Biabani, M.A.F. & Laatsch, H. (1998). Advances in chemical studies on low-molecular weight metabolites of marine fungi. *J. Prakt. Chem. Ztg.* **340**, 589-607.
2. Fenical, W. (1993). Chemical studies of marine bacteria - Developing a new resource. *Chem. Rev.* **93**, 1673-1683.
3. Davidson, B.S. (1995). New dimensions in natural products research: Cultured marine microorganisms. *Curr. Opin. Biotechnol.* **6**, 284-291.
4. Pietra, F. (1997). Secondary metabolites from marine microorganisms: bacteria, protozoa, algae and fungi. Achievements and prospects. *Nat. Prod. Rep.* **14**, 453-464.
5. Jensen, P.R. & Fenical, W. (1996). Marine bacterial diversity as a resource for novel microbial products. *J. Ind. Microbiol. Biotechnol.* **17**, 346-351.
6. Jensen, P.R. & Fenical, W. (1994). Strategies for the discovery of secondary metabolites from marine bacteria - Ecological perspectives. *Annu. Rev. Microbiol.* **48**, 559-584.
7. Liberra, K. & Lindequist, U. (1995). Marine fungi - a prolific resource of biologically active natural products. *Pharmazie* **50**, 583-588.
8. Jensen, P.R. & Fenical, W. (2000). Marine microorganisms and drug discovery: Current status and future potential. *In* Drugs from the sea. N. Fusetani, editor. Karger, Basel. 6-29.
9. Numata, A., Takahashi, C., Matsushita, T., Miyamoto, T., Kawai, K., Usami, Y., Matsumura, E., Inoue, M., Ohishi, H. & Shingu, T. (1992). Fumiquinazolines, novel metabolites of a fungus isolated from a saltfish. *Tetrahedron Lett.* **33**, 1621-1624.
10. Cui, C.B., Kakeya, H., Okada, G., Onose, R., Ubukata, M., Takahashi, I., Isono, K. & Osada, H. (1995). Tryprostatins A and B, novel mammalian cell cycle inhibitors produced by *Aspergillus fumigatus*. *J. Antibiot.* **48**, 1382-1384.
11. Varoglu, M., Corbett, T.H., Valeriote, F.A. & Crews, P. (1997). Asperazine, a selective cytotoxic alkaloid from a sponge-derived culture of *Aspergillus niger*. *J. Org. Chem.* **62**, 7078-7079.
12. Toske, S.G., Jensen, P.R., Kauffman, C.A. & Fenical, W. (1998). Aspergillamides A and B: Modified cytotoxic tripeptides produced by a marine fungus of the genus *Aspergillus*. *Tetrahedron* **54**, 13459-13466.

13. Belofsky, G.N., Jensen, P.R., Renner, M.K. & Fenical, W. (1998). New cytotoxic sesquiterpenoid nitrobenzoyl esters from a marine isolate of the fungus *Aspergillus versicolor*. *Tetrahedron* **54**, 1715-1724.
14. Renner, M.K., Jensen, P.R. & Fenical, W. (1998). Neomangicols: Structures and absolute stereochemistries of unprecedented halogenated sesterterpenes from a marine fungus of the genus *Fusarium*. *J. Org. Chem.* **63**, 8346-8354.
15. Numata, A., Amagata, T., Minoura, K. & Ito, T. (1997). Gymnastatins, novel cytotoxic metabolites produced by a fungal strain from a sponge. **38**, 5675-5678.
16. Amagata, T., Doi, M., Ohta, T., Minoura, K. & Numata, A. (1998). Absolute stereostructures of novel cytotoxic metabolites, gymnastatins A-E, from a *Gymnascella* species separated from a *Halichonbdria* sponge. *J. Chem. Soc. Perk. Trans. 1* 3585-3599.
17. Amagata, T., Minoura, K. & Numata, A. (1998). Gymnasterones, novel cytotoxic metabolites produced by a fungal strain from a sponge. *Tetrahedron Lett.* **39**, 3773-3774.
18. Takahashi, C., Numata, A., Matsumura, E., Minoura, K., Eto, H., Shingu, T., Ito, T. & Hasegawa, T. (1994). Leptosins I and J, cytotoxic substances produced by a *Leptosphaeria* sp.: Physico-chemical properties and structures. *J. Antibiot.* **47**, 1242-1249.
19. Shigemori, H., Wakuri, S., Yazawa, K., Nakamura, T., Sasaki, T. & Kobayashi, J. (1991). Fellutamides A and B, cytotoxic peptides from a marine fish-possessing fungus *Penicillium fellutanum*. *Tetrahedron* **47**, 8529-8534.
20. Numata, A., Takahashi, C., Ito, Y., Takada, T., Kawai, K., Usami, Y., Matsumura, E., Imachi, M., Ito, T. & Hasegawa, T. (1993). Communesins, cytotoxic metabolites of a fungus isolated from a marine alga. *Tetrahedron Lett.* **34**, 2355-2358.
21. Numata, A., Takahashi, C., Ito, Y., Minoura, K., Yamada, T., Matsuda, C., Nomoto, K. (1996). Penochalasin, a novel class of cytotoxic cytochalasins from a *Penicillium* species separated from a marine alga: structure determination and solution conformation. *J. Chem. Soc. Perkin Trans.* 239-245.
22. Takahashi, C., Numata, A., Yamada, T., Minoura, K., Enomoto, S., Konishi, K., Nakai, M., Matsuda, C. & Nomoto, K. (1996). Penostatins, novel cytotoxic metabolites from a *Penicillium* species separated from a green alga. *Tetrahedron Lett.* **37**, 655-658.
23. Amagata, T., Minoura, K. & Numata, A. (1998). Cytotoxic metabolites produced by a fungal strain from a Sargassum alga. *J. Antibiot.* **51**, 432-434.

24. Iwamoto, C., Minoura, K., Hagishita, S., Nomoto, K. & Numata, A. (1998). Penostatins F-I, novel cytotoxic metabolites from a *Penicillium* species separated from an *Enteromorpha* marine alga. *J. Chem. Soc. Perkin Trans. 1* 449-456.
25. Numata, A., Iritani, M., Yamada, T., Minoura, K., Matsumura, E., Yamori, T. & Tsuruo, T. (1997). Novel antitumour metabolites produced by a fungal strain from a sea hare. *Tetrahedron Lett.* **38**, 8215-8218.
26. Namikoshi, M., Kobayashi, H., Yoshimoto, T. & Hosoya, T. (1997). Phomopsidin, a new inhibitor of microtubule assembly produced by *Phomopsis* sp. isolated from coral reef in Pohnpei. *J. Antibiot.* **50**, 890-892.
27. Amagata, T., Usami, Y., Minoura, K., Ito, T. & Numata, A. (1998). Cytotoxic substances produced by a fungal strain from a sponge: Physico-chemical properties and structures. *J. Antibiot.* **51**, 33-40.
28. McDonald, L.A., Abbanat, D.R., Barbieri, L.R., Bernan, V.S., Discafani, C.M., Greenstein, M., Janota, K., Korshalla, J.D., Lassota, P., Tischler, M. & Carter, G.T. (1999). Spiroxins, DNA cleaving antitumor antibiotics from a marine-derived fungus. *Tetrahedron Lett.* **40**, 2489-2492.
29. Son, B., Jensen, P.R., Kauffman, C., Fenical, W. (1999). New cytotoxic epidithiodioxopiperazines related to verticillin A from a marine isolate of the fungus *Penicillium*. *Nat. Prod. Rep.* **13**, 213-222.
30. Amagata, T., Doi, M., Tohgo, M., Minoura, K. & Numata, A. (1999). Dankasterone, a new class of cytotoxic steroid produced by a *Gymnascella* species from a marine sponge. *Chem. Commun.* 2131.
31. Beilofsky, G.N., Jensen, P.R. & Fenical, W. (1999). Sansalvamide: A new cytotoxic cyclic depsipeptide produced by a marine fungus of the genus *Fusarium*. *Tetrahedron Lett.* **40**, 2913-2916.
32. Cueto, M., Jensen, P.R. & Fenical, W. (2000). N-methylsansalvamide, a cytotoxic cyclic depsipeptide from a marine fungus of the genus *Fusarium*. *Phytochemistry* **55**, 223-226.
33. Laurent, D., Guella, G., Roquebert, M.F., Farinole, F., Mancini, I. & Pietra, F. (2000). Cytotoxins, mycotoxins and drugs from a new deuteromycete, *Acremonium neo-caledoniae*, from the southwestern lagoon of New Caledonia. *Planta Med.* **66**, 63-66.
34. Suenaga, K., Aoyama, S., Xi, W., Arimoto, H., Yamaguchi, K., Yamada, K., Tsuji, T., Yamada, A. & Uemura, D. (2000). Isolation and structure of kasarín, a novel azetinone compound, isolated from a marine microorganism. *Heterocycles* **52**, 1033-1036.



35. Brauers, G., Edrada, R.A., Ebel, R., Proksch, P., Wray, V., Berg, A., Grafe, U., Schachtele, C., Totzke, F., Finkenzeller, G., Marme, D., Kraus, J., Munchbach, M., Michel, M., Bringmann, G. & Schaumann, K. (2000). Anthraquinones and betaenone derivatives from the sponge-associated fungus *Microsphaeropsis* species: Novel inhibitors of protein kinases. *J. Nat. Prod.* **63**, 739-745.
36. Afiyatullo, S.S., Kuznetsova, T.A., Isakov, V.V., Pivkin, M.V., Prokofeva, N.G. & Elyakov, G.B. (2000). New diterpenic altrosides of the fungus *Acremonium striatisporum* isolated from a sea cucumber. *J. Nat. Prod.* **63**, 848-850.
37. Namikoshi, M., Akano, K., Meguro, S., Kasuga, I., Mine, Y., Takahashi, T. & Kobayashi, H. (2001). A new macrocyclic trichothecene, 12,13-deoxyroridin E, produced by the marine-derived fungus *Myrothecium roridum* collected in Palau. *J. Nat. Prod.* **64**, 396-398.
38. Lorenz, P., Jensen, P.R., Fenical, W. (1998). Mactanamide, A new fungistatic diketopiperazine produced by a marine *Aspergillus* sp. *Nat. Prod. Rep.* **12**, 55-60.
39. Holler, U., Konig, G.M. & Wright, A.D. (1999). Three new metabolites from marine-derived fungi of the genera *Coniothyrium* and *Microsphaeropsis*. *J. Nat. Prod.* **62**, 114-118.
40. Furuya, K., Okudaira, M., Shindo, T. and Sato, A. (1985). *Corollospora pulchella*, a marine fungus producing antibiotics, melinacidins III, IV and gancidin W. *Annu. Rep. Sankyo Res. Lab.* **37**, 140-142.
41. Schlingmann, G., Milne, L., Williams, D.R. & Carter, G.T. (1998). Cell wall active antifungal compounds produced by the marine fungus *Hypoxylon oceanicum* LL-15G256: II. Isolation and structure determination. *J. Antibiot.* **51**, 303-316.
42. Poch, G.K. & Gloer, J.B. (1991). Auranticins A and B: Two new depsidones from a mangrove isolate of the fungus *Preussia aurantiaca*. *J. Nat. Prod.* **54**, 213-217.
43. Abrell, L.M., Borgeson, B. & Crews, P. (1996). A new polyketide, secocurvularin, from the salt water culture of a sponge derived fungus. *Tetrahedron Lett.* **37**, 8983-8984.
44. Wang, G.Y.S., Abrell, L.M., Avelar, A., Borgeson, B.M. & Crews, P. (1998). New hirsutane based sesquiterpenes from salt water cultures of a marine sponge-derived fungus and the terrestrial fungus *Coriolus consors*. *Tetrahedron* **54**, 7335-7342.
45. Liberra, K., Jansen, R. & Lindequist, U. (1998). Corollosporine, a new phthalide derivative from the marine fungus *Corollospora maritima* Werderm. *Pharmazie* **53**, 578-581.

46. Daferner, M., Mensch, S., Anke, T. & Sterner, O. (1999). Hypoxysordarin, a new sordarin derivative from *Hypoxylon croceum*. *Z. Naturforsch. C.* **54**, 474-480.
47. Shigemori, H., Komatsu, K., Mikami, Y. & Kobayashi, J.i. (1999). Seragakinone A, a new pentacyclic metabolite from a marine-derived fungus. *Tetrahedron* **55**, 14925-14930.
48. Nielsen, J., Nielsen, P.H. & Frisvad, J.C. (1999). Fungal depside, guisinol, from a marine derived strain of *Emericella unguis*. *Phytochemistry* **50**, 263-265.
49. Bugni, T.S., Abbanat, D., Berman, V.S., Maiese, W.M., Greenstein, M., Van Wagoner, R.M. & Ireland, C.M. (2000). Yanuthones: Novel metabolites from a marine isolate of *Aspergillus niger*. *J. Org. Chem.* **65**, 7195-7200.
50. Osterhage, C., Kaminsky, R., König, G.M. & Wright, A.D. (2000). Ascosalipyrrolidinone A, an antimicrobial alkaloid, from the obligate marine fungus *Ascochyta salicorniae*. *J. Org. Chem.* **65**, 6412-6417.
51. Belofsky, G.N., Anguera, M., Jensen, P.R., Fenical, W. & Kock, M. (2000). Oxepinamides A-C and fumiquinazolines H-I: Bioactive metabolites from a marine isolate of a fungus of the genus *Acremonium*. *Eur. J. Chem.* **6**, 1355-1360.
52. Alvi, K.A., Casey, A. & Nair, B.G. (1998). Pulchellalactam: A CD45 protein tyrosine phosphatase inhibitor from the marine fungus *Corollospora pulchella*. *J. Antibiot.* **51**, 515-517.
53. Yu, C.M., Curtis, J.M., Walter, J.A., Wright, J.L.C., Ayer, S.W., Kaleta, J., Querengesser, L. & Fathi-Afshar, Z.R. (1996). Potent inhibitors of cysteine proteases from the marine fungus *Microascus longirostris*. *J. Antibiot.* **49**, 395-397.
54. Omura, S., Tomoda, H., Tabata, N., Ohyama, Y., Abe, T. & Namikoshi, M. (2000). Roselipins, novel fungal metabolites having a highly methylated fatty acid modified with a mannose and an arabinitol. *J. Antibiot.* **53**, C1.
55. Kakeya, H., Takahashi, I., Okada, G., Isono, K. & Osada, H. (1995). Epolactaene, a novel neurotogenic compound in human neuroblastoma cells, produced by a marine fungus. *J. Antibiot.* **48**, 733-735.
56. Sugano, M., Sato, A., Iijima, Y., Furuya, K., Haruyama, H., Yoda, K. & Hata, T. (1994). Phomactins, novel PAF antagonists from marine fungus *Phoma* sp. *J. Org. Chem.* **59**, 564-569.
57. Sugano, M., Sato, A., Iijima, Y., Oshima, T., Furuya, K., Kuwano, H., Hata, T. & Hanzawa, H. (1991). Phomactin A, a novel PAF antagonist from a marine fungus *Phoma* sp. *J. Am. Chem. Soc.* **113**, 5463-5464.

58. Hugenholtz, P. & Pace, N.R. (1996). Identifying microbial diversity in the natural environment: A molecular phylogenetic approach. *14*, 190-197.
59. Delong, E.F. (1997). Marine microbial diversity: The tip of the iceberg. *Trends Biotechnol.* **15**, 203-207.
60. Giovannoni, S.J., Britschgi, T.B., Moyer, C.L. & Field, K.G. (1990). Genetic diversity in Sargasso sea North Atlantic ocean bacterioplankton. *Nature* **345**, 60-63.
61. Britschgi, T.B. & Giovannoni, S.J. (1991). Phylogenetic analysis of a natural marine bacterioplankton population by ribosomal RNA gene cloning and sequencing. *Appl. Environ. Microbiol.* **57**, 1707-1713.
62. Kameyama, T., Takahashi, A., Kurasawa, S., Ishizuka, M., Okami, Y., Takeuchi, T. & Umezawa, H. (1987). Bisucaberin a new siderophore sensitizing tumor cells to macrophage-mediated cytotoxicity I. Taxonomy of the producing organism isolation and biological properties. *J. Antibiot.* **40**, 1664-1670.
63. Takahashi, A., Nakamura, H., Kameyama, T., Kurasawa, S., Naganawa, H., Okami, Y., Takeuchi, T., Umezawa, H. & Itaka, Y. (1987). Bisucaberin A new siderophore sensitizing tumor cells to macrophage-mediated cytotoxicity II. Physico-chemical properties and structure determination. *J. Antibiot.* **40**, 1671-1676.
64. Shigemori, H., Bae, M.A., Yazawa, K., Sasaki, T. & Kobayashi, J. (1992). Alteramide-A, a new tetracyclic alkaloid from a bacterium-*Alteromonas* sp. associated with the marine sponge *Halichondria okadai*. *J. Org. Chem.* **57**, 4317-4320.
65. Wang, G.Y.S., Kuramoto, M., Yamada, K., Yazawa, K. & Uemura, D. (1995). Homocereulide, an extremely potent cytotoxic depsipeptide from the marine bacterium *Bacillus cereus*. *Chem. Lett.* 791-792.
66. Trischman, J.A., Jensen, P.R. & Fenical, W. (1994). Halobacillin - a cytotoxic cyclic acylpeptide of the iturin class produced by a marine *Bacillus* sp. *Tetrahedron Lett.* **35**, 5571-5574.
67. Canedo, L.M., Puentes, J.L.F. & Baz, J.P. (1997). PM-94128, a new isocoumarin antitumor agent produced by a marine bacterium. *J. Antibiot.* **50**, 175-176.
68. Kitahara, T., Naganawa, H., Okazaki, T., Okami, Y. & Umezawa, H. (1975). The structure of SS-228Y, an antibiotic from *Chainia* sp. *J. Antibiot.* **28**, 208-5.
69. Okazaki, T., Kitahara, T. & Okami, Y. (1975). Studies on marine microorganisms. IV. A new antibiotic SS-228 Y produced by *Chainia* isolated from shallow sea mud. *J. Antibiot.* **28**, 176-84.

70. Romero, F., Espliego, F., Baz, J.P., DeQuesada, T.G., Gravalos, D., DelaCalle, F. & FernandezPuertes, J.L. (1997). Thiocoraline, a new depsipeptide with antitumor activity produced by a marine *Micromonospora* .1. Taxonomy, fermentation, isolation, and biological activities. *J. Antibiot.* **50**, 734-737.
71. Baz, J.P., Canedo, L.M., Puentes, J.L.F. & Elipe, M.V.S. (1997). Thiocoraline, a novel depsipeptide with antitumor activity produced by a marine *Micromonospora* .2. Physico-chemical properties and structure determination. *J. Antibiot.* **50**, 738-741.
72. Imamura, N., Nishijima, M., Takadera, T., Adachi, K., Sakai, M. & Sano, H. (1997). New anticancer antibiotics pelagiomicins, produced by a new marine bacterium *Pelagibacter variabilis*. *J. Antibiot.* **50**, 8-12.
73. Takahashi, C., Takada, T., Yamada, T., Minoura, K., Uchida, K., Matsumura, E. & Numata, A. (1994). Halichomycin, a new class of potent cytotoxic macrolide produced by an actinomycete from a marine fish. *Tetrahedron Lett.* **35**, 5013-5014.
74. Takahashi, A., Ikeda, D., Nakamura, H., Naganawa, H., Kurasawa, S., Okami, Y., Takeuchi, T. & Iitaka, Y. (1989). Altemicidin, a new acaricidal and antitumor substance: II. Structure determination. *J. Antibiot.* **42**, 1562-1566.
75. Takahashi, A., Kurasawa, S., Ikeda, D., Okami, Y. & Takeuchi, T. (1989). Altemicidin, a new acaricidal and antitumor substance: I. Taxonomy, fermentation, isolation and physico-chemical and biological properties. *J. Antibiot.* **42**, 1556-1561.
76. Tapiolas, D.M., Roman, M., Fenical, W., Stout, T.J. & Clardy, J. (1991). Octalactin-A and octalactin-B - Cytotoxic 8-membered-ring lactones from a marine bacterium, *Streptomyces* sp. *J. Am. Chem. Soc.* **113**, 4682-4683.
77. Schumacher, R.W. & Davidson, B.S. (1995). Gamma-indomycinone, a new pluramycin metabolite from a deep-sea derived actinomycete. *J. Nat. Prod.* **58**, 613-617.
78. Biabani, M.A.F., Laatsch, H., Helmke, E. & Weyland, H. (1997). Delta-indomycinone: A new member of pluramycin class of antibiotics isolated from marine *Streptomyces* sp. *J. Antibiot.* **50**, 874-877.
79. Harrigan, G.G., Harrigan, B.L. & Davidson, B.S. (1997). Kailuins A-D, new cyclic acyldepsipeptides from cultures of a marine-derived bacterium. *Tetrahedron* **53**, 1577-1582.

80. Cañedo, L.M., de la Fuente, J.A., Gesto, C., Ferreiro, M.J., Jimenez, C. & Riguera, R. (1999). Agrochelin, a new cytotoxic alkaloid from the marine bacteria *Agrobacterium* sp. *Tetrahedron Lett.* **40**, 6841-6844.
81. Kalinovskaya, N.I., Kuznetsova, T.A., Rashkes, Y.V., Milgrom, Y.M., Milgrom, E.G., Willis, R.H., Wood, A.I., Kurtz, H.A., Carabedian, C., Murphy, P. & Elyakov, G.B. (1995). Surfactin-Like structures of fivecyclic depsipeptides from the marine isolate of *Bacillus pumilus*. *Russ. Chem. Bull.* **44**, 951-955.
82. Cañedo, L.M., Puentes, J.L.F., Baz, J.P., Huang, X.H. & Rinehart, K.L. (2000). IB-96212, a novel cytotoxic macrolide produced by a marine *Micromonospora* - II. Physico-chemical properties and structure determination. *J. Antibiot.* **53**, 479-483.
83. Fernandez-Chimeno, R.I., Cañedo, L., Espliego, F., Gravalos, D., De la Calle, F., Fernandez-Puentes, J.L. & Romero, F. (2000). IB-96212, a novel cytotoxic macrolide produced by a marine *Micromonospora* - I. Taxonomy, fermentation, isolation and biological activities. *J. Antibiot.* **53**, 474-478.
84. Hernandez, L.M.C., Blanco, J.A.D., Baz, J.P., Puentes, J.L.F., Millan, F.R., Vazquez, F.E., Fernandez-Chimeno, R.I. & Gravalos, D.G. (2000). 4'-N-methyl-5'-hydroxystaurosporine and 5'-hydroxystaurosporine, new indolocarbazole alkaloids from a marine *Micromonospora* sp strain. *J. Antibiot.* **53**, 895-902.
85. Hardt, I.H., Jensen, P.R. & Fenical, W. (2000). Neomarinone, and new cytotoxic marinone derivatives, produced by a marine filamentous bacterium (*actinomycetales*). *Tetrahedron Lett.* **41**, 2073-2076.
86. Bae, M.A., Yamada, K., Ijuin, Y., Tsuji, T., Yazawa, K., Tomono, Y. & Uemura, D. (1996). Aburatubolactam A, a novel inhibitor of superoxide anion generation from a marine microorganism. *Heterocycl. Comm.* **2**, 315-318.
87. Bae, M.-A., Yamada, K., Uemura, D., Seu, J.H. & Kim, Y.H. (1998). Aburatubolactam C, a novel apoptosis-inducing substance produced by marine *Streptomyces* sp. SCRC A-20. *J. Microb. Biotech.* **8**, 455-460.
88. Pathirana, C., Jensen, P.R. & Fenical, W. (1992). Marinone and debromomarinone - Antibiotic sesquiterpenoid naphthoquinones of a new structure class from a marine bacterium. *Tetrahedron Lett.* **33**, 7663-7666.
89. Gerard, J., Haden, P., Kelly, M.T. & Andersen, R.J. (1996). Loloatin B, a cyclic decapeptide antibiotic produced in culture by a tropical marine bacterium. **37**, 7201-7204.

90. Gerard, J.M., Haden, P., Kelly, M.T. & Andersen, R.J. (1999). Loloatins A-D, cyclic decapeptide antibiotics produced in culture by a tropical marine bacterium. *J. Nat. Prod.* **62**, 80-85.
91. Shiozawa, H., Kagasaki, T., Kinoshita, T., Haruyama, H., Domon, H., Utsui, Y., Kodama, K. & Takahashi, S. (1993). Thiomarinol, a new hybrid antimicrobial antibiotic produced by a murine bacterium: Fermentation, isolation, structure, and antimicrobial activity. *J. Antibiot.* **46**, 1834-1842.
92. Shiozawa, H., Kagasaki, T., Torikata, A., Tanagk, N., Hata, T., Furukawa, Y. & Takahashi, S. (1995). Thiomarinols B and C, new antimicrobial antibiotics produced by a marine bacterium. *J. Antibiot.* **48**, 907-909.
93. Shiozawa, H., Shimada, A. & Takahashi, S. (1997). Thiomarinols D, E, F and G, new hybrid antimicrobial antibiotics produced by a marine bacterium: Isolation, structure, and antimicrobial activity. *J. Antibiot.* **50**, 449-452.
94. Andersen, R.J., Wolfe, M.S. & Faulkner, D.J. (1974). Autotoxic antibiotic production by a marine *Chromobacterium*. *Mar. Biol.* **27**, 281.
95. Pathirana, C., Tapiolas, D., Jensen, P.R., Dwight, R. & Fenical, W. (1991). Structure determination of maduralide - a new 24-membered ring macrolide glycoside produced by a marine bacterium (*Actinomycetales*). *Tetrahedron Lett.* **32**, 2323-2326.
96. Wratten, S.J., Wolfe, M.S., Andersen, R.J. & Faulkner, D.J. (1977). Antibiotic metabolites from a marine pseudomonad. *Antimicrob. Agents Chemother.* **11**, 411-414.
97. Yoshikawa, K., Takadera, T., Adachi, K., Nishijima, M. & Sano, H. (1997). Korormicin, a novel antibiotic specifically active against marine gram-negative bacteria, produced by a marine bacterium. *J. Antibiot.* **50**, 949-953.
98. Jayatilake, G.S., Thornton, M.P., Leonard, A.C., Grimwade, J.E. & Baker, B.J. (1996). Metabolites from an antarctic sponge-associated bacterium, *Pseudomonas aeruginosa*. *J. Nat. Prod.* **59**, 293-296.
99. Lovell, F.M. (1966). The structure of a bromine-rich antibiotic. *J. Am. Chem. Soc.* **59**, 4510.
100. Needham, J., Kelly, M.T., Ishige, M. & Andersen, R.J. (1994). Andrimid and moriamides A-C, metabolites produced in culture by a marine isolate of the bacterium *Pseudomonas fluorescens*: Structure elucidation and biosynthesis. *J. Org. Chem.* **59**, 2058-2063.

101. Gerard, J., Lloyd, R., Barsby, T., Haden, P., Kelly, M.T. & Andersen, R.J. (1997). Massetolides A-H, antimycobacterial cyclic depsipeptides produced by two pseudomonads isolated from marine habitats. *J. Nat. Prod.* **60**, 223-229.
102. Okami, Y., Okazaki, T., Kitahara, T. & Umezawa, H. (1976). Studies on marine microorganisms. V. A new antibiotic, aplasmomycin, produced by a streptomycete isolated from shallow sea mud. *J. Antibiot.* **29**, 1019-1025.
103. Nakamura, H., Iitaka, Y., Kitahara, T., Okazaki, T. & Okami, Y. (1977). Structure of aplasmomycin. *J. Antibiot.* **30**, 714-719.
104. Sato, K., Okazaki, T., Maeda, K. & Okami, Y. (1978). New antibiotics, aplasmomycins B and C. *J. Antibiot.* **31**, 632-635.
105. Stout, T.J., Clardy, J., Pathirana, I.C. & Fenical, W. (1991). Aplasmomycin-C - structural studies of a marine antibiotic. *Tetrahedron* **47**, 3511-3520.
106. Okami, Y., Hotta, K., Yoshida, M., Ikeda, D., Kondo, S. & Umezawa, H. (1979). New aminoglycoside antibiotics, istamycins A and B. *J. Antibiot.* **32**, 964-966.
107. Hotta, K., Yoshida, M., Hamada, M. & Okami, Y. (1980). Studies on new aminoglycoside antibiotics, istamycins, from an actinomycete isolated from a marine environment. III. Nutritional effects on istamycin production and additional chemical and biological properties of istamycins. *J. Antibiot.* **33**, 1515-1520.
108. Pathirana, C., Jensen, P.R., Dwight, R. & Fenical, W. (1992). Rare phenazine L-quinovose esters from a marine actinomycete. *J. Org. Chem.* **57**, 740-742.
109. Imamura, N., Nishijima, M., Adachi, K. & Sano, H. (1993). Novel antimycin antibiotics, urauchimycin-A and urauchimycin-B, produced by marine actinomycete. *J. Antibiot.* **46**, 241-246.
110. Berman, V.S., Montenegro, D.A., Korshalla, J.D., Maiese, W.M., Steinberg, D.A. & Greenstein, M. (1994). Bioxalomycins, new antibiotics produced by the marine *Streptomyces* sp. Ll-31f508 - Taxonomy and fermentation. *J. Antibiot.* **47**, 1417-1424.
111. Sitachitta, N., Gadepalli, M. & Davidson, B.S. (1996). New alpha-pyrone-containing metabolites from a marine-derived actinomycete. *Tetrahedron* **52**, 8073-8080.
112. Ritzau, M., Keller, M., Wessels, P., Stetter, K.O. & Zeeck, A. (1993). Secondary metabolites by chemical screening .25. New cyclic polysulfides from hyperthermophilic archaea of the genus *Thermococcus*. *Lieb. Ann. Ch.* 871-876.

113. Gandhi, N.M., Nazareth, J., Divekar, P.V., Kohl, H. & De Souza, N.J. (1973). Magnesidin, a novel magnesium-containing antibiotic. *J. Antibiot.* **26**, 797-798.
114. Kohl, H., Bhat, S.V., Patell, J.R., Gandhi, N.M., Nazareth, J., Divekar, P.V., De Souza, N.J., Berscheid, H.G. & Fehlhaver, H.W. (1974). Structure of magnesidin, a new magnesium containing antibiotic from *Pseudomonas magnesoruba*. *Tetrahedron Lett.* **12**, 983.
115. Imamura, N., Adachi, K. & Sano, H. (1994). Magnesidin A, a component of marine antibiotic magnesidin, produced by *Vibrio gazogenes* ATCC 29988. *J. Antibiot.* **47**, 257-261.
116. Oclarit, J.M., Ohta, S., Kamimura, K., Yamaoka, Y. & Ikegami, S. (1994). Production of the antibacterial agent, O-aminophenol, by a bacterium isolated from the marine sponge, *Adocia* sp. *Fish. Sci.* **60**, 559-562.
117. Kobayashi, M., Aoki, S., Gato, K., Matsunami, K., Kurosu, M. & Kitagawa, I. (1994). Marine natural products .34. Trisindoline, a new antibiotic indole trimer, produced by a bacterium of *Vibrio* sp. separated from the marine sponge *Hyrtios altum*. *Chem. Pharm. Bull.* **42**, 2449-2451.
118. Cho, K.W. & Mo, S.J. (1999). Screening and characterization of eicosapentaenoic acid-producing marine bacteria. *Biotechnol. Lett.* **21**, 215-218.
119. Capon, R.J., Skene, C., Lacey, E., Gill, J.H., Wicker, J., Heiland, K. & Friedel, T. (2000). Lorneamides A and B: Two new aromatic amides from a southern Australian marine actinomycete. *J. Nat. Prod.* **63**, 1682-1683.
120. Barsby, T., Kelly, M.T., Gagne, S.M. & Andersen, R.J. (2001). Bogorol A produced in culture by a marine *Bacillus* sp. reveals a novel template for cationic peptide antibiotics. *Org. Lett.* **3**, 437-440.
121. Jaruchoktaweechai, C., Suwanborirux, K., Tanasupawatt, S., Kittakoop, P. & Menasveta, P. (2000). New macrolactins from a marine *Bacillus* sp. Sc026. *J. Nat. Prod.* **63**, 984-986.
122. Gustafson, K., Roman, M. & Fenical, W. (1989). The macrolactins, a novel class of antiviral and cytotoxic macrolides from a deep-sea marine bacterium. *J. Am. Chem. Soc.* **111**, 7519-7524.
123. Davidson, B.S. & Schumacher, R.W. (1993). Isolation and synthesis of caprolactins A and B, new caprolactams from a marine bacterium. *Tetrahedron* **49**, 6569-6574.
124. Trischman, J.A., Tapiolas, D.M., Jensen, P.R., Dwight, R., Fenical, W., McKee, T.C., Ireland, C.M., Stout, T.J. & Clardy, J. (1994). Salinamide-A and



- Salinamide-B - Anti-inflammatory depsipeptides from a marine streptomycete. *J. Am. Chem. Soc.* **116**, 757-758.
125. Moore, B.S., Trischman, J.A., Seng, D., Kho, D., Jensen, P.R. & Fenical, W. (1999). Salinamides, antiinflammatory depsipeptides from a marine streptomycete. *J. Org. Chem.* **64**, 1145-1150.
126. Renner, M.K., Shen, Y.C., Cheng, X.C., Jensen, P.R., Frankmoelle, W., Kauffman, C.A., Fenical, W., Lobkovsky, E. & Clardy, J. (1999). Cyclomarins A-C, new antiinflammatory cyclic peptides produced by a marine bacterium (*Streptomyces* sp.). *J. Am. Chem. Soc.* **121**, 11273-11276.
127. Jiang, Z.D., Jensen, P.R. & Fenical, W. (1999). Lobophorins A and B, new antiinflammatory macrolides produced by a tropical marine bacterium. *Bioorg. Med. Chem. Lett.* **9**, 2003-2006.
128. Izumida, H., Adachi, K., Mihara, A., Yasuzawa, T. & Sano, H. (1997). Hydroxyakalone, a novel xanthine oxidase inhibitor produced by a marine bacterium, *Agrobacterium aurantiacum*. *J. Antibiot.* **50**, 916-918.
129. Takaishi, S., Tuchiya, N., Sato, A., Negishi, T., Takamatsu, Y., Matsushita, Y., Watanabe, T., Iijima, Y., Haruyama, H., Kinoshita, T., Tanaka, M. & Kodama, K. (1998). B-90063, a novel endothelin converting enzyme inhibitor isolated from a new marine bacterium, *Blastobacter* sp. SANK 71894. *J. Antibiot.* **51**, 805-815.
130. Kobayashi, J., Mikami, S., Shigemori, H., Takao, T., Shimonishi, Y., Izuta, S. & Yoshida, S. (1995). Flavocristamides A and B, new DNA polymerase alpha inhibitors from a marine bacterium *Flavobacterium* sp. *Tetrahedron* **51**, 10487-10490.
131. Aoyama, T., Kojima, F., Imada, C., Muraoka, Y., Naganawa, H., Okami, Y., Takeuchi, T. & Aoyagi, T. (1995). Pyrostatins a and B, new inhibitors of N-acetyl-beta-D-glucosaminidase, produced by *Streptomyces* sp. Sa-3501. *J. Enzym. Inhib.* **8**, 223-232.
132. Kono, K., Tanaka, M., Mizuno, T., Kodama, K., Ogita, T. & Kohama, T. (2000). B-5354a, b and c, new sphingosine kinase inhibitors, produced by a marine bacterium; Taxonomy, fermentation, isolation, physico-chemical properties and structure determination. *J. Antibiot.* **53**, 753-758.
133. Kono, K., Tanaka, M., Ogita, T. & Kohama, T. (2000). Characterization of B-5354c, a new sphingosine kinase inhibitor, produced by a marine bacterium. *J. Antibiot.* **53**, 759-764.
134. Jensen, P.R., Kauffman, C.A. & Fenical, W. (1996). High recovery of culturable bacteria from the surfaces of marine algae. *Mar. Biol.* **126**, 1-7.

135. Harnden, M.R. (1985). *Approaches to antiviral agents. Distribution for USA and Canada* VCH Publishers, Deerfield Beach FL USA. xii, 326 pp.
136. Becker, Y. (1980). Antiviral agents from natural sources. *Pharmacol. Ther.* **10**, 119-59.
137. Gerzon, K., DeLong, D.C. & Cline, J.C. (1971). C-nucleosides: aspects of chemistry and mode of action. *Pure Appl. Chem.* **28**, 489-497.
138. Shannon, W.M. (1977). Selective inhibition of RNA tumor virus replication in vitro and evaluation of candidate antiviral agents in vivo. *Ann. N Y Acad. Sci.* **284**, 472-507.
139. Ishida, N., Homma, M., Kumagai, K., Shimizu, Y. & Matsumoto, S. (1967). Studies on the antiviral activity of formycin. *J. Antibiot.* **20**, 49-52.
140. Pugh, C.S., Borchardt, R.T. & Stone, H.O. (1978). Sinefungin, a potent inhibitor of virion mRNA(guanine-7-)-methyltransferase, mRNA(nucleoside-2')-methyltransferase, and viral multiplication. *J. Biol. Chem.* **253**, 4075-4077.
141. Subak-Sharpe, J.H., Timbury, M.C. & Williams, J.F. (1969). Rifampicin inhibits the growth of some mammalian viruses. *Nature* **222**, 341-345.
142. Lampis, G., Deidda, D., Maullu, C., Petruzzelli, S., Pompei, R., Dellemonache, F. & Satta, G. (1996). Karalicin, a new biologically active compound from *Pseudomonas fluorescens putida* .2. Biological properties. *J. Antibiot.* **49**, 263-266.
143. Matsuzaki, K., Ikeda, H., Masuma, R., Tanaka, H. & Omura, S. (1995). Isochromophilones I and II, novel inhibitors against GP120-CD4 binding produced by I FO-2338 .1. Screening, taxonomy, fermentation, isolation and biological activity. *J. Antibiot.* **48**, 703-707.
144. Tomassini, J.E., Davies, M.E., Hastings, J.C., Lingham, R., Mojena, M., Raghoobar, S.L., Singh, S.B., Tkacz, J.S. & Goetz, M.A. (1996). A novel antiviral agent which inhibits the endonuclease of influenza viruses. *Antimicrob. Agents Chemother.* **40**, 1189-1193.
145. Nishihara, Y., Tsujii, E., Yamagishi, Y., Sakamoto, K., Tsurumi, Y., Furukawa, S., Ohtsu, R., Kino, T., Hino, M., Yamashita, M. & Hashimoto, S. (2001). FR198248, a new anti-influenza agent isolated from *Aspergillus terreus* no. 13830 I. Taxonomy, fermentation, isolation, physico-chemical properties and biological activities. *J. Antibiot.* **54**, 136-143.
146. Gustafson, K.R., Li, R.C.S., Henderson, L.E., Li, J.H.C., McMahon, J.B., Rajamani, U., Pannell, L.K. & Boyd, M.R. (1997). Isolation, primary sequence determination, and disulfide bond structure of cyanovirin-N, an anti-HIV (Human

- Immunodeficiency Virus) protein from the cyanobacterium *Nostoc ellipsosporum*. **238**, 223-228.
147. Boyd, M.R., Gustafson, K.R., McMahon, J.B., Shoemaker, R.H., O'Keefe, B.R., Mori, T., Gulakowski, R.J., Wu, L., Rivera, M.I., Laurencot, C.M., Currens, M.J., Cardellina, J.H.I., Buckheit, R.W., Narra, P.L., Pannell, L.K., Sowder, R.C.I. & Henderson, L.E. (1997). Discovery of cyanovirin-N, a novel human immunodeficiency virus-inactivating protein that binds viral surface envelope glycoprotein gp120: Potential applications to microbicide development. *Antimicrob. Agents Chemother.* **41**, 1521-1530.
148. Chu, M., Mierzwa, R., Truumees, I., King, A., Patel, M., Pichardo, J., Hart, A., Dasmahapatra, B., Das, P.R. & Puar, M.S. (1996). SCH 65676 - a novel fungal metabolite with the inhibitory activity against the cytomegalovirus protease. *Tetrahedron Lett.* **37**, 3943-3946.
149. Chu, M., Mierzwa, R., Truumees, I., King, A., Patel, M., Berrie, R., Hart, A., Butkiewicz, N., Dasmahapatra, B., Chan, T.M. & Puar, M.S. (1996). Structure of SCH 68631 - a new hepatitis C virus proteinase inhibitor from *Streptomyces* sp. *Tetrahedron Lett.* **37**, 7229-7232.
150. Hennes, K.P., Suttle, C.A. & Chan, A.M. (1995). Fluorescently labeled virus probes show that natural virus populations can control the structure of marine microbial communities. *Appl. Environ. Microb.* **61**, 3623-3627.
151. Proctor, L.M. & Fuhrman, J.A. (1990). Viral mortality of marine bacteria and cyanobacteria. *Nature* **343**, 60-62.
152. Borsheim, K.Y. (1993). Native marine bacteriophages. *FEMS Microbiol. Ecol.* **102**, 141-159.
153. Thingstad, T.F., Heldal, M., Bratbak, G. & Dundas, I. (1993). Are viruses important partners in pelagic food webs. *Trend. Ecol. Evolut.* **8**, 209-213.
154. Hara, S., Koike, I., Terauchi, K., Kamiya, H. & Tanoue, E. (1996). Abundance of viruses in deep oceanic waters. *Mar. Ecol. Progr. Ser.* **145**, 269-277.
155. Suttle, C.A. & Feng, C. (1992). Mechanisms and rates of decay of marine viruses in seawater. *Appl. Environ. Microbiol.* **58**, 3721-3729.
156. Girones, R., Jofre, J. & Bosch, A. (1989). Natural inactivation of enteric viruses in seawater. *J. Environ. Qual.* **18**, 34-39.
157. Kamei, Y., Yoshimizu, M., Ezura, Y. & Kimura, T. (1987). Screening of bacteria with antiviral activity against infectious hematopoietic necrosis virus HNV from estuarine and marine environments. *Nip. Suis. Gakk.* **53**, 2179-2186.

158. Kimura, T., Yoshimizu, M., Ezura, Y. & Kamei, Y. (1990). An antiviral agent (46NW-04A) produced by *Pseudomonas* sp. and its activity against fish viruses. *J. Aquat. Anim. Health* **2**, 12-20.

159. Myouga, H., Yoshimizu, M., Tajima, K. & Ezura, Y. (1995). Purification of an antiviral substance produced by *Alteromonas* sp. and its virucidal activity against fish viruses. *Fish Path.* **30**, 15-22.

### **Chapter 3. Discovery of Crude Extracts Produced by Marine Microorganisms Active Against the Herpes Simplex Virus-1**

This chapter describes a program designed to explore marine microorganisms as a resource for the discovery of antiviral agents. The herpes simplex virus was selected as the biomedical target for this experiment due to the genuine need for new therapeutics needed to treat infections of this human pathogen. HSV was an also an appropriate choice because a high-throughput, cell based assay could be developed to for the rapid screening of several thousand extracts. The extracts evaluated in this study were generated through the laboratory culture of bacteria and fungi collected throughout the world's oceans. In all, approximately 7000 crude extracts were assayed for anti-HSV metabolites, and the hit rate was around 1%. Advanced fermentation and chemistry studies were pursued on the most promising of the active extracts, and one series of antiviral agents were identified as novel inhibitors of this viral pathogen. Presented in this first part of this chapter is a short background on the herpes simplex viruses and the current methods used to treat these infections. Part two of this chapter discusses the strategies and methods I used to identify anti-HSV activity and the results of this investigation.

The interdisciplinary nature of this endeavor necessitated my collaboration with many of the accomplished scientists in the Fenical laboratory. Paul Jensen, Chris Kauffman, and Sy Teisan were instrumental in all matters concerning the isolation and fermentation of marine microorganisms. Sara Kelley took over the operation of the HSV assay in order to allow me to focus on pursuing the bioactive leads. Without the

collaboration of these and other scientists in the Fenical lab, this project would not have been possible.

### **3.1 The Herpes Simplex Virus**

The herpes simplex virus-1 (HSV-1) was selected as the primary target in this program for three reasons: (1) HSV-1 is an important biomedical target for which new clinical treatments possessing novel modes of action are needed, (2) a reasonably high-throughput, infectious virus assay involving a mammalian cell line could be developed for the screening of crude microbial extracts, and (3) the handling of infectious HSV-1 requires a Biosafety Level 2 facility that exists in the Fenical laboratory.

#### **3.1.1 Biological Background**

The family Herpesviridae includes nearly 100 herpesviruses that are distributed throughout nature. Most animal species have yielded at least one herpesvirus and eight so far have been isolated from humans. These include the herpes simplex virus-1 (HSV-1), herpes simplex virus-2 (HSV-2), human cytomegalovirus (HCMV), varicella-zoster virus (VZV), Epstein-Barr virus (EBV), and the human herpesviruses 6-8 (HHV6, HHV7, and HHV8).<sup>1</sup> HHV8 has been implicated as the causative agent of Kaposi's sarcoma, a skin cancer commonly associated with AIDS.<sup>2</sup> HSV-1, HSV-2, VZV, and HHV8 are members of the subfamily alphaherpesvirinae on the basis of variable host range, relatively short reproduction cycle, efficient destruction of infected cells, rapid spread in cell culture, and the ability to maintain a latent infection

in sensory ganglia. HSV-1 and HSV-2 are further taxonomically grouped in the genera *Simplexvirus*.<sup>1</sup>

Herpes simplex viruses are well known for their ability to cause a wide variety of infections, to remain latent in their host for life, and to reactivate and cause lesions at or near the initial site of infection.<sup>3</sup> Typical infections include those of oral and genital mucosal tissues, eyes (keratitis), and central nervous system (encephalitis and meningitis). The latter are rare but life-threatening infections, even in immunocompetent hosts. Incidence of HSV-2, the serotype most commonly correlated with genital infection, has risen by 30% in the United States since the late 1970s, and now infects one in five Americans above the age of twelve.<sup>4</sup> Now, the incidence of HSV-1 associated genital herpes is increasing worldwide.<sup>5,6</sup> Herpes lesions aid in the sexual transmission of other diseases such as HIV.

There is an immediate need for new antiviral drugs to combat HSV in immunocompromised hosts, especially those suffering from AIDS. With the body's immune capabilities collapsing, HSV infections reactivate with serious consequences. The lesions are broader and deeper, and increase the victims vulnerability to bacterial and fungal superinfections. HSV infections persisting for longer than one month are an AIDS defining illness.<sup>7</sup>

An aspect of great concern in current HSV chemotherapy is that drug resistant strains are emerging.<sup>8</sup> During viral replication in immunocompromised patients undergoing long term antiviral chemotherapy, strains have evolved that contain genetic mutations making them impervious to current drugs. These emergent strains have caused progressive disease in immunocompromised patients. Only time will tell

if more virulent and drug-resistant strains will emerge. Obviously, new HSV antivirals with novel modes of action are already needed.

### **3.1.2 Replication of HSV-1**

The life cycle of the herpes simplex virus involves periods of latent infection in neuronal cells and recurrent outbreaks of infection involving epithelial cells. The molecular mechanisms involved in reactivation of latent virus are poorly understood. However, reactivation generally occurs in response to local stimuli such as injury to tissue innervated by neurons harboring latent virus, or in response to systemic stimuli such as emotional or physical stress.<sup>3</sup> Both the body's immune defenses and our current methods of antiviral chemotherapy are incapable of eradicating latent virus. Therefore, herpes simplex virus infections are life long.

Transmission of HSV-1 and HSV-2 occur via direct skin-to-skin contact, and especially those involving mucous membranes when HSV lesions are present. However, transmission can also happen when lesions are absent, such as in the case of asymptomatic shedding.<sup>9</sup> Studies have indicated that sexual transmission of HSV-2 generally occurs when the infected individual is unaware of any lesions present.<sup>10,11</sup>

The infectious HSV virion itself is composed of four elements including (1) an electron opaque core, (2) an icosahedral capsid surrounding the core, (3) an amorphous tegument surrounding the capsid, and (4) a lipid envelope. The envelope is likely acquired from the cytoplasmic membrane of the host cell.<sup>3</sup> The HSV genome is linear, double stranded DNA of approximately 150 kbp. There are 30+ gene products, at least 9 of which are eventually located on the virion outer envelope.<sup>3</sup>

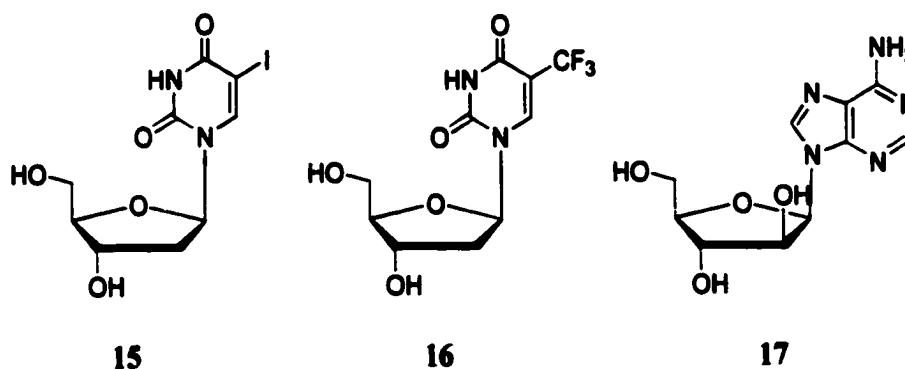


The herpes simplex infection process begins with the attachment of the virus to cell surface receptors. Several viral glycoproteins are likely to be involved. Since HSV must infect at least two very different cell types during its life history, epithelial cells and neurons, it likely has evolved multiple attachment pathways.<sup>3</sup> Therefore, drugs designed to bind to a specific HSV receptor are unlikely to be effective in preventing infection. For instance, Spear and coworkers identified heparin sulfate as an important factor in HSV attachment.<sup>12,13</sup> Cells deficient in heparin sulfate show reduced levels of viral infection, and heparin itself is a potent inhibitor of viral attachment. However, neither the absence of heparin sulfate on a cell surface nor competition by heparin can fully prevent HSV infection. One explanation is that alternate mechanisms of HSV attachment exist.

After attachment, fusion of the viral envelope with the plasma membrane follows, releasing the capsid into the cell. The capsid is transported to the nuclear pores where the viral DNA is released into the nucleus. The DNA circularizes immediately upon entry of the cell nucleus. Tightly regulated transcription of viral DNA in the nucleus is performed by host cell RNA polymerase II, but is mediated by viral factors. There are at least five groups of products sequentially formed during gene expression, including DNA-binding proteins and enzymes involved in DNA replication. The viral DNA is packaged into pre-assembled capsids that then bud out from the nuclear membrane. The entire replication cycle occurs in approximately 18 to 20 hours.<sup>3</sup>

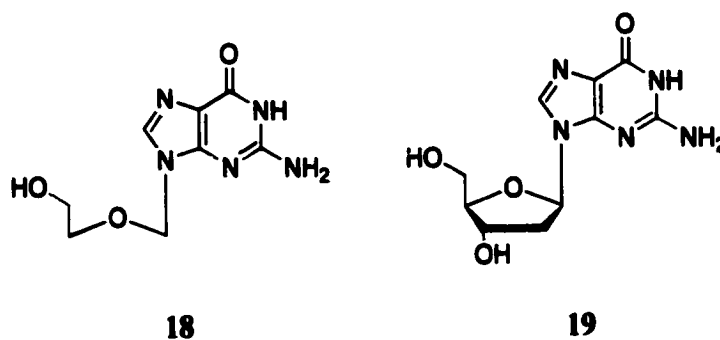
### 3.1.3 Clinically Used Antiviral Agents Against HSV Infections

In the early 1960s, several pyrimidine nucleosides were under investigation for their inhibitory properties against the herpes simplex virus-1. Two of these included 5-iodo-2'-deoxyuridine (IDU, **15**) and 5-trifluoromethyl-2'-deoxyuridine (TFT, **16**) that were later approved for the topical treatment of HSV keratitis. Unfortunately, toxicity issues prevented systemic applications. The first purine nucleoside that was discovered to have beneficial antiviral activity was arabinosyl adenine (Ara-A, **17**) in the mid-sixties. This compound could be used intravenously but lacked a large therapeutic index.<sup>14</sup> The identification of these antiviral agents set the stage for the synthetic effort that led to the discovery of acyclovir.



The development of acyclovir (**18**) was a breakthrough in the clinical management of herpesvirus infections, and clearly represented a milestone achievement in the development of safe and effective antiviral chemotherapies. Initially launched in the United Kingdom in 1981 as an eye ointment, it has since been formulated as tablets, creams, and intravenous preparations. Acyclovir, or ACV, is an

acyclic congener of guanosine deoxyriboside (19), a natural component of DNA. ACV lacks the 2'- and 3'-carbons and 3'-hydroxyl group of the deoxyribose ring in the natural substrate. ACV thus acts as a chain terminating agent during DNA polymerization. What is astonishing about acyclovir is its selectivity for inhibiting the viral DNA polymerase versus cellular homologs. Since viruses replicate inside of cells, molecules that inhibit replication of viral genes can also disrupt normal cellular DNA polymerization leading to toxicity problems. Remarkably, however, ACV is selectively monophosphorylated by the herpes virus-encoded thymidine kinase (TK), whereas cellular thymidine kinases do not recognize ACV as a substrate.<sup>14</sup> Conversion to the acyclovir diphosphate analog is accomplished by the cell enzyme guanylate kinase, and the final phosphorylation can be completed by a number of other cellular enzymes. The triphosphate derivative is the active antiviral agent.

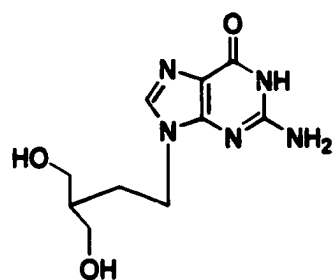


In *in vitro* tests, ACV (18) inhibits 50% of HSV-1 viral replication ( $IC_{50}$ ) at a concentration of 0.1  $\mu$ M. It is less active against HSV-2 ( $IC_{50} = 2 \mu$ M), the varicella-zoster virus ( $IC_{50} = 4 \mu$ M), and the human cytomegalovirus ( $IC_{50} = 100 \mu$ M).<sup>14</sup> When the cytotoxicity is measured against mammalian cells, ACV has an  $IC_{50}$  of

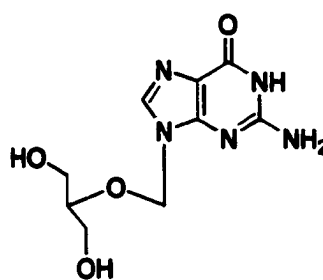
approximately 300  $\mu\text{M}$ , or a therapeutic index of around 3000.<sup>14</sup> This is the primary reason why acyclovir has proven to be such a safe medication.

As mentioned earlier, viral resistance to acyclovir has become an increasing problem in immunocompromised hosts. The mechanisms of resistance can be traced back to mutations in either the virus-encoded thymidine kinase or DNA polymerase enzymes.<sup>15-17</sup> Fortunately, most of these clinical mutants are less virulent and do not pose health risks to healthy individuals. One can only speculate as to whether this will continue to be the case. However, new drugs will need to be discovered if we are committed to ensuring effective antiviral medications for our immunocompromised population.

Other anti-herpes drugs have been developed since the discovery of acyclovir, most of which are also nucleoside-based molecules with similar modes of action. Penciclovir (PCV, **20**) is an acyclic guanosine analog with much the same biological properties as ACV. Oral ganciclovir (**21**) is the preferred clinical treatment of human cytomegalovirus infections in immunocompromised patients. Ganciclovir is 25-100 fold more active *in vitro* than acyclovir against HCMV due to a higher intracellular concentration of the triphosphate derivative in infected cells.<sup>18</sup> Unfortunately, neutropenia, a reduction in neutrophils leading to a decrease in host defense against infectious disease, is an important dose-limiting, adverse side effect in humans.<sup>19</sup>

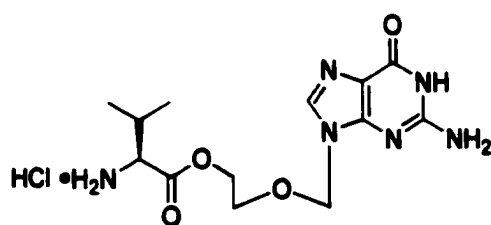


20

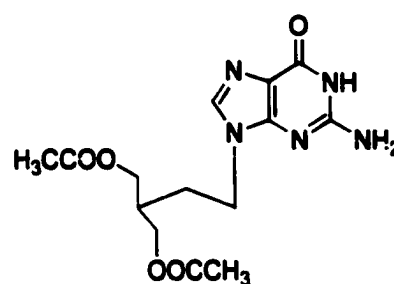


21

Valacyclovir (22) and famciclovir (23) were developed as prodrugs of ACV and PCV, respectively, because of their superior oral bioavailability. Valacyclovir, the L-valyl ester of acyclovir, is better absorbed through the gut wall and then is rapidly hydrolyzed by enzymes in the liver and intestinal wall to ACV and L-valine. The bioavailability of ACV after oral administration of valacyclovir is increased 25-40%.<sup>20</sup>



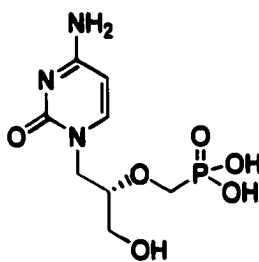
22



23

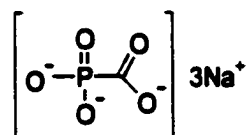
Famciclovir is the diacetyl ester prodrug of penciclovir. It is also better absorbed in the upper intestine and then undergoes metabolism in the intestinal wall and liver to the active component.<sup>21</sup>

Cidofovir (**24**) is a phosphonate nucleoside derivative with broad spectrum activity against HSV-1, HSV-2, VZV, CMV, EBV, and human papillomaviruses. Phosphonates involve a carbon-phosphorous bond rather than the C-O-P linkage found in nucleoside monophosphates that provides an enzymatically stable monophosphate derivative.<sup>22</sup> Because it does not require conversion by the viral thymidine kinase to the monophosphate, cidofovir is active against ACV resistant strains arising from TK mutations. Cellular enzymes phosphorylate cidofovir to the mono- and diphosphate metabolites, and the active diphosphate derivative selectively interacts with the DNA polymerase. Incorporation of two molecules of CDV separated by less than two nucleotides in the elongating DNA results in complete chain termination.<sup>22</sup> Cidofovir is currently limited to intravenous administration.

**24**

Foscarnet (**25**) interferes with viral DNA polymerization by preventing cleavage of the pyrophosphates from the deoxynucleotide triphosphates. As a direct inhibitor of the DNA polymerase, it also finds clinical use for the treatment of herpesvirus infections that are acyclovir resistant. However, foscarnet is poorly

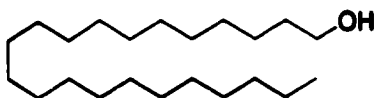
absorbed by oral administration, and a major side effect is irreversible nephrotoxicity.<sup>23</sup>



25

*n*-Docosanol (26) is formulated as a 10% cream for the topical treatment of herpes simplex infections. The 22-carbon, saturated fatty alcohol also exerts an antiviral effect against a wide range of other lipid-enveloped viruses including influenza A, respiratory syncytial virus, cytomegalovirus, varicella-zoster virus, and HIV. The *in vitro* antiviral IC<sub>50</sub> values against these viruses range from a very modest 3 to 12 mM. However, a favorable therapeutic index exists for the drug since concentrations as high as 300 mM are not cytotoxic.<sup>24</sup> *n*-Docosanol does not directly inactivate the herpes simplex virus because pre-incubation of the virus with the compound does not reduce infectivity. Further, attachment of radiolabeled virions to cell surfaces is not affected, indicating that *n*-docosanol does not specifically or sterically block HSV binding receptors.<sup>25</sup> Evidence instead supports that the drug blocks the biophysical process of viral/cell fusion.<sup>24</sup> The optimal antiviral effect of *n*-docosanol is achieved in cells pre-exposed to drug prior to viral infection,<sup>25</sup> and the activity may in part be due to metabolic products formed from the fatty alcohol and retained in the cell membrane.<sup>24</sup> The half-life of *n*-docosanol is around three hours,

but since it is formulated as a cream for topical treatments, a constant reservoir remains at the site of the infection.



26

Our current ability to treat herpesvirus infections finds limitation in that all of the systemically used drugs ultimately target the viral DNA polymerase. It is conceivable that mutation of the viral DNA polymerase might result in a replication competent virus resistant to all current herpes drugs. With the exception of cidofovir, all of the nucleoside drugs require activation by the viral thymidine kinase, and TK mutations that confer resistance to one nucleoside generally confer resistance to others as well. A lesson learned from the treatment of HIV infections is that multi-drug chemotherapies are more effective methods to treat viral infections. Hence, new drugs with novel modes of action are highly desirable for the management of HSV.

## **3.2 Screening Program for Identification of Antiviral Agents Against HSV-1**

### **3.2.1 Choice of Assay Design**

The replication cycles of most viruses involve reactions catalyzed by both cellular and virus-encoded enzymes. The later represent attractive targets for drug development since their structures and functions are likely to be very different than those of normal cellular enzymes. Therefore, biochemical assays targeting virus



specific enzymes are attractive screening tools. Indeed, many programs have successfully involved such strategies, including the work presented in chapters 6 and 7 of this thesis. However, enzyme-based screening methods have several drawbacks. First, they reduce the chances of success by targeting only one of many possible mechanisms in the viral replication cycle. Also, compounds that require metabolic activation would not be detected (i.e. acyclovir). Once enzyme inhibitors are identified, there are no guarantees that the inhibitory compounds will adequately penetrate cell membranes to provide antiviral effects. Lastly, a number of additional enzyme assays must be employed to ensure that the molecule in question is a selective inhibitor of the viral process.

Cell-based assays are an alternative to biochemical methods. These techniques involve infection of living cells with virus and then probe for the ability of test compounds to inhibit viral cytopathic effects. A typical endpoint of an assay is the measurement of cell survival versus a control using metabolic indicators or the enumeration of viral plaques on a lawn of cells.<sup>26</sup> Alternatively, ELISA methods that detect the production of viral proteins expressed on cell surfaces can be employed. Regardless, these methods simultaneously screen against many possible mechanisms of action, and give a better probability of *in vivo* activity since cell penetration issues are concurrently addressed. Of course, drawbacks still exist with these methods. The presence of cytotoxic components in crude extracts or semi-purified fractions can mask the presence of selective antiviral compounds. Also, the observed antiviral effects can be due to inhibition of a process common to both viral replication and host

cell metabolism. Lastly, once an antiviral agent has been discovered, mechanism of action studies must be initiated to determine the exact nature of the inhibitory process.

After careful consideration, a cell-based assay was selected for this investigation in order to maximize the potential for identifying novel antiviral agents. The criteria for choosing the assay format included that (1) it must allow for relatively high-throughput evaluation of a large number of samples, and (2) the estimation of antiviral activity must be quantitative. An assay employing Vero cells, African Green Monkey kidney cells, and infectious HSV-1 (Schooler strain) was adopted. The assay strategy involved growing the cells in 96-well microtiter plates, infecting the cells with virus, and then adding test compounds to probe for antiviral effects. After five days incubation, a simple work-up involved the addition of a metabolic indicator followed by quantitative colorimetric endpoint analysis using an ELISA plate reader. To institute the assay, several hundred stock vials containing the herpes simplex virus-1 at known viral titers had to be produced, a Vero cell line needed to be established and maintained, and a strategy for screening crude extracts had to be implemented. The remainder of this chapter is devoted to describing the nature of this assay and the results obtained from the screening of nearly 7000 marine microbial extracts.

### **3.2.2 Production and Titer of Viral Stocks**

The strain of herpes simplex virus-1 used in this program was graciously provided by Bristol-Myers Squibb and was described as the Schooler strain. During a one day visit to the Virology Department of Bristol-Myers Squibb in Waterbury, Connecticut in 1996, I received expert advice from Stephanie Danetz, a technician, on

the production and titer determination of HSV stocks. Based upon this information, viral stocks were prepared for the *in vitro* assays as follows:

1. Vero cells were grown to confluency over five days in four T150 tissue culture flasks.
2. The media in these flasks was removed and 10 mL of a viral inoculant was introduced at an approximate multiplicity of infection, or MOI, of 0.01. The inoculant was prepared by dilution of BMS viral stock ( $2.4 \times 10^8$  pfu/mL) in MEM containing 1% Pen/Strep and 1% glutamine to achieve a final viral titer of  $1.5 \times 10^4$  pfu/mL. The amount of cells in a confluent T150 flask was estimated to be  $1.5 \times 10^7$  cells (personal communication from Stephanie Danetz, BMS).
3. The cells were incubated for one hour at 37 °C and 5% CO<sub>2</sub>.
4. The inoculum was removed and 30 mL of MEM containing 1% FBS was added. The flasks were then incubated for five days.
5. The infected cells slide easily from the sides of the tissue culture bottles. The media from each flask was transferred to 50 mL sterile centrifuge tubes and sonicated for 30 seconds in an ice water bath. The cell debris was then pelleted by centrifugation at 1500 rpm for 10 minutes.
6. Aliquots of ~1 mL were pipetted into cryovials and stored at -80 °C.

The viral titer is defined as the number of infectious viruses per given volume of liquid and is expressed in the units pfu/mL, where pfu stands for plaque forming units. Determination of this value is critical for delivering a discrete number of infectious viral units to an assay. By also controlling the number of cells in an assay,

the multiplicity of infection, or MOI, is determined. The viral titer of the stock solutions was determined in a plaque assay as follows:

1. Two milliliters of a Vero cell suspension, at a concentration of  $2 \times 10^4$  cells/mL in 2% MEM, was seeded into six-well tissue culture plates. The cells were incubated overnight at 37 °C and 5% CO<sub>2</sub>.
2. The media was aspirated from each well, and the cell monolayers were washed with PBS.
3. Viral solutions had been prepared in advance. The viral stock (0.2 mL) was diluted into 1.8 mL of 0% MEM and vortexed for 30 seconds. This viral suspension (0.2 mL) was then further diluted into 1.8 mL of 0% MEM and vortexed. This dilution scheme was continued nine times. The dilutions were kept in ice water baths until used.
4. In triplicate, cell monolayers were treated with 0.5 mL of each viral dilution. The plates were swiveled to completely cover the monolayers with inoculum, and then placed in an incubator for one hour.
5. The viral media was aspirated. An agar overlay, prepared ahead of time and stored at 45°C (see below), was allowed to cool slightly, and then two milliliters was added to each well. The agar was allowed to gently run down the sides of the wells in order not to harm the cells. The plates were inverted and incubated for 2 days.
6. The agar overlay was then gently flipped out of each well with a spatula and the monolayers were stained with 2 mL of crystal violet. After 15 minutes, the stain

was removed, the wells rinsed with cold water, and the plates let stand to air dry.

Plaques were counted as clear zones in a blue field.

The agar overlay was composed of the following: 8.5 mL water, 2.5 mL 2X MEM, 0.5 mL 1% DEAE dextran, 15 mL 2% agar, and 1 mL 5% NaHCO<sub>3</sub>. Everything was combined and stored at 45 °C in preparation of the assay. The agar was prepared by combining 10g oxoid agar with 500 mL H<sub>2</sub>O and autoclaving. The 2X MEM was composed of the following: 100 mL 10X MEM, 340 mL H<sub>2</sub>O, 6 mL 35% BSA, 10 mL glutamine, 10 mL 1M HEPES, 10 mL of penicillin/streptomycin, 24 mL 5% NaHCO<sub>3</sub>. The 1% DEAE dextran was prepared by dissolving one gram of DEAE in 100 mL of H<sub>2</sub>O, autoclaving, and stored at 4 °C. The crystal violet solution was prepared by combining 40 mL of 1% crystal violet with 50 mL of methanol and 150 mL of deionized water.

The 10<sup>-3</sup> viral dilution produced too many plaques to accurately count. The 10<sup>-4</sup> viral dilution produced counts of 63, 59, and 57 plaques per well, and the 10<sup>-5</sup> dilution had counts of 4, 4, and 1. The viral titer can then be calculated using the following equation:

$$\text{Titer} = (\text{average \# of plaques}) \times (\text{reciprocal of the dilution}) \times (\text{reciprocal of the inoculant volume in mL})$$

Based on the results from the 10,000-fold dilution, the titer of the viral stock solution is then calculated as:

$$\text{Titer} = 60. \text{ pfu} \times 10^5 \times 2.0 \text{ mL}^{-1} = 1.2 \times 10^6 \text{ pfu/mL}$$

The plaque assay was carried out twice and the average of the two results, 1.36 x 10<sup>6</sup> pfu/mL, was taken as the final viral titer of the HSV-1 stock solutions.

### **3.2.3 Standard Assay Protocol for Screening Extract Library**

The *in vitro* antiviral activities of extracts and pure compounds were assessed in a live cell assay using infectious HSV-1. Vero cells were dispensed in 96-well plates at a concentration of 10,000 cells/well in 100  $\mu$ L of minimum essential medium (MEM) containing 5% fetal bovine serum (FBS). The cells were incubated overnight at 37 °C under 5% CO<sub>2</sub>. The media was removed by aspiration, and 100  $\mu$ L of phosphate buffered saline (PBS) was added to each well and then aspirated. The wells were treated with 100  $\mu$ L of MEM containing 50 plaque forming units (pfu) of virus and incubated for one hour (MOI = 0.005). Each well was then overlaid with 100  $\mu$ L of media containing 2% FBS and serial dilutions of the halovirs (the compounds had been first dissolved in DMSO before dilution in the media). After incubation for five days, each well was treated with 20  $\mu$ L of a solution comprising 10 mg/mL of MTS in phosphate buffered saline (PBS). The plates were incubated for four hours during which time viable cells metabolize the MTS to a soluble blue formazan. The amount of formazan produced is directly proportional to the amount of surviving cells. The optical density of the wells at 490 nm was then assessed using an ELISA plate reader. The plate reader was linked with a computer outfitted with the Softmax© software for data manipulation.

MTS, also known as Owen's reagent, is an aqueous soluble indicator of metabolic activity. When combined with a solution of phenazine methosulfate, an electron coupling reagent, the tetrazolium salt is bio-reduced by live cells to a formazan that is also soluble in tissue culture media.<sup>27,28</sup>

A variation of this method substitutes MTT for MTS as the colorimetric indicator to determine the extent of cell survival. An assay using MTT results in the production of an insoluble formazan salt and requires additional steps in the final work-up procedure.<sup>29</sup> After incubating the plates for four hours in the presence of MTT, the media must be carefully aspirated, and then 100  $\mu$ L of acidified isopropanol is added to dissolve any formazan produced. The acidified isopropanol solution is prepared by adding 50 mL Triton X100 and 2 mL concentrated HCL to 450 mL isopropanol. The danger of this method lies in the aspiration of the media prior to adding the acidified isopropanol. It is possible to inadvertently suction away small amounts of formazan salt and thereby compromise the accuracy of the assay. For this reason, the MTT method used in the early stages of this program was replaced by one using MTS.

Two controls, four wells each, were included on each assay plate in order to calculate the antiviral effects of test compounds. A positive growth control (PG) contained non-infected Vero cells grown in the presence of 0.2% DMSO. A viral death control (VD) contained cells infected with HSV-1 and grown in the presence of 0.2% DMSO. The DMSO content reflects the maximum amount present in wells treated with a compound or extract. Also, an acyclovir control was used to verify the consistency of the assay. ACV was serially diluted and an  $IC_{50}$  was determined for each assay plate.

The antiviral effect of a test compound or extract can then be calculated as a percent survival using the following formula:

$$\% \text{ Survival} = \frac{(PG - OD_{\text{test}})}{(PG - VD)}$$

where,

**PG** = the average OD of four wells containing non-infected cells,

**OD<sub>test</sub>** = the OD of a well containing HSV-1 infected cells treated with a compound or extract,

and **VD** = the average OD of four wells containing cells infected with HSV-1.

### **3.2.4 Strategy for the Discovery of Antivirals**

The strategy for discovering novel anti-HSV agents produced via saline fermentation of marine microorganisms was as follows:

1. Screen as many microbial extracts as possible at a single concentration.
2. Confirm the activity of all “hits” in a second assay with the extracts in serially dilution.
3. Repeat one-liter fermentations of the most promising hits, and then re-confirm activity.
4. Pursue bioassay-guided fractionations of active one-liter extracts.

Approximately 7000 crude extracts generated from the saline fermentation of marine microorganisms were assayed for anti-HSV activity. These extracts were primarily accessed from the library that exists and continues to expand within the Fenical laboratory (see section 3.2.7). The crude microbial extracts within this library are stored in DMSO at a concentration of 25 mg/mL in deep 96-well plates, a format conducive to a rapid screening process. In preparation of an assay, the extracts are



first diluted in MEM containing 2% FBS, and then delivered to the assay to produce a final reaction concentration of 25 µg/mL extract and 0.2% DMSO. This percentage of DMSO is well tolerated by the Vero cells during a five-day assay, but even slightly higher concentrations begin to create cell toxicity problems. Testing each extract once at a single concentration allowed for the greatest number samples to be evaluated.

### 3.2.5 Screening Results

As an initial screen to assess the potential for success in this endeavor, nearly nine hundred marine microbial extracts were evaluated for antiviral activity against HSV-1. Table 3 details the results from this primary screening effort. "Actives" were defined as extracts which reduced cell mortality due to viral infection by greater than 40% at concentrations ranging from 5-20 µg/mL.

Table 3. Initial Screening Results for Crude Extract Antiviral Activities Versus HSV-1

<u>Extract type</u>	<u># Screened</u>	<u># HSV-1 Active</u>	<u>Percentage</u>
fungal broth	435	8	1.8%
fungal mycelia	123	7	5.7%
actinomycete	93	2	2.2%
bacteria	240	4	1.7%
total	891	21	2.4%

Fungal mycelia were identified as having the highest percentage of actives. The most promising of these extracts was generated from the mycelium of fungal strain CNL240. A series of lipophilic, linear peptides was subsequently isolated from a large-scale fermentation of this fungus. A detailed description of this project is the subject of the following chapter.

Since the preliminary screening showed promise, a larger scale screening of marine microbial extracts was undertaken. In this second phase, a total of 6160 extracts were evaluated for inhibition against HSV-1, bringing the total number of extracts studied in this investigation to over 7000. Criteria were established in order to select a manageable number of the most promising for further evaluation. Extracts that produced an inhibitory effect registering in excess of 70% cell survival at the initial test concentration of 25 µg/mL were advanced for retesting to confirm activity. Retests were carried out in 2-fold serial dilutions with a concentration range of 0.78-100 µg/mL. The IC<sub>50</sub>'s and maximum percent cell survival were recorded for each retest to prioritize further advancement. In addition, extracts that provided a cell protective effect of greater than 70% at multiple concentrations were considered most favorably.

Of these 6160 extracts, 261 demonstrated a protective effect of greater than 70% and thus met the first pass criteria to be further evaluated. This represents an initial "hit rate" of four percent. During retesting of these active extracts in serial dilutions, 62 confirmed the initial activity. IC<sub>50</sub> values for these actives ranged from 3-39 µg/mL. The second-pass hit rate was therefore 1%. Based primarily upon potency, 51 of these actives were re-fermented in one-liter scale. Of these "regrows", only eleven (21%) reproduced the initial activity and were further evaluated in chemical studies. Table 4 summarizes the activities for the extracts that were pursued through additional fermentations.

Table 4. Crude Marine Microbial Extracts Exhibiting Anti-HSV Activity.

Extract (Strain + Culture Medium)	Initial screen (% survival)	Retest IC <sub>50</sub> (µg/mL)	Retest % Survival	Regrow Activity IC <sub>50</sub> (%Survival)
CNC798 YPM/ST	74	3	68	2.5 (88%)
CNK113 CK1/SH	78	28	112	NSA
CNK119 M1/ST	89	21	69	NSA
CNK126 M1/ST	96	24	64	4 (82%)
CNK145 CK1/SH	130	34	127	2.5 (51%)
CNK196 CK1/SH	76	17	68	86 (73%)
CNK395 CK1/SH	76	20	98	4.9 (74%)
CNK398 YPMBFe/SH	78	6	100	1.5 (90%)
CNK408 CK1/SH	87	20	91	NSA
CNK427 CK1/ST	77	4	88	NSA
CNK445 MAR2/SH	82	27	80	NSA
CNL 010 YPM/SH	84	20	110	NSA
CNL367 CK1/SH	88	36	109	NSA
CNL417CK1/SH	185	18	134	NSA
CNL820 YPM/ST	98	27	94	20 (82%)
CNL940 YPM/SH	88	20	65	NSA
CNL943 CK1/SH	92	24	68	NSA
CNL962 CK1/SH	96	22	56	NSA
CNL966 CK1/SH	103	26	93	NSA
CNL988 CK1/SH	70	31	86	NSA
CNM545 CK1/SH	101	23	133	NSA
CNM546 YPMBFe/ST	99	23	103	NSA
CNM552 YPM/SH	79	39	81	NSA
CNM557 YPM/SH	76	23	73	NSA
CNM562 YPMBFe	86	22	63	NSA
CNM566 M1/SH	84	23	68	NSA
CNM687 M1/ST	71	12	73	NSA
CNM707 CK1/SH	70	9	86	NSA
CNM748 YPM/ST	79	24	78	NSA
CNM749 YPM/ST	107	27	132	NSA
CNM760 M1/SH	92	22	79	NSA
CNM777 M1/ST	83	6	76	22 (68%)
CNM778 M1/ST	78	21	61	NSA
CNM784 CK1/SH	82	24	68	NSA
CNM785 YPM/SH	81	12	79	42 (106%)
CNM790 YPMBFe/SH	76	16	63	NSA
CNM806 M1/ST	94	29	67	NSA
CNM808 CK1/SH	70	20	91	NSA
CNM831 YPMBFe/SH	81	11	63	NSA
CNM832 M1/ST	79	24	71	NSA
CNM869 YPM/ST	92	25	74	NSA
CNM879 YPMBFe/ST	79	34	78	4.9 (72%)
CNM881 YPMBFe/SH	86	18	108	NSA
CNM884 YPM/ST	158	5	122	NSA
CNM891 M1/ST	70	21	81	NSA
CNM892 CK1/SH	72	12	76	NSA
CNM893 CK1/SH	75	19	73	NSA
CNM895 M1/ST	71	21	73	NSA
CNM905 M1/ST	84	22	70	6 (85%)
CNM911 M1/ST	71	21	82	7 (83%)
CNM913 M1/ST	82	24	70	NSA

NSA = No Significant Activity

### **3.2.6 Description of Extracts Used in this Study**

The 240 bacterial extracts evaluated in the initial screening effort were generated with the assistance of Daniel Thomassen, an undergraduate researcher who worked several months under my guidance. Bacteria isolates were removed from cryogenic storage and added to 100 mL of sterile marine media. Cultures were shaken at ~ 250 rpm for one week and then extracted with 150 mL of EtOAc. The organic layers were dried over MgSO<sub>4</sub> or Na<sub>2</sub>SO<sub>4</sub>, filtered, and concentrated *in vacuo*. Each isolate was grown in two different media that were selected with the help of Paul Jensen, an expert in the fermentation of marine microorganisms.

An expert fermentation team comprising Paul Jensen, Christopher Kauffman, and Sy Teisan prepared all the fungal extracts. Fungi were typically grown in 100 mL scale using multiple different fermentation conditions and extracted whole with ethyl acetate. Both static (ST) and shake (SH) methods were employed.

### **3.2.7 Summary and Discussion**

Presented in this chapter is a cell-based assay established to investigate the production of antiviral metabolites produced by marine microorganisms. Specifically, this assay assessed the ability of crude extract components to ameliorate the infection of HSV-1 in Vero cells. A microtiter plate format and an automated, quantitative colorimetric endpoint analysis allowed for high-throughput of samples. In total, 7051 crude extracts were evaluated for anti-HSV activity. The hit rate for extracts demonstrating better than 70% cell protection at 25 µg/mL was approximately 4%

(from 6160 samples). Retesting of the active extracts identified 62 with significant activity (1%).

The low hit rate encountered in this study is perhaps not surprising. Relative to the discovery of antibiotics and cytotoxic agents, selective antiviral compounds are more rarely encountered. This is primarily due to the fact that many viral replication processes are related to events in normal cellular metabolism. It must also be considered that many extracts produced by marine microorganisms display cell toxicity effects. The identical extracts tested in the second phase of this investigation were also evaluated in a human colon tumor cell (HCT-116) model. In this assay, approximately 3-5% of the extracts caused at least 50% cell death at 25  $\mu\text{g/mL}$ . Although Vero cells and HCT cells likely have different sensitivities to cytotoxic agents, it would be reasonable to expect that around this percentage of extracts would be eliminated from consideration.

The low rate of reproducibility for the antiviral activities in the secondary fermentations is a troubling matter, but one that is addressable through further investigation. The production of secondary metabolites can be related to specific chemical and physical parameters. For instance, nutrient concentrations, temperature, pH, agitation, inoculum size and age, and fermentation time can all influence the growth, and thus the secondary metabolism, of an organism. Sometimes increasing the scale of fermentation, even from 100 mL to 1 L, can result in the loss of the activity of interest. Life history events such as reproduction can also play a dominant role in turning on biochemical pathways. For example, the halovir peptides discussed in the following chapter are only isolated when the producing fungal strain is

speculating. All these parameters need to be considered when the activity of interest is lost in subsequent cultivation attempts. This is a time intensive endeavor and was not pursued to any appreciable extent in this study.

This experiment tested for antiviral activity of a small number of marine microbial extracts against one particular viral pathogen. The discovery of sixty-two lead extracts at a hit rate of 1% represented a manageable number of projects for further consideration through additional fermentation and chemical investigation. I believe that these results support the hypothesis that marine microorganisms represent a viable resource for the discovery of antiviral agents. More studies are certainly warranted to more broadly access marine bacteria and fungal diversity in the pursuit of finding novel inhibitors against wide ranging viral diseases.

### References

1. Roizman, B. (1996). *Herpesviridae*. In Fields Virology. B.N. Fields, D.M. Knipe, and P.M. Howley, editors. Lippincott-Raven Publishers, Philadelphia. 2221-2230.
2. Foreman, K.E., Friborg, J., Kong, W.P., Woffendin, C., Polverini, P.J., Nickoloff, B.J. & Nabel, G.J. (1997). Propagation of a human herpesvirus from AIDS-associated Kaposi's sarcoma. *N. Engl. J. Med.* **336**, 163-171.
3. Roizman, B. & Sears, A.E. (1996). Herpes simplex viruses and their replication. In Fundamental Virology. B.N. Fields, D.M. Knipe, and P.M. Howley, editors. Lippincott-Raven Publishers, Philadelphia. 1043-1107.
4. Fleming, D.T., McQuillan, G.M., Johnson, R.E., Nahmias, A.J., Aral, S.O., Lee, F.K. & StLouis, M.E. (1997). Herpes simplex virus type 2 in the United States, 1976 to 1994. *N. Engl. J. Med.* **337**, 1105-1111.
5. Christie, S.N., McCaughey, C., McBride, M. & Coyle, P.V. (1997). Herpes simplex type 1 and genital herpes in Northern Ireland. *Int. J. Std. AIDS* **8**, 68-69.

6. Rodgers, C.A. & Omahony, C. (1995). High prevalence of herpes simplex virus type 1 in female anogenital herpes simplex. *Int. J. Std. AIDS* **6**, 144-144.
7. Wood, M.J. (1996). Antivirals in the context of HIV disease. *J. Antimicrob. Chemother.* **37**, 97-112.
8. Coen, D.M. (1996). Antiviral Drug Resistance in Herpes Simplex Virus. In *Antiviral chemotherapy 4 : new directions for clinical application and research*. J. Mills, P. Volberding, and L. Corey, editors. Plenum Press, New York. 49-57.
9. Wald, A., Zeh, J., Selke, S., Ashley, R.L. & Corey, L. (1995). Virologic characteristics of subclinical and symptomatic genital herpes infections. *N. Eng. J. Med.* **333**, 770-775.
10. Mertz, G.J., Schmidt, O., Jourden, J.L., Guinan, M.E., Remington, M.L., Fahnlander, A., Winter, C., Holmes, K.K. & Corey, L. (1985). Frequency of acquisition of 1st-episode genital infection with herpes simplex virus from symptomatic and asymptomatic source contacts. *Sex. Trans. Dis.* **12**, 33-39.
11. Mertz, G.J., Benedetti, J., Ashley, R., Selke, S.A. & Corey, L. (1992). Risk factors for the sexual transmission of genital herpes. *Ann. Intern. Med.* **116**, 197-202.
12. Shieh, M.T., Wudunn, D., Montgomery, R.I., Esko, J.D. & Spear, P.G. (1992). Cell surface receptors for herpes simplex virus are heparan sulfate proteoglycans. *J. Cell Biol.* **116**, 1273-1281.
13. Wudunn, D. & Spear, P.G. (1989). Initial interaction of herpes simplex virus with cells is binding to heparan sulfate. *J. Virol.* **63**, 52-58.
14. Elion, G.B. (1993). Acyclovir: Discovery, mechanism of action, and selectivity. *J. Med. Virol.* **S1**, 2-6.
15. Coen, D.M. & Schaffer, P.A. (1980). Two distinct loci confer resistance to acycloguanosine in herpes simplex virus type 1. *Proc. Nat. Acad. Sci. USA* **77**, 2265-2269.
16. Schnipper, L.E. & Crumpacker, C.S. (1980). Resistance of herpes simplex virus to acycloguanosine: role of viral thymidine kinase and DNA polymerase loci. *Proc. Nat. Acad. Sci. USA* **77**, 2270-2273.
17. Reusser, P. (1996). Herpesvirus resistance to antiviral drugs - a review of the mechanisms, clinical importance and therapeutic options. *J. Hosp. Infect.* **33**, 235-248.
18. Cole, N.L. & Balfour, H.H., Jr. (1987). *In vitro* susceptibility of cytomegalovirus isolates from immunocompromised patients to acyclovir and ganciclovir. *Diag. Microb. Infect. Dis.* **6**, 255-262.

19. Balfour, H.H., Jr. (1990). Management of cytomegalovirus disease with antiviral drugs. *Rev. Infect. Dis.* **12**, S849-S860.
20. Perry, C.M. & Faulds, D. (1996). Valaciclovir - a review of its antiviral activity, pharmacokinetic properties and therapeutic efficacy in herpesvirus infections. *Drugs* **52**, 754-772.
21. Vere Hodge, R.A. (1993). Famciclovir and penciclovir: The mode of action of famciclovir including its conversion to penciclovir. *Antivir. Chem. Chemother.* **4**, 67-84.
22. Snoeck, R. (2000). Antiviral therapy of herpes simplex. *Int. J. Antimicrob. Agents* **16**, 157-159.
23. Sasadeusz, J.J. & Sacks, S.L. (1993). Systemic antivirals in herpesvirus infections. *Dermatol. Ther.* **11**, 171-185.
24. Pope, L.E., Marcelletti, J.F., Katz, L.R., Lin, J.Y., Katz, D.H., Parish, M.L. & Spear, P.G. (1998). The anti-herpes simplex virus activity of n-docosanol includes inhibition of the viral entry process. *Antivir. Res.* **40**, 85-94.
25. Katz, D.H., Marcelletti, J.F., Khalil, M.H., Pope, L.E. & Katz, L.R. (1991). Antiviral activity of 1-docosanol, an inhibitor of lipid-enveloped viruses including herpes simplex. *Proc. Nat. Acad. Sci. USA* **88**, 10825-10829.
26. Mahy, B.W.J. & Kangro, H. (1996). *Virology methods manual*. Academic Press, London ; San Diego. x, 374 pp.
27. Barltrop, J.A., Owen, T.C., Cory, A.H. & Cory, J.G. (1991). 5-(3-Carboxymethoxyphenyl)-2-(4,5-dimethylthiazolyl)-3-(4-sulfophenyl)tetrazolium, inner salt (MTS) and related analogs of 3-(4,5-dimethylthiazolyl)-2,5-diphenyltetrazolium bromide (MTT) reducing to purple water-soluble formazans as cell-viability indicators. *Bioorg. Med. Chem. Lett.* **1**, 611-614.
28. Cory, A.H., Owen, T.C., Barltrop, J.A. & Cory, J.G. (1991). Use of an aqueous soluble tetrazolium-formazan assay for cell growth assays in culture. *Cancer Comm.* **3**, 207-212.
29. Takeuchi, H., Baba, M. & Shigeta, S. (1991). An application of yetrazolium (MTT) colorimetric assay for the screening of anti-herpes simplex virus compounds. *J. Virol. Meth.* **33**, 61-71.



## **Chapter 4. Halovirs A-F, Novel Antiviral Agents from a Marine Fungus**

From the screening program described in chapter three, a crude extract derived from the cultivation of marine fungal strain CNL240 displayed consistent and potent activity against HSV-1. Scale-up fermentations of this fungus reproduced the desired antiviral activity, and a chemical investigation was pursued to uncover the molecules responsible. Five linear, lipophilic peptides named the halovirs A-E were identified as the active constituents. This chapter presents the isolation and structure determination of the halovirs, their bioactivities, and further presents experiments designed to elucidate the mechanisms by which the novel compounds exert their antiviral effects.

### **4.1 Isolation and Structural Characterization of Halovirs A-C**

Marine fungal strain CNL240 was obtained from a sample of the seagrass *Halodule wrightii* during a research expedition to the Bahamas in August 1996 aboard the R/V Seward Johnson (Harbor Branch Oceanographic Institute). The seagrass sample was air-dried, cut into small pieces, and placed onto seawater based agar medium containing the antibiotics penicillin G and streptomycin sulfate to inhibit bacterial growth. Following incubation, a small section of hyphae growing outward from the plant material was carefully transferred to a secondary isolation plate containing agar medium. Following adequate growth, portions of the fungus were removed and cryopreserved at  $-80\text{ }^{\circ}\text{C}$  in sterile vials containing growth medium enriched with 10% glycerol. Marine fungal strain CNL240 was identified as a *Scytalidium* sp. by fatty acid analysis as applied to a fungal similarity index.<sup>1</sup> The

similarity index for this genus was 0.897. CNL240 was deposited with the American Type Culture Collection in Manassas, Virginia, and has the ATCC designation 74470.

Nineteen one-liter fermentations of strain CNL240 were conducted in a sterilized medium consisting of 2 grams peptone, 2 grams yeast extract, and 4 grams mannitol in one-liter of filtered seawater. After approximately 20 days, the fermentations appeared as white mycelial mats with randomly dispersed thick, black spore suspensions resting on the surface. The mats were separated from the broth, lyophilized, and extracted with a 1:1 mixture of dichloromethane and methanol. Concentration *in vacuo* yielded 375 mg of crude extract per liter. Assay results indicated a strong antiviral effect at 10-20 µg/mL against HSV infected cells.

Bioassay-guided fractionation was pursued on the mycelial extract to determine the nature of the antiviral components (Figure 2). The first step was separation by high-speed countercurrent chromatography using a solvent system composed of 10% hexanes, 30% ethyl acetate, 30% methanol, and 30% water. The upper layer of this biphasic system was used as the mobile phase, and five fractions were generated. The third of these fractions was determined to possess the antiviral activity and was subjected to further separation by reversed-phase silica gel flash chromatography using a gradient of 10% to 0% water in methanol. The fourth and fifth fractions of this purification procedure concentrated the antiviral activity. The fifth fraction was further separated by silica gel flash chromatography followed by isocratic C18 HPLC to afford halovirs A (27), B (28), and C (29) as the major antiviral components.

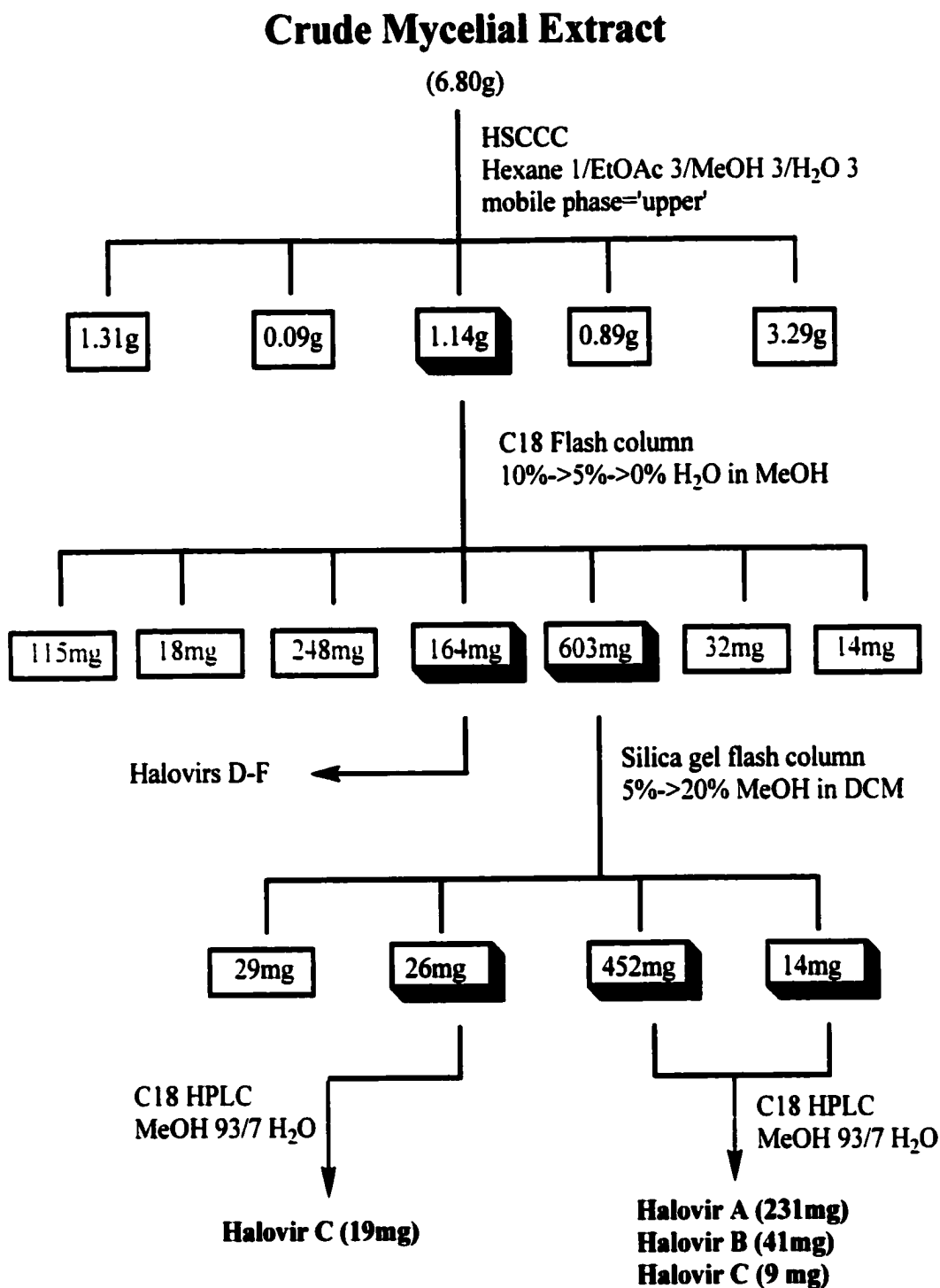


Figure 2. Bioassay-guided fractionation of extract CNL240 used in the purification of halovirs A-C. The shaded boxes indicate fractions demonstrating antiviral activity.

Halovir A (**27**) was obtained as a colorless, amorphous solid in 12 mg/L yield. A molecular formula of  $C_{45}H_{83}O_9N_7$  was determined based on high resolution FAB mass spectrometry  $[[M+Na]^+ m/z 888.6119$ ; calculated 888.6150] coupled with  $^1H$  and  $^{13}C$  NMR data. The IR spectrum displayed absorptions at  $1640\text{ cm}^{-1}$  and  $1540\text{ cm}^{-1}$  characteristic of amide carbonyls groups, and a broad absorption at  $3290\text{ cm}^{-1}$  consistent with the presence of OH and NH functionalities.

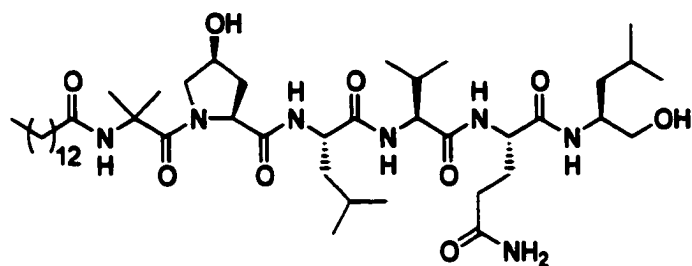
Initial inspection of the  $^1H$  and  $^{13}C$  NMR spectra of **27** in pyridine- $d_5$  revealed features consistent with a peptide. In the  $^1H$  spectrum, resonances typical of amide protons were visible between  $\delta$  7-9, and several resonance bands between  $\delta$  4-5 were suggestive of amino acid  $\alpha$ -hydrogens. A prominent characteristic of this spectrum was a large, broad peak at  $\delta$  1.2 indicative of at least one aliphatic chain. The  $^{13}C$  spectrum displayed seven carbonyl resonances and eight peaks between  $\delta$  50-70, which is the region of the spectrum at which  $\alpha$ -carbons of a peptide normally occur. A region of significantly overlapping peaks was observed in the region of 30 ppm, and  $^{13}C$  NMR DEPT experiments indicated that all were methylenes. DEPT experiments further revealed that this molecule contained 9  $CH_3$ , 9  $CH$ , and at least one quaternary carbon.

The planar structure of halovir A was deduced by extensive analysis of homo- and heteronuclear 2D NMR data. The amino acids leucine, valine, 4-hydroxyproline, and glutamine, as well as a leucinol (Lol) moiety, were identified by their spin systems observed in TOCSY and COSY experiments and by analysis of NMR chemical shift data. Two methyl groups, both singlets in the  $^1H$  NMR spectrum, were observed to

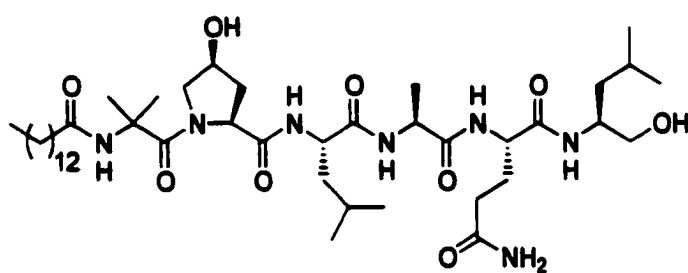
correlate with both a quaternary carbon at  $\delta$  57.3 and each other in HMBC experiments, helping to establish the presence of an  $\alpha$ -aminoisobutyric acid residue (Aib). HMBC correlations further verified the other amino acid substructures. ROESY correlations between the  $\gamma$  and  $\epsilon$  hydrogens of Gln helped establish its connectivity. The features of a fatty acid derived component were also apparent from these experiments, but the connectivity was quickly lost after C4 due to significant signal overlap in both the  $^1\text{H}$  and  $^{13}\text{C}$  NMR spectra.

The linear peptide sequence was elucidated by correlations observed in the HMBC and ROESY experiments. Amide NH and  $\alpha$ -protons correlated with their neighboring carbonyls in the HMBC spectrum. Strong sequential  $d_{\text{NN}}(i,i+1)$  and  $d_{\alpha\text{N}}(i,i+1)$  NOE signals were present in the ROESY spectrum further supporting the proposed peptide sequence. ROESY signals were also observed from the singlet NH of the Aib residue to a  $\delta$ -proton on the hydroxyproline and both the  $\alpha$ - and  $\beta$ -methylenes of the fatty acid moiety. All other HMBC and ROESY correlations observed were consistent with the proposed structure (Figure 3). The molecular formula, coupled with the  $^1\text{H}$  and  $^{13}\text{C}$  NMR data, indicated that the terminal fatty acid was myristic acid.

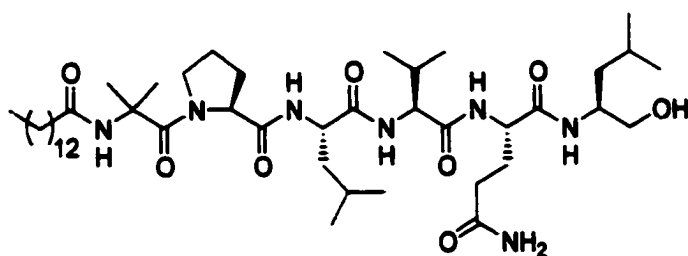
The sequence of **27** was further confirmed by the analysis of fragment ions, or daughter ions, produced during electrospray mass spectrometry. Fragmentation of molecules can be induced during mass analysis, and the resulting daughter ions provide structural information about the parent compound. In particular, linear peptides are known to fragment in predictable patterns, predominately across the



27



28



29

Figure 3. The structures of the halovir peptides A (27), B (28), and C(29).

Table 5.  $^1\text{H}$  and  $^{13}\text{C}$  Assignments for Halovirs A-C in pyridine- $d_5$ .

	Halovir A (27)		Halovir B (28)		Halovir C (29)		
	$\delta^{13}\text{C}^a$	$\delta^1\text{H}^b$	$\delta^{13}\text{C}$	$\delta^1\text{H}$	$\delta^{13}\text{C}$	$\delta^1\text{H}$	
Lol	1	66.0	4.04 (m)	66.0	4.04 (m)	65.9	4.03 (m)
	2	50.8	4.62 (m)	50.9	4.61 (m)	50.7	4.63 (m)
	3	41.2	1.94 (m), 1.76 (m)	41.3	1.95 (m), 1.76 (m)	41.1	1.95 (m), 1.72 (m)
	4	25.6	1.9 (m)	25.6	1.85 (m)	25.5	1.97 (m)
	5	24.3	0.98 (d, 6.3)	24.3	0.99 (d)	24.1	0.99 (d, 6.35)
	6	22.8	0.98 (d, 6.3)	22.7	0.99 (d)	22.7	0.99 (d, 6.35)
NH		7.76 (d, 9.3)		7.74 (d, 8.7)		7.78 (d, 8.79)	
OH		5.83		5.96		5.87 (bs)	
Gln	1	172.8		172.7		172.7	
	2	55.4	5.05 (m)	55.1	5.05 (m)	55.5	5.05 (m)
	3	29.4	2.68 (m)	29.4	2.74 (m)	29.4	2.76 (m)
	4	33.8	2.95 (m)	33.7	2.95 (m)	33.8	2.95 (m)
	5	175.5		175.5		175.4	
NH <sub>2</sub>		8.09 (s), 7.57 (s)		8.08 (s), 7.55 (s)		8.14 (s), 7.62 (s)	
NH		8.12 (d, 7.3)		8.01 (d, 7.8)		8.13 (d, 7.3)	
Val/Ala	1	172.8		174.1		172.7	
	2	61.9	4.67 (m)	51.8	4.6 (m)	61.7	4.67 (m)
	3	30.3	2.68 (m)	17.5	1.75 (d, 5.7)	30.0	2.65 (m)
	4	19.6	1.30 (d, 6.8)			19.6	1.28 (d, 6.8)
	5	20.1	1.21 (d, 6.8)			20.0	1.20 (d, 6.8)
NH		8.12 (d, 7.3)		8.40 (d, 6.3)		8.03 (d, 7.3)	
Leu	1	175.8		175.6		175.0	
	2	55.4	4.67 (m)	55.2	4.68 (m)	55.3	4.65 (m)
	3	40.3	2.33 (m), 2.06 (m)	40.0	2.32 (m), 2.04 (m)	40.1	2.33 (m), 2.03 (m)

a) 100 MHz b) 300 MHz Assignments by DEPT and HMQC methods.

Table 5.  $^1\text{H}$  and  $^{13}\text{C}$  Assignments for Halovir A-C in pyridine- $d_5$ . (con't)

	Halovir A (27)		Halovir B (28)		Halovir C (29)	
	$\delta^{13}\text{C}^a$	$\delta^1\text{H}^b$	$\delta^{13}\text{C}$	$\delta^1\text{H}$	$\delta^{13}\text{C}$	$\delta^1\text{H}$
Leu						
4	26.0	2.05 (m)	26.0	2.05 (m)	25.9	2.02 (m)
5	24.1	1.14 (d, 5.86)	24.0	1.13 (d)	21.5	1.12 (d, 5.4)
6	21.6	1.02 (d, 5.86)	21.6	1.00 (d)	23.9	1.00 (d, 5.4)
NH		8.62 (d, 6.35)		8.58 (d, 6.3)		8.50 (d, 6.35)
Hyp/Pro						
1	175.4		175.9		175.0	
2	63.3	5.25 (dd, 9.8, 8.0)	63.6	5.26 (m)	64.4	4.77 (t, 7.3)
3a	38.4	2.72 (dd, 8.0, 13)	38.4	2.73 (m)	29.7	2.31 (m)
3b		2.08 (dd, 10, 13)		2.06 (m)		1.80 (m)
4	70.9	4.75 (m)	71.0	4.77 (m)	26.8	1.80 (m)
5a	58.2	4.34(d, 11.2)	58.2	4.33 (m)	49.5	3.58 (m)
5b		3.81 (dd, 11.2, 2.5)		3.82 (m)		4.02 (m)
OH		6.99 (d, 2.5)		7.03 (bs)		
Aib						
1	175.1		175.4		174.2	
2	57.3		57.3		57.2	
3	27.2	1.80 (s)	27.0	1.75 (s)	27.2	1.78 (s)
4	24.4	1.60 (s)	24.3	1.57 (s)	24.0	1.56 (s)
NH		9.60 (s)		9.64 (s)		9.62 (s)
Myr						
1	174.7		174.8		174.7	
2	36.3	2.56 (m)	36.2	2.54 (m)	36.2	2.51 (t, 7.3)
3	26.4	1.77 (m)	26.3	1.80 (m)	26.2	1.77 (m)
4	32.6	1.25 (m)	32.6	1.24 (m)	32.5	1.25 (m)
5-12	30	1.2 (m)	30	1.2-1.4 (m)	30.0	1.2 (m)
13	23.4	1.25 (m)	23.4	1.2 (m)	23.3	1.25 (m)
14	14.8	0.88 (t)	14.8	0.87 (t)	14.7	0.88 (t)

a) 100 MHz b) 300 MHz Assignments by DEPT and HMQC methods.



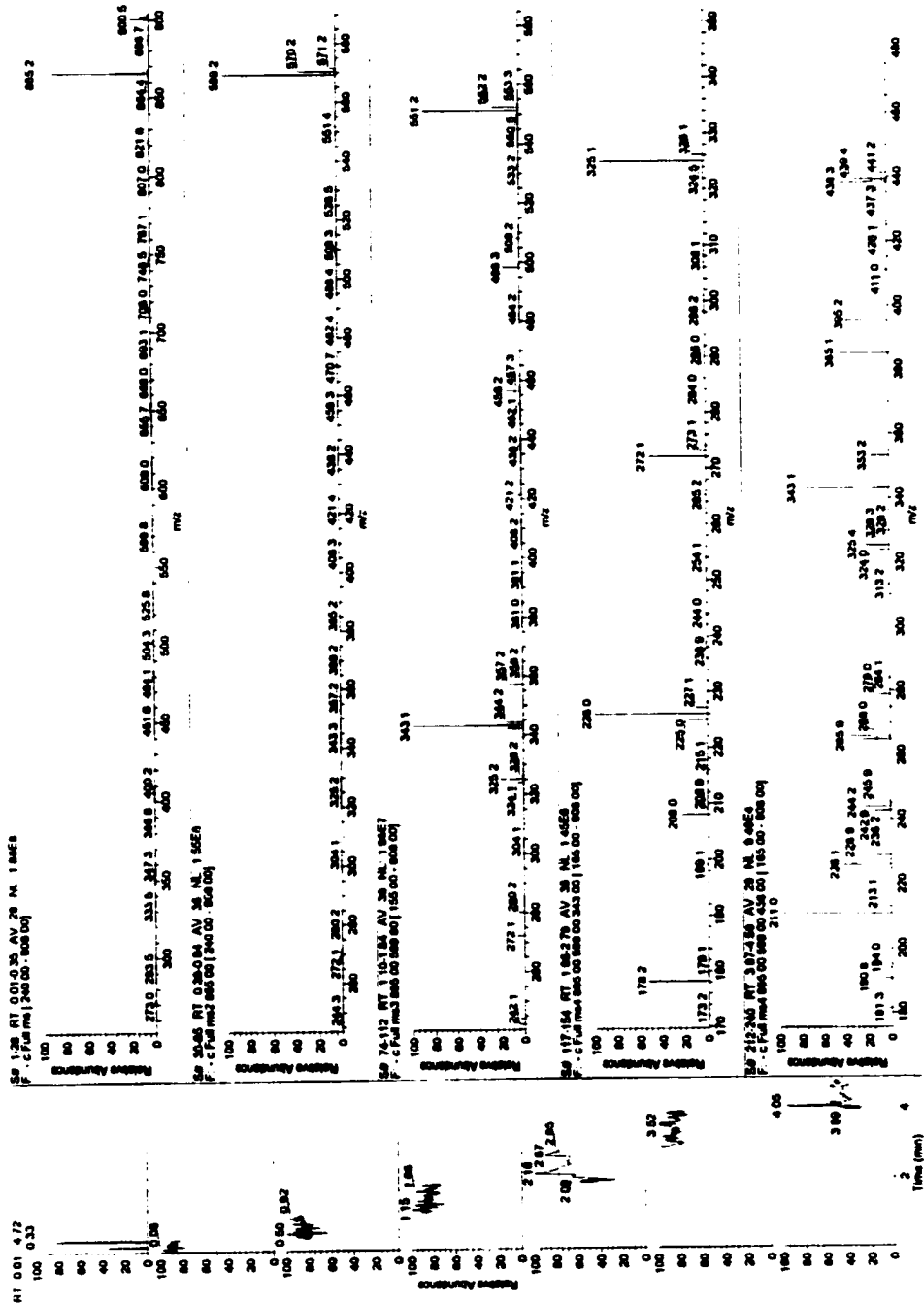


Figure 4. Fragment ions generated during an MS<sup>2</sup> experiment involving halovir A (27). The experiment was conducted on a Finnegan LCQ mass spectrometer operated in the negative ion mode.

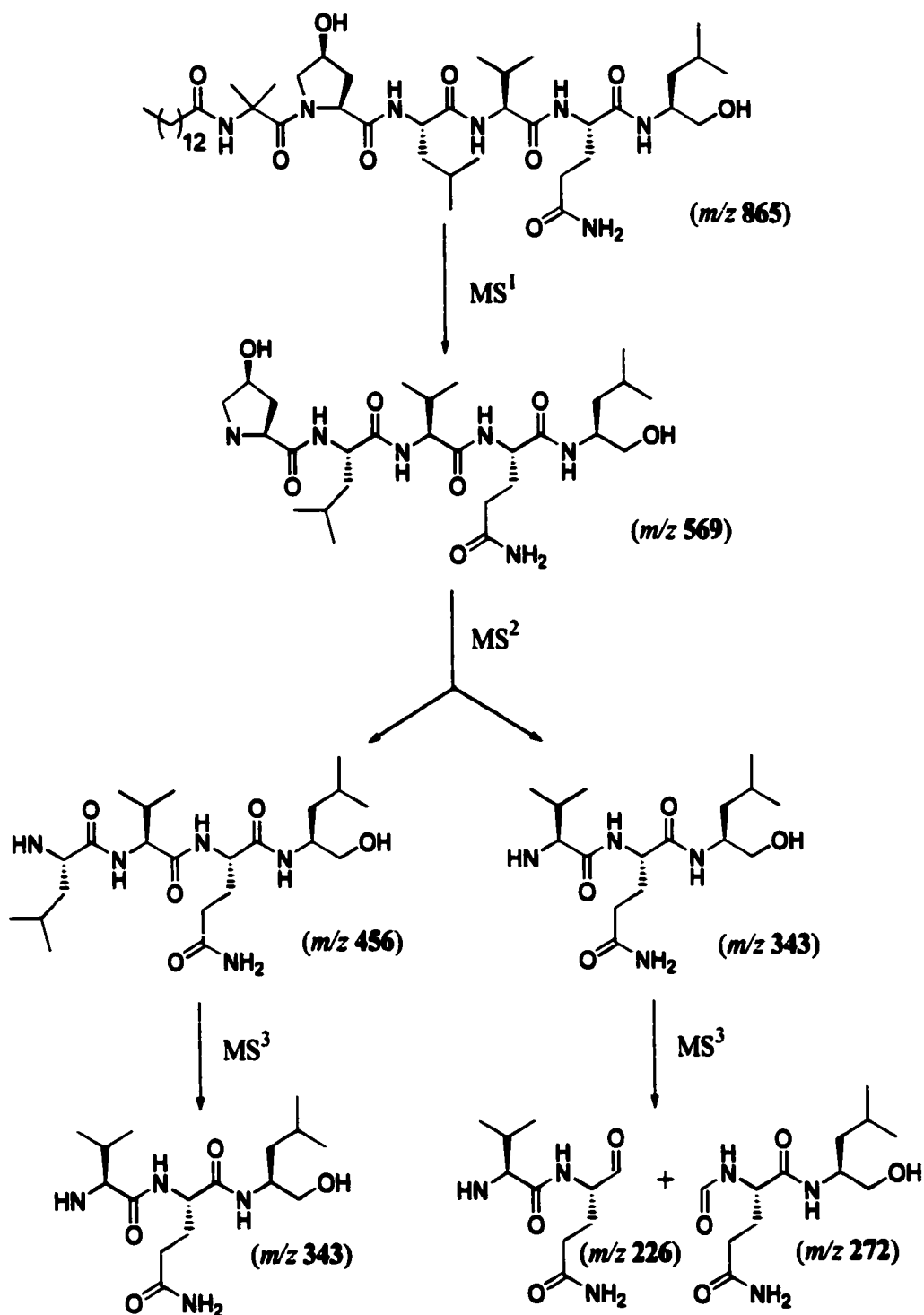


Figure 5. Negative-mode electrospray  $MS^3$  analysis of halovir A (27). The numbers refer to the mass to charge ratios of the observed ions.

peptide bonds, and sequence information is possible by analyzing the serial loss of amino acids from the chain. Figures 4 and 5 show the dominant daughter ions generated in a MS<sup>3</sup> experiment performed on a Finnigan LCQ mass spectrometer. Cleavage across the Aib-Hyp amide bond is the initial dominant fragment. Further collision induced dissociation of the major ion (*m/z* 569) shows serial loss of the Hyp and Leu residues, each with a molecular weight of 113. MS<sup>3</sup> analysis of the Val-Gln-Lol granddaughter ion showed x<sub>1</sub>-cleavage across the valine and b<sub>1</sub>-dissociation from loss of the Lol. Thus, electrospray ionization tandem mass spectrometry further supported the proposed structure.

Halovir B (**28**) was isolated in a yield of 2 mg/L and determined to have a molecular formula of C<sub>43</sub>H<sub>79</sub>N<sub>7</sub>O<sub>9</sub> by high-resolution electrospray ionization mass spectrometry (HREIMS). Carbon NMR DEPT experiments showed that **28** differed from **27** by having one less methyl group and methine carbon. Analysis of spin systems from TOCSY and COSY data indicated that halovir B contained alanine in place of the valine unit in **27**. HMQC, HMBC, and ROESY NMR data, in addition to ms/ms experiments (Figure 6), all confirmed the presence of alanine and the peptide sequence of halovir B.

Halovir C (**29**) was isolated in a yield of 1.5 mg/L and determined to have a molecular formula of C<sub>45</sub>H<sub>83</sub>N<sub>7</sub>O<sub>8</sub> by HREIMS. The difference in the molecular formula of an oxygen from halovir A was attributed to the presence of a proline residue in place of hydroxyproline. The <sup>1</sup>H NMR spectra lacked the presence of an OH signal around δ 7.0 found in **27** and **28**, and the proline β- and γ-methylenes were all appropriately shifted upfield relative to halovirs A and B. HMQC, HMBC,

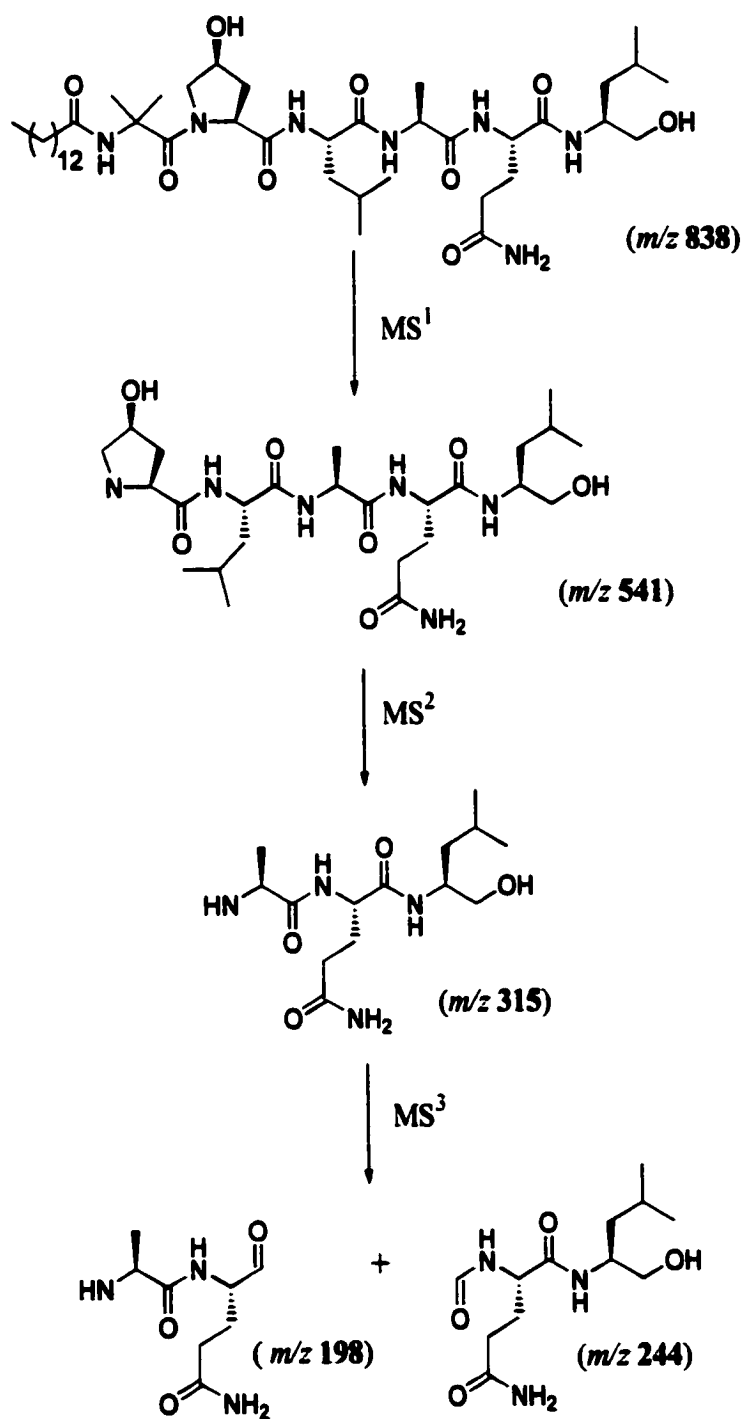


Figure 6. Negative-mode electrospray MS<sup>3</sup> analysis of halovir B (29). The numbers refer to the mass to charge ratios of the observed ions.

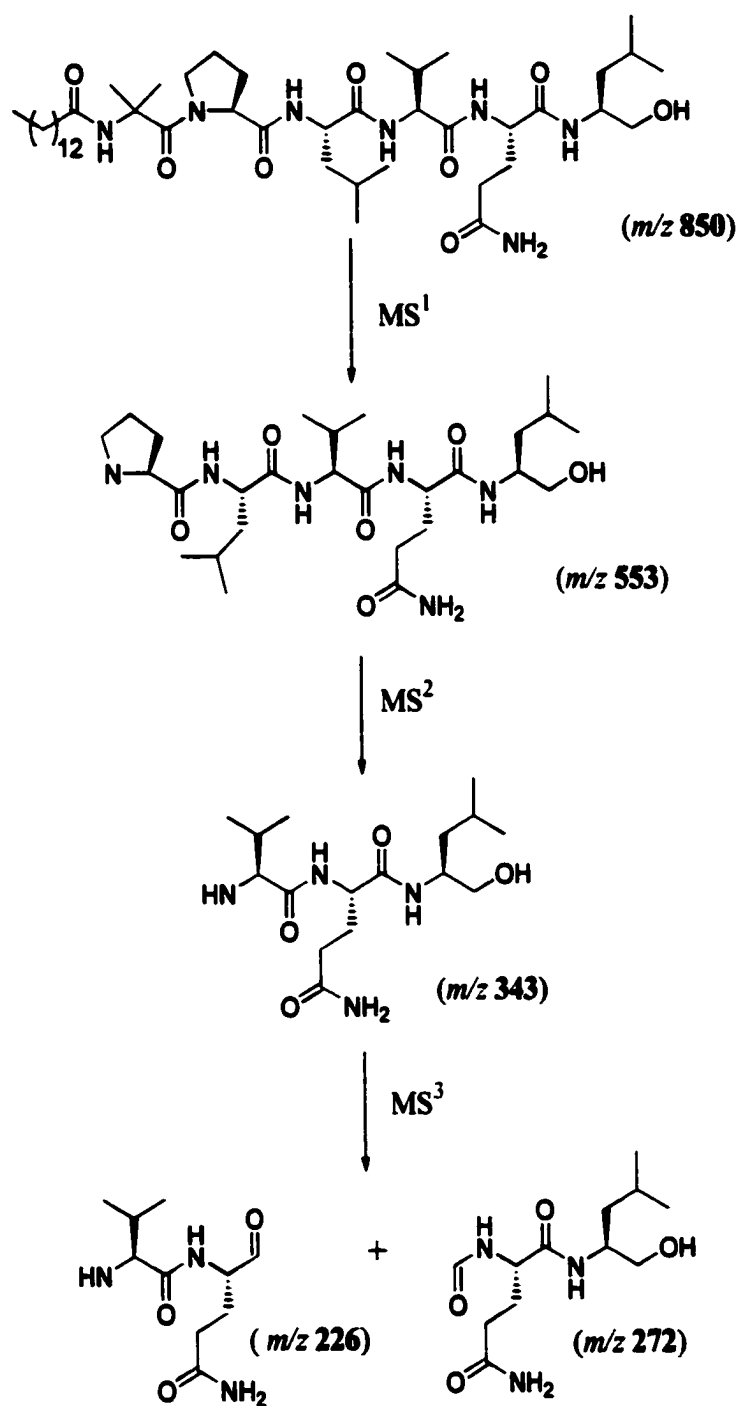


Figure 7. Negative-mode electrospray MS<sup>3</sup> analysis of halovir C (29). The numbers refer to the mass to charge ratios of the observed ions.

ROESY, and DEPT NMR data, in combination with ms/ms experiments (Figure 7), were consistent with the presence of proline and the peptide sequence assigned for halovir C.

The stereochemistry of the halovirs was addressed using chiral GC-FID and Mosher's ester analysis. Halovirs A, B, and C were subjected to acid hydrolysis and then derivatized to form the isopropyl ester pentafluoropropionamide amino acid derivatives. These were then characterized by GC-FID on a Chirasil-Val capillary column by comparison and co-injection with identically prepared standards. Using these methods, halovir A was determined to contain L-leucine, L-valine, and L-glutamine. Halovir C additionally contained L-proline. Halovir B was composed of L-alanine, L-leucine, and L-glutamine. In order to determine the stereochemistry of the leucinol (Lol) carboxyl terminus, halovir A was oxidized with Jones reagent to yield the corresponding C-terminal carboxylic acid. Acid hydrolysis, amino acid derivatization, and chiral GC-FID analysis of this derivative showed the presence of only L-leucine, indicating that the original leucinol of halovir A is of the *S*-configuration.

The absolute stereochemistry at C-3 of the 3-hydroxyproline residue in halovir A was established by application of the modified Mosher's method (Figure 8).<sup>2</sup> This method involves the esterification of secondary alcohols with both the (*S*)- and (*R*)-isomers of 2-methoxy-2-phenyl-2-(trifluoromethyl)acetic acid chlorides (MTPA). The resulting esters normally adopt a preferred conformation in solution whereby the carbonyl proton, the ester carbonyl, and the trifluoromethyl group align approximately in a plane. Protons that are situated behind the benzene ring are shielded due to its

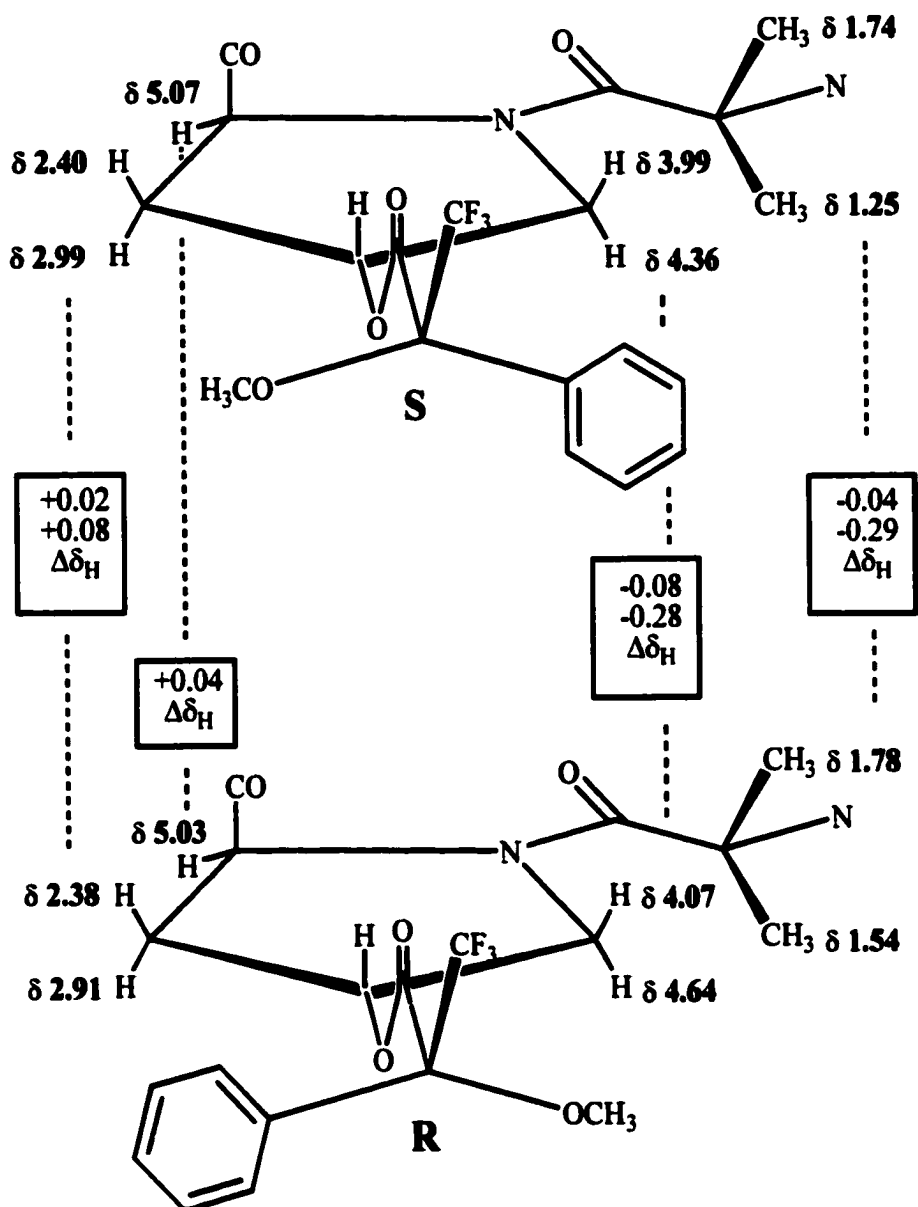


Figure 8. Mosher's ester diagram of (*R*)- and (*S*)-MTPA esters of halovir A.  $^1\text{H}$  NMR assignments were made in pyridine- $d_6$  (300 MHz).

diamagnetic effect, and their resulting  $^1\text{H}$  NMR signals are shifted upfield relative to their normal positions. The opposite is true of protons influenced by the methoxyl group. The assignment of as many proton signals differentially shielded by both the (*S*)- and (*R*)-MTPA esters then allows for calculations of the type  $\Delta\delta = \delta_S - \delta_R$ . A model can then be constructed with protons having positive  $\Delta\delta$  values on one side of the MTPA plane and those with negative  $\Delta\delta$  values on the other. The molecular model then provides means for predicting the absolute configuration of the secondary alcohol. Halovir A was esterified with both the (*S*)- and (*R*)-MTPA acid chlorides. The  $^1\text{H}$  NMR signals of the esters were assigned using a combination of 1D-TOCSY and  $^1\text{H}$  NMR experiments. The use of 1D-TOCSY experiments proved valuable for the assignment of crucial proton resonances significantly overlapped in the  $^1\text{H}$  NMR spectrum. Analysis of the  $\Delta\delta$  values established the Hyp-C3 absolute stereochemistry as the *R*-configuration. This determination, coupled with the finding of L-proline in halovir C, shows that the hydroxyproline residues of halovirs A and B possess the L-4-*trans*-configuration.

## 4.2 Secondary Structure of Halovir A

Peptide molecules often adopt regular secondary structures in solution that are intimately associated with their biological properties. These polypeptide conformations are stabilized through the formation of hydrogen bonds between amide proton and carbonyl oxygens in the peptide backbone, leading to such common peptide conformations as  $\alpha$ - and  $3_{10}$ -helices and  $\beta$ -sheets. I initially suspected that the halovir peptides may have regular secondary structure due to slow deuterium



exchange rates of the Lol, Gln, Val, and Leu backbone amide protons in methanol- $d_4$  and also DMSO- $d_6$  spiked with D<sub>2</sub>O, a typical property of protons involved in hydrogen bonding. The Aib NH,  $\epsilon$ -NH<sub>2</sub> of the Gln residue, and both hydroxyl groups all rapidly exchanged under the same experimental conditions. Therefore, a more detailed inspection of the halovir A polypeptide secondary structure was undertaken through further investigation of hydrogen bonding evidence and also by NOE/ROESY observations of short and medium range <sup>1</sup>H-<sup>1</sup>H distances in the peptide backbone.

The temperature dependence of amide proton chemical shifts correlate with their inaccessibility to solvent, and hence are one indicator of protons potentially involved in hydrogen bonding interactions.<sup>3</sup> It is generally accepted that  $\Delta\delta/\Delta T$  coefficients less than  $4.0 \times 10^{-3}$  ppm/K in polar solvents are consistent with amide protons shielded from solvent, while coefficients greater than  $5.0 \times 10^{-3}$  ppm/K are indicative of solvated protons such as those of linear extended peptide conformations.<sup>4</sup> The temperature coefficients for the backbone amide protons of **27** were measured in DMSO- $d_6$  over a range of 298-388 K (Table 6, Figure 9). The Leu, Val, Gln, and Lol NHs all clearly satisfy the criteria of having coefficients less than  $4.0 \times 10^{-3}$  ppm/K, indicating inaccessibility to solvent and hence possible participation in hydrogen bonding. The middle Val and Leu residues showed the lowest temperature dependence with coefficients of  $0.8 \times 10^{-3}$  and  $1.3 \times 10^{-3}$ , respectively, indicating significant shielding from solvent.

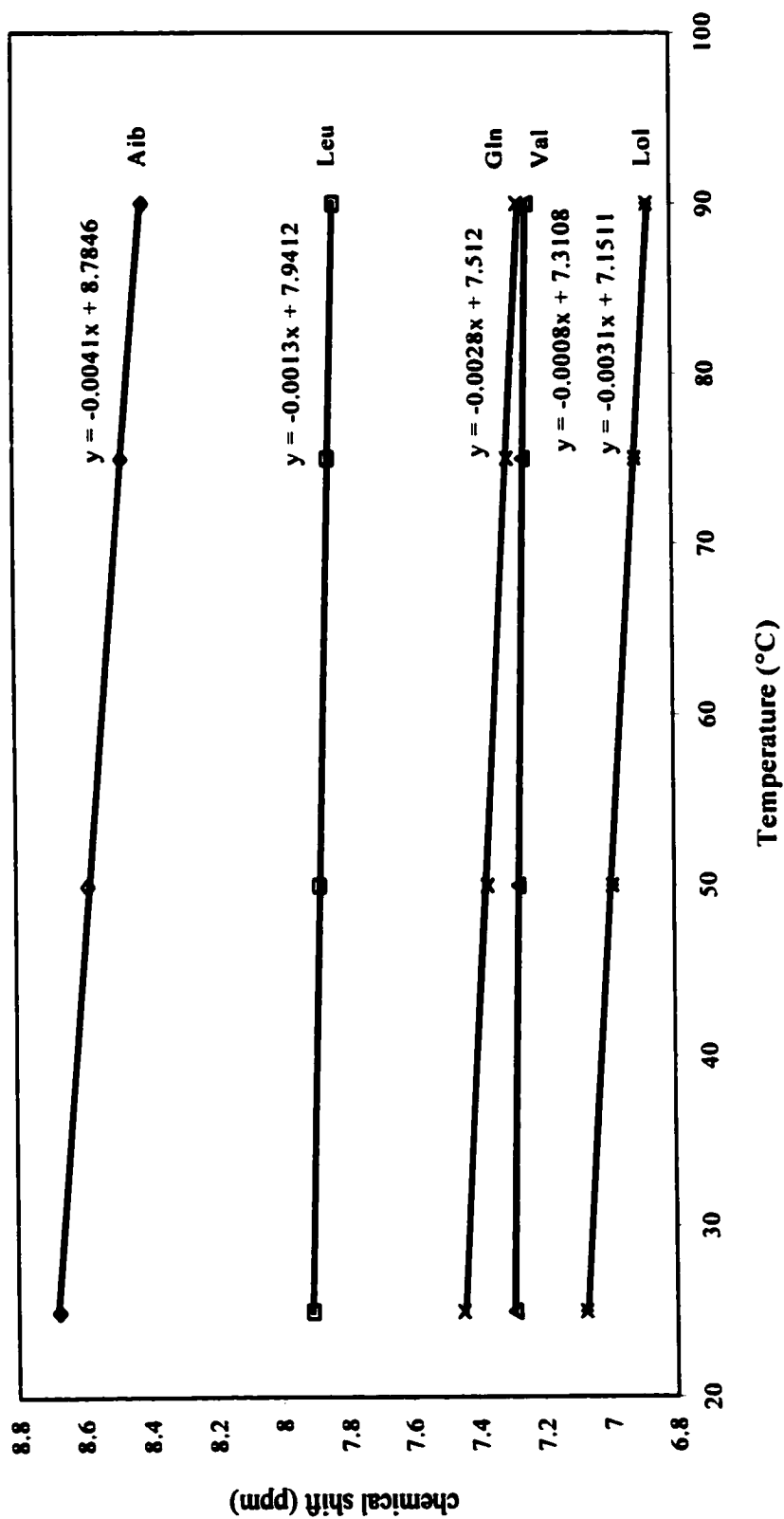


Figure 9. <sup>1</sup>H NMR chemical shift temperature dependence of the backbone amide protons of halovir A (27) measured in DMSO-*d*<sub>6</sub> (300 MHz).

Table 6. Temperature Dependence of Amide Backbone Protons of Halovir A (27)

	Aib	Leu	Val	Gln	Lol
$\Delta\delta/\Delta T$	$4.1 \times 10^{-3}$	$1.3 \times 10^{-3}$	$0.8 \times 10^{-3}$	$2.8 \times 10^{-3}$	$3.1 \times 10^{-3}$

As a second test of hydrogen bonding potential, the solvent dependence of NH chemical shifts was measured as a function of DMSO- $d_6$  concentration in CDCl<sub>3</sub> (Figure 10).<sup>5</sup> In this experiment, protons with greater exposure to a polar solvent such as dimethyl sulfoxide are better able to participate in intermolecular H-bonding and consequently demonstrate greater chemical shift changes. Such was observed with the Aib NH, which showed a chemical shift perturbation of nearly 0.75 ppm as the DMSO concentration was increased from 5 to 40 percent. However, the chemical shifts of the Leu, Val, Gln, and Lol amide protons were practically independent of solvent composition. These data essentially mirror those of the temperature dependence experiment, strongly supporting the participation of the Leu, Val, Gln, and Lol backbone amide protons in hydrogen bonding.

The common secondary structures of polypeptides provide for regular short, medium, and long range <sup>1</sup>H-<sup>1</sup>H distances that are sufficiently close enough for observation by NOE experiments. Some of these NOEs are suitable for distinguishing between conformations such as  $\alpha$ - and  $3_{10}$ -helices and  $\beta$ -sheets.<sup>6</sup> Therefore, the secondary structure of **27** was further investigated by analysis of NOE correlations as measured in a ROESY experiment conducted in DMSO- $d_6$ . Strong sequential  $d_{NN(i,i+1)}$  signals were observed in the ROESY spectrum between the Leu, Val, Gln, and Lol residues. Such interresidue correlations are a distinctive feature of polypeptides residing in helical conformations.<sup>6</sup> A complete tracing of successive

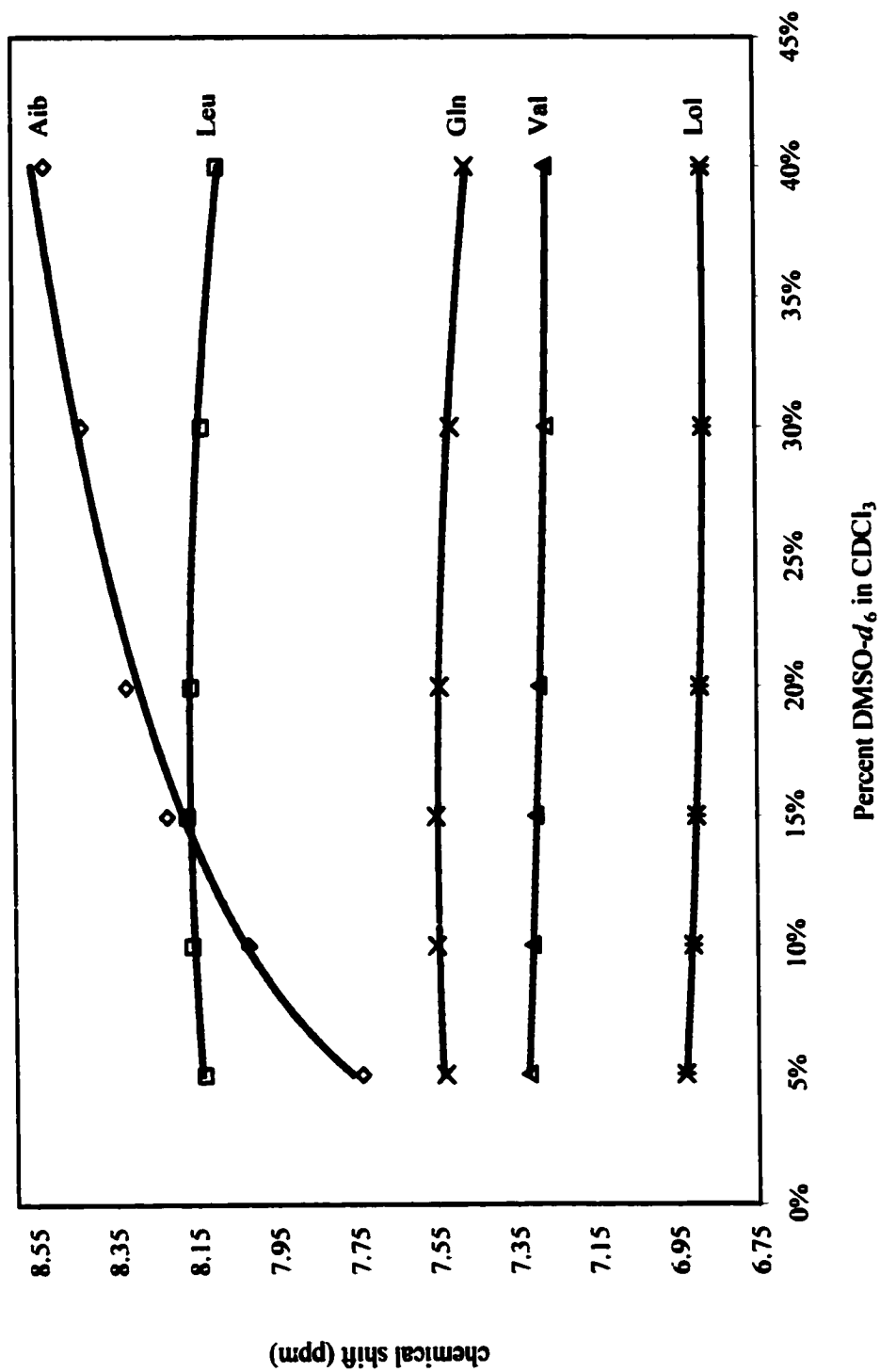


Figure 10. Solvent dependence of NH chemical shifts of halovir A as a function of DMSO-d<sub>6</sub> concentration in CDCl<sub>3</sub>.

$d_{\text{NN}(i,i+1)}$  correlations through the helical backbone was precluded by the hydroxyproline residue. Dipeptide segments containing proline frequently reside in a *cis*, rather than *trans*, configuration. *Cis-trans* isomerization has a dominant influence on sequential  $^1\text{H}$ - $^1\text{H}$  distances, with *cis* forms favoring shorter distances between  $\text{NH}_i$  and  $\alpha\text{H}_{(i+1)}$ , and *trans* configurations providing closer contact between  $\text{NH}_i$  and  $\delta\text{CH}_{2(i+1)}$ .<sup>7</sup> In the case of the Leu-Hyp dipeptide segment of halovir A, a NOE was observed between the Leu NH and the higher field Hyp  $\delta\text{CH}$  in support of a geometry approaching a *trans*-configuration and a continuing helix through the Leu-Hyp linkage. Looking further down the peptide chain at the Aib-Hyp segment, a strong NOE was observed between the Aib NH and the lower field hydroxyproline  $\delta\text{CH}_2$  (3.68 ppm,  $\text{DMSO-}d_6$ ), indicative of a *trans*-configuration. Taken together, these data are consistent with the hexapeptide segment of **27** as residing in a helical conformation.

Both  $\alpha$ - and  $3_{10}$ -helices are further distinguished from  $\beta$ -sheet formations by close approach of interresidue  $i$  and  $(i+3)$  backbone protons. Other medium-range NOEs are individually characteristic of the two helical types. Short distances prevail between residues  $i$  and  $(i+4)$  in a  $\alpha$ -helix, while the more tightly wound  $3_{10}$ -helix is characterized by close approach of the  $i$  and  $(i+2)$  amino acid backbone hydrogens.<sup>7</sup> From the Hyp  $\alpha$ -H,  $d_{\alpha\text{N}(i,i+2)}$  and  $d_{\alpha\text{N}(i,i+3)}$  correlations were observed to the valine and glutamine amide protons, respectively. A NOESY correlation was measured between the leucinol NH and either the Val  $\alpha$ -H ( $(i, i+2)$ ), the Leu  $\alpha$ -H ( $(i, i+3)$ ), or both, but signal overlap precluded distinction between these two. Aib does not

contain an  $\alpha$ -proton, but weak  $d_{\beta\text{N}}(i,i+2)$  and  $d_{\beta\text{N}}(i,i+3)$  correlations were observed between an Aib  $\beta$ -methyl and the leucine and valine NHs, respectively. A  $d_{\alpha\beta}(i,i+3)$  crosspeak was also observed between the Gln  $\alpha$ -H and Hyp  $\beta$ -CH<sub>2</sub>. These medium-range NOEs are further supportive of a helical solution structure for **27**. Few possible NOE correlations exist to distinguish between  $\alpha$  and  $3_{10}$  helices in such a short peptide. However, at least one, and possibly two,  $(i,i+2)$  type backbone  $^1\text{H}$ - $^1\text{H}$  distances lend support in favor of a  $3_{10}$ -helix.

Taken together, the hydrogen bonding evidence and the above NOE data fit with a representation of halovir A in a  $3_{10}$ -helix (Figure 11). In such a conformation, regular  $\text{CO}_i\text{-NH}_{i+3}$  hydrogen bonds are expected to stabilize the tightly twisted secondary structure. If the myristoyl carbonyl were considered to be  $\text{CO}_i$ , then in a  $3_{10}$ -helical model it would be involved in a hydrogen bond with the leucine NH. Alternatively, an  $\alpha$ -helix is characterized by a series of  $\text{CO}_i\text{-NH}_{i+4}$  hydrogen bonds, and would result in the Myr CO hydrogen bonding with the valine NH. Therefore, an  $\alpha$ -helical model of halovir A does not provide a logical hydrogen bonding sequence involving the leucine amide proton.

Figure 12 shows a 3-dimensional representation of the peptide portion of halovir A in a  $3_{10}$ -helical secondary structure. The myristoyl lipophilic chain has been omitted for clarity. It is interesting to note that the model predicts an amphiphilic conformation. The polar primary amide of the Gln and Hyp hydroxyl groups align on one side of the molecule, while the leucine and leucinol lipophilic side chains arrange

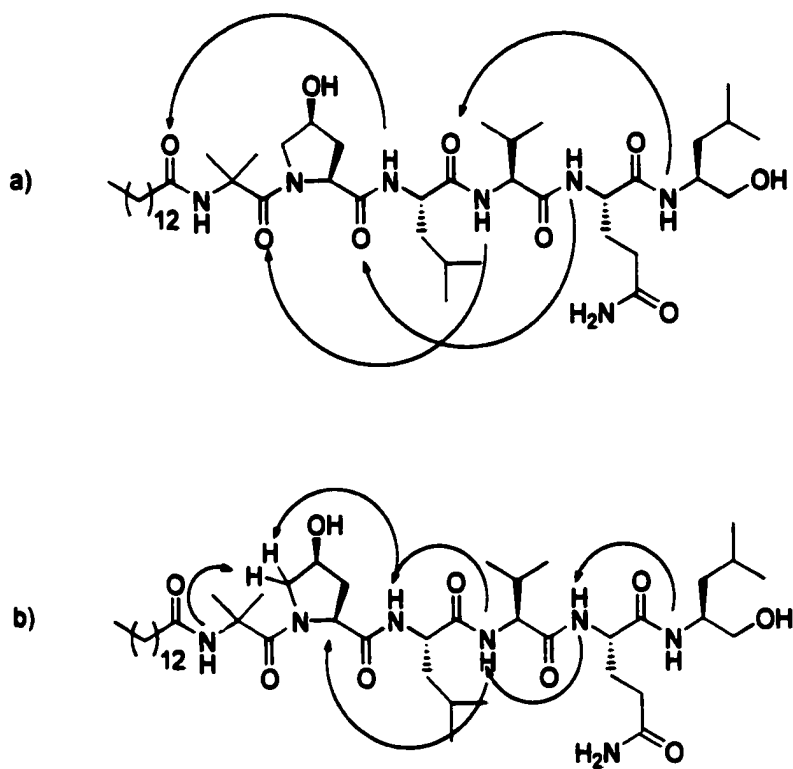


**Figure 11 (a) Proposed 3<sub>10</sub>-helical hydrogen-bonding scheme, and (b) observed ROESY correlations relevant to the helical nature of halovir A (27).**

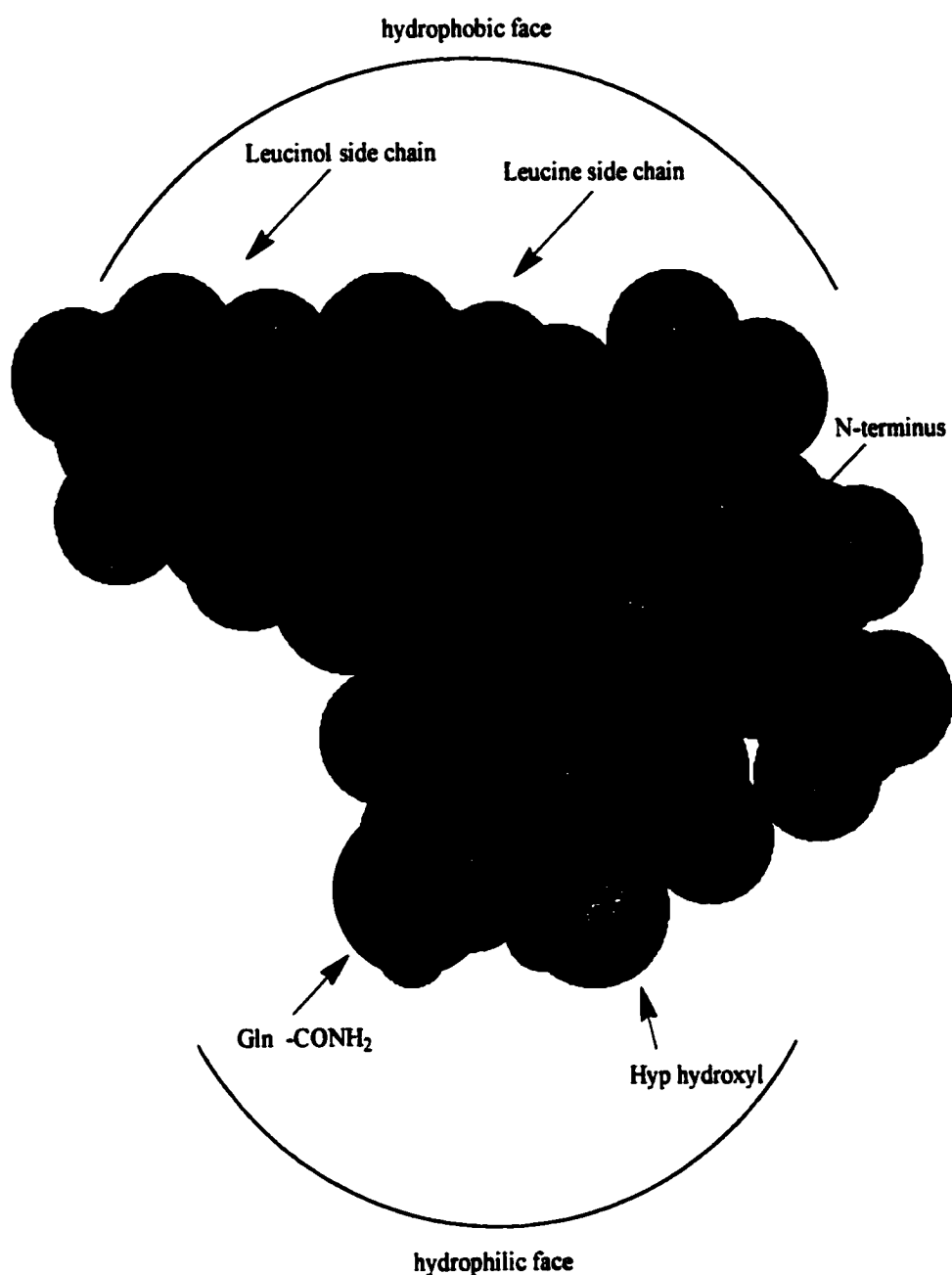


**Figure 12.** Three-dimensional space-filling model of halovir A in a  $3_{10}$ -helix formation. Twelve carbons of the myristoyl chain have been omitted for clarity. The N-terminus of the peptide backbone appears to extend furthest from the page. Hydrogen atoms appear as light blue, oxygen atoms as red, nitrogen atoms as navy blue, and carbon atoms as gray.



on the opposite side. Such conformations are common among membrane-active peptides (see later discussion).<sup>8</sup>

### **4.3 Discovery of Halovirs D-F by LC/MS Analysis**

During bioassay-guided fractionations, it is possible to overlook compounds structurally related to the active components of initial interest because they either lack activity or are masked by the presence of other compounds in the assay. The latter can be due to dilution of active constituents present only in trace quantities or else to the presence of molecules with competing bioactivities (i.e. cytotoxicity). The identification and biological evaluation of structural analogs can provide valuable information in defining the molecular features crucial for the activity of interest. Structure-Activity Relationships, or SAR, are based on comparison of the biological activities of structurally related molecules. This information can then effectively feed back into synthetic programs designed to optimize the desired biological effects of the lead compound. Therefore, it is often prudent to pursue chemical screening of “non-active” fractions for the purpose of discovering structural analogs.

In the case of the bioassay-guided fractionation of the antiviral CNL240 extract, chemical analysis of inactive fractions using C18 HPLC coupled to an electrospray mass spectrometry detector led to the discovery of three additional halovir analogs. The fraction yielding these compounds contained metabolites slightly more polar in nature than halovirs A-C and had previously displayed cytotoxic activity in the Vero cell assay. This cytotoxicity was potent enough to prevent detection of antiviral activity. Figure 13 shows a HPLC chromatogram of the fraction with the y-

axis as a function of the total ion current measured in the mass detector. The compounds were separated on an analytical C18 HPLC column using a gradient of 5->100% MeCN (1% CH<sub>3</sub>COOH) in H<sub>2</sub>O over 20 minutes. Under these conditions the halovirs A- C had been determined to elute at longer retention times. As labeled in the figure, one peak in the chromatogram measured  $[M + H^+]$  and  $[M + Na^+]$  molecular ions of 838.5 and 860.5 indicating a molecular weight equivalent to that of halovir B. Two other peaks displayed ions consistent with compound molecular weights of 810 and 821. Even taken alone, such molecular weights would warrant further investigation to evaluate if these compounds were halovir structural analogs. However, optimization of the capillary and fragmentor voltages allowed for more detailed analysis of the unknowns by their fragmentation patterns (Figure 14).

When compared to the fragmentation patterns observed for pure halovirs A-C analyzed under identical conditions, the unknowns clearly contained related peptide segments. In the example shown in Figure 14, the ions 571, 494, 593, and 721 matched ions corresponding to the C-terminal peptapeptide segment of halovir A. Similar analysis indicated that the 810 and 821 molecular ions were derived from compounds structurally related to halovirs B and C, respectively. The mass differences of 28 in the molecular ions should then be associated with structural differences in the Aib-myristoyl portion of the molecules. This might be accounted for by substitution of a glycine for the Aib or, alternatively, a C12 lauroyl *N*-acylation. Unfortunately, a distinction between these two could not be unambiguously made due to a lack of further characteristic ions. Also, since the HPLC peaks do not guarantee

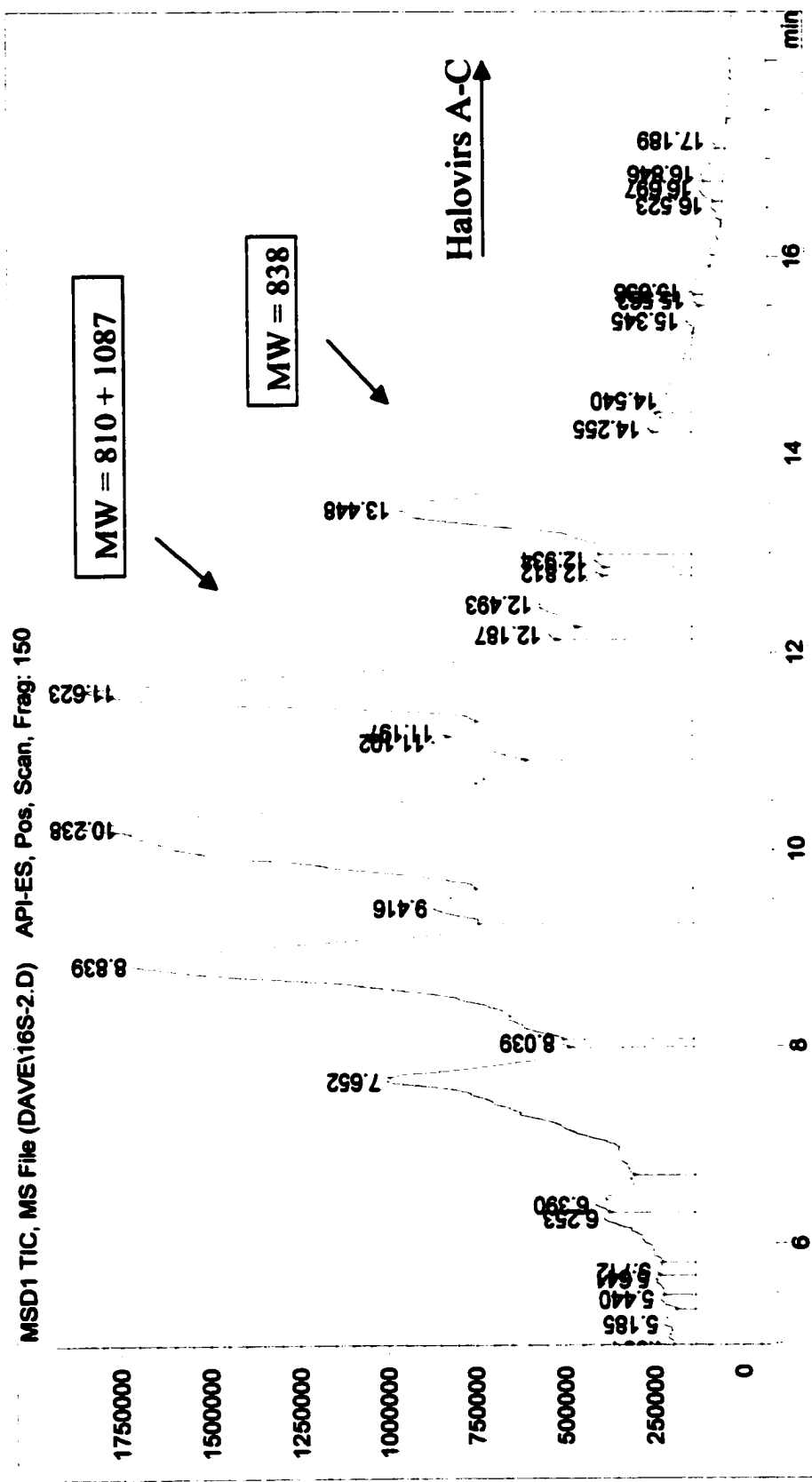


Figure 13. LC/MS chromatogram of a CNL240 fraction containing the halovirs D-F. The y-axis is a measure of the total ion current entering the mass detector.

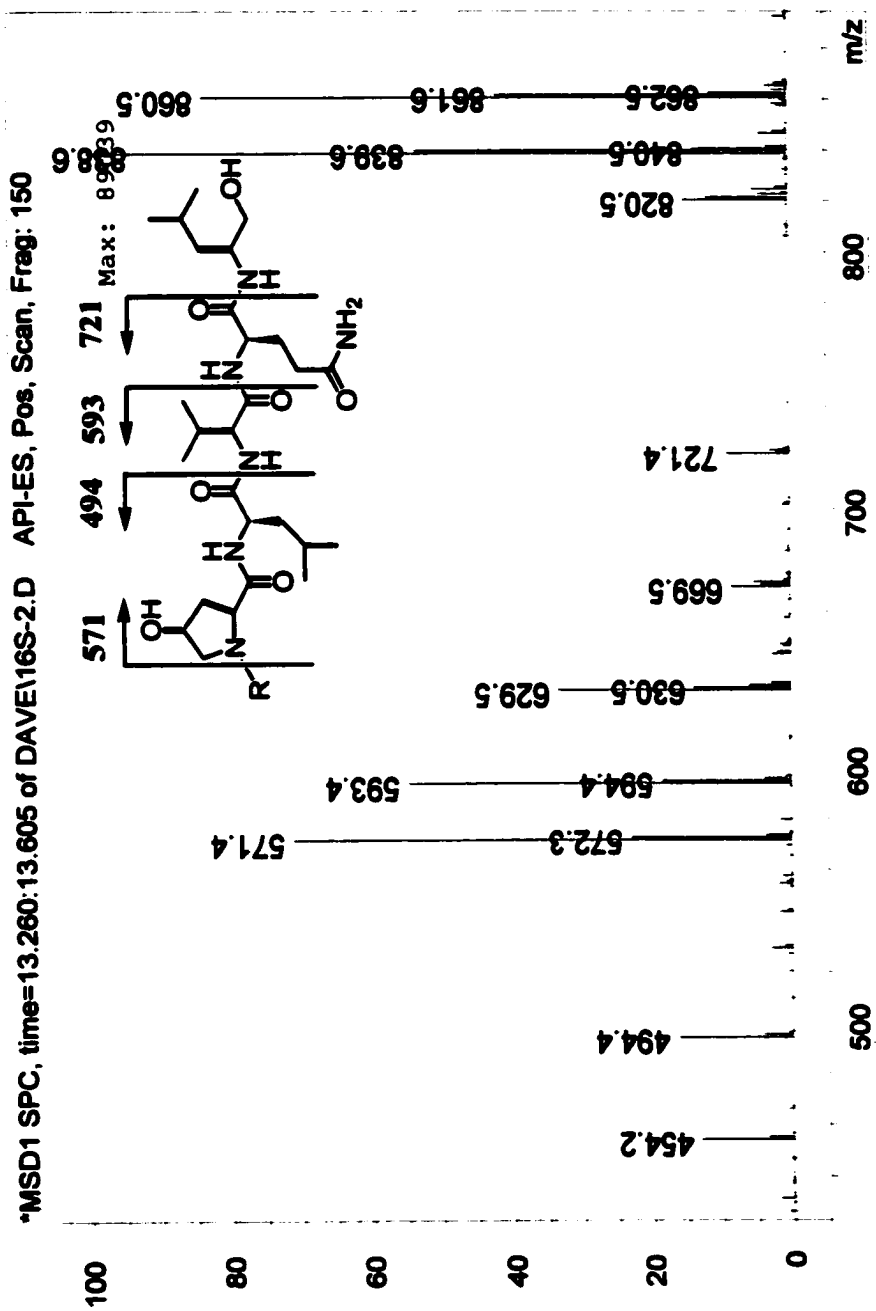
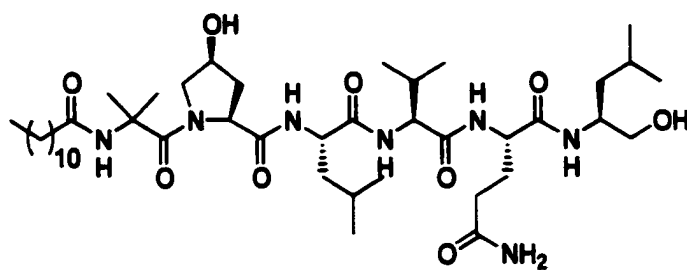
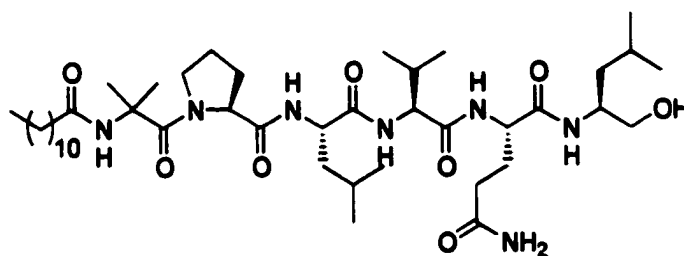


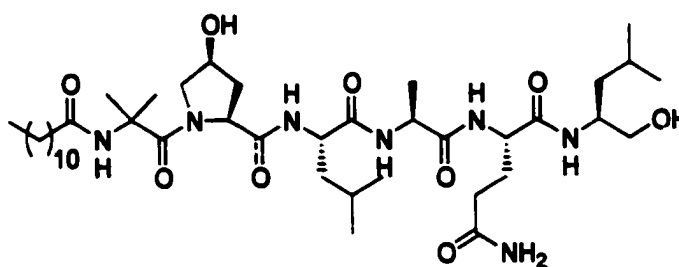
Figure 14. Mass chromatogram showing molecular ions and fragmentation peaks for halovir D during an LC/MS experiment. The 838.6 and 860.5 peaks correspond to the  $[M + H]^+$  and  $[M + Na]^+$  molecular ions, respectively.



30



31



32

Figure 15. The structures of the halovir peptides D (30), E (31), and proposed F (32).

Table 7.  $^1\text{H}$  and  $^{13}\text{C}$  NMR Assignments for Halovir D (30) in  $\text{DMSO}-d_6$ .

Amino acid		$\delta^{13}\text{C}^a$	$\delta^1\text{H}^b$	C mult	m, J (Hz)
Lol	1	63.8	3.30, 3.16	$\text{CH}_2$	m
	2	48.6	3.77	CH	m
	3	39.8	1.30	$\text{CH}_2$	m
	4	24.1	1.58	CH	m
	5	21.8	0.80	$\text{CH}_3$	d
	6	20.7	0.79	$\text{CH}_3$	d
	NH		7.10		d, 9.2
	OH		4.57		bt
Gln	1	170.3		C	
	2	52.9	4.09	CH	m
	3	27.8	1.80	$\text{CH}_2$	m
	4	31.6	2.05	$\text{CH}_2$	m
	5	173.2		C	
	NH <sub>2</sub> NH		7.23, 6.73 7.46		s d, 8.4
Val	1	170.1		C	
	2	58.8	4.00	CH	m
	3	29.4	2.08	CH	m
	4	19.1	0.86	$\text{CH}_3$	d
	5	18.3	0.87	$\text{CH}_3$	d
	NH		7.29		d, 8.4
Leu	1	172.5		C	
	2	52.5	4.00	CH	m
	3	39.0	1.70	$\text{CH}_2$	m
	4	24.5	1.57	CH	m
	5	23.5	0.82	$\text{CH}_3$	d
	6	23.1	0.87	$\text{CH}_3$	d
	NH		7.91		d, 6.8
Hyp	1	172.4		C	
	2	61.0	4.38	CH	dd, 8
	3	36.8	2.13, 1.60	$\text{CH}_2$	m
	4	68.9	4.26	CH	m
	5	56.3	3.71, 3.23	$\text{CH}_2$	m
	OH		5.16		bs
Aib	1	173.1		C	
	2	55.6		C	
	3	26.0	1.34	$\text{CH}_3$	s
	4	23.5	1.36	$\text{CH}_3$	s
	NH		8.70		s
Myr	1	172.7		C	
	2	34.6	2.20	$\text{CH}_2$	m
	3	24.8	1.48	$\text{CH}_2$	m
	4	31.3	1.22	$\text{CH}_2$	m
	5-10	28.7-29.0	1.22	$\text{CH}_2$	m
	11	22.1	1.22	$\text{CH}_2$	m
	12	14.0	0.85	$\text{CH}_3$	t

a) 100 MHz b) 300 MHz Assignments by DEPT and HMQC methods.

Table 8.  $^1\text{H}$  and  $^{13}\text{C}$  NMR Assignments for Halovir E (31) in  $\text{DMSO-}d_6$ .

Amino acid		$\delta^{13}\text{C}^a$	$\delta^1\text{H}^b$	C mult	m, J (Hz)
Lol	1	63.8	3.16, 3.28	$\text{CH}_2$	m
	2	48.6	3.75	CH	m
	3	39.6	1.30	$\text{CH}_2$	m
	4	24.1	1.60	CH	m
	5	23.5	0.86	$\text{CH}_3$	d
	6	19.2	0.87	$\text{CH}_3$	d
	NH		7.11		d, 8.8
	OH		4.56		bs
Gln	1	170.3		C	
	2	52.9	4.07	CH	m
	3	27.8	1.78	$\text{CH}_2$	m
	4	31.6	2.05	$\text{CH}_2$	m
	5	173.3		C	
	NH <sub>2</sub>		7.21, 6.72		s
	NH		7.45		d, 7.6
Val	1	170.1		C	
	2	58.6	4.02	CH	m
	3	29.5	2.08	CH	m
	4	20.6	0.83	$\text{CH}_3$	d
	5	18.3	0.88	$\text{CH}_3$	d
	NH		7.28		d, 8.4
Leu	1	172.5		C	
	2	52.6	4.02	CH	m
	3	38.3	1.75	$\text{CH}_2$	m
	4	24.6	1.54	CH	m
	5	23.2	0.81	$\text{CH}_3$	d
	6	21.8	0.90	$\text{CH}_3$	d
	NH		7.91		d, 7.2
Pro	1	172.4		C	
	2	62.4	4.29	CH	dd, 8
	3	28.7	2.20, 1.59	$\text{CH}_2$	m
	4	25.5	1.82	$\text{CH}_2$	m
	5	48.2	3.75, 3.28	$\text{CH}_2$	m
Aib	1	172.5		C	
	2	55.7		C	
	3	26.1	1.36	$\text{CH}_3$	s
	4	23.4	1.34	$\text{CH}_3$	s
	NH		8.71		s
Myr	1	172.8		C	
	2	34.7	2.20	$\text{CH}_2$	m
	3	24.8	1.51	$\text{CH}_2$	m
	4	31.3	1.22	$\text{CH}_2$	m
	5-10	28.7-29.0	1.22	$\text{CH}_2$	m
	11	22.1	1.26	$\text{CH}_2$	m
	12	14.0	0.84	$\text{CH}_3$	t

a) 100 MHz b) 300 MHz Assignments by DEPT and HMQC methods.

analysis of single molecular entities, some caution must be taken in assigning significance to peaks.

Preparatory-scale purification was undertaken using C18 HPLC and leading to the isolation of the lesser abundant analogs halovirs D (30) and E (31). Insufficient material prevented isolation of the putative halovir F (32) which was only present in trace amounts. Analysis of the  $^1\text{H}$  and  $^{13}\text{C}$  NMR spectra immediately identified the congeners as containing an Aib residue. Therefore, halovirs D and E are analogs of A and C, respectively, containing a lauric acid moiety on the nitrogen terminus (Figure 15).

#### 4.4 Biological Properties of the Halovir Peptides

The halovirs possess potent *in vitro* activity against herpes simplex virus-1 (Figure 16). Halovirs A, B, and C display  $\text{IC}_{50}$  values of approximately 1  $\mu\text{M}$  when added to cells which had been previously infected with HSV-1 for one hour. Halovirs D and E, possessing a slightly shorter lipophilic chain, were slightly less active with  $\text{IC}_{50}$ 's of 2 and 3  $\mu\text{M}$ , respectively. These values were determined by averaging at least ten replicates. All of these molecules also demonstrated cytotoxicity against uninfected Vero cells, as well as against human colon tumor cells (HCT-116).

Variations of the standard assay were designed and executed in order to investigate the nature of the antiviral activities of these peptides. Halovir A was studied as a representative compound due to its more abundant culture production. Two initial assays were designed to determine whether the peptides might be directly inactivating HSV-1. Figure 17 shows the result of pre-incubating infectious HSV-1



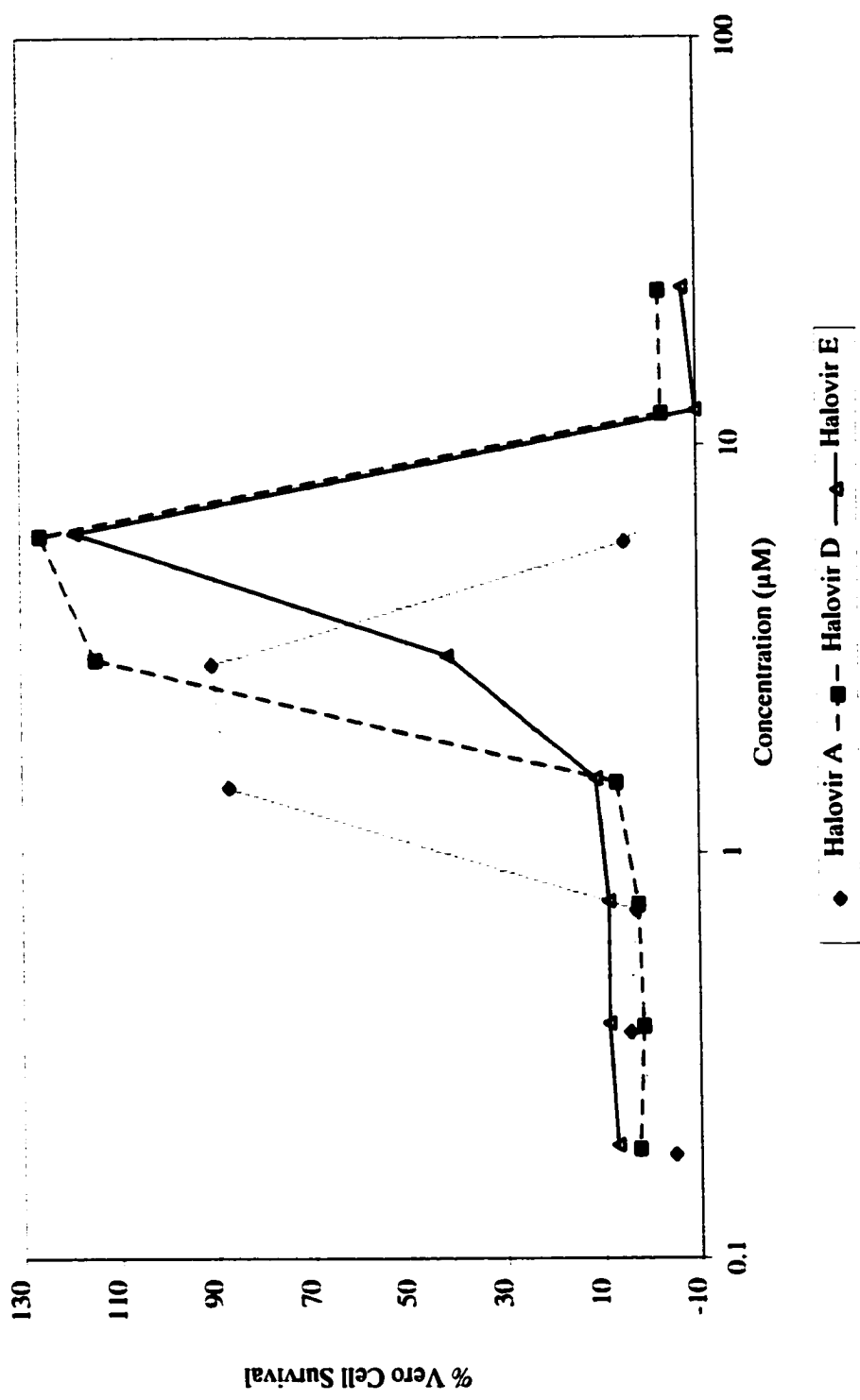
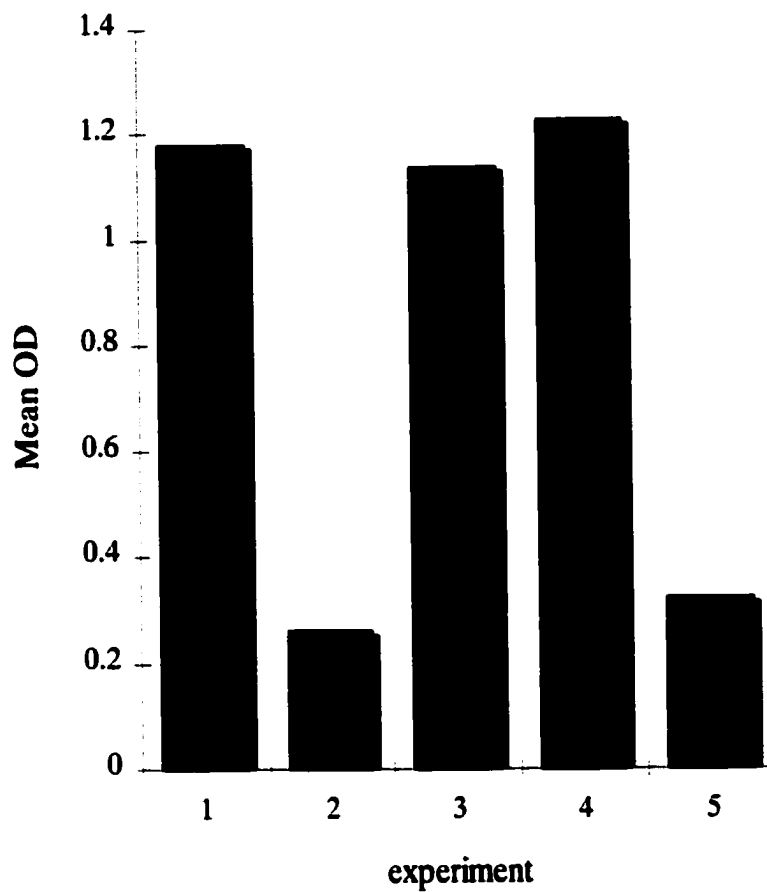


Figure 16. Comparative antiviral activities of halovir A, D, and E against HSV-1 in pre-infected Vero cells.



**Figure 17. Inactivation study of halovir A (27) versus HSV-1. After 2.5 hours, the solutions from each experiment were added to Vero cells and incubated for five days. Experiment 1 pre-incubated HSV-1 with 0.85  $\mu$ M halovir A. Experiment 2 pre-incubated virus with DMSO carrier and represents total cell death due to virus. Experiment 3 contained only media with DMSO and represents 100% cell survival. Experiment 4 contains 0.85  $\mu$ M halovir A. Experiment 5 represents the results of treating pre-infected cells with 0.85  $\mu$ M halovir A.**

with halovir A prior to addition to cells. A suspension of HSV-1 at 50,000 pfu/mL was exposed to 150 µg/mL of compound for 2.5 hours, then diluted 100-fold and added to Vero cells in microtiter plates (experiment 1). Control experiments included virus processed identically in the absence of halovir A (experiment 2), and media identically handled but with no virus or compound (experiment 3). Additionally, media spiked with halovir A was used to assess compound cytotoxicity (experiment 4), and a “normal assay” was conducted to test for halovir potency on cells pre-infected with virus for one hour (experiment 5). The final assay concentrations of 27 were 0.85 µM, and the results were monitored after 5 days of incubation. The experiment clearly demonstrated the virucidal effect of halovir A on HSV-1. Nearly 100% cell survival was achieved by pre-exposing the virus to compound. Column 5 demonstrates that 0.85 µM of 27 is insufficient to effectively protect cells pre-infected with HSV-1. Therefore, the major antiviral effects are achieved prior to cell infection. Further, no appreciable cell cytotoxicity was witnessed at this assay concentration.

A second assay was designed to explore the concentration and time dependence of the viral inactivation process. In this experiment, viral suspensions consisting of 500 pfu/mL of HSV-1 in microtiter plates were treated with serial dilutions of halovir A ranging from 10 down to 0.08 µg/mL. The plates were then incubated for 0, 15, 30, and 60 minutes prior to addition of the virus to cells. The results were again recorded after five days. Figure 18 shows that halovir A inactivates HSV-1 in a time dependent manner. IC<sub>50</sub> values decrease with the longer pre-incubation times, with the maximum effects being reached after approximately one hour.

The virucidal effects of halovirs A-C were compared in a 30-minute inactivation assay. Figure 19 shows that each of the peptides potently inhibits cell death with  $IC_{50}$  values around 0.5  $\mu$ M. However, small variations in the peptide chain affect the cell toxicity profile, and thus the *in vitro* therapeutic index, of these antiviral agents. Halovir B displays a markedly lower cytotoxicity than A in this assay, while C is somewhat more cytotoxic than A. It is also interesting to note the apparently high levels of percent cell survival attained in this and other assay. Perhaps the halovirs promote cell growth over the course of the assay. Alternatively, if the halovir peptides are indeed membrane active, they may be facilitating increased levels of MTS uptake, leading to higher optical density readings at the assay conclusion. However, this remains an unresolved issue.

A variation of the time-dependent inactivation experiment involved the removal of compound and unattached virus after 3 hours (Figure 20). In the above assays, the compound exerts a cytotoxic effect at moderately higher doses than is observed for the antiviral activity. Since the peptides remain in contact with the cells over the course of five days, I was interested to know whether the virus could be inactivated in a short time frame with subsequent removal of the compound, thereby preventing the cytopathic effects. Three hours after the treated viral suspensions were added to the Vero cells, the test wells were aspirated and washed with PBS, aspirated again and overlaid with MEM (1% FBS). The results show that the antiviral activities are not significantly attenuated in this study. The compound cytotoxic properties are somewhat reduced, but not entirely eliminated. This would suggest that the toxic effects are incurred shortly after cell exposure, or else that significant cellular uptake

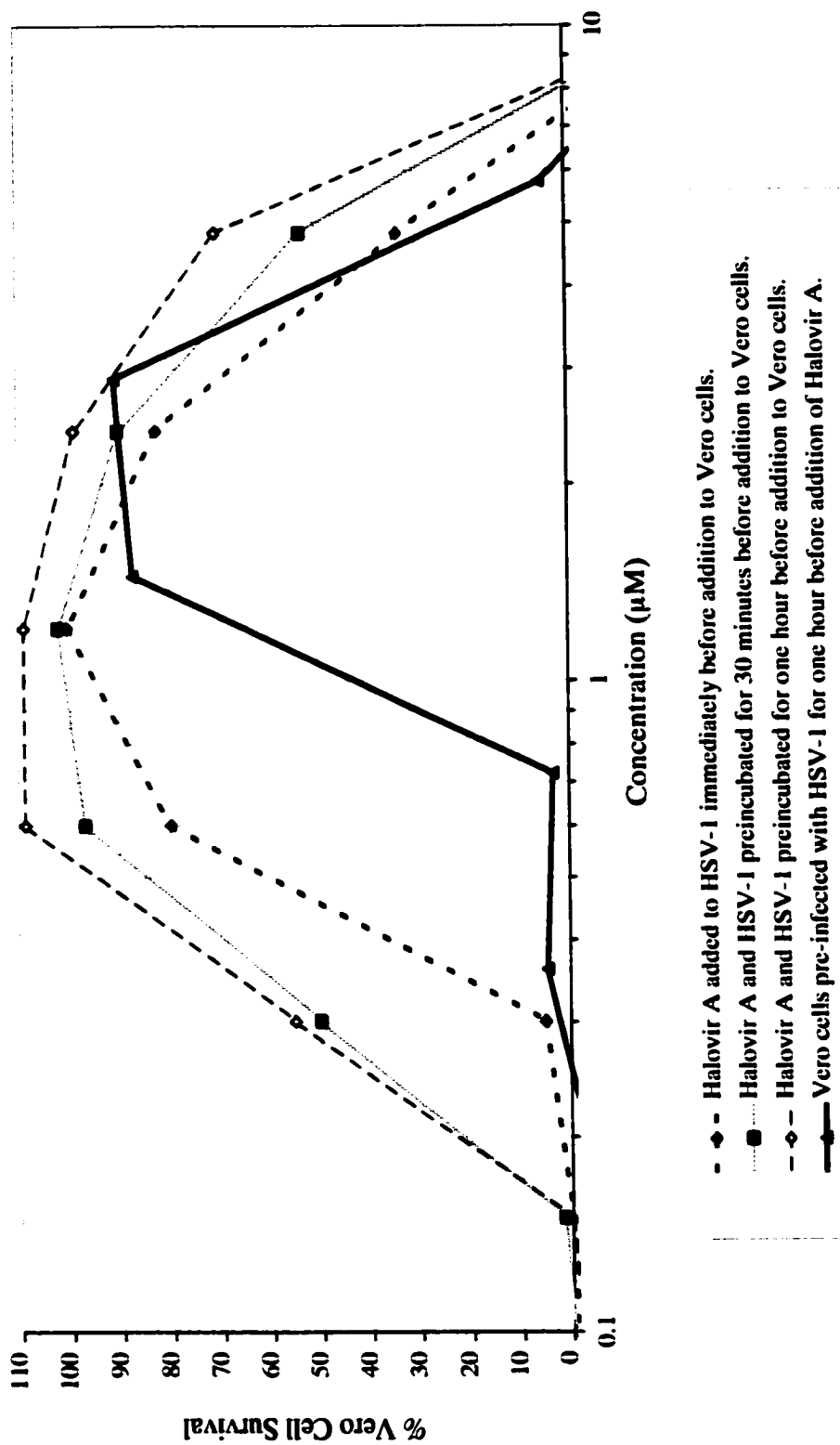


Figure 18. Time and concentration dependent inactivation of HSV-1 by halovir A (27).

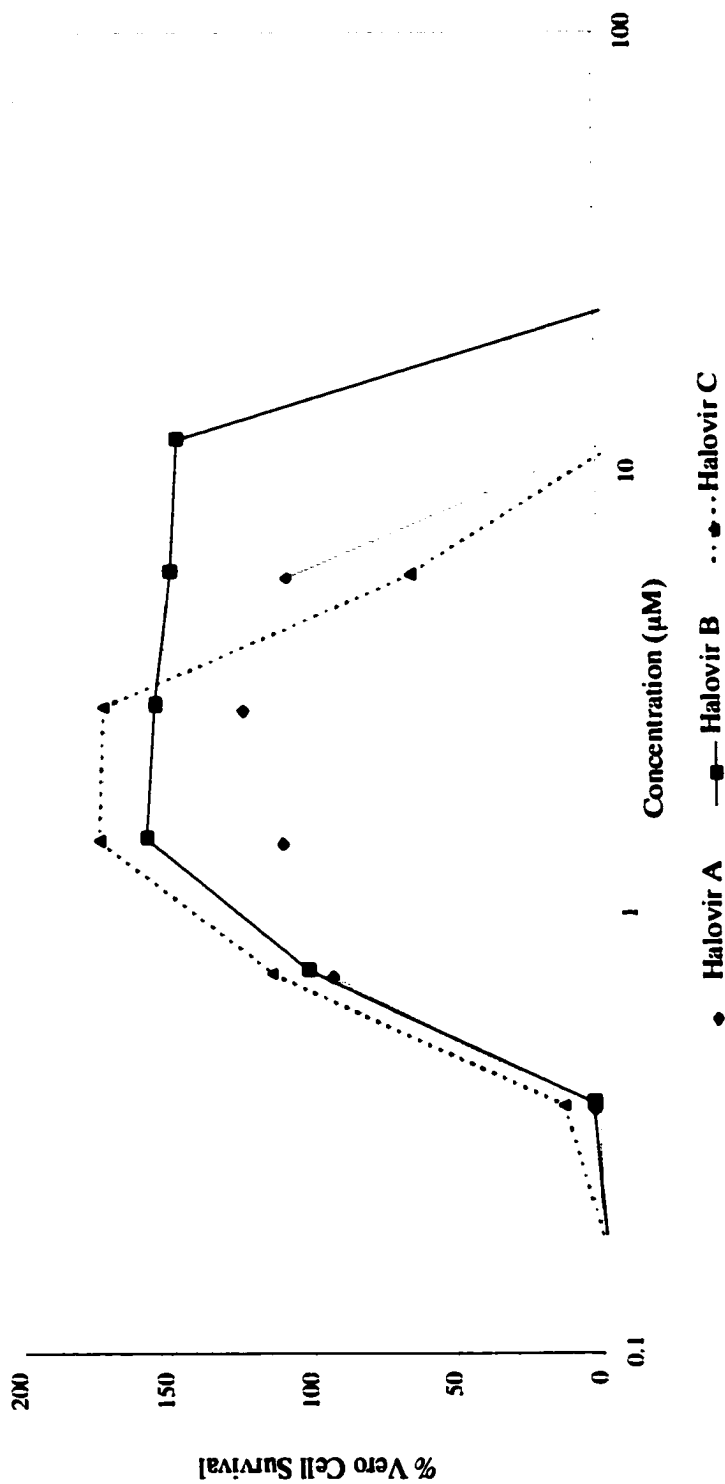


Figure 19. Comparison of virucidal activities of halovir A, B, and C. Compound and HSV-1 were pre-incubated for 30 minutes.

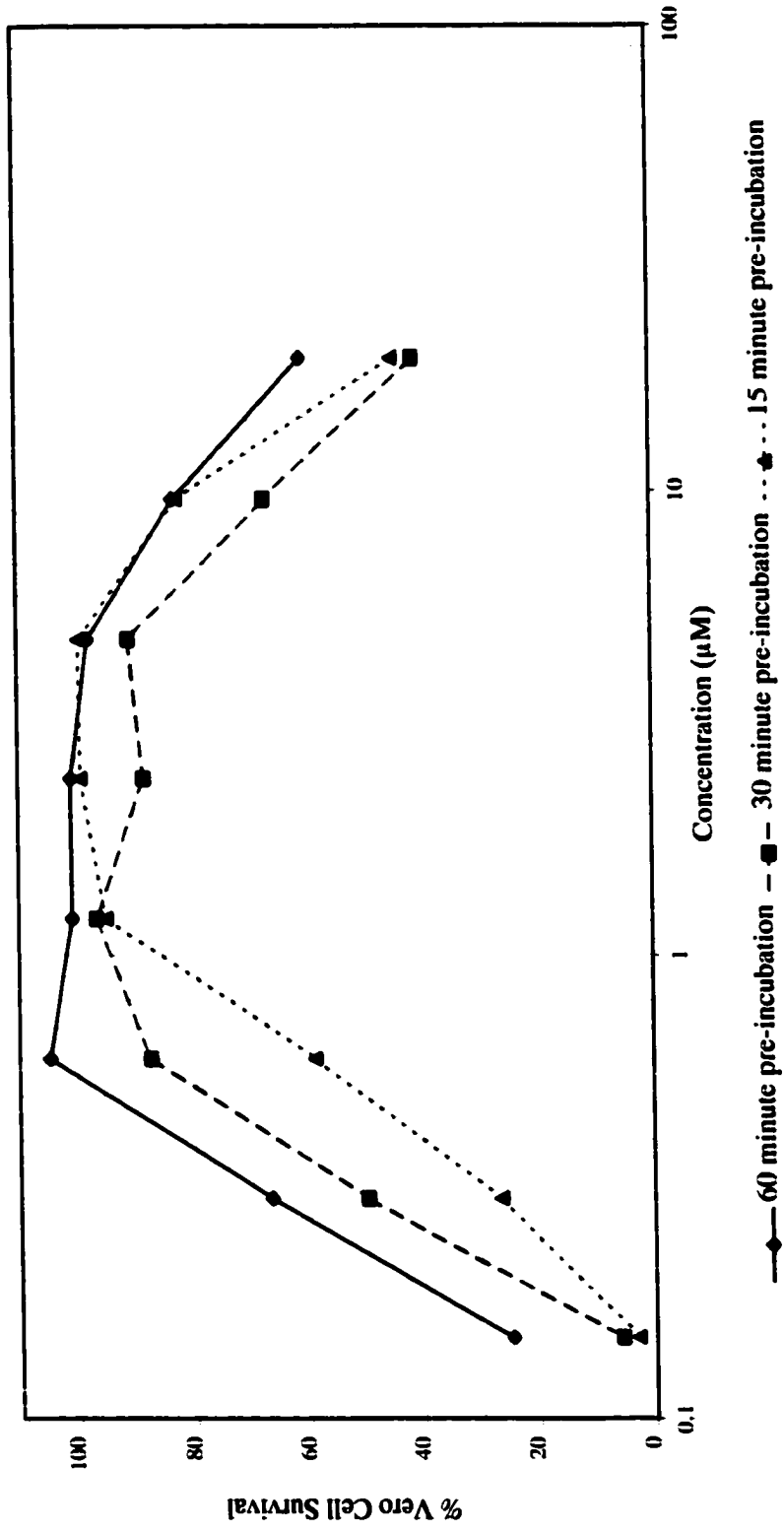


Figure 20. Time dependent inactivation of HSV-1 by incubation with halovir A with subsequent removal of drug. Unabsorbed compound and unattached virus was removed from Vero cells after 3 hours.

of the compounds occurs in the three hour period leading to the observed toxicity after five days.

A fifth assay probed the effects of pre-incubating the Vero cells with compound prior to the addition of the virus. Such an assay might indicate if there are alternate mechanisms by which halovir A exerts an antiviral effect against HSV-1. Serial dilutions of **27** were added to cells in microtiter plates and incubated for 30, 60, 120, or 240 minutes. The media was then aspirated, the cells washed with PBS, and 50 pfu HSV-1 added to test wells. The effects were quantified using the MTS method after five days. Figure 21 shows that a much more modest antiviral effect was achieved in this assay. However, pre-treatment of the cells with 20  $\mu\text{M}$  of compound for at least one hour provided 100% cell survival.

The specificity of this antiviral activity was investigated in several assays. Experiments to test for activity against HSV-2 were conducted at MDS Pharma Services, formerly MDS Panlabs, a biotechnology company. Halovir A was determined to equally inhibit replication of HSV-1 and HSV-2 with an  $\text{IC}_{50} < 0.3 \mu\text{M}$  (Figure 22) in a standard plaque reduction assay.<sup>9</sup> Halovirs A and B were evaluated in the anti-HIV screen conducted at the National Cancer Institute. The assay involves the killing of T4 lymphocytes by HIV, and is designed to detect agents that inhibit any stage of the viral reproductive cycle.<sup>10</sup> The compounds were tested in ten-fold serial dilutions at eight concentrations starting with  $1.00 \times 10^{-4}$  M. Unfortunately, significant cytotoxicity was encountered in this screen ( $\text{IC}_{50} = 5.7 \mu\text{M}$ ), and no antiviral activity was observed. Halovirs A and B were submitted to the National Cancer Institute for testing in the 60 tumor cell line panel and displayed non-selective



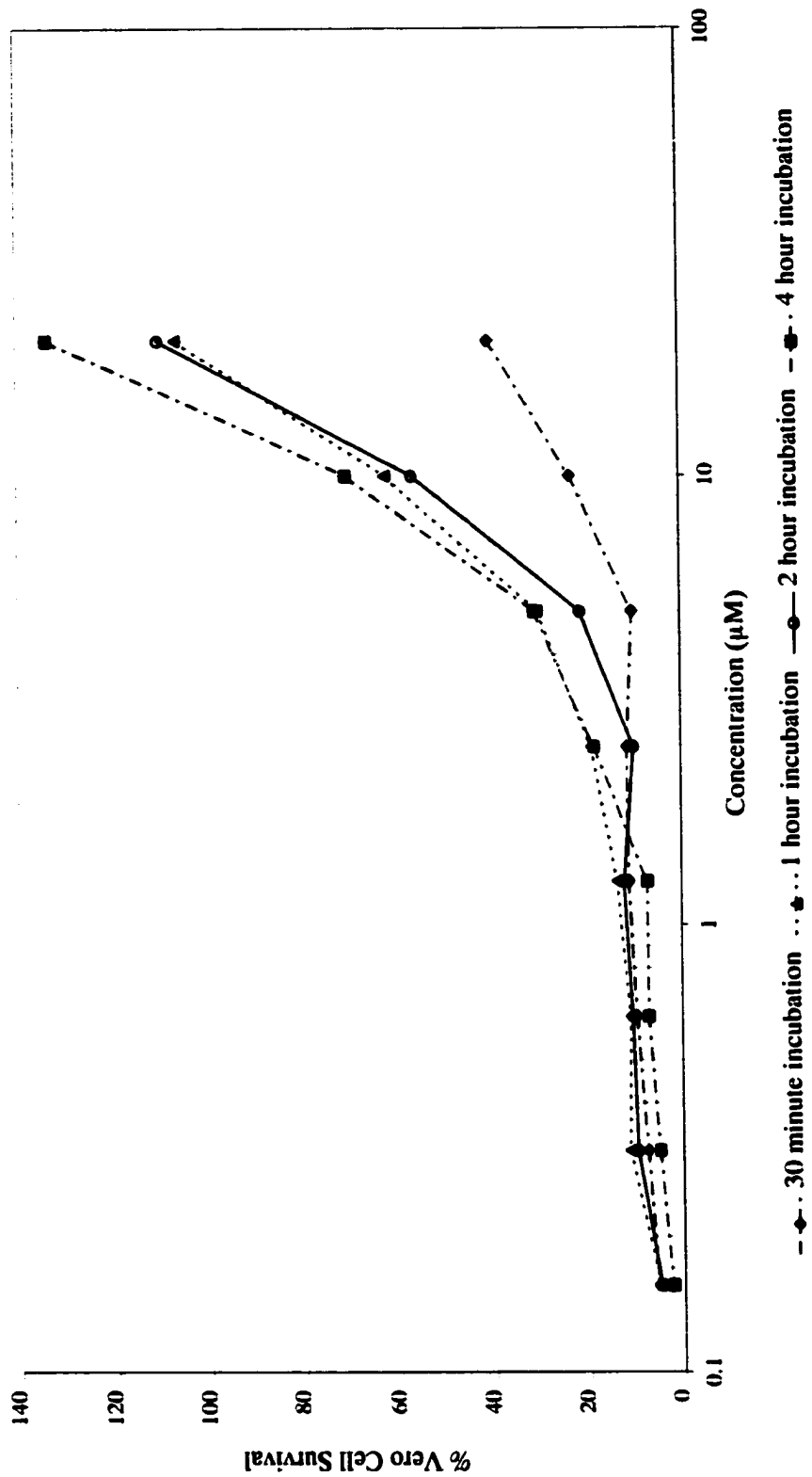


Figure 21. Pre-incubation of halovir A with Vero cells prior to infection with HSV-1.

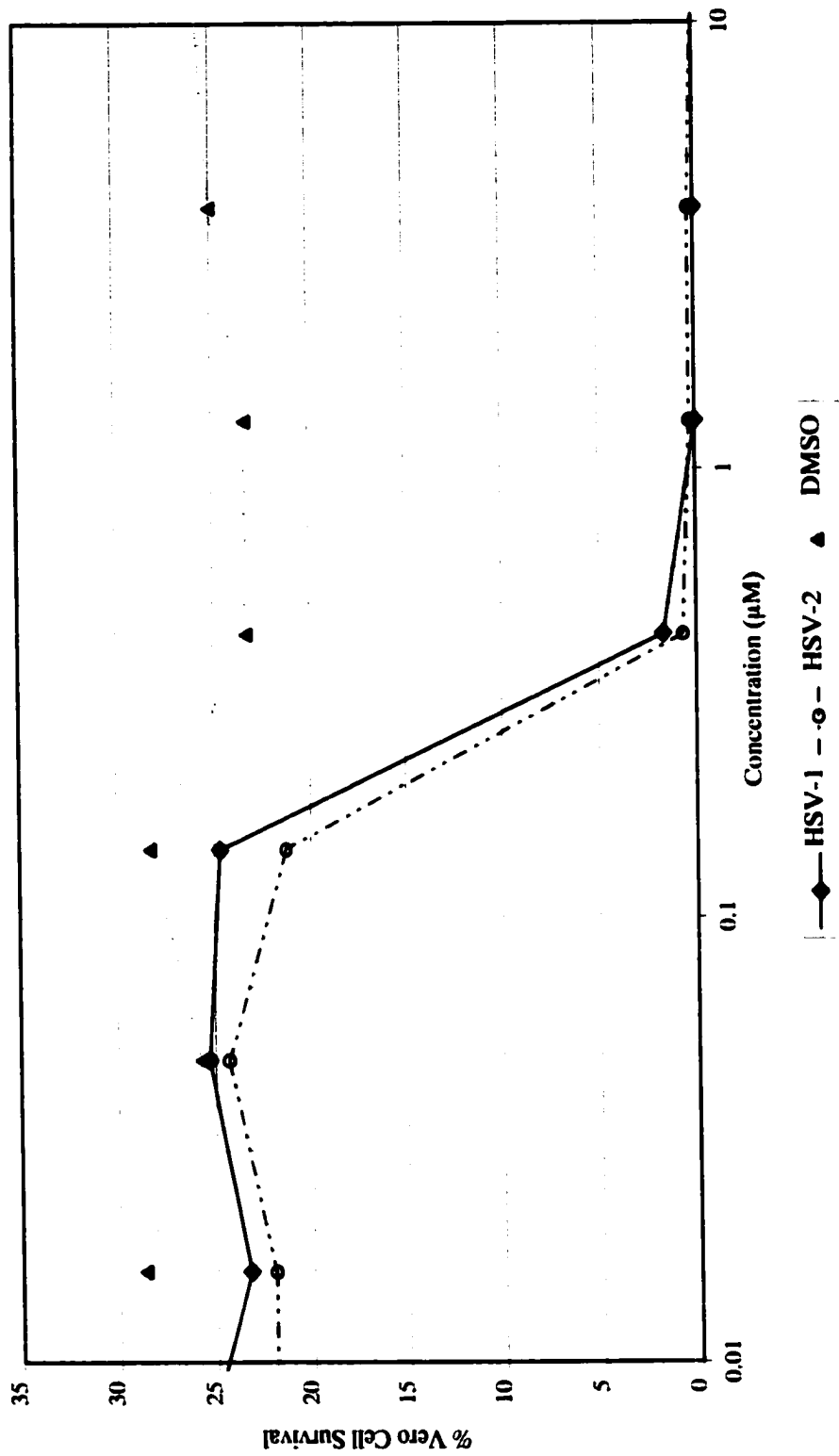


Figure 22. Plaque assay of halovir A against herpes simplex viruses 1 and 2.

cytotoxic activities between 10 and 20 $\mu$ M. The halovirs were inactive against the MCV topoisomerase and HIV integrase assays conducted in the Bushman laboratory at the Salk Institute for Biological Studies.

#### 4.5 Discussion

A series of linear, lipophilic hexapeptides, designated halovirs A-F, have been isolated from the laboratory cultivation of a marine fungal isolate identified as a *Scytalidium* sp.. Although these are short peptides, hydrogen-bonding evidence, coupled with NOE experiments, suggest a  $3_{10}$ -helical secondary structure leading to an overall amphipathic character. The halovirs demonstrate activity against both serotypes of the herpes simplex virus in cell-based assays at low micromolar concentrations. Time and concentration dependent inactivation of HSV-1 has been shown, strongly suggesting a virucidal mechanism of action.

The presence of an Aib residue likely contributes to the helical nature of the halovirs. The additional  $\alpha$ -methyl group of Aib restricts the allowed regions of conformational space to those favorable for helices,<sup>11</sup> and Aib has been shown to stabilize  $3_{10}$ - and  $\alpha$ -helical peptide conformations.<sup>12</sup> Analysis of Aib-containing peptides of varying lengths indicates that  $3_{10}$ -helices are preferred for peptides with eight or less residues,<sup>12</sup> likely due to the stabilizing effect of the additional hydrogen bond present in the more tightly wound configuration.<sup>13</sup>

Other peptides have been reported to directly inactivate the herpes simplex virus, all of which differ from the halovirs by their charged nature. MCP-1 and MCP-2 are highly cationic, 33 amino acid residue polypeptides isolated from rabbit

leukocytes that inactivate several enveloped viruses including HSV-1 and HSV-2, Vesicular stomatitis virus, and influenza.<sup>14</sup> Inactivation of HSV-1 by MCP-1 and -2 was dependent upon peptide concentration, ineffective at temperatures below 20° C, and optimum at a pH of 6.<sup>14</sup> The magainins are another group of cationic peptides with HSV-1 inactivating capability. Originally isolated from the skin of the African clawed frog *Xenopus laevis*, synthetic derivatives of this class that are lysine rich show modest virucidal activities between 12.5 and 50 µg/mL.<sup>15</sup>

Synthetic polyhistidine, polylysine, and polyarginine peptides, all of highly cationic character, have also been demonstrated to possess HSV inactivating properties.<sup>16</sup> Polyhistidines require a minimum chain length of at least 24 residues with optimum activities achieved at longer lengths, and activity is highly dependent on a pH between 5 and 6. Polylysine and polyarginine show slightly better activities at higher pH between 7 and 8. The optimum pH difference between these inhibitors likely stems from the differences in the pKs of histidine, lysine, and arginine residues. At neutral pH or higher, the imidazole side chain of histidine, with a pK<sub>a</sub> of around 6, would only be minimally charged and would be unable to bind to negatively charged surfaces of an HSV virion.<sup>16</sup> These peptides are only mildly potent, however, displaying inactivating properties at concentrations of 100 µg/mL.

Saturated fatty acids have also been demonstrated to possess antiviral activities.<sup>17</sup> Myristic and lauric acids are inhibitors of HSV-1 and vesicular stomatitis virus (VSV) at concentrations of 16 and 10 mM, respectively. Shorter or longer saturated fatty acids are less active. The unsaturated linoleic (18:2) and arachidonic (20:4) fatty acids are somewhat more active at 3.6 and 1.6 mM concentrations.

Incubation of intact VSV virions with 0.5 mg/mL of linoleic acid caused leakage of the viral envelopes. The halovirs are more active by a factor of  $10^4$  than the free fatty acids. Clearly, the hexapeptide portion is critical to the potent virucidal nature of these molecules, perhaps by intensifying the interaction of the inhibitors with the viral envelope.

The halovirs share structural similarities with a group of fungal metabolites known as the lipopeptaibols. In 1992, Auvin-Guette and coworkers reported the isolation of trichogin A IV from a fermentation of the fungus *Trichoderma longibrachiatum* undergoing sporulation.<sup>18</sup> The peptide was determined to have a mixed  $3_{10}$ - and  $\alpha$ -helical solution conformation, with the *N*-terminal region folding into a  $3_{10}$ -helix, and the central and *C*-terminal portions adopting a mainly  $\alpha$ -helical structure.<sup>18,19</sup> The proposed conformation of this molecule leads to an overall amphiphilic character, with the hydrophobic residues Leu, Ile, Lol, and the lipophilic chain on one side of the helix, and the less hydrophobic Gly residues on the more polar face. Like many other helical, amphiphilic peptides, trichogin A IV displays membrane-modifying properties in a carboxy-fluorescein leakage model.<sup>20</sup> Larger peptides, such as the 19-residue alamethicin, have been demonstrated to induce aqueous leakage of liposomes, putatively by forming ion-channels across the membrane.<sup>12</sup> However, the length of the trichogin peptide chain is too short to span a lipid bilayer and form conductance channels. Thus, the mode of action of this membrane-active peptide is not clear.

**Trichogin A IV: Oct-Aib-Gly-Leu-Aib-Gly-Gly-Leu-Aib-Gly-Ile-Lol**

Monaco and coworkers studied the interaction of trichogin A IV with phospholipid membranes by electron spin resonance (ESR) experiments involving synthetic analogs.<sup>19,21,22</sup> Nitroxide spin-labeled analogs were prepared by substituting Aib residues with TOAC (2,2,6,6-tetramethylpiperidine-1-oxyl-4-amino-4-carboxylic acid). ESR spectra of double spin labeled peptides are diagnostic of peptide conformation, and can discriminate between  $3_{10}$ - and  $\alpha$ -helical geometries. Double substitutions of TOAC for Aib did not influence the helical geometry of trichogin, and the identical membrane modifying properties were retained.<sup>19</sup> To study the orientation of trichogin with respect to the membrane bilayers, analysis of the hyperfine interaction of the radical with the nitrogen nucleus allowed for the determination that the peptide is oriented parallel to the membrane surface. The hydrophobic face of trichogin is imbedded in the membrane interior and the glycine-rich side is exposed to the surrounding water.<sup>22</sup> The octanoyl chain is proposed to be anchored in the lipid membrane.

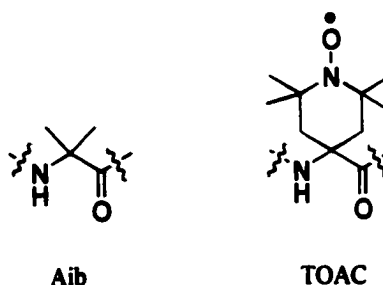


Figure 23. Structure of Aib and TOAC residues.

Another study assessed the ability of trichogin analogs with single TOAC substitutions to quench the fluorescence of phospholipid bilayers labeled with the

fluorophore BODIPY (4,4-difluoro-4-bora-3a,4a-diaza-S-indecene).<sup>21</sup> The fluorophore was covalently linked to a phospholipid so as to reside at different depths within the bilayer. The results of this study supported the concept that trichogin A IV does not penetrate membrane bilayers deeply, but rather orients itself along the surface. This orientation is consistent with a “carpet-like” mechanism of action for membrane destabilization.<sup>21</sup> This mechanism proposes peptide helices to float on membrane surfaces with the hydrophilic residues extended outward toward the aqueous surroundings. The exact nature of how the physical properties of the membrane are altered to allow for greater permeability has not been clarified.

Halovir A may interact with the lipid envelope of the HSV virus in a manner analogous with the proposed mechanism of action of trichogin A IV. Structurally, these peptides are neutrally charged, lipophilic, helical, and amphiphilic. Trichogin has a slightly longer peptide segment, but a shorter lipophilic chain. Membrane destabilization of the viral envelope by halovir A would be consistent with a direct inactivation mechanism, as evidenced by the non-specific interactions of the charged peptides discussed above. In this instance, the viral particle would perhaps be more sensitive to membrane disruptions than live cells. Greater membrane permeability might also explain why percent survival measurements of greater than 100% are observed for Vero cells treated with the halovir peptides. If more MTS reagent is able to penetrate the cell membranes during the work-up procedure, then a proportionally higher percentage will be metabolized by the mitochondria, thus leading to an overestimation of the percent cell survival.

Other lipopeptaibols have been reported. The trikoningins KB I and II are lipopeptides closely related to trichogin A IV produced by the fungus *Trichoderma koningii*.<sup>23</sup> Although the structure of KB I only differs from A IV by the replacement of the leucines at positions 3 and 7 with valine residues, this molecule was 25-fold less active in the carboxy-fluorescein leakage model. The authors suggest that this is due to the decreased hydrophobicity of valine versus leucine, leading to an overall reduced interaction with the lipid membranes. The trikoningins also possess modest antibacterial activity against *Staphylococcus aureus*, but were inactive against *Escherichia coli*. The trichodecinins-I and -II are lipopeptaibols derived from a seven amino acid peptide chain N-acylated with a (Z)-4-decenoyl group.<sup>24</sup> No biological activities were reported for these molecules. The hydrophilic moieties found in the halovirs should be expected to increase their overall amphiphilicity.

Trikoningin KB I: nOct-Aib-Gly-Val-Aib-Gly-Gly-Val-Aib-Gly-Ile-Lol

Trikoningin KB II: nOct-D-Iva-Gly-Val-Aib-Gly-Gly-Val-Aib-Gly-Ile-Lol

Trichodecinin-I: (Z)-4-decenoyl-Gly-Gly-Leu-Aib-Gly-Ile-Lol

Trichodecinin-II: (Z)-4-decenoyl-Gly-Gly-Leu-Aib-Gly-Leu-Lol

The lipopeptaibols are related to a larger class of peptides termed the peptaibols. These channel forming molecules are linear, typically 14-20 amino acids in length, and are characterized by a reduced carboxyl terminus, a high percentage (up to 50%) of Aib residues, and an acetylated N-terminal amino acid.<sup>12</sup> As already mentioned, Aib is strongly helicogenic, and structural studies on these peptides have



shown that they reside in amphiphilic, helical conformations. The majority of residues form 1 ← 5 (i.e.  $\alpha$ -helical) H-bonds, but deviations including 1 ← 4 (i.e.  $3_{10}$ ) H-bonds are also observed. Peptaibols contain at least one central proline residue, occasionally hydroxylated, and usually neighboring an Aib, which induces a kink in the in the helical structure. It has been proposed that this kink may have a dynamic role in the membrane modifying properties of the peptaibols, acting as a molecular hinge to allow movement between the N- and C-terminal helical segments. This flexibility may help facilitate insertion of the peptides into lipid membranes during channel formation.<sup>12</sup>

Unlike the above lipopeptaibols, the halovirs contain an Aib-Pro dipeptide segment common to the larger peptaibols. The studies here indicate that halovir peptides form a continuous helical chain in DMSO. However, other investigations have shown that the exact conformations of short Aib-containing peptides are sensitive to the polarity of their environment.<sup>25</sup> Therefore, alternate conformations of the halovirs are possible in hydrophobic environments, such as in the presence of a lipid bilayer. Although the Aib-Pro segment could act as a hinge between the fatty acyl chain and the remainder of the peptide portion, it is not immediately apparent why this should be necessary since the saturated hydrocarbon already has inherent flexibility.

Peptaibols such as alamethicin are noted for their ability to alter membrane permeability by forming ion channels. The channels are formed by intermolecular aggregation of multiple peptides. The membrane modifying properties of the peptaibols are likely responsible for their reported biological properties, including antibiotic activity<sup>23,26</sup> and the uncoupling of oxidative phosphorylation.<sup>27</sup> The peptavirins A and B are 19-amino acid peptaibols that display inhibitory activity

against infection of the tobacco plant *Nicotiana tabacum* by the tobacco mosaic virus at concentrations around 10  $\mu\text{g/mL}$ .<sup>28</sup> To my knowledge, no peptaibols or lipopeptaibols have been recognized for their ability to selectively inactivate membrane-enveloped viruses such as HSV-1.

Extensive biological evaluation is required to fully assess the potential of the halovirs as antiviral agents. Further studies to elucidate the exact mechanism of action are needed. Additional *in vitro* testing against a range of other viruses, and especially enveloped viruses such as HIV and CMV, is warranted to explore the specificity of the observed activity. Also, many *in vivo* animal models are well established for the evaluation of antiviral agents against herpesvirus infections. A guinea pig or mouse model for HSV vaginitis might be particularly applicable in this case, especially to assess the potential of the halovirs to inhibit sexual transmission. Vaginal microbicides are currently needed in order to help halt transmission of HIV, HSV, and other sexually transmitted diseases.<sup>29</sup>

#### 4.6 Experimental

General. Proton and  $^{13}\text{C}$  NMR spectra were recorded at 300 MHz and 100 MHz, respectively. NMR spectra were recorded in pyridine-*d*<sub>5</sub> or DMSO-*d*<sub>6</sub>. DEPT experiments were used to determine the number of attached protons, and all carbon assignments were consistent with DEPT results. HMBC and HMQC experiments were optimized for  $^nJ_{\text{CH}} = 4, 6, 8, \text{ and } 10 \text{ Hz}$  and  $^1J_{\text{CH}} = 150 \text{ Hz}$ , respectively. ROESY experiments were recorded in DMSO-*d*<sub>6</sub> and used a mixing time of 300 ms. HPLC separations were accomplished using a Rainin DYNAMAX-60Å C18 column (250 x

10 mm) at a flow rate of 3 mL/min with refractive index detection. Electrospray ionization mass spectrometry was completed on either a HP 1100 MSD or Finnigan LCQ mass spectrometers.

Bioassay-Guided Isolation of the Halovirs A-C. The crude mycelial extract was fractionated by high speed counter-current chromatography using a solvent system composed of 10% hexanes, 30% EtOAc, 30% MeOH, and 30% H<sub>2</sub>O. The upper layer of the biphasic system was used as the mobile phase. The third of five fractions tested positive for antiviral activity and was further fractionated by reversed-phase silica gel chromatography using 10% → 0% H<sub>2</sub>O in MeOH as the eluant. The fifth of seven fractions was subjected to silica column chromatography using 5% → 20% MeOH in DCM. Reversed-phase HPLC (C18 Dynamax, of antiviral fractions 2-4 using 7% H<sub>2</sub>O in MeOH yielded pure **27** (231 mg), **28** (41 mg), and **29** (28 mg).

Halovir A (**27**) was obtained as a colorless, non-crystalline solid (12 mg/L fermentation yield): HRFABMS [M+Na]<sup>+</sup> obsd *m/z* 888.6119; calcd 888.6150 for C<sub>45</sub>H<sub>43</sub>N<sub>7</sub>O<sub>9</sub>Na (Δ 3.5 ppm); [α]<sub>D</sub> -13° (c 0.73, MeOH); UV (MeOH) λ<sub>max</sub>, nm (log ε), 226 (2.58). IR(neat) 3284, 2920, 1643, 1537 cm<sup>-1</sup>. See Table 5 for <sup>1</sup>H and <sup>13</sup>C NMR spectral data.

Halovir B (**28**) was obtained as a colorless, non-crystalline solid (2 mg/L fermentation yield): HREIMS [M+Cs]<sup>+</sup> obsd *m/z* 970.4954; calcd 970.4994 for C<sub>43</sub>H<sub>79</sub>N<sub>7</sub>O<sub>9</sub>Cs (Δ 4.1 ppm); [α]<sub>D</sub> -8° (c 0.25, MeOH), UV (MeOH) λ<sub>max</sub>, nm (log ε), 225 (3.01). IR(neat) 3282, 2928, 1637, 1541 cm<sup>-1</sup>. See Table 5 for <sup>1</sup>H and <sup>13</sup>C NMR spectral data.

Halovir C (29) was obtained as a colorless, non-crystalline solid (1.5 mg/L fermentation yield): HREIMS  $[M+Cs]^+$  obsd  $m/z$  982.5320; calcd 982.5357 for  $C_{45}H_{83}N_7O_8Cs$  ( $\Delta$  3.8 ppm);  $[\alpha]_D -20^\circ$  (c 0.38, MeOH); UV (MeOH)  $\lambda_{max}$ , nm (log  $\epsilon$ ), 227 (2.90). IR(neat) 3282, 2928, 1637, 1536  $cm^{-1}$ . See Table 5 for  $^1H$  and  $^{13}C$  NMR spectral data.

Halovir D (30) was obtained as a colorless, non-crystalline solid: MALDI-FTMS  $[M+Na]^+$  obsd  $m/z$  860.5828; calcd 860.5831 for  $C_{43}H_{79}N_7O_9Na$  ( $\Delta$  0.3 ppm);  $[\alpha]_D -27^\circ$  (c 0.28, MeOH); IR(neat) 3281, 2926, 1641, 1542, 1419  $cm^{-1}$ . See Table 7 for  $^1H$  and  $^{13}C$  NMR spectral data.

Halovir E (31) was obtained as a colorless, non-crystalline solid: MALDI-FTMS  $[M+Na]^+$  obsd  $m/z$  844.5856; calcd 844.5882 for  $C_{43}H_{79}N_7O_8Na$  ( $\Delta$  3.1 ppm);  $[\alpha]_D -14^\circ$  (c 0.42, MeOH); IR(neat) 3272, 2926, 2855, 1651, 1538  $cm^{-1}$ . See Table 8 for  $^1H$  and  $^{13}C$  NMR spectral data.

Acid Hydrolysis of 1-3 and Chiral GC Analysis. Peptides 1 (5.6 mg), 2 (1.8 mg), and 3 (0.6 mg) were each dissolved in 1 mL of 6N HCl and heated to 105°C for 15 hours in sealed vials. After solvent evaporation under a stream of  $N_2$  at 105 °C, the crude hydrolysates were treated with isopropyl alcohol (1 mL) and acetyl chloride (250  $\mu$ L), sealed, and heated to 105 °C for one hour. The crude products were concentrated under  $N_2$  at 105 °C, cooled to ambient temperature, treated with pentafluoropropionic anhydride (250  $\mu$ L) in  $CH_2Cl_2$  (1 mL), sealed, and heated to 110 °C for 20 minutes. The vials were cooled to ambient temperature and concentrated under a stream of  $N_2$ . The derivatized hydrolysates were dissolved in  $CH_2Cl_2$  at a

concentration of 1 mg/mL, and 100  $\mu$ L aliquots were injected onto a Chirasil-Val capillary column, which was ramped upwards from 90  $^{\circ}$ C at 4  $^{\circ}$ C/minute. Elution times were measured by GC-FID and compared to derivatized amino acid standards prepared identically. Halovir A (27) was identified as being composed L-leucine, L-valine, and L-glutamine. Halovir B (28) included L-alanine in the place of L-valine. Halovir C (29) was identified to contain L-proline.

Preparation of Carboxylic Acid Derivative of Halovir A, Acid Hydrolysis, and Chiral GC Analysis. Compound 27 (7.9 mg, 9.0  $\mu$ mol) was dissolved in 2 ml acetone at ambient temperature and treated dropwise with Jones reagent until a brown color persisted for 5 minutes. A vigorous reaction was initially observed. (Jones reagent was prepared by dissolving 0.67 g of  $\text{CrO}_3$  in 19 mL of distilled  $\text{H}_2\text{O}$  and adding 5.8 mL of  $\text{H}_2\text{SO}_4$  at  $0^{\circ}\text{C}$ .) The reaction was quenched with 0.5 mL of *i*-PrOH, and then partitioned between 25 mL each of EtOAc and  $\text{H}_2\text{O}$ . The phases were separated and the aqueous phase was further extracted with 2x25 mL of EtOAc. The combined organic phases were dried over  $\text{Na}_2\text{SO}_4$ , filtered, and concentrated *in vacuo*. The desired compound was semi-purified by C18 reversed-phase HPLC using 10% aqueous MeCN with 0.1% TFA. This synthetic product was more polar than the starting peptide, and a distinctive peak in the  $^1\text{H}$  NMR spectrum was observed at 12.3 ppm. The carboxylic acid was subjected to acid hydrolysis, amino acid derivatization, and chiral GC-FID analysis as described above. The hydrolysate was identified as containing only L-leucine by comparison and co-injection with standards. This result indicates that the leucinol moiety of halovir A (27) corresponds to the reduced form of L-leucine.

**Preparation of (R)-MTPA ester of Halovir A.** A solution of **27** (8.5 mg, 9.8  $\mu\text{mol}$ ) in 500  $\mu\text{L}$  of  $\text{CH}_2\text{Cl}_2$  was treated with 10 equivalents of (S)-MTPA chloride (18.3  $\mu\text{L}$ , 98  $\mu\text{mol}$ ), diisopropylethylamine (35  $\mu\text{L}$ , 200  $\mu\text{mol}$ ), and a catalytic amount of DMAP. The reaction was stirred at ambient temperature under  $\text{N}_2$  for 15 hours. The solution was concentrated *in vacuo*, and the crude product was subjected to C18 reversed-phase HPLC using 2.5%  $\text{H}_2\text{O}$  in MeOH to yield 9.6 mg of the desired product (75%).

$^1\text{H}$  NMR (300 MHz, pyridine- $d_5$ ) 9.70 (s, 1H), 8.61 (d, 6.0, 1H), 8.16 (d, 7.8, 1H), 8.04 (s, 1H), 8.03 (d, 7.2, 1H), 7.92 (d, 7.2, 1H), 7.81 (d, 7.5, 2H), 7.72 (m, 2H), 7.40-7.51 (m, 7H), 5.90 (m, 1H), 5.03 (m, 1H), 5.00 (m, 1H), 4.6-4.8 (m, 6H), 4.03 (dd, 1H), 3.76 (s, 3H), 3.58 (s, 3H), 2.60-2.94 (m, 5H), 2.52 (t, 6, 2H), 2.24-2.42 (m, 2H), 2.06 (m, 2H), 1.7-2.0 (m, 4H), 1.79 (s, 3H), 1.54 (s, 3H), 1.22-1.40 (m, 25H), 1.18 (d, 6.3, 3H), 1.12 (d, 5.1, 3H), 0.98 (d, 5.1, 3H), 0.84-0.92 (m, 9H)

**(S)-MTPA Ester.** Prepared by the same procedure as described for the preparation of the (R)-MTPA ester.  $^1\text{H}$  NMR (300 MHz, pyridine- $d_5$ ) 9.62 (s, 1H), 8.61 (d, 6.3, 1H), 8.09 (d, 7.8, 1H), 8.02 (bs, 1H), 7.93 (d, 7.5, 1H), 7.91 (d, 6.9, 1H), 7.81 (d, 7.8, 2H), 7.67 (m, 2H), 7.36-7.51 (m, 7H), 5.95 (m, 1H), 5.06 (m, 1H), 5.00 (m, 1H), 4.73 (m, 2H), 4.64 (m, 3H), 4.36 (dd, 12.9, 1H), 3.99 (dd, 12.9, 1H), 3.75 (s, 3H), 3.64 (s, 3H), 3.00 (m, 1H), 2.6-2.9 (m, 5H), 2.51 (m, 2H), 2.4 (m, 1H), 2.29 (m, 1H), 1.7-2.1 (m, 6H), 1.74 (s, 3H), 1.22-1.50 (m, 25H), 1.18 (d, 6.7, 3H), 1.13 (d, 5.7, 3H), 1.00 (d, 5.4, 3H), 0.93 (d, 6.0, 3H), 0.91 (d, 6.3, 3H), 0.89 (t, 6.9, 3H)

**Viral Inactivation Assay #1.** Five solutions were prepared as described below. All solutions were vortexed for 30 seconds and shaken at ambient temperature for 2.5

hours. They were vortexed again, and then 100  $\mu$ L of each was diluted with 9.9 mL of MEM (100x dilution). Microtiter plates had been prepared with Vero cells overnight, aspirated, washed with PBS, and aspirated again. One hundred  $\mu$ L of diluted solution 1 was added to each well of a microtiter plate. This was repeated for each of the other dilute solutions. The plates were incubated at 37 °C under 5% CO<sub>2</sub> for one hour. At that time, solution 1-4 plates were overlaid with 100  $\mu$ L of MEM (2% FBS) and incubated for 5 days. The solution 5 plate was overlaid with 100  $\mu$ L of dilute solution 4. The final test concentrations of halovir A were 0.85  $\mu$ M. After 5 days incubation, the plates were processed using the standard MTT procedure. Solution 1: HSV-1 at 50,000 pfu/ml and 150  $\mu$ g/mL Halovir A in MEM with 0.6% DMSO. Solution 2: HSV-1 at 50,000 pfu/ml in MEM with 0.6% DMSO. This is a control to measure cell death due to viral infection. Solution 3: MEM with 0.6% DMSO. This is a control to measure 100% cell survival. Solution 4: Halovir A at 150  $\mu$ g/mL in MEM with 0.6% DMSO. This is a test for cell cytotoxicity due to halovir A. Solution 5: HSV-1 at 50,000 pfu/ml in MEM with no DMSO. This solution mimics the conditions of the standard assay where cells are pre-infected for one hour.

Viral Inactivation Assay #2. This assay is a variation of the standard assay described previously. In a 96-well microtiter plate, 25  $\mu$ L aliquots of a HSV-1 suspension (3000 pfu/mL in MEM) were added to 2-fold serial dilutions of 27 prepared in 125  $\mu$ L of MEM. After incubating at room temperature for 0, 15, 30, or 60 minutes, 100  $\mu$ L of the treated suspensions were transferred to a microtiter plate containing Vero cells. These cells had been prepared overnight in the usual manner.

After a one-hour incubation at 37 °C under 5% CO<sub>2</sub>, the cells were further overlaid with 100 µL of MEM containing 2% FBS. The plates were further incubated for 5 days, and then worked-up using the MTS method. Acyclovir was used as a control.

Viral Inactivation Assay #3. This assay is carried out as above, except that the media containing unadsorbed virus and drug was aspirated after three hours of incubation with the cells. The cells were washed with PBS and aspirated, and then overlaid with 200 µL of MEM containing 1% FBS. The plates were incubated for five days, and then evaluated using the standard MTS work-up.

Vero Cell Absorption Assay. Two-fold serial dilutions of halovir A were prepared and 100 µL aliquots were added to Vero cells prepared in microtiter plates. The plates were incubated at 37 °C and 5% CO<sub>2</sub> for 30, 60, 120, or 240 minutes. Each well was then aspirated, washed with PBS and aspirated, and then overlaid with 50 pfu of HSV-1 in 100 µL of MEM. After incubating for one hour, 100 µL of MEM containing 2% FBS was added to each well, the plates were incubated for five days, and then evaluated using the standard MTS work-up. Acyclovir was used as a control.

### References

1. Graham, J.H., Hodge, N.C. & Morton, J.B. (1995). Fatty acid methyl ester profiles for characterization of glomalean fungi and their endomycorrhizae. *Appl. Environ. Microbiol.* **61**, 58-64.
2. Ohtani, I., Kusumi, T., Kashman, Y. & Kakisawa, H. (1991). High-Field FTNMR application of Mosher method - the absolute configurations of marine terpenoids. *J. Am. Chem. Soc.* **113**, 4092-4096.



3. Stevens, E.S., Sugawara, N., Bonora, G.M. & Toniolo, C. (1980). Conformational analysis of linear peptides. 3. Temperature dependence of NH chemical shifts in chloroform. *J. Am. Chem. Soc.* **102**, 7048-7050.
4. Vervoort, H., Fenical, W. & Epifanio, R.D. (2000). Tamandarins A and B: New cytotoxic depsipeptides from a Brazilian ascidian of the family Didemnidae. *J. Org. Chem.* **65**, 782-792.
5. Karle, I.L., Flippen-Anderson, J.L., Uma, K., Balaram, H. & Balaram, P. (1990). Peptide design: Influence of a gust Aib-Pro segment of the stereochemistry of an oligo-Val sequence: Solution conformations and crystal structure of Boc-(Val)2-Aib-Pro-(Val)3-OMe. *Biopolymers* **29**, 1433-1442.
6. Wüthrich, K., Billeter, M. & Braun, W. (1984). Polypeptide secondary structure determination by nuclear magnetic resonance observation of short proton-proton distances. *J. Mol. Biol.* **180**, 715-40.
7. Wüthrich, K. (1986). NMR of proteins and nucleic acids. Wiley, New York. xv, 292 pp.
8. Takahashi, S. (1990). Conformation of membrane fusion-active 20-residue peptides with or without lipid bilayers: Implication of  $\alpha$ -helix formation for membrane fusion. *Biochemistry* **29**, 6257-6264.
9. Mahy, B.W.J. & Kangro, H. (1996). Virology methods manual. Academic Press, London ; San Diego. x, 374 pp.
10. Weislow, O.S., Kiser, R., Fine, D.L., Bader, J., Shoemaker, R.H. & Boyd, M.R. (1989). New soluble formazan assay for HIV-1 cytopathic effects: Application to high-flux screening of synthetic and natural products for AIDS-antiviral activity. *J. Nat. Can. Inst.* **81**, 577-586.
11. Balaram, P. (1992). Non-standard amino acids in peptide design and protein engineering. *Curr. Opin. Struct. Biol.* **2**, 845-851.
12. Sansom, M.S.P. (1993). Structure and function of channel-forming peptaibols. *Q. Rev. Biophys.* **26**, 365-421.
13. Marshall, G.R., Hodgkin, E.E., Langs, D.A., Smith, G.D., Zabrocki, J. & Leplawy, M.T. (1990). Factors governing helical preference of peptides containing multiple alpha,alpha-dialkyl amino acids. *Proc. Nat. Acad. Sci. USA* **87**, 487-491.
14. Lehrer, R.I., Daher, K., Ganz, T. & Selsted, M.E. (1985). Direct inactivation of viruses by MCP-1 and MCP-2, natural peptide antibiotics from rabbit leukocytes. *J. Virol.* **54**, 467-472.

15. Egal, M., Conrad, M., MacDonald, D.L., Maloy, W.L., Motley, M. & Genco, C.A. (1999). Antiviral effects of synthetic membrane-active peptides on herpes simplex virus, type 1. *Int. J. Antimicrob. Agents* **13**, 57-60.
16. Docherty, J.J. & Pollock, J.J. (1987). Inactivation of herpes simplex virus types 1 and 2 by synthetic histidine peptides. *Antimicrob. Agents Chemother.* **31**, 1562-1566.
17. Thormar, H., Isaacs, C.E., Brown, H.R., Barshatzky, M.R. & Pessolano, T. (1987). Inactivation of enveloped viruses and killing of cells by fatty acids and monoglycerides. *Antimicrob. Agents Chemother.* **31**, 27-31.
18. Auvin-Guette, C., Rebuffat, S., Prigent, Y. & Bodo, B. (1992). Trichogin A IV, an 11-residue lipopeptaibol from *Trichoderma longibrachiatum*. *J. Am. Chem. Soc.* **114**, 2170-2174.
19. Monaco, V., Formaggio, F., Crisma, M., Toniolo, C., Hanson, P., Millhauser, G., George, C., Deschamps, J.R. & Flippen-Anderson, J.L. (1999). Determining the occurrence of a 3(10)-helix and an alpha-helix in two different segments of a lipopeptaibol antibiotic using TOAC, a nitroxide spin-labeled C-alpha-tetrasubstituted alpha-amino acid. *Bioorg. Med. Chem.* **7**, 119-131.
20. El Hajji, M., Rebuffat, S., Le Doan, T., Klein, G., Satre, M. & Bodo, B. (1989). Interaction of trichorzianins A and B with model membranes and with the amoeba *Dictyostelium*. *Bioch. Biophys. Acta* **978**, 97-104.
21. Epand, R.F., Epand, R.M., Monaco, V., Stoia, S., Formaggio, F., Crisma, M. & Toniolo, C. (1999). The antimicrobial peptide trichogin and its interaction with phospholipid membranes. *Eur. J. Biochem.* **266**, 1021-1028.
22. Monaco, V., Formaggio, F., Crisma, M., Toniolo, C., Hanson, P. & Millhauser, G.L. (1999). Orientation and immersion depth of a helical lipopeptaibol in membranes using TOAC as an ESR probe. *Biopolymers* **50**, 239-253.
23. Auvin-Guette, C., Rebuffat, S., Vuidepot, I., Massias, M. & Bodo, B. (1993). Structural Elucidation of Trikonigin-KA and Trikonigin-KB, Peptaibols from *Trichoderma koningii*. *J. Chem. Soc. Perk. Trans. 1* 249-255.
24. Fujita, T., Wada, S.-I., Iida, A., Nishimura, T., Kanai, M. & Toyama, N. (1994). Fungal metabolites. XIII. Isolation and structural elucidation of new peptaibols, trichodecenins-I and -II, from *Trichoderma viride*. *Chem. Pharm. Bull.* **42**, 489-494.
25. Karle, I.L., Flippen-Anderson, J.L., Sukumar, M. & Balam, P. (1988). Monoclinic polymorph of Boc-Trp-Ile-Ala-Aib-Ile-Val-Aib-Leu-Aib-Pro-OMe

- (anhydrous): Parallel packing of  $3_{10}$ -/alpha-helices and a transition of helix type. *Int. J. Pept. Prot. Res.* **31**, 567-576.
26. Ritzau, M., Heinze, S., Dornberger, K., Berg, A., Fleck, W., Schlegel, B., Haertl, A. & Graefe, U. (1997). Ampullosporin, a new peptaibol-type antibiotic from *Sepedonium ampullosporum* HKI-0053 with neuroleptic activity in mice. *J. Antibiot.* **50**, 722-728.
27. Takaishi, Y., Terada, H. & Fujita, T. (1980). The effect of two new peptide antibiotics, the hypelcins, on mitochondrial function. *Experientia* **36**, 550-2.
28. Yun, B.S., Yoo, I.D., Kim, Y.H., Kim, Y.S., Lee, S.J., Kim, K.S. & Yeo, W.H. (2000). Peptaivirins A and B, two new antiviral peptaibols against TMV infection. *Tetrahedron Lett.* **41**, 1429-1431.
29. The International Working Group On Vaginal Microbicides. (1996). Recommendations for the development of vaginal microbicides. *Aids* **10**, 1-6.

## **Chapter 5. Synthesis and Structure-Activity Relationships of the Halovirs**

### **5.1 Introduction**

Based upon the promising antiviral activity of the halovir peptides against the herpes simplex virus-1, a synthesis program was undertaken in order to more fully explore the structure-activity relationships of these molecules. Analysis of the five natural halovirs had already indicated that both the length of the fatty acyl chain and the amino acid components of the peptide impacted the antiviral potency as well as the cytotoxic properties. These observations implied that strategic manipulation of the halovir molecular scaffold via a synthetic effort might lead to more potent and selective inhibitors with increased clinical potential. Further, these manipulations would assist in elucidating the critical structural features necessary for antiviral activity. Such a synthetic effort could also supply further halovir material for advanced biological evaluations.

At the outset, three salient structural features of the general halovir structure presented themselves for chemical modification in a SAR investigation: the fatty  $N^\alpha$ -acyl substituent, the amino acid composition of the peptide segment, and the reduced carboxyl terminus. The  $N^\alpha$ -acyl chain provides substantial lipophilic character to these molecules. Since these inhibitors appear to exert their antiviral activity through direct association with the virus, one cannot discount that the hydrophobic chain might be involved in membrane association. The less potent halovirs D and E incorporate an  $N^\alpha$ -dodecanoyl substituent versus the tetradecanoyl chain found in halovirs A-C, alluding to the biological importance of the acyl substituent. Therefore, the length of

the acyl chain is worthy of investigation, as well as the effects of unsaturation to limit chain flexibility and the incorporation of polar groups to reduce lipophilicity.

The variations in the amino acid composition of halovirs A, B, and C and the associated differences in the antiviral and cytotoxic activities indicate that this portion of the molecule also modulates biological properties. Due to the amphiphilic nature and the short length of these peptides, one might suspect that even small changes to the amino acid sequence might have profound consequences. Of particular interest is the Aib-Hyp dipeptide segment. As discussed in chapter four, Aib-Pro and Aib-Hyp functionality is frequently positioned centrally in peptaibols, producing a kink in the helical nature of these molecules, and has been proposed to act as a 'molecular hinge' between the resulting two helices.<sup>1</sup> The Aib-Hyp dipeptide segment might therefore play an important role in the antiviral activities of the present molecules, possibly acting as a 'hinge' between the hydrophobic acyl chain and the remainder of the peptide.

Lastly, modification of the reduced carboxyl terminus deserves attention. This is perhaps the easiest structural feature to investigate because modifications can be accomplished via the natural product. The primary alcohol, a characteristic common to linear peptides of fungal origin, might add to the overall amphiphilic character. Hence, alternate C-terminal functionalities would provide interesting analogs.

The initial strategy was to pursue solution-phase methodologies in the construction of the core peptide sequence. This approach offered the advantage of working on a multi-gram scale that would provide additional halovir A for advanced biological evaluation. All the synthetic products of this study were subjected to

biological evaluation, and the results of those antiviral and cytotoxic tests then influenced the direction of further synthetic efforts. Therefore, biological results are presented alongside the synthetic details in this chapter. All the antiviral activities presented in this chapter were determined using the standard assay where the Vero cells are pre-infected with HSV-1 prior to addition of compound (see chapter 3.2.3).

## 5.2 Synthesis and Biological Activities of Halovir Analogs

Figure 24 outlines the construction of the core peptide sequence for halovir A. None of the peptides prepared in the synthesis of this hexapeptide intermediate displayed any antiviral or cytotoxic properties. Peptide couplings were accomplished by activation of carboxylic acids with 1-(3-dimethylaminopropyl)-3-ethylcarbodiimide (EDC), and 1-hydroxybenzotriazole (HOBt) was utilized to suppress racemization. *N*<sup>α</sup>-*t*-Butyloxycarbonyl (Boc) protected amino acids were cleaved using trifluoroacetic acid (TFA) or ethanolic HCl. As anticipated, deprotections involving ethanolic HCl involved partial transesterification of the C-terminal methyl esters to the corresponding ethyl esters. This was not a concern here since reduction of either ester to the primary alcohol, as present in the natural products, would result in the identical product. Also, the ethyl ester would provide an additional congener of the peptide scaffold.

The total synthesis of halovir A was completed as shown in figure 25. The coupling of the amine trifluoroacetate salt of **36** with myristic acid proceeded in 89% yield. The C-terminal methyl ester of compound **37** was then efficiently reduced with lithium borohydride to yield the desired target. Synthetic halovir A matched the

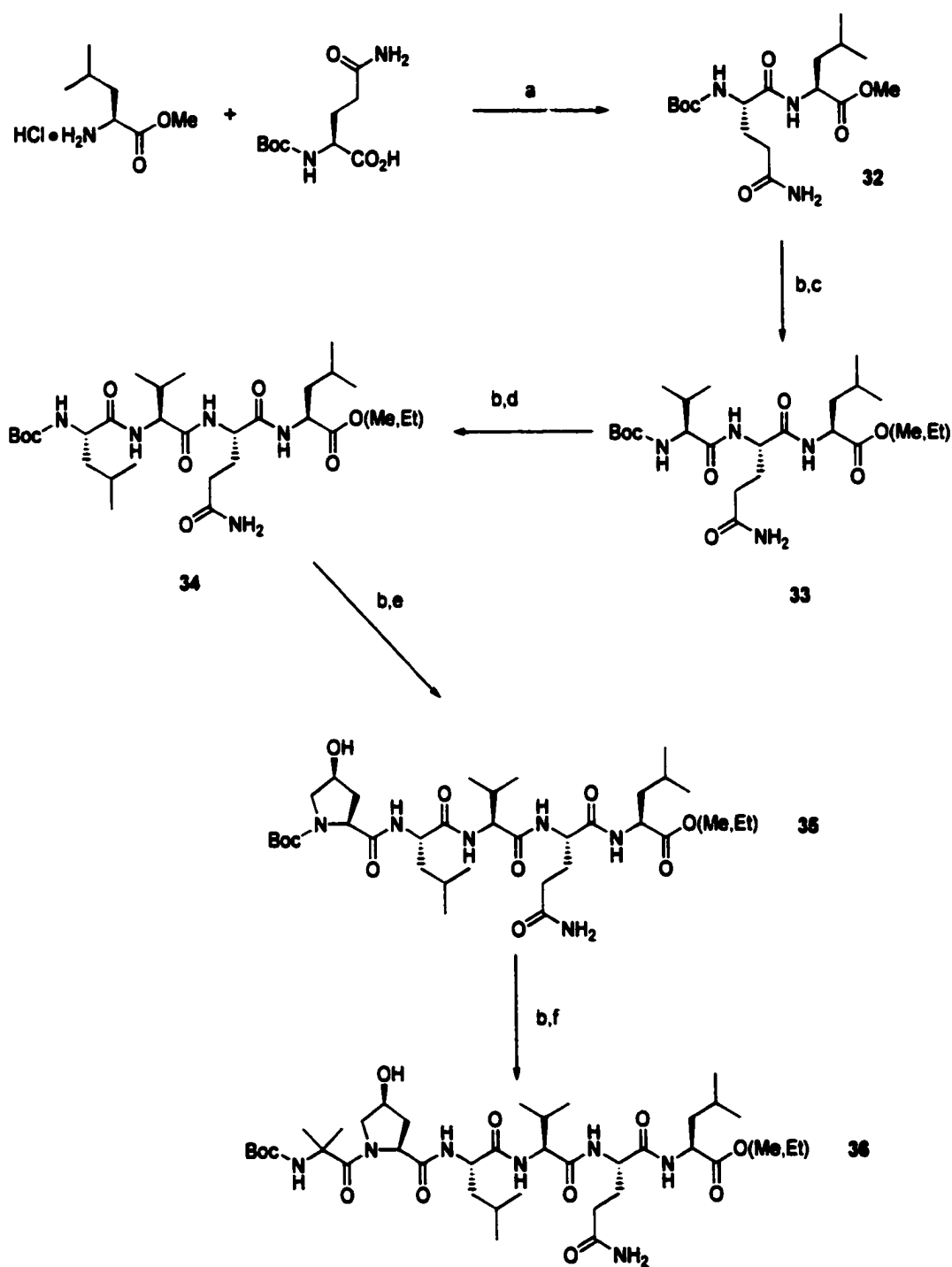
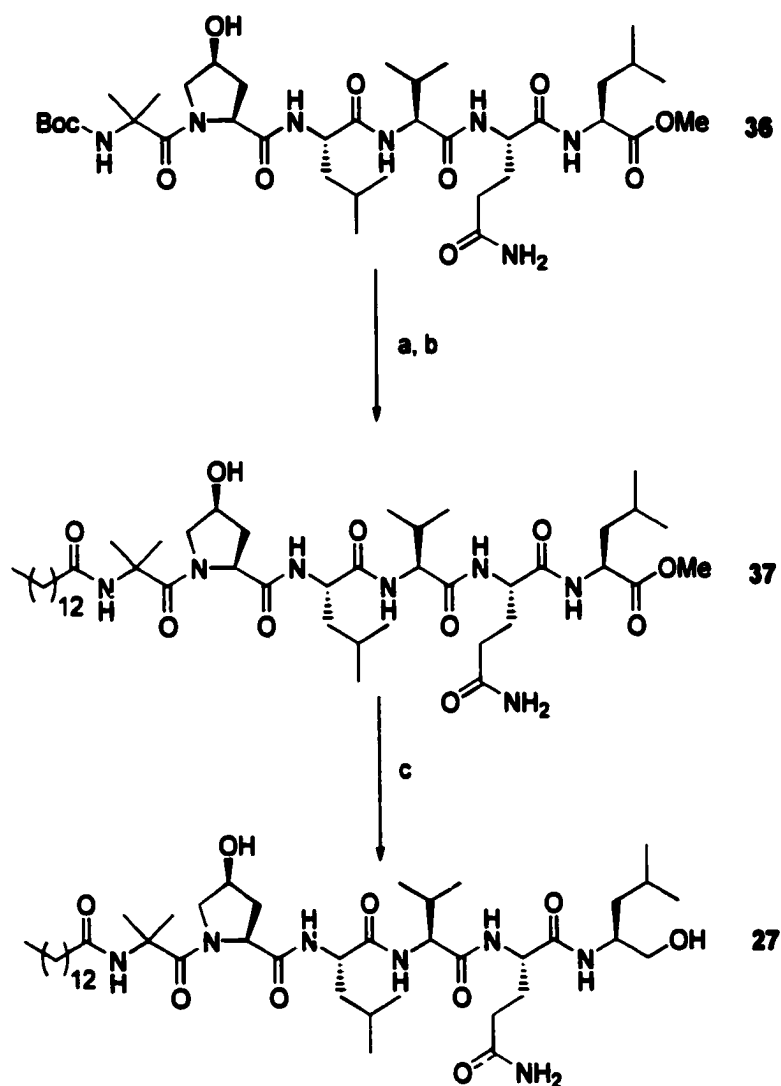


Figure 24. Synthesis of halovir A peptide fragment. *Reagents and conditions:* (a) EDC, HOBT, DIEA, MeCN, 84%; (b) HCl, EtOH, 0° to room temperature, ~ quant.; (c) *N*<sup>α</sup>-Boc-L-valine, EDC, HOBT, DIEA, MeCN, 87%; (d) *N*<sup>α</sup>-Boc-L-leucine, EDC, HOBT, DIEA, MeCN/DMF, 69%; (e) *N*<sup>α</sup>-Boc-L-trans-4-hydroxyproline, EDC, HOBT, DIEA, MeCN, 88%; (f) *N*<sup>α</sup>-Boc-aminoisobutyric acid, EDC, HOBT, DIEA, MeCN/DMF, 57%.



**Figure 25.** Completion of synthesis of halovir A. *Reagents and conditions:* (a) TFA, room temperature, ~ quant.; (b) myristic acid, EDC, HOBT, DIEA, DMF, 89%; (c)  $\text{LiBH}_4$ , THF, 82%.



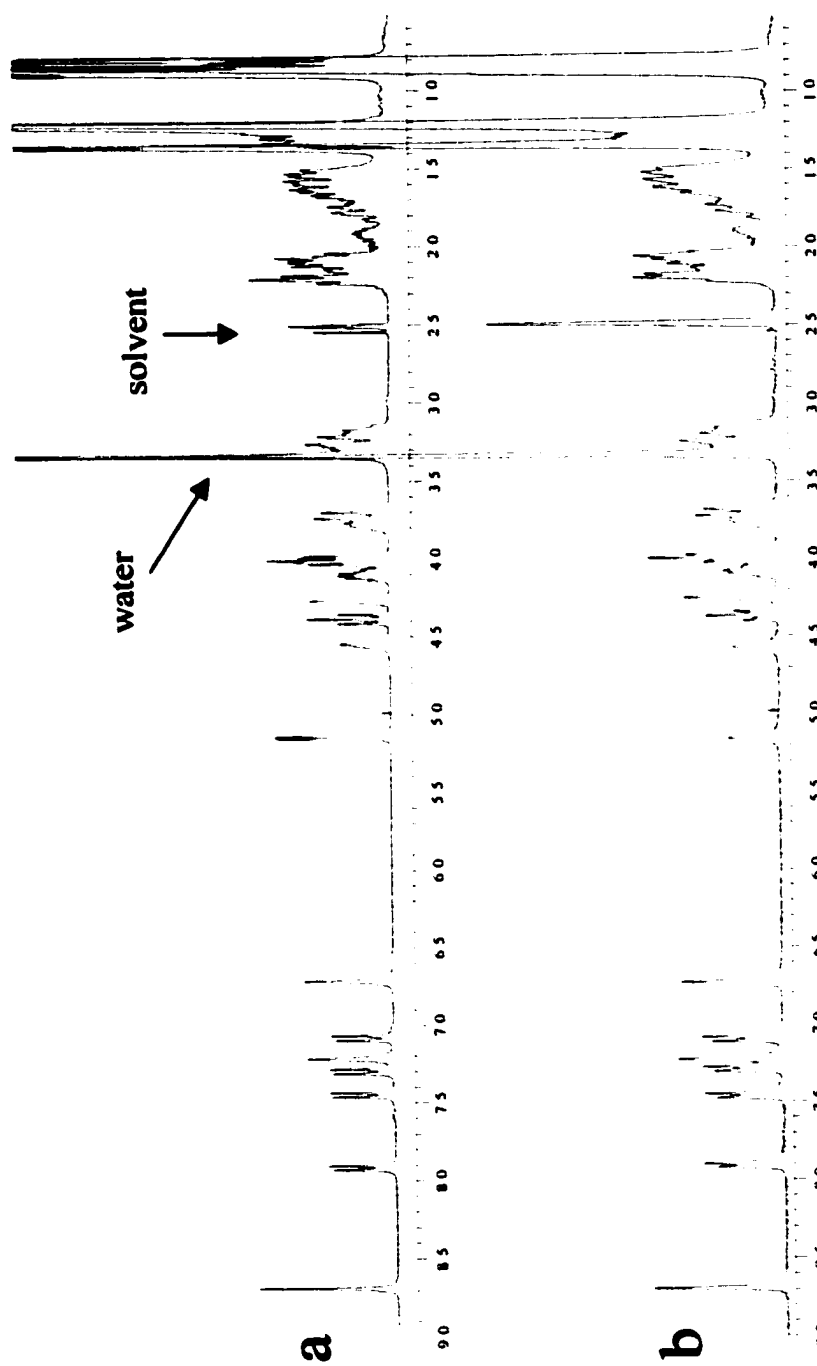


Figure 26.  $^1\text{H}$  NMR of (a) natural and (b) synthetic halovir A in  $\text{DMSO}-d_6$ .

natural substrate in all chemical and biological aspects. Figure 26 shows a comparison of the  $^1\text{H}$  NMR spectra of both natural and synthetic halovir A in  $\text{DMSO-}d_6$ . Perhaps of greater interest in this total synthesis was the discovery that compound **37**, the methyl ester derivative of the natural substrate, demonstrated nearly equivalent anti- $\text{HSV-1}$  activity ( $\text{IC}_{50} = 2.3 \mu\text{M}$ ), but slightly less cytotoxicity than halovir A (Figure 27).

The  $N^\alpha$ -acetyl analog of halovir A was prepared as an initial investigation of the importance of the lipophilic  $N^\alpha$ -acyl chain (Figure 28). The ethyl ester derivative of intermediate **36** was deprotected with ethanolic  $\text{HCl}$ . The amine hydrochloride salt was then treated with acetic anhydride to produce the di-acetylated hexapeptide **38**. Both the C-terminal ethyl ester and the acetylated hydroxyproline were reduced with  $\text{LiBH}_4$  to the corresponding alcohols to achieve the desired target **39**. Assay of this compound against  $\text{HSV-1}$  showed no signs of antiviral activity (Figure 27), and no cytotoxicity was observed against either Vero or HCT-116 cells. This demonstrates the requirement of the  $N^\alpha$ -acyl hydrophobic substituent for the bioactivity of the halovirs.

Figure 29 shows the completion of several targets designed to determine the length of the  $N^\alpha$ -acyl chain required to retain antiviral activity. It was decided to prepare these analogs as the C-terminal methyl esters due to the improved biological activities already determined for compound **37**. Intermediate **36** was deprotected with  $\text{TFA}$ , and the resulting amine trifluoroacetate salt was subsequently coupled with hexanoic, decanoic, palmitic, and stearic acids. Biological evaluation of these derivatives clearly established that saturated lipophilic chains shorter than fourteen

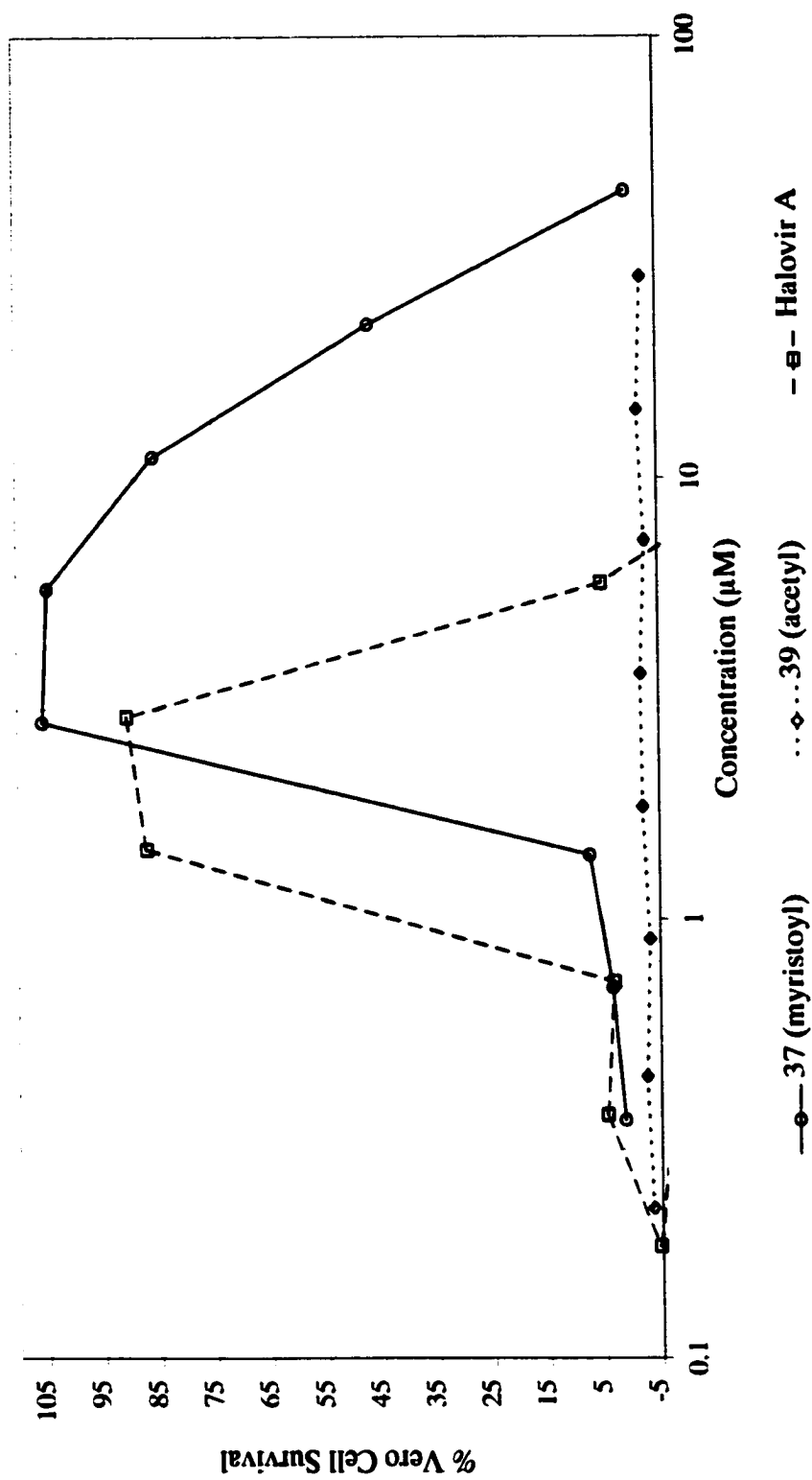


Figure 27. Anti-HSV-1 activity of halovir A versus the Leu-OMe and  $N''$ -acetyl analogs.

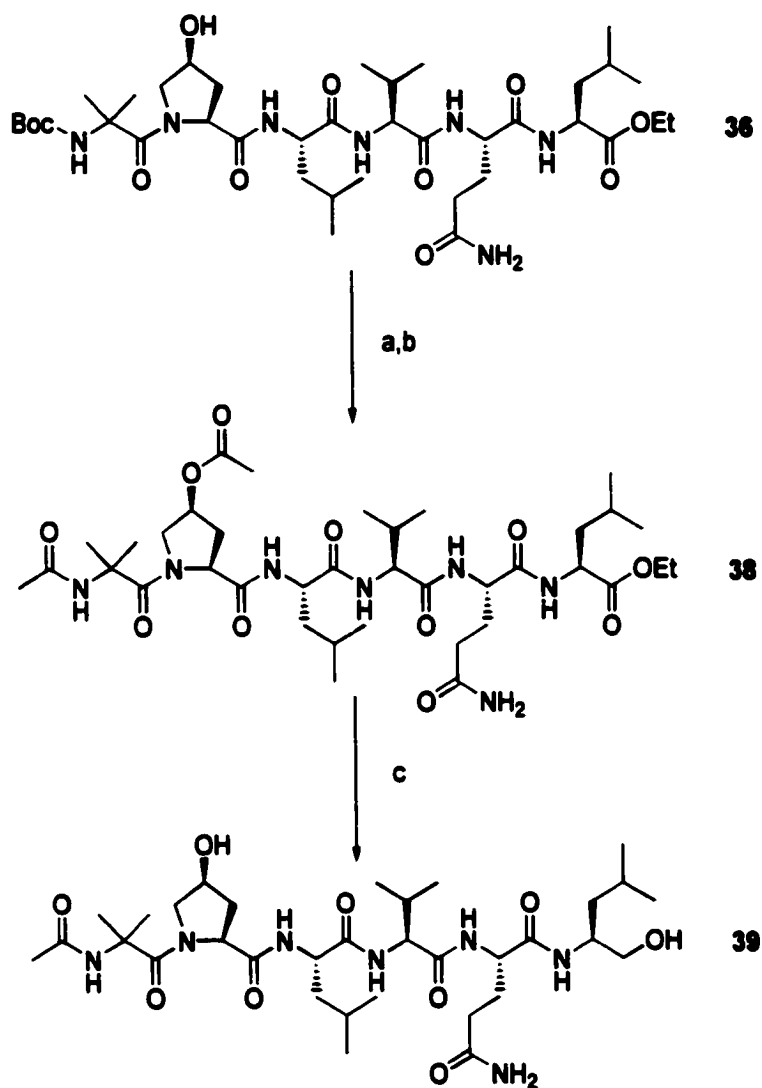


Figure 28. Synthesis of *N*-acetyl halovir analog. *Reagents and conditions:* (a) HCl, EtOH, 0° to room temperature, ~ quant.; (b) Ac<sub>2</sub>O, pyridine, DMAP, 68%; (c) LiBH<sub>4</sub>, THF, 93%.

carbons have reduced antiviral potencies (Figure 30). The  $N^{\alpha}$ -decanoyl derivative **41** was about 3-fold less active than **37** and the  $N^{\alpha}$ -hexanoyl analog **40** demonstrated no observable activity. The  $N^{\alpha}$ -myristoyl (**37**),  $N^{\alpha}$ -palmitoyl (**42**), and  $N^{\alpha}$ -stearoyl (**43**) analogs all possessed similar anti-HSV-1 activities.

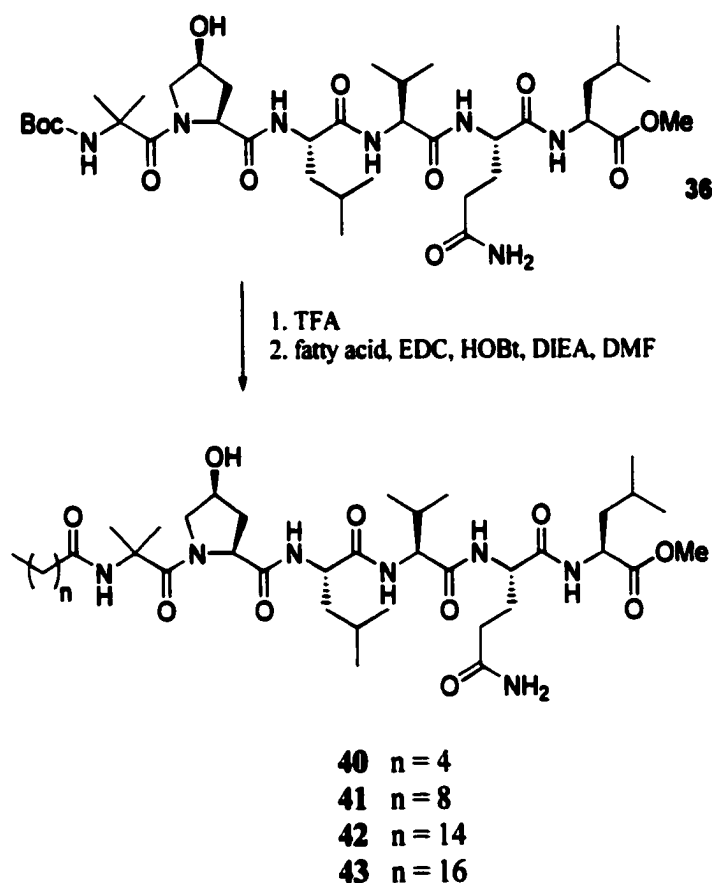


Figure 29. Synthesis of halovir analogs with different lipophilic chain lengths.

The effects of unsaturation in the lipophilic acyl chain were next investigated. Myristoleic (**44**), linoleic (**45**), and linolenic (**46**) acids were selected for this purpose since they are commercially available, and the targets were prepared analogously to

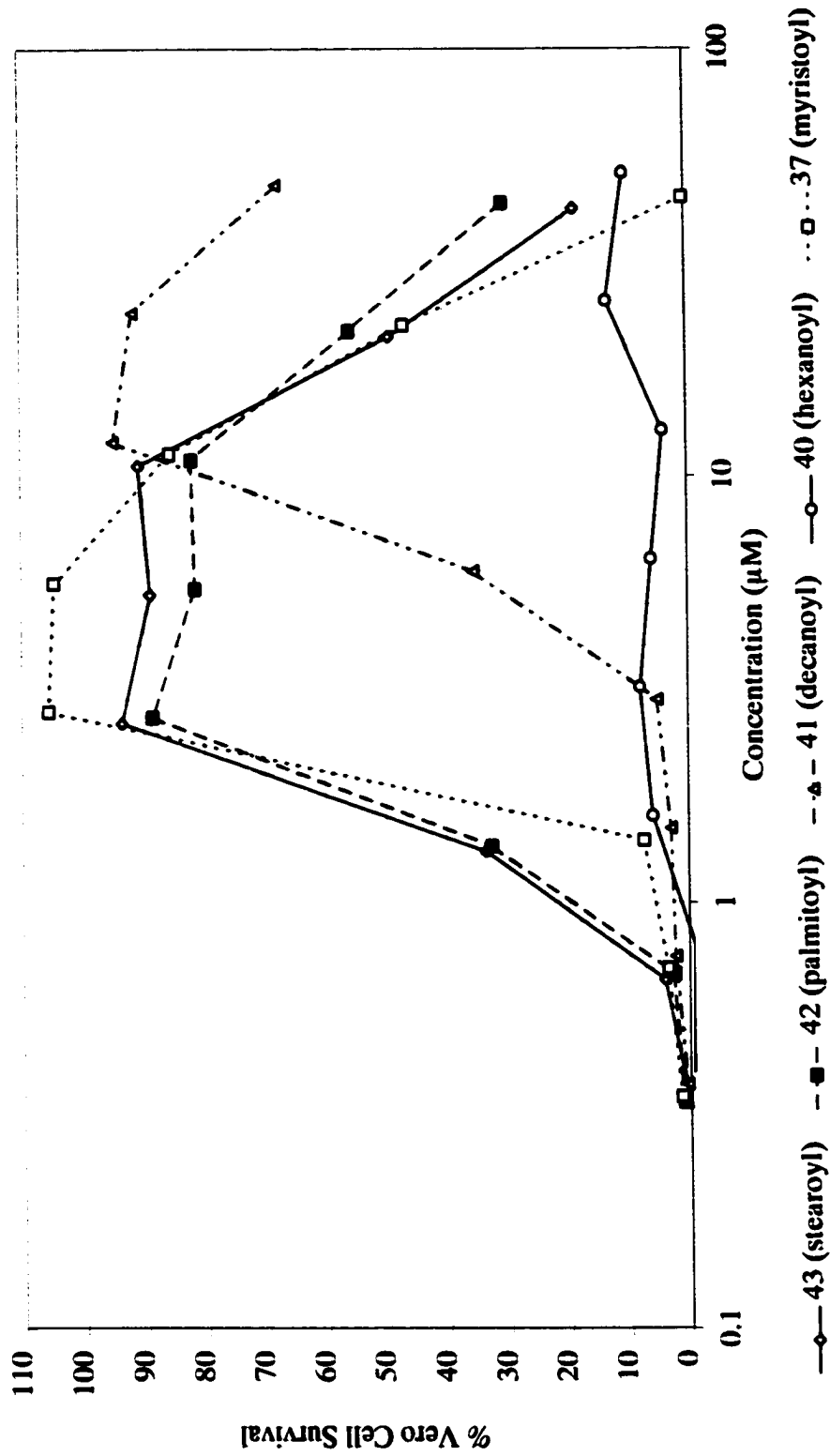
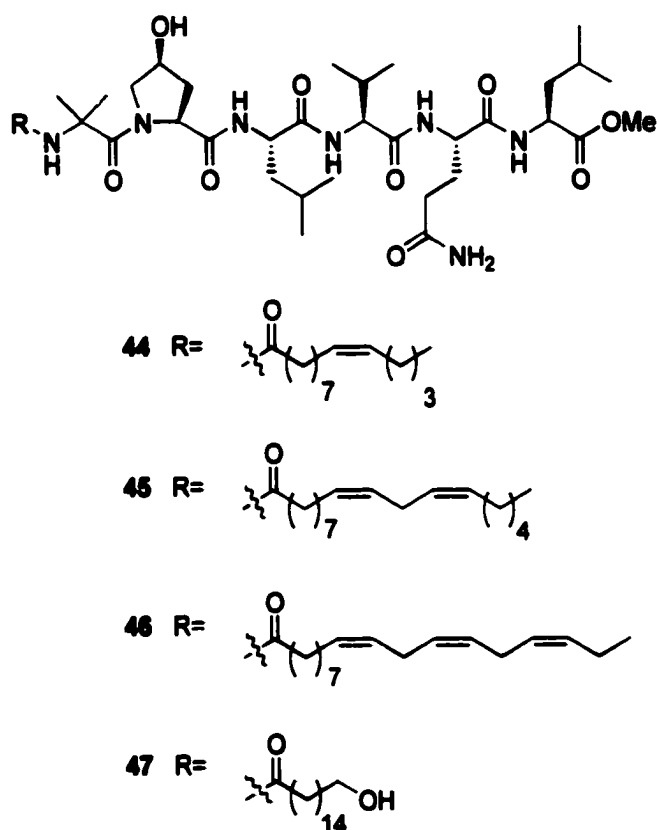


Figure 30. Anti-HSV-1 activities of halovir A methyl ester analogs with various lipophilic chain lengths.

those above. Myristoleic acid is a C14 fatty acid incorporating one degree of unsaturation, while linoleic and linolenic acids are C18 fatty acids with two and three double bonds, respectively. Figure 31 shows that increasing degrees of unsaturation result in loss of potency against HSV-1. Compound 47, an analog incorporating a *N*<sup>α</sup>-16-hydroxyhexadecanoyl substituent, showed a slight decrease the anti-HSV-1 activity ( $IC_{50} = 2.3 \mu\text{M}$ ) relative to the palmitoyl analog 42 ( $IC_{50} = 1.7 \mu\text{M}$ ).



Several synthetic targets were designed to determine the importance of the Aib-Hyp dipeptide segment on the antiviral properties. Figure 32 outlines the synthesis of an analog that incorporates an L-alanine substitution for the *N*-terminal

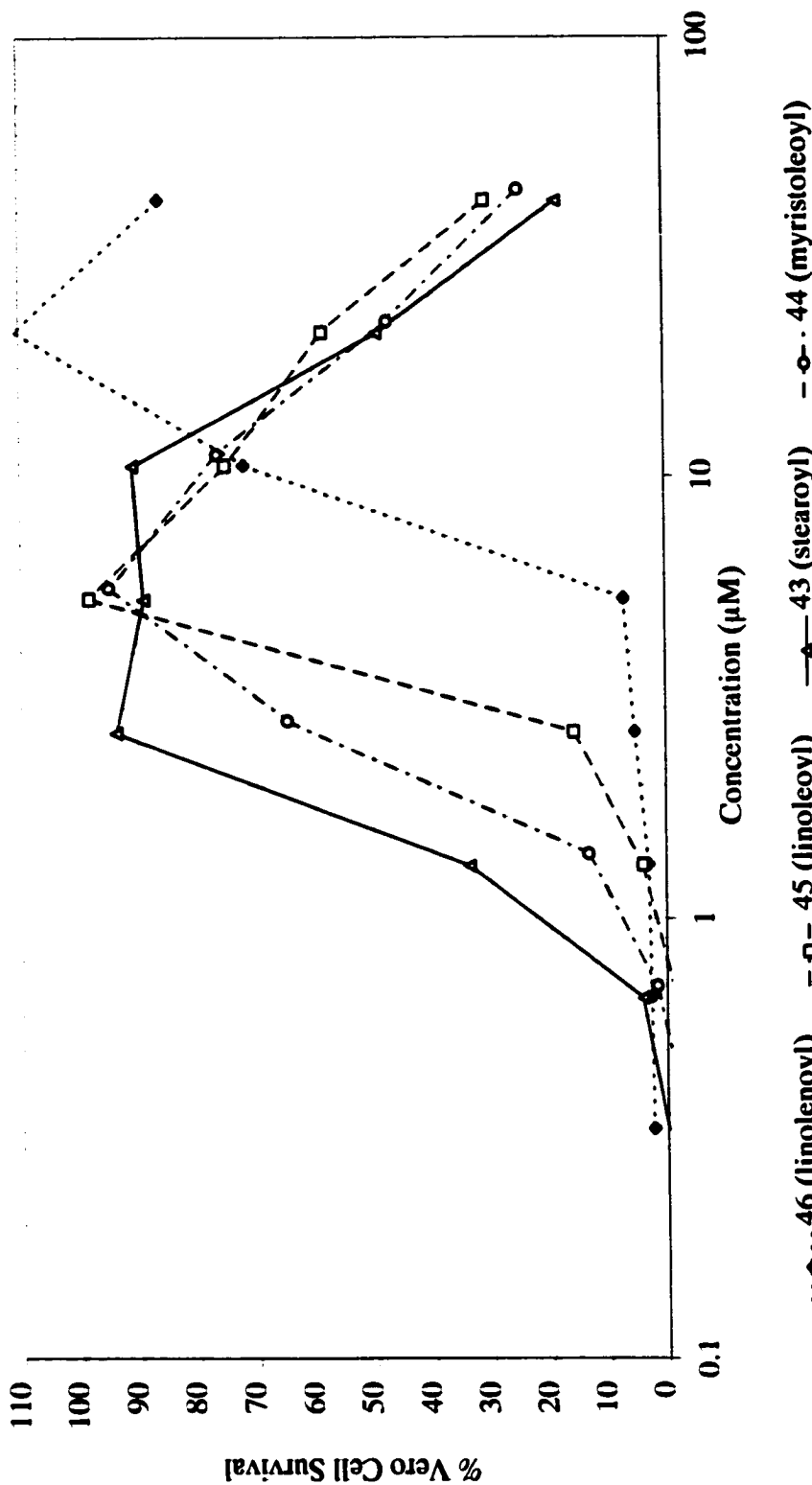
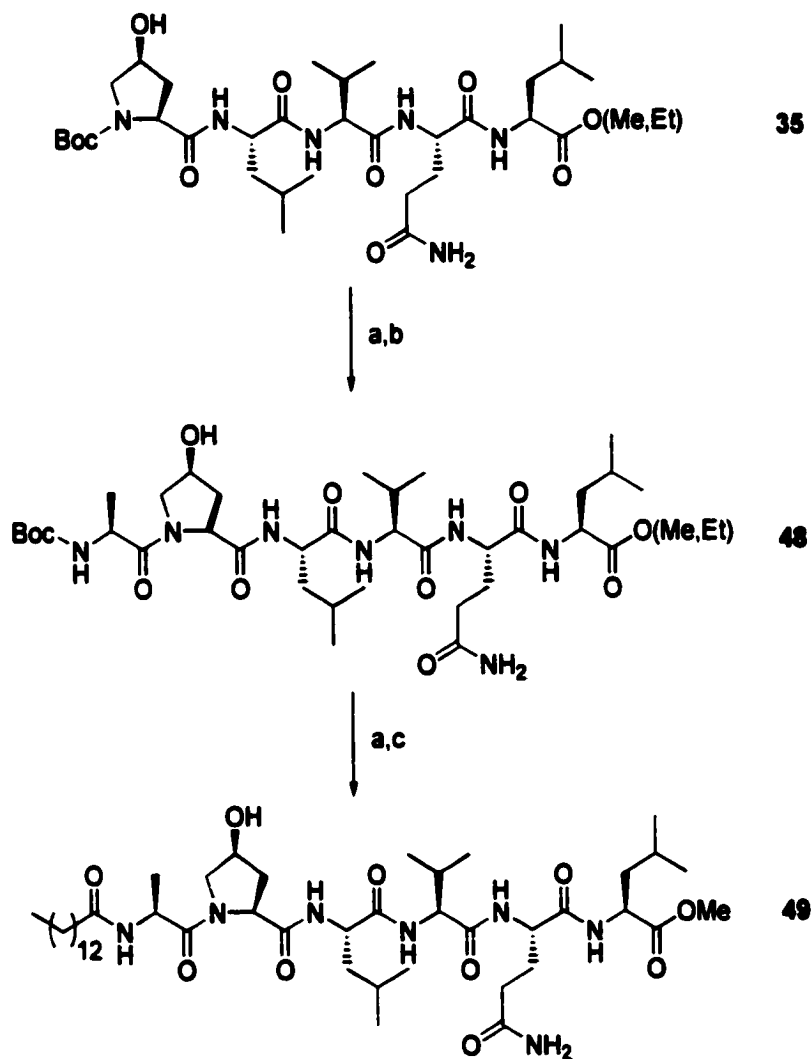


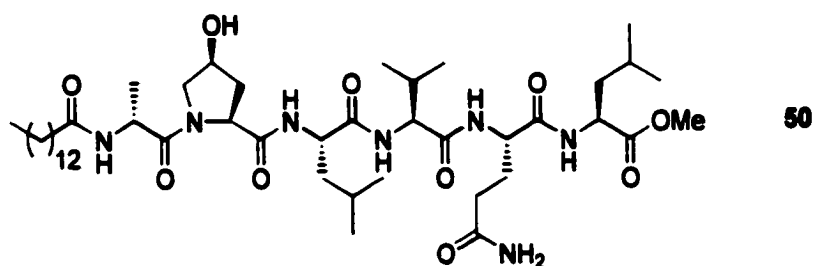
Figure 31. The effects of unsaturation in the lipophilic chain on the anti-HSV-1 activities of halovir A methyl ester analogs.





**Figure 32.** Synthesis of a halovir analog with an L-Ala substitution for the Aib residue.  
**Reagents and conditions:** (a) TFA, room temperature, ~ quant.; (b)  $N^\alpha$ -Boc-L-alanine, EDC, HOBT, DIEA, DMF, 48%. (c) myristic acid, EDC, HOBT, DIEA, DMF, 97%.

Aib unit (**49**). The D-alanine stereoisomer **50** was prepared in the identical manner. Both L- and D-alanine derivatives were synthesized in order to determine if either methyl of the Aib residue was critical to the anti-HSV properties. Figure 33 shows the synthesis of compound **53**, a target that substitutes sarcosine for the hydroxyproline residue of **37**. Sarcosine was selected as a replacement for Hyp because it induces flexibility in the peptide chain while maintaining the tertiary amine of the parent compound. Figure 34 demonstrates the detrimental effects of these three amino acid substitutions on the anti-HSV-1 activity of the halovir peptides.



In addition to methyl ester analog **37**, two additional derivatives were prepared to test the effects of modifications at the carbon terminus of the peptide. The ethyl ester **54** was synthesized in a manner analogous to compound **37**, and possessed nearly equivalent antiviral activity ( $IC_{50} = 1.9 \mu M$ ). Also, the natural substrate halovir C (**29**) was acylated with myristoyl chloride to form the C-terminal myristoylated peptide **55**. Halovir C was chosen for this experiment due to compound availability and because only a single product was anticipated from the reaction. This extremely lipophilic peptide was inactive in both the herpes simplex assay and the HCT-116 cytotoxicity assay.

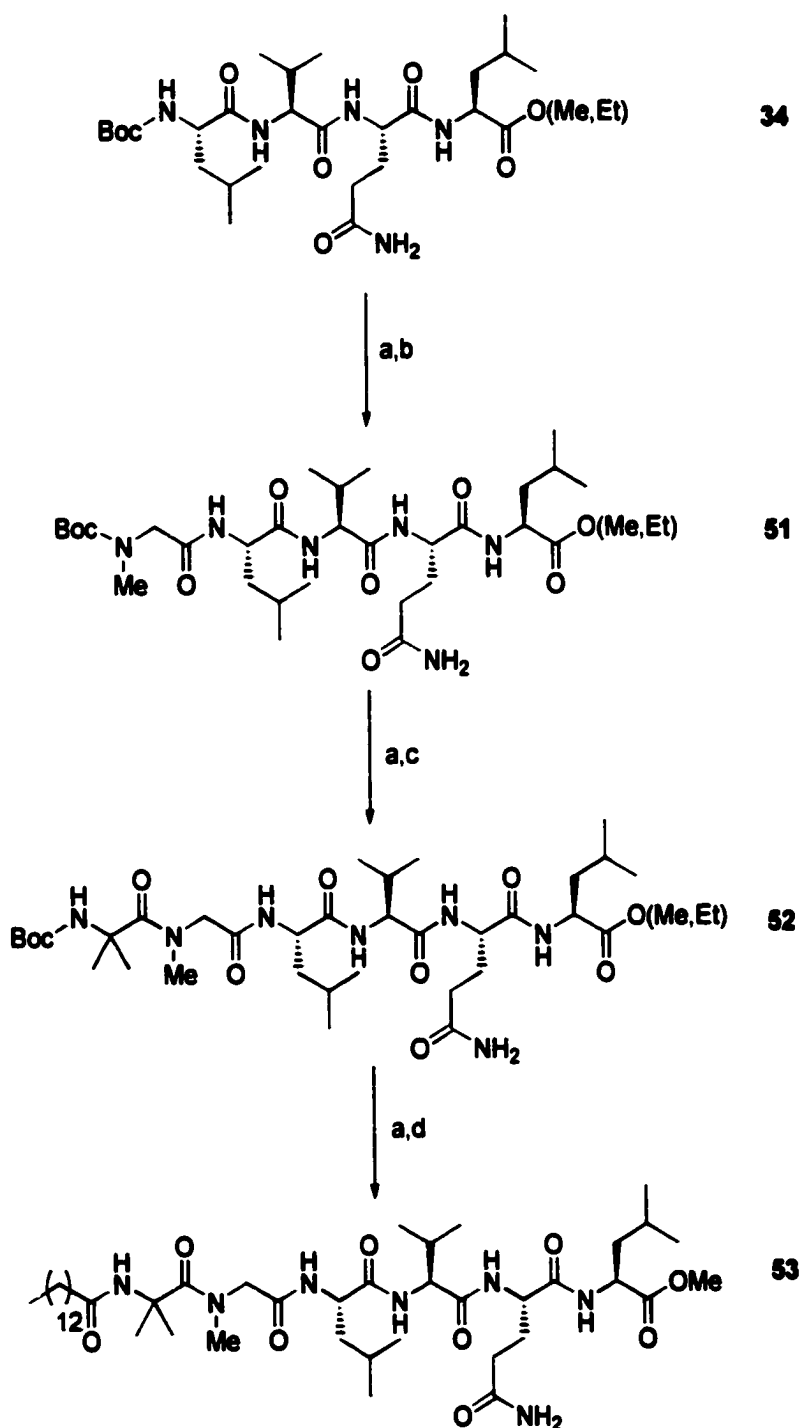


Figure 33. Synthesis of a halovir peptide analog incorporating a sarcosine substitution at the proline position. *Reagents and conditions:* (a) HCl, EtOH, 0° to room temperature, ~quant.; (b) *N*<sup>α</sup>-Boc-Sar, EDC, HOBT, DIEA, DMF, 92%; (c) *N*<sup>α</sup>-Boc-Aib, EDC, HOBT, DIEA, DMF, 37%; (d) myristic acid, EDC, HOBT, DIEA, DMF, 23%.

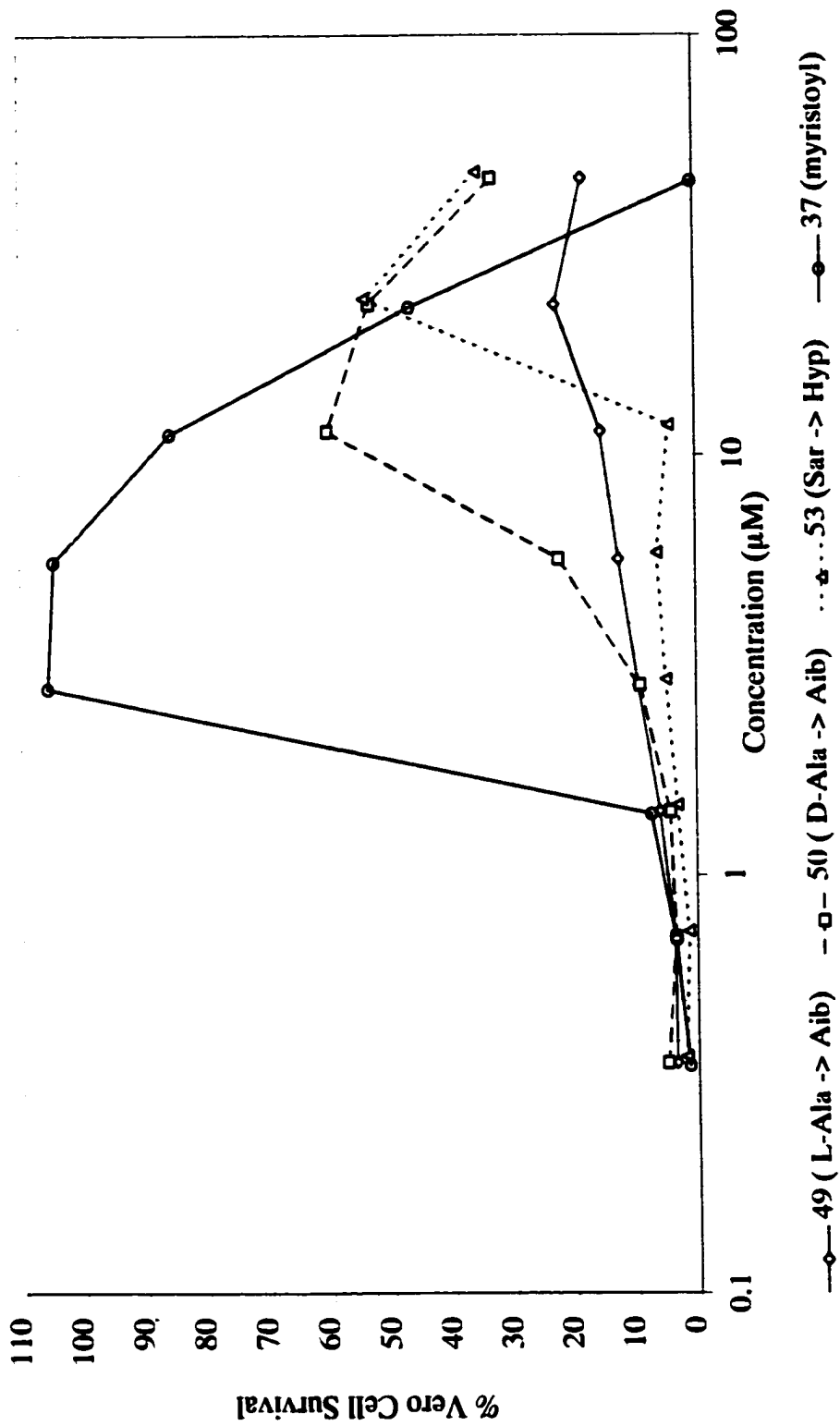


Figure 34. The effects of amino acid substitutions on the anti-HSV-1 activities of halovir A methyl ester analogs.

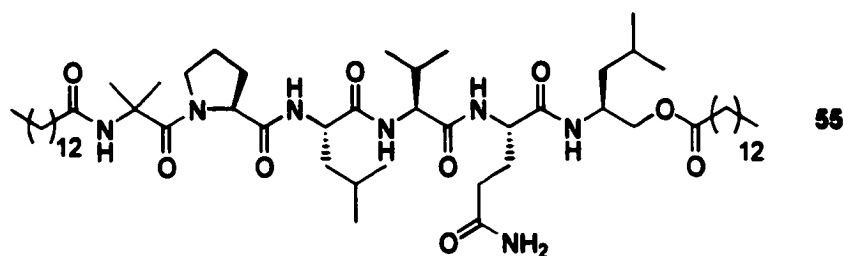
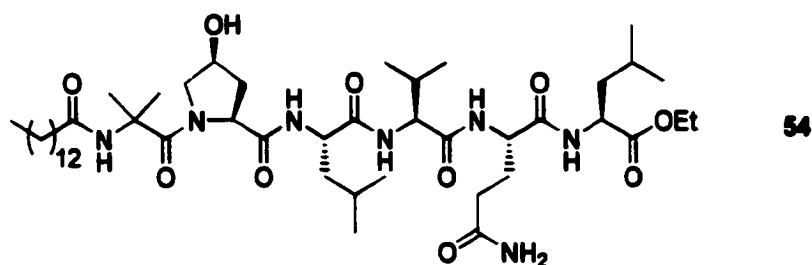
**Table 9. Summary of Biological Activities for the Synthetic Halovir Analogs**

Derivative	Antiviral IC <sub>50</sub> (μM)	Vero Cell IC <sub>50</sub> (μM) <sup>a</sup>	TI <sup>b</sup>	HCT-116 IC <sub>50</sub> (μM)
<b>37</b> (methyl ester)	2.3	20	8.7	7.0
<b>54</b> (ethyl ester)	1.9	28	14	11
<b>43</b> (stearoyl)	1.6	25	15	3.4
<b>42</b> (palmitoyl)	1.7	21	12	9.1
<b>41</b> (decanoyl)	7.0	59	8.4	NSA <sup>c</sup>
<b>40</b> (hexanoyl)	NSA	NSA		NSA
<b>44</b> (myristoleoyl)	2.2	>45	>20	22
<b>45</b> (linoleoyl)	3.4	28	8.4	13
<b>46</b> (linolenoyl)	8.5	>42	>4.9	13
<b>47</b> (juniperoyl)	2.3	>43	>19	14
<b>49</b> (L-Ala -> Aib)	NSA	36		75
<b>50</b> (D-Ala -> Aib)	NSA	48		22
<b>53</b> (Sar -> Hyp)	NSA	NSA		NSA
<b>55</b> (C-myristoyl)	NSA	NSA		NSA

a) Cytotoxicity of compound against Vero cells.

b) Therapeutic Index = Antiviral IC<sub>50</sub> / Vero Cell Cytotoxicity IC<sub>50</sub>

c) No Significant Activity



### 5.3 Discussion

Synthetic analogs of the halovir peptides were prepared *de novo* and evaluated *in vitro* against HSV-1 in order to establish structure-activity relationships relevant to their antiviral properties. The study focused on modifications of the lipophilic  $N^{\alpha}$ -acyl substituent, the Aib-Hyp dipeptide segment, and the reduced carboxyl terminus. Also, a total synthesis of halovir A was completed. Synthetically derived halovir A was identical to the natural substrate in all chemical and biological aspects, thereby giving further evidence of the proposed structure.

This study has shown that the  $N^{\alpha}$ -myristoyl and  $N^{\alpha}$ -lauroyl chains of the naturally occurring halovirs play a major role in the antiviral nature of these molecules. Specifically, an  $N^{\alpha}$ -acyl chain of at least fourteen carbons is required to maintain the maximum anti-HSV-1 potency. Shorter saturated chains of six or less carbons lost all observable antiviral and cytotoxic activities. Interestingly,  $N^{\alpha}$ -acyl

chain length modulated the cytotoxic properties analogously to the measured differences in the antiviral properties, hinting that similar mechanisms might be involved. These results suggest that it is unlikely that the antiviral mechanism of action involves the hexapeptide portion engaged in a receptor-binding phenomenon. As discussed in the previous chapter, non-specific interaction of the lipopeptides with the lipid envelope of the virus and cellular membrane remains a plausible explanation.

Tonolio and coworkers found similar results while investigating the significance of the *N*-terminal fatty acyl chain length of trichogin A IV analogs (see chapter 4 discussion) on membrane destabilization.<sup>2</sup> Incremental extension of the lipid chain length from C3 to C10 resulted in continuous increase of the membrane-modifying properties. However, longer chain lengths resulted in slower kinetics of liposome permeabilization, and a C16 analog had significantly reduced activity. This study also found that the C-terminal methyl ester analog of trichogin GA IV retained the biological properties of the native compound.

Congeners of halovir A incorporating unsaturated lipid chains were found to possess decreased anti-HSV-1 activity. The addition of one point of unsaturation, as demonstrated with the myristoleoyl derivative **44**, only slightly affected HSV inhibition. However, the linoleoyl (**45**) and linolenoyl (**46**) targets were two and five fold less active, respectively, than the saturated stearoyl compound **43**. Thus, increases in unsaturation incrementally decreased the antiviral activity. This raises the possibility that lipid chain flexibility is an important factor in HSV-1 inhibition. These results are in contrast to the antiviral activities of fatty acids themselves, where

it was found that unsaturated linoleic (18:2) and arachidonic (20:4) fatty acids were more active against HSV-1 than saturated fatty acids.<sup>3</sup>

The modifications to the Aib-Hyp dipeptide segment in this study nearly abolished the antiviral activity. In fact, substitution of the aminoisobutyric residue with L-alanine resulted in a completely inactive compound (49). Interestingly, the D-alanine isomer inhibited some HSV induced cell death, although a maximum of only 60% cell survival was achieved (11  $\mu$ M). Elimination of the cyclic Hyp residue by substitution with a sarcosine also resulted in a nearly inactive peptide. A common effect of these three amino acid substitutions is a reduction in the steric hindrance to rotation between the Aib and Hyp residues. Hindered rotation between the Aib and Hyp residue may provide for a conformational bias in the presence of a lipid membrane leading to observed biological effects. However, further studies are needed to explore this possibility.

Unfortunately, none of the peptide modifications in this study led to the identification of a more potent inhibitor of HSV-1 than halovir A, and little headway was made towards improving the *in vitro* therapeutic index. However, interesting insights into the structure-activity relationships of these inhibitors was gained. The indispensability of a sufficiently long  $N^{\alpha}$ -acyl chain has been established, and modification of the C-terminal group has been shown to modulate the toxicity of these compounds. Particularly intriguing is the requirement for the Aib-Pro dipeptide segment. Further conformational studies, especially of the natural substrate in the presence of a lipid bilayer, may provide further insight into why this unusual structural feature is crucial to the biological activity.



## 5.4 Materials and Methods

Amino acids derivatives were purchased from Calbiochem-Novabiochem Corp.. All materials and reagents were of reagent grade and used without further purification. The reaction solvents (DMF, MeCN, THF, and CH<sub>2</sub>Cl<sub>2</sub>) were anhydrous as purchased. Purifications were accomplished on a gradient HPLC system comprising a Waters Prep LC 4000 System equipped with a Knauer variable wavelength UV detector set to 210 nm. The column consisted of a Waters PrepLC 25 mm Module fitted sequentially with two 25 x 100 mm Prep Nova-Pak ® C18 6µm 60Å cartridges. Flow rates were typically 12 mL/minute. Normal-phase silica gel chromatography was performed using Merck Silica gel, 230-400 mesh, 60Å. Electrospray mass spectrometry was accomplished on a HP 1100 MSD. The <sup>1</sup>H NMR data were recorded on either a Varian Inova 300 MHz or Gemini 400 MHz instrument.

*N<sup>α</sup> - t-Butyloxycarbonyl – glutaminyl – leucine methyl ester (N<sup>α</sup>-Boc-Gln-Leu-OMe)*  
(32)

*N<sup>α</sup>*-Boc-Gln-OH (10.0 g, 55.0 mmol) and H-Leu-OMe (13.6 g, 55.0 mmol) were dissolved in 250 mL anhydrous MeCN at ambient temperature and treated with EDC (11.1g, 57.8 mmol, 1.05 eq) and HOBt (8.18 g, 60.5 mmol, 1.1 eq). After stirring under N<sub>2</sub> for 10 minutes, 18.4 mL of DIEA (105 mmol, 1.9 eq, pH 8) was added and the reaction stirred overnight. After concentration *in vacuo*, the crude residue was partitioned between 300 mL EtOAc and 125 mL 1N HCl. The organic phase was separated, washed sequentially with 125 mL saturated NaHCO<sub>3</sub> and 125 mL H<sub>2</sub>O. The aqueous phases were back-extracted in order with 200 mL EtOAc. The

combined organic layers were dried over  $\text{MgSO}_4$ , filtered, and concentrated *in vacuo*. Purification by silica gel chromatography using 5% MeOH in  $\text{CH}_2\text{Cl}_2$  yielded 17.2 g (84%) of the desired product.

*N $\alpha$*  - *t*-Butyloxycarbonyl – valyl – glutaminy – leucine methyl, ethyl ester (*N $\alpha$* -Boc-Val-Gln-Leu-OMe, *N $\alpha$* -Boc-Val-Gln-Leu-OEt) (33)

Compound **32** (17.1 g, 45.8 mmol) was treated with 75 mL saturated HCl in EtOH at  $-20^\circ\text{C}$ . After warming to ambient temperature over 10 minutes, all gas evolution had stopped. The reaction was concentrated *in vacuo* to a white foam (15.4 g). The  $^1\text{H}$  NMR spectrum showed complete loss of the Boc-protecting group and a small amount of the trans-esterification product. The amine hydrochloride salt, *N $\alpha$* -Boc-Val-OH (11.4 g, 52.4 mmol), EDC (10.0 g, 52.4 mmol), and HOBt (7.39g, 54.7 mmol) were dissolved in 250 mL anhydrous MeCN and stirred under  $\text{N}_2$  at ambient temperature for 20 minutes. The homogeneous solution was treated with DIEA (19.9 mL, 114 mmol, 2.5 eq, final pH 8). Within 5 minutes, a thick precipitate formed, 750 mL MeCN were added, and stirred for 3.5 hours. Analysis by TLC showed formation of one major product ( $\text{CH}_2\text{Cl}_2$ :MeOH (9/1),  $\text{KMnO}_4$ ,  $R_f = 0.1$ ). After concentration *in vacuo*, the crude residue was partitioned between 700 mL EtOAc and 200 mL 1N HCl. The organic phase was separated, washed sequentially with 200 mL saturated  $\text{NaHCO}_3$  and 125 mL  $\text{H}_2\text{O}$ . Due to the formation of emulsions, the aqueous phases were extensively back-extracted with EtOAc and  $\text{CH}_2\text{Cl}_2$ . The combined organic layers were dried over  $\text{MgSO}_4$ , filtered, and concentrated *in vacuo* (17.8 g, 106%

crude yield). Recrystallization from hot EtOAc yielded 18.7 g of white solids as the desired product **33** (87%).

*N<sup>α</sup> - t-Butyloxycarbonyl – leucyl - valyl - glutaminy – leucine methyl, ethyl ester (N<sup>α</sup>-Boc-Leu-Val-Gln-Leu-OMe, N<sup>α</sup>-Boc-Leu-Val-Gln-Leu-OEt) (34)*

Compound **33** (18.2 g, 38.6 mmol) was treated with 75 mL saturated HCl in EtOH (-20° C). After warming to ambient temperature over 20 minutes, the reaction was concentrated *in vacuo* to a white foam (17.3 g). The resulting hydrochloride amine salt, *N<sup>α</sup>-Boc-Leu-OH* (10.6 g, 42.3 mmol), EDC (8.10 g, 42.3 mmol, 1.1 eq), and HOBT (5.97 g, 44.2 mmol, 1.15 eq) were dissolved in 75 mL anhydrous MeCN and 75 mL DMF and stirred under N<sub>2</sub> at ambient temperature for 20 minutes. The homogeneous solution was treated with DIEA (17.9 mL, 103 mmol, 2.7 eq, final pH 8). After stirring under N<sub>2</sub> at ambient temperature for 4.5 hours, analysis by TLC showed formation of new product (CH<sub>2</sub>Cl<sub>2</sub>:MeOH (9/1), KMnO<sub>4</sub> R<sub>f</sub> = 0.25). A significant formation of white precipitate had occurred that were filtered off (10.1 g). The MeCN was stripped off *in vacuo*, and resulting solution was partitioned between 400 mL EtOAc and 400 mL 1N HCl. The separated organic layer was subsequently extracted with 300 mL each NaHCO<sub>3</sub> and H<sub>2</sub>O. Significant emulsion necessitated extensive back extraction of the aqueous phases with EtOAc and CH<sub>2</sub>Cl<sub>2</sub>. The combined organic layers were dried over MgSO<sub>4</sub>, filtered, and concentrated *in vacuo* (19.4 g, 86% crude yield). Purification by silica gel chromatography using 5-20% MeOH in CH<sub>2</sub>Cl<sub>2</sub> yielded 15.5 g (69%) of the desired product **34**.

*N<sup>α</sup> - t-Butyloxycarbonyl – (trans -4 -hydroxy) prolyl - leucyl - valyl - glutaminyl – leucine methyl, ethyl ester (N<sup>α</sup>-Boc-trans-4-Hyp-Leu-Val-Gln-Leu-OMe, N<sup>α</sup>-Boc-trans-4-Hyp-Leu-Val-Gln-Leu-OEt) (35)*

Compound **34** (4.05 g, 6.86 mmol) was treated with 4 mL of TFA at ambient temperature for 30 minutes. The reaction was concentrated *in vacuo*, and the resulting TFA amine salt, *N<sup>α</sup>-Boc-L-trans-4-Hyp-OH* (1.75 g, 7.57 mmol, 1.1 eq), EDC (1.58 g, 8.25 mmol, 1.2 eq), and HOBt (1.12 g, 8.25 mmol, 1.2 eq) were dissolved in 20 mL DMF and stirred under N<sub>2</sub> at ambient temperature for 10 minutes. The solution was treated with DIEA (4.79 mL, 27.5 mmol, 4.0 eq, final pH 8). After stirring under N<sub>2</sub> overnight, the homogeneous reaction was partitioned between 400 mL EtOAc and 250 mL 1N HCl. Added 40 mL *i*-PrOH to break an emulsion. The separated organic phase was extracted with 250 mL NaHCO<sub>3</sub> and H<sub>2</sub>O, dried over MgSO<sub>4</sub>, filtered, and concentrated *in vacuo* to a white solid (4.20 g, 87.5%).

*N<sup>α</sup> - t-Butyloxycarbonyl – (α - methyl) alanyl –(trans -4 -hydroxy) prolyl - leucyl - valyl - glutaminyl – leucine methyl, ethyl ester (N<sup>α</sup>-Boc-Aib-(trans-4-hydroxy)Pro-Leu-Val-Gln-Leu-OMe, N<sup>α</sup>-Boc-Aib-(trans-4-hydroxy)Pro-Leu-Val-Gln-Leu-OEt) (36)*

Compound **35** (3.11 g, 4.43 mmol) was treated with 10 mL of TFA at ambient temperature for 20 minutes, and then concentrated under reduced pressure. The resulting amine salt was dissolved in 15 mL DMF and treated with DIEA (6.10 mL, 35.0 mmol, 7.95 eq). In a separate flask, the *N<sup>α</sup>-Boc-Aib-OH* (1.08 g, 5.32 mmol, 1.2 eq), EDC (1.58 g, 8.25 mmol, 1.2 eq), and HOBt (1.12 g, 8.25 mmol, 1.2 eq) were

dissolved in 15 mL DMF and stirred under N<sub>2</sub> at ambient temperature for 10 minutes. The two solutions were then combined and stirred under N<sub>2</sub> for 2 days. The homogeneous reaction was partitioned between 500 mL EtOAc and 500 mL 1N HCl. The separated organic phase was extracted with 500 mL NaHCO<sub>3</sub> and H<sub>2</sub>O, dried over MgSO<sub>4</sub>, filtered, and concentrated *in vacuo* to an orange foam (1.4 g). Reversed-phase HPLC purification using a 25-100% gradient yielded 1.13 g of the methyl ester, 502 mg of the ethyl ester, and 358 mg of a mixture of the two esters as the desired products. (57% yield)

*Myristoyl - (α - methyl)alanyl -(trans -4 -hydroxy) prolyl - leucyl - valyl - glutaminy - leucine methyl ester (Myr-Aib-(trans-4-hydroxy)Pro-Leu-Val-Gln-Leu-OMe) (37)*

Intermediate **36** (500 mg, 0.638 mmol) was treated with 10 mL of TFA at ambient temperature for 20 minutes, and then concentrated under reduced pressure. The resulting amine salt was dissolved in 5 mL DMF and treated with DIEA (445 μL, 2.55 mmol, 4 eq). In a separate flask, the myristic acid (218 mg, 0.957 mmol, 1.5 eq), EDC (183.5 mg, 0.957 mmol, 1.5 eq), and HOBt (129 mg, 0.957 mmol, 1.5 eq) were dissolved in 5 mL DMF and stirred under N<sub>2</sub> at ambient temperature for 10 minutes. The two solutions were then combined and stirred under N<sub>2</sub> overnight. The homogeneous reaction was purified directly by C18 HPLC using a 0-100% gradient of MeOH in H<sub>2</sub>O, and the desired product **37** was obtained as a white foam (509 mg, 89% yield). ESI-MS [M + H]<sup>+</sup> = 894.6, [M + Na]<sup>+</sup> = 916.6; <sup>1</sup>H NMR (300 MHz, DMSO-*d*<sub>6</sub>):

$\delta$  0.85 (m, 21H), 1.22 (m, 20H), 1.34 (s, 3H), 1.35 (s, 3H), 1.45-1.75 (m, 10H), 1.89 (m, 1H), 2.09 (m, 3H), 2.18 (m, 3H), 3.20 (dd,  $J = 12, 2.9$  Hz, 1H), 3.60 (s, 3H), 3.70 (d,  $J = 12$  Hz, 1H), 4.06 (m, 2H), 4.25 (m, 3H), 4.38 (t,  $J = 8.8$  Hz, 1H), 5.13 (bs, 1H), 6.75 (s, 1H), 7.22 (s, 1H), 7.24 (d,  $J = 8.7$  Hz, 1H), 7.59 (d,  $J = 7.8$  Hz, 1H), 7.88 (d,  $J = 7.8$  Hz, 1H), 7.98 (d,  $J = 7.8$  Hz, 1H), 8.66 (s, 1H)

*Myristoyl - ( $\alpha$  - methyl)alanyl - (trans -4 -hydroxy) prolyl - leucyl - valyl - glutaminyl - leucinol (Myr-Aib-(trans-4-hydroxy)Pro-Leu-Val-Gln-Lol) (27)*

Compound **37** (96.4 mg, 0.106 mmol) was dissolved in 4 mL anhydrous THF and treated with 250  $\mu$ L LiBH<sub>4</sub> (2.0M in THF). After 90 minutes of vigorous stirring under N<sub>2</sub>, the TLC (CH<sub>2</sub>Cl<sub>2</sub> 9:1 MeOH, KMnO<sub>4</sub>) showed no starting material remained. The reaction was quenched with 2 mL of MeOH and then concentrated *in vacuo*. The residue was taken up in MeOH, filtered, and purified by C18 HPLC (75-100% MeOH in H<sub>2</sub>O, 15 minutes). Pure synthetic halovir A (75 mg) was obtained as the desired product. (82% yield); [ $\alpha$ ]<sub>D</sub> -10° (c 0.62, MeOH); MALDI FTMS [M + Na]<sup>+</sup> obsd  $m/z$  888.6175; calcd 888.6144 for C<sub>45</sub>H<sub>83</sub>N<sub>7</sub>O<sub>9</sub>Na ( $\Delta$  3.5 ppm).

*Acetyl - ( $\alpha$  - methyl)alanyl - (trans -4 -acetoxy) prolyl - leucyl - valyl - glutaminyl - leucine ethyl ester (Acetyl-Aib-(trans-4-acetoxy)Pro-Leu-Val-Gln-Leu-OEt) (38)*

Intermediate **36** (40 mg, 0.050 mmol) was treated with saturated HCl in EtOH (-20° C). After warming to ambient temperature, the reaction was concentrated *in vacuo* to yellow oil, and 1 mL of anhydrous pyridine, 1 mL of acetic anhydride, and a

catalytic amount of 4-dimethylaminopyridine were added. The reaction stirred at room temperature overnight, was concentrated under reduced pressure, and then subjected to reversed-phase HPLC (5-100% MeOH in H<sub>2</sub>O, 25 minutes). The desired product was obtained as a clear oil (26.5 mg, 68%). TLC R<sub>f</sub> = 0.25 in CH<sub>2</sub>Cl<sub>2</sub> 9:1 MeOH, KMnO<sub>4</sub>. ESI-MS [M + Na]<sup>+</sup> = 804, [M - H]<sup>-</sup> = 780.

*Acetyl - (α - methyl)alanyl - (trans -4 -hydroxy) prolyl - leucyl - valyl - glutaminyl - leucinol (Acetyl-Aib-(trans-4-hydroxy)Pro-Leu-Val-Gln-Lol) (39)*

Compound **38** (14 mg, 0.018mmol) was dissolved in 1 mL anhydrous THF at ambient temperature and treated with 60 μL of LiBH<sub>4</sub> (2.0 M in THF). After 2 hours, the homogeneous reaction had formed a white precipitate. After 3 hours, TLC analysis indicated the complete conversion to a single product (CH<sub>2</sub>Cl<sub>2</sub> 9:1 MeOH, KMnO<sub>4</sub>, R<sub>f</sub> = 0.05). C18 reversed-phase HPLC (5-100% MeOH in H<sub>2</sub>O, 25 minutes) afforded the desired product as a colorless oil (26.5 mg, 68%). ESI-MS [M + Na]<sup>+</sup> = 720, [M - H]<sup>-</sup> = 696; <sup>1</sup>H NMR (300 MHz, pyridine-*d*<sub>6</sub>):

δ 0.96 (m, 9H), 1.06 (d, *J* = 3.9 Hz, 3H), 1.19 (d, *J* = 5.7 Hz, 3H), 1.28 (d, *J* = 5.4 Hz, 3H), 1.56 (s, 3H), 1.74 (s, 3H), 1.75 (m, 1H), 1.98 (m, H), 2.16 (s, 3H), 2.33 (t, *J* = 9.6 Hz, 1H), 2.7 (m, H), 2.92 (m, 2H), 3.73 (d, *J* = 11 Hz, 1H), 4.04 (m, 2H), 4.32 (d, *J* = 11 Hz, 1H), 4.65 (m, 4H), 5.24 (t, *J* = 9.3 Hz, 1H), 5.91 (t, *J* = 6.3 Hz, 1H), 7.02 (s, 1H), 7.62 (s, 1H), 7.80 (d, *J* = 9.6 Hz, 1H), 8.07 (d, *J* = 7.2 Hz, 1H), 8.14 (s, 1H), 8.15 (d, *J* = 7.5 Hz, 1H), 8.58 (d, *J* = 5.7 Hz, 1H), 9.74 (s, 1H)

*Hexanoyl - ( $\alpha$  - methyl)alanyl - (trans -4 -hydroxy) prolyl - leucyl - valyl - glutaminyl - leucine methyl ester (Hexanoyl-Aib-(trans-4-hydroxy)Pro-Leu-Val-Gln-Leu-OMe) (40)*

Compound **36** (28 mg, 0.036 mmol) was treated with 0.3 mL of TFA at ambient temperature for 45 minutes and then concentrated under reduced pressure. The resulting amine trifluoroacetate salt was dissolved in 0.5 mL DMF and treated with DIEA (30  $\mu$ L, 0.18 mmol, 5 eq, final pH 8.5). In a separate flask, hexanoic acid (5.5  $\mu$ L, 0.044 mmol, 1.25 eq), EDC (8.4 mg, 0.044 mmol, 1.25 eq), and HOBt (5.9 mg, 0.044 mmol, 1.25 eq) were dissolved in 0.5 mL DMF and stirred under N<sub>2</sub> at ambient temperature for 10 minutes. The two solutions were then combined and stirred under N<sub>2</sub> at ambient temperature overnight. The homogeneous reaction was purified directly by C18 HPLC using a 0-100% gradient of MeOH in H<sub>2</sub>O over 15 minutes, and the desired product **40** was obtained as a clear, colorless glass (21 mg, 81% yield). ESI-MS [M + Na]<sup>+</sup> = 804.4; <sup>1</sup>H NMR (300 MHz, DMSO-*d*<sub>6</sub>):

$\delta$  0.83 (m, 21H), 1.24 (m, 4H), 1.34 (s, 3H), 1.36 (s, 3H), 1.45-1.80 (m, 10H), 1.90 (m, 1H), 2.09 (m, 3H), 2.19 (m, 3H), 3.21 (dd,  $J = 11, 3.3$  Hz, 1H), 3.60 (s, 3H), 3.70 (d,  $J = 11$  Hz, 1H), 4.06 (m, 2H), 4.24 (m, 3H), 4.39 (t,  $J = 9.0$  Hz, 1H), 5.13 (bd, 1H), 6.73 (s, 1H), 7.21 (s, 1H), 7.24 (d,  $J = 9.3$  Hz, 1H), 7.58 (d,  $J = 7.8$  Hz, 1H), 7.87 (d,  $J = 7.8$  Hz, 1H), 7.96 (d,  $J = 7.5$  Hz, 1H), 8.65 (s, 1H)

*Decanoyl - ( $\alpha$  - methyl)alanyl - (trans -4 -hydroxy) prolyl - leucyl - valyl - glutaminyl - leucine methyl ester (Decanoyl-Aib-(trans-4-hydroxy)Pro-Leu-Val-Gln-Leu-OMe) (41)*



Intermediate **36** (25 mg, 0.033 mmol) was treated with saturated HCl in EtOH (-20° C). After warming to ambient temperature over 10 minutes, the reaction was concentrated *in vacuo* to a white powder. To a solution of the resulting amine hydrochloride salt in 1 mL DMF was added decanoic acid (7.8  $\mu$ L, 0.041 mmol, 1.25 eq), EDC (13 mg, 0.066 mmol, 2 eq), and HOBT (9.4 mg, 0.069 mmol, 2.1 eq). After stirring under N<sub>2</sub> at ambient temperature for 10 minutes, the DIEA (12  $\mu$ L, 0.66 mmol, 2 eq) was added, and the reaction stirred overnight. The homogeneous reaction was purified directly by C18 HPLC using a 75-100% gradient of MeCN in H<sub>2</sub>O over 30 minutes, and the desired product **41** was obtained as a clear, colorless glass (12.5 mg, 45% yield). ESI-MS [M + H]<sup>+</sup> = 838.5; <sup>1</sup>H NMR (400 MHz, DMSO-*d*<sub>6</sub>):

$\delta$  0.78 (d, *J* = 5.6 Hz, 3H), 0.84 (m, 18H), 1.22 (m, 12H), 1.34 (s, 3H), 1.36 (s, 3H), 1.45-1.80 (m, 10H), 1.91 (m, 1H), 2.09 (m, 3H), 2.19 (m, 3H), 3.21 (dd, *J* = 11, 2.8 Hz, 1H), 3.60 (s, 3H), 3.70 (d, *J* = 11 Hz, 1H), 4.03 (m, 1H), 4.09 (m, 1H), 4.20 (m, 1H), 4.25 (m, 2H), 4.39 (t, *J* = 8.8 Hz, 1H), 5.14 (d, *J* = 3.2 Hz, 1H), 6.74 (s, 1H), 7.22 (s, 1H), 7.24 (d, *J* = 8.8 Hz, 1H), 7.58 (d, *J* = 8.4 Hz, 1H), 7.88 (d, *J* = 7.6 Hz, 1H), 7.97 (d, *J* = 7.2 Hz, 1H), 8.66 (s, 1H)

*Hexadecanoyl - ( $\alpha$  - methyl)alanyl - (trans -4 -hydroxy) prolyl - leucyl - valyl - glutaminyl - leucine methyl ester (Palmitoyl-Aib-(trans-4-hydroxy)Pro-Leu-Val-Gln-Leu-OMe) (42)*

Compound **36** (17 mg, 0.021 mmol) was treated with 1 mL of TFA at ambient temperature for 90 minutes, and then concentrated under reduced pressure. The

resulting amine salt was dissolved in 0.5 mL DMF and treated with DIEA (22  $\mu$ L, 0.13 mmol, 6 eq, final pH 9). In a separate flask, palmitic acid (22 mg, 0.085 mmol, 4 eq), EDC (16 mg, 0.085 mmol, 4 eq), and HOBt (11 mg, 0.085 mmol, 4 eq) were dissolved in 1 mL DMF and stirred under N<sub>2</sub> at ambient temperature for 15 minutes. The two solutions were then combined and stirred under N<sub>2</sub> at ambient temperature overnight. The homogeneous reaction was purified directly by C18 HPLC using a 0-100% gradient of MeOH in H<sub>2</sub>O over 15 minutes. The enriched fraction was re-chromatographed using a 70-100% gradient of MeOH in H<sub>2</sub>O and the desired product **42** was obtained as a clear, colorless glass (17 mg, 86% yield). ESI-MS [M + H]<sup>+</sup> = 922.6, [M + Na]<sup>+</sup> = 944.6; <sup>1</sup>H NMR (400 MHz, DMSO-*d*<sub>6</sub>):

$\delta$  0.84 (m, 21H), 1.22 (m, 24H), 1.34 (s, 3H), 1.36 (s, 3H), 1.45-1.80 (m, 10H), 1.91 (m, 1H), 2.11 (m, 3H), 2.18 (m, 3H), 3.21 (d, *J* = 11 Hz, 1H), 3.60 (s, 3H), 3.71 (d, *J* = 11 Hz, 1H), 4.03 (m, 1H), 4.09 (m, 1H), 4.22 (m, 3H), 4.39 (t, *J* = 9.2 Hz, 1H), 5.14 (bs, 1H), 6.74 (s, 1H), 7.23 (s, 1H), 7.24 (d, 1H), 7.58 (d, *J* = 6.8 Hz, 1H), 7.88 (d, *J* = 7.6 Hz, 1H), 7.96 (d, *J* = 6.4 Hz, 1H), 8.66 (s, 1H)

*Octadecanoyl - ( $\alpha$  - methyl)alanyl -(trans -4 -hydroxy) prolyl - leucyl - valyl - glutaminyl - leucine methyl ester (Stearoyl-Aib-(trans-4-hydroxy)Pro-Leu-Val-Gln-Leu-OMe) (43)*

Intermediate **36** (17 mg, 0.022 mmol) was treated with 1 mL of TFA at ambient temperature and then concentrated under reduced pressure. The resulting amine salt was dissolved in 0.75 mL DMF and treated with DIEA (23  $\mu$ L, 0.13 mmol, 6 eq, final pH 9). In a separate flask, stearic acid (19 mg, 0.066 mmol, 3 eq), EDC (13

mg, 0.066 mmol, 3 eq), and HOBt (8.9 mg, 0.066 mmol, 3 eq) were dissolved in 0.75 mL DMF and stirred under N<sub>2</sub> at ambient temperature for 10 minutes. The two solutions were then combined and stirred under N<sub>2</sub> at ambient temperature overnight. The homogeneous reaction was purified directly by C18 HPLC using a 0-100% gradient of MeOH in H<sub>2</sub>O over 15 minutes. The enriched fraction was re-chromatographed using a 70-100% gradient of MeOH in H<sub>2</sub>O and the desired product was obtained as a clear, colorless glass (19 mg, 90% yield). ESI-MS [M + H]<sup>+</sup> = 950.7, [M + Na]<sup>+</sup> = 972.7; <sup>1</sup>H NMR (400 MHz, DMSO-*d*<sub>6</sub>):

δ 0.84 (m, 21H), 1.23 (m, 28H), 1.34 (s, 3H), 1.36 (s, 3H), 1.45-1.80 (m, 10H), 1.91 (m, 1H), 2.10 (m, 3H), 2.18 (m, 3H), 3.21 (dd, *J* = 11 Hz, 1H), 3.60 (s, 3H), 3.71 (d, *J* = 11 Hz, 1H), 4.03 (m, 1H), 4.09 (m, 1H), 4.24 (m, 3H), 4.39 (t, *J* = 8.8 Hz, 1H), 5.13 (bs, 1H), 6.74 (s, 1H), 7.22 (s, 1H), 7.24 (d, *J* = 9.6 Hz, 1H), 7.57 (d, *J* = 8.4 Hz, 1H), 7.88 (d, *J* = 7.2 Hz, 1H), 7.95 (d, *J* = 6.8 Hz, 1H), 8.66 (s, 1H)

*Myristoleoyl* - (*α* - methyl)alanyl - (*trans* -4 -hydroxy) prolyl - leucyl - valyl - glutaminy! - leucine methyl ester (*Myristoleoyl* -Aib-(*trans*-4-hydroxy)Pro-Leu-Val-Gln-Leu-OMe) (44)

Compound 36 (17 mg, 0.022 mmol) was treated with 1 mL of TFA at ambient temperature for 90 minutes, and then concentrated under reduced pressure. The resulting amine trifluoroacetate salt was dissolved in 0.5 mL DMF and treated with DIEA (23 μL, 0.13 mmol, 6 eq). In a separate flask, myristoleic acid (15 mg, 0.066 mmol, 3 eq), EDC (13 mg, 0.066 mmol, 3 eq), and HOBt (8.9 mg, 0.066 mmol, 3 eq) were dissolved in 1 mL DMF and stirred under N<sub>2</sub> at ambient temperature for 15

minutes. The two solutions were then combined and stirred under N<sub>2</sub> overnight at ambient temperature. The homogeneous reaction was purified directly by C18 HPLC using a 0-100% gradient of MeOH in H<sub>2</sub>O over 15 minutes, and the desired product was obtained as a clear, colorless glass (15 mg, 73% yield). MALDI FTMS [M + Na]<sup>+</sup> obsd *m/z* 914.5906; calcd 914.5937 for C<sub>46</sub>H<sub>81</sub>N<sub>7</sub>O<sub>10</sub>Na ( $\Delta$  3.4 ppm); <sup>1</sup>H NMR (400 MHz, DMSO-*d*<sub>6</sub>):

$\delta$  0.84 (m, 21H), 1.22 (m, 12H), 1.34 (s, 3H), 1.36 (s, 3H), 1.45-1.80 (m, 10H), 1.97 (m, 5H), 2.11 (m, 3H), 2.18 (m, 3H), 3.21 (d, *J* = 12, 1H), 3.60 (s, 3H), 3.71 (d, *J* = 12 Hz, 1H), 4.03 (m, 1H), 4.07 (m, 1H), 4.23 (m, 3H), 4.39 (t, *J* = 8.8 Hz, 1H), 5.13 (bs, 1H), 5.31 (m, 2H), 6.74 (s, 1H), 7.23 (s, 1H), 7.24 (d, 1H), 7.58 (d, *J* = 8.0 Hz, 1H), 7.88 (d, *J* = 7.2 Hz, 1H), 7.96 (d, *J* = 7.2 Hz, 1H), 8.66 (s, 1H)

*Linoleoyl - ( $\alpha$  - methyl)alanyl -(trans -4 -hydroxy) prolyl - leucyl - valyl - glutaminy - leucine methyl ester (Linoleoyl-Aib-(trans-4-hydroxy)Pro-Leu-Val-Gln-Leu-OMe) (45)*

Compound 36 (17 mg, 0.021 mmol) was treated with 1 mL of TFA at ambient temperature for 35 minutes, and then concentrated under reduced pressure. The resulting amine trifluoroacetate salt was dissolved in 0.5 mL DMF and treated with DIEA (22  $\mu$ L, 0.13 mmol, 6 eq). In a separate flask, linoleic acid (26 mg, 0.085 mmol, 4 eq), EDC (16 mg, 0.085 mmol, 4 eq), and HOBt (11 mg, 0.085 mmol, 4 eq) were dissolved in 1 mL DMF and stirred under N<sub>2</sub> at ambient temperature for 15 minutes. The two solutions were then combined and stirred under N<sub>2</sub> overnight at ambient temperature. The homogeneous reaction was purified directly by C18 HPLC

using a 0-100% gradient of MeOH in H<sub>2</sub>O over 15 minutes, and the desired product was obtained as a clear, colorless glass (19 mg, 96% yield). ESI-MS [M + H]<sup>+</sup> = 946.5, [M + Na]<sup>+</sup> = 968.6.

*Linolenoyl - (α - methyl)alanyl -(trans -4 -hydroxy) prolyl - leucyl - valyl - glutaminyl -leucine methyl ester (Linolenoyl-Aib-(trans-4-hydroxy)Pro-Leu-Val-Gln-Leu-OMe) (46)*

Compound **36** (41 mg, 0.052 mmol) was treated with 1 mL of TFA at ambient temperature for 20 minutes, and then concentrated under reduced pressure. The resulting amine salt was dissolved in 1 mL DMF and treated with DIEA (54 μL, 0.31 mmol, 6 eq). In a separate flask, the linolenic acid (64 μL, 0.21 mmol, 4 eq), EDC (40 mg, 0.21 mmol, 4 eq), and HOBt (28 mg, 0.21 mmol, 4 eq) were dissolved in 1 mL DMF and stirred under N<sub>2</sub> at ambient temperature for 10 minutes. The two solutions were then combined and stirred under N<sub>2</sub> overnight. The homogeneous reaction was purified directly by C18 HPLC using a 0-100% gradient of MeOH in H<sub>2</sub>O over 20 minutes. The enriched fraction was re-chromatographed using an 80-100% gradient of MeOH in H<sub>2</sub>O and the desired product was obtained as a clear, colorless glass (34 mg, 70% yield). MALDI FTMS [M + Na]<sup>+</sup> obsd *m/z* 966.6291; calcd 966.6249 for C<sub>50</sub>H<sub>85</sub>N<sub>7</sub>O<sub>10</sub>Na (Δ 4.2 ppm).

*16 - Hydroxyhexadecanoyl - ( $\alpha$  - methyl)alamyl - (trans -4 -hydroxy) prolyl - leucyl - valyl - glutaminyll - leucine methyl ester (16-hydroxydecanoyl-Aib-(trans-4-hydroxy)Pro-Leu-Val-Gln-Leu-OMe) (47)*

Intermediate **36** (18 mg, 0.022 mmol) was treated with 1 mL of TFA at ambient temperature for 20 minutes, and then concentrated under reduced pressure. The resulting amine trifluoroacetate salt was dissolved in 0.5 mL DMF and treated with DIEA (24  $\mu$ L, 0.14 mmol, 6 eq). In a separate flask, juniperic acid (24 mg, 0.090 mmol, 4 eq), EDC (17 mg, 0.090 mmol, 4 eq), and HOBt (12 mg, 0.090 mmol, 4 eq) were dissolved in 1 mL DMF and stirred under N<sub>2</sub> at ambient temperature for 20 minutes. The two solutions were then combined and stirred under N<sub>2</sub> overnight at ambient temperature. The cloudy reaction was filtered through a C18 plug with MeOH, concentrated under reduced pressure, and purified by C18 HPLC using a 0-100% gradient of MeOH in H<sub>2</sub>O over 15 minutes. The desired product was obtained as a clear, colorless glass (13 mg, 62% yield). ESI-MS [M + H]<sup>+</sup> = 938.6, [M + Na]<sup>+</sup> = 960.6; <sup>1</sup>H NMR (400 MHz, DMSO-*d*<sub>6</sub>):

$\delta$  0.84 (m, 18H), 1.23 (m, 24H), 1.34 (s, 3H), 1.36 (s, 3H), 1.45-1.80 (m, 10H), 1.90 (m, 1H), 2.10 (m, 3H), 2.18 (m, 3H), 3.21 (dd, *J* = 11, 1H), 3.36 (t, *J* = 6.8, 2H), 3.60 (s, 3H), 3.70 (d, *J* = 11 Hz, 1H), 4.03 (m, 1H), 4.09 (m, 1H), 4.22 (m, 3H), 4.39 (t, *J* = 8.8 Hz, 1H), 5.1 (bs, 1H), 6.74 (s, 1H), 7.22 (s, 1H), 7.23 (d, *J* = 9.6 Hz, 1H), 7.58 (d, *J* = 8.0 Hz, 1H), 7.88 (d, *J* = 7.6 Hz, 1H), 7.97 (d, *J* = 7.6 Hz, 1H), 8.66 (s, 1H)

*N<sup>α</sup> - t-Butyloxycarbonyl – alanyl –(trans –4 –hydroxy) prolyl - leucyl - valyl - glutaminyl – leucine methyl, ethyl ester (N<sup>α</sup> -Boc-Ala-(trans-4-hydroxy)Pro-Leu-Val-Gln-Leu-OMe (48a), N<sup>α</sup> -Boc-Ala-(trans-4-hydroxy)Pro-Leu-Val-Gln-Leu-OEt (48b))*

Compound **35** (200 mg, 0.285 mmol) was deprotected by treatment with 3 mL of TFA over 45 minutes. The TFA was removed under reduced pressure. To a solution of the amine trifluoroacetate salt residue in 6 mL DMF was added Boc-L-Ala-OH (64.7 mg, 0.342 mmol, 1.2 eq), EDC (65.5 mg, 0.342 mmol, 1.2 eq), and HOBT (48.1 mg, 0.356 mmol, 1.25 eq). The reaction stirred under N<sub>2</sub> at ambient temperature for 15 minutes, and was then treated with DIEA (0.248 mL, 1.13 mmol, 4 eq, pH 9) and stirred overnight. The reaction was injected onto a C18 HPLC column and eluted with a 0-100% gradient of MeOH in H<sub>2</sub>O. A second reversed-phase HPLC purification using a 40-100% gradient yielded 58.6 mg of the methyl ester and 46.6 mg of the ethyl ester as the desired products (48% yield).

*Myristoyl – alanyl –(trans –4 –hydroxy) prolyl - leucyl - valyl - glutaminyl – leucine methyl ester (Myr-Ala-(trans-4-hydroxy)Pro-Leu-Val-Gln-Leu-OMe) (49)*

Intermediate **48** (10.3 mg, 0.013 mmol) was treated with 2 mL of TFA at ambient temperature for 20 minutes, and then concentrated under reduced pressure. The resulting amine salt was dissolved in 0.75 mL DMF and treated with DIEA (14 μL, 0.080 mmol, 6 eq). In a separate flask, myristic acid (12.2 mg, 0.054 mmol, 4 eq), EDC (10.3 mg, 0.054 mmol, 4 eq), and HOBT (7.2 mg, 0.054 mmol, 4 eq) were dissolved in 0.75 mL DMF and stirred under N<sub>2</sub> at ambient temperature for 10 minutes. The two solutions were then combined and stirred under N<sub>2</sub> overnight. The

homogeneous reaction was purified directly by C18 HPLC using a 0-100% gradient, and the desired product was obtained as a clear glass (11.4 mg, 97% yield). MALDI FTMS  $[M + Na]^+$  obsd  $m/z$  902.5909; calcd 902.5937 for  $C_{45}H_{81}N_7O_{10}Na$  ( $\Delta$  3.1 ppm);  $^1H$  NMR (400 MHz, DMSO- $d_6$ ):

$\delta$  0.84 (m, 21H), 1.14 (d,  $J = 6.8$  Hz, 3H), 1.23 (m, 20H), 1.45-1.75 (m, 9H), 1.85 (m, 2H), 1.95 (m, 2H), 2.08 (m, 4H), 3.47 (d,  $J = 10$ , 1H), 3.57 (d,  $J = 10$  Hz, 1H), 3.61 (s, 3H), 4.15 (m, 1H), 4.26 (m, 4H), 4.36 (t,  $J = 8.0$  Hz, 1H), 4.47 (t,  $J = 7.2$  Hz, 1H), 5.11 (d,  $J = 3.2$  Hz, 1H), 6.77 (s, 1H), 7.24 (s, 1H), 7.47 (d,  $J = 8.8$  Hz, 1H), 7.97 (d,  $J = 7.6$  Hz, 1H), 8.02 (d,  $J = 7.6$  Hz, 1H), 8.06 (d,  $J = 7.2$  Hz, 1H), 8.22 (d,  $J = 8.0$  Hz, 1H)

*N $\alpha$  - t-Butyloxycarbonyl - D - alanyl -(trans -4 -hydroxy) prolyl - leucyl - valyl - glutaminy - leucine methyl, ethyl ester (N $\alpha$  -Boc-D-Ala-(trans-4-hydroxy)Pro-Leu-Val-Gln-Leu-OMe, N $\alpha$  -Boc-D-Ala-(trans-4-hydroxy)Pro-Leu-Val-Gln-Leu-OEt)*

Compound 35 (227 mg, 0.323 mmol) was deprotected by treatment with 5 mL of TFA for 20 minutes, and then concentrated under reduced pressure. To a solution of the amine trifluoroacetate salt residue in 4 mL DMF was added Boc-D-Ala-OH (73.4 mg, 0.380 mmol, 1.2 eq), EDC (74.4 mg, 0.380 mmol, 1.2 eq), and HOBT (54.6 mg, 0.404 mmol, 1.25 eq). The reaction was stirred under  $N_2$  at ambient temperature for 15 minutes, and was then treated with DIEA (0.225 mL, 1.29 mmol, 4 eq, pH 9) and stirred for 28 hours. The reaction was injected directly onto a C18 HPLC column and eluted with a 0-100% gradient of MeOH in  $H_2O$ . A second reversed-phase HPLC



purification using a 50-100% gradient of MeCN in H<sub>2</sub>O yielded 68.4 mg of the methyl ester and 46.3 mg of the ethyl ester as the desired products (38% yield).

*Myristoyl - D - alanyl - (trans -4 -hydroxyl) prolyl - leucyl - valyl - glutaminyll - leucine methyl ester (Myr-D-Ala-(trans-4-hydroxy)Pro-Leu-Val-Gln-Leu-OMe) (50)*

The above compound (48 mg, 0.062 mmol) was treated with 1 mL of TFA at ambient temperature for 20 minutes, and then concentrated under reduced pressure. The resulting amine salt was dissolved in 1 mL DMF and treated with DIEA (65  $\mu$ L, 0.37 mmol, 6 eq). In a separate flask, myristic acid (57.0 mg, 0.250 mmol, 4 eq), EDC (47.8 mg, 0.250 mmol, 4 eq), and HOBt (33.7 mg, 0.250 mmol, 4 eq) were dissolved in 1 mL DMF and stirred under N<sub>2</sub> at ambient temperature for 15 minutes. The two solutions were then combined and stirred under N<sub>2</sub> for 24 hours. The reaction was then injected onto a C18 HPLC column and eluted using a 0-100% MeOH in H<sub>2</sub>O gradient. A second C18 HPLC purification using 75-100% MeOH in H<sub>2</sub>O yielded the desired product as a clear glass (40.0 mg, 73% yield). ESI-MS [M + H]<sup>+</sup> = 880.6, [M + Na]<sup>+</sup> = 902.6, [M + K]<sup>+</sup> = 916.6; MALDI FTMS [M + Na]<sup>+</sup> obsd *m/z* 902.5970; calcd 902.5937 for C<sub>45</sub>H<sub>81</sub>N<sub>7</sub>O<sub>10</sub>Na ( $\Delta$  3.7 ppm).

*N<sup>α</sup> - t-Butyloxycarbonyl - sarcosyl - leucyl - valyl - glutaminyll - leucine methyl, ethyl ester (N<sup>α</sup>-Boc-Sar-Leu-Val-Gln-Leu-OMe, N<sup>α</sup>-Boc-Sar-Leu-Val-Gln-Leu-OEt) (51)*

Compound **34** was deprotected by treatment with 3 mL saturated HCl in EtOH at -20° C. After warming to room temperature over 10 minutes, all gas evolution had

stopped. The reaction was concentrated *in vacuo* to a white foam (281 mg). The amine hydrochloride salt, *N*<sup>α</sup>-*t*-Boc-sarcosine (182 mg, 0.962 mmol, 2 eq), EDC (198 mg, 1.03 mmol, 2.15 eq), and HOBt (142.7 mg, 1.06 mmol, 2.2 eq) were dissolved in 5 mL DMF and stirred vigorously under N<sub>2</sub> at ambient temperature for 5 minutes. DIEA (167 μL, 0.96 mmol, 2 eq) was then added, and the reaction continued for 24 hours. The reaction, now cloudy and viscous, was partitioned between 350 mL EtOAc (cloudy) and 200 mL 1N HCl. The organic layer was further extracted with NaHCO<sub>3</sub> and H<sub>2</sub>O. The aqueous layers were back extracted sequentially with 200 mL EtOAc. The combined organic layers were concentrated under reduced pressure and used directly in the next reaction. (300 mg, 92%)

*N*<sup>α</sup> - *t*-Butyloxycarbonyl - (α - methyl)alanyl - sarcosyl - leucyl - valyl - glutaminyl - leucine methyl, ethyl ester (*N*<sup>α</sup> -Boc -Aib-Sar-Leu-Val-Gln-Leu-OMe, *N*<sup>α</sup> -Boc -Aib-Sar-Leu-Val-Gln-Leu-OEt) (52)

Compound 51 (300 mg, 0.457 mmol) was treated with 3 mL saturated HCl in EtOH at -20° C, warmed to room temperature, and concentrated *in vacuo* to a yellow foam. The resulting amine hydrochloride salt, Boc-Aib-OH (203 mg, 1.00 mmol), EDC (192 mg, 1.00 mmol), and HOBt (149 mg, 1.10 mmol) were dissolved in 5 mL DMF and stirred vigorously under N<sub>2</sub> at ambient temperature for 5 minutes. DIEA (0.348 mL, 2.0 mmol, final pH 9) was then added. The reaction proceeded for 20 hours and was then partitioned between 250 mL each EtOAc and 1N HCl. The organic phase was further extracted with 250 mL each of NaHCO<sub>3</sub> and H<sub>2</sub>O. After back extracting with 200 mL EtOAc, the combined organic layers were concentrated

under reduced pressure to yield an amorphous yellow solid. C18 HPLC using a gradient of 5-100% MeCN in H<sub>2</sub>O over 25 minutes yielded 67 mg of the methyl ester and 58 mg of the ethyl ester as the desired compounds. (~37% yield)

Methyl ester (C<sub>35</sub>H<sub>63</sub>N<sub>7</sub>O<sub>10</sub>): ESI-MS [M+H]<sup>+</sup> = 743, [M+Na]<sup>+</sup> = 765, [M-H]<sup>-</sup> = 741.

Ethyl ester (C<sub>36</sub>H<sub>65</sub>N<sub>7</sub>O<sub>10</sub>): ESI-MS [M+H]<sup>+</sup> = 757, [M+Na]<sup>+</sup> = 779, [M-H]<sup>-</sup> = 755.

*Myristoyl - (α - methyl)alanyl - sarcosyl - leucyl - valyl - glutaminy - leucine methyl ester (Myr-Aib-Sar-Leu-Val-Gln- Leu-OMe) (53)*

Compound **52** (56 mg, 0.076 mmol) was treated with 2 mL saturated HCl in EtOH at -20° C, warmed to room temperature, and concentrated *in vacuo* to a yellow foam. The resulting amine hydrochloride salt, myristic acid (52 mg, 0.23 mmol, 3 eq), EDC (45 mg, 0.24 mmol, 3 eq), and HOBT (33 mg, 0.24 mmol, 3.2 eq) were dissolved in 2 mL DMF, stirred vigorously for 5 minutes, and then treated with DIEA (40 μL, 0.23 mmol, 3 eq). After stirring overnight, the reaction was purified directly by C18 HPLC (60-100% MeCN in H<sub>2</sub>O over 25 minutes) to yield 14.8 mg (23%) of the desired compound **53**. MALDI FTMS [M + Na]<sup>+</sup> obsd *m/z* 874.6001; calcd 874.5988 for C<sub>44</sub>H<sub>81</sub>N<sub>7</sub>O<sub>9</sub>Na (Δ 1.5 ppm); <sup>1</sup>H NMR (400 MHz, DMSO-*d*<sub>6</sub>):

δ 0.85 (m, 21H), 1.22 (m, 20H), 1.34 (s, 3H), 1.35 (s, 3H), 1.45-1.75 (m, 9H), 1.86 (m, 1H), 1.89 (m, 1H), 2.08 (m, 2H), 2.15 (m, 2H), 3.08 (s, 3H), 3.60 (s, 3H), 3.88 (s, 2H), 4.13-4.25 (m, 4H), 6.75 (s, 1H), 7.23 (m, 2H), 7.88 (d, *J* = 7.6 Hz, 2H), 8.17 (d, *J* = 7.6 Hz, 1H), 8.60 (s, 1H)

*Myristoyl – (α - methyl)alanyl –(trans-4 -hydroxyl) prolyl - leucyl - valyl - glutaminyll – leucine ethyl ester (Myr-Aib-(trans-4-hydroxy)Pro-Leu-Val-Gln-Leu-OEt) (54)*

Intermediate **36** (31 mg, 0.032 mmol) was treated with 1 mL of TFA at ambient temperature for 30 minutes, and then concentrated under reduced pressure. The resulting amine salt was dissolved in 0.5 mL DMF and treated with DIEA (33 μL, 0.19 mmol, 6 eq, pH 9). In a separate flask, myristic acid (16 mg, 0.070 mmol, 2.2 eq), EDC (13 mg, 0.070 mmol, 2.2 eq), and HOBt (9.5 mg, 0.070 mmol, 2.2 eq) were dissolved in 1 mL DMF and stirred under N<sub>2</sub> at ambient temperature for 10 minutes. The two solutions were then combined and stirred under N<sub>2</sub> overnight. The homogeneous reaction was purified directly by C18 HPLC using a 0-100% gradient of MeOH in H<sub>2</sub>O over 15 minutes. A second reversed-phase HPLC purification using a 60-100% gradient of MeOH in H<sub>2</sub>O yielded 21 mg of the desired product (73% yield). ESI-MS [M + H]<sup>+</sup> = 908.6, [M + Na]<sup>+</sup> = 930.6; <sup>1</sup>H NMR (400 MHz, DMSO-*d*<sub>6</sub>):

δ 0.84 (m, 21H), 1.16 (t, 3H, *J* = 6 Hz), 1.22 (m, 20H), 1.34 (s, 3H), 1.36 (s, 3H), 1.45-1.80 (m, 10H), 1.91 (m, 1H), 2.11 (m, 3H), 2.18 (m, 3H), 3.21 (d, *J* = 11, 1H), 3.71 (d, *J* = 11 Hz, 1H), 4.06 (m, 4H), 4.22 (m, 3H), 4.39 (t, *J* = 8.4 Hz, 1H), 5.13 (s, 1H), 6.74 (s, 1H), 7.22 (s, 1H), 7.24 (d, 1H), 7.58 (d, *J* = 8.0 Hz, 1H), 7.88 (d, *J* = 7.2 Hz, 1H), 7.95 (d, *J* = 7.6 Hz, 1H), 8.66 (s, 1H)

*Myristoyl – (α - methyl)alanyl – prolyl - leucyl - valyl - glutaminyll – leucinol myristyl ester (Myr-Aib-Pro-Leu-Val-Gln-Lol-OMyr) (55)*

Halovir C (**29**) (16.7 mg, 0.0196 mmol) was dissolved in 2 mL CH<sub>2</sub>Cl<sub>2</sub> and treated with myristoyl chloride (26.7  $\mu$ L, 0.982 mmol, 5 eq) and stirred at room temperature under N<sub>2</sub> overnight. The reaction was concentrated *in vacuo*, and filtered over silica gel using CH<sub>2</sub>Cl<sub>2</sub> 9:1 MeOH. The enriched fraction was further purified by C18 HPLC (70-100% MeCN over 15 minutes) to yield 16 mg of compound **55** (76% yield). ESI-MS [M + H]<sup>+</sup> = 1061, [M + Na]<sup>+</sup> = 1083; <sup>1</sup>H NMR (400 MHz, DMSO-*d*<sub>6</sub>):  $\delta$  0.85 (m, 24H), 1.22 (m, 40H), 1.34 (s, 3H), 1.36 (s, 3H), 1.46-1.90 (m, 13H), 2.09 (m, 3H), 2.20 (m, 3H), 2.27 (t, *J* = 7.2 Hz, 2H), 3.28 (m, 1H), 3.75 (m, 1H), 3.84 (m, 1H), 3.90 (m, 1H), 4.02 (m, 4H), 4.28 (t, *J* = 7.6 Hz, 1H), 6.72 (s, 1H), 7.20 (s, 1H), 7.28 (d, *J* = 6.4 Hz, 2H), 7.45 (d, *J* = 7.6 Hz, 1H), 7.92 (d, *J* = 6.4 Hz, 1H), 8.68 (s, 1H)

### References

1. Sansom, M.S.P. (1993). Structure and function of channel-forming peptaibols. *Q. Rev. Biophys.* **26**, 365-421.
2. Toniolo, C., Crisma, M., Formaggio, F., Peggion, C., Monaco, V., Goulard, C., Rebuffat, S. & Bodo, B. (1996). Effect of N-alpha-acyl chain length on the membrane-modifying properties of synthetic analogs of the lipopeptaibol trichogin GA IV. *J. Am. Chem. Soc.* **118**, 4952-4958.
3. Thormar, H., Isaacs, C.E., Brown, H.R., Barshatzky, M.R. & Pessolano, T. (1987). Inactivation of enveloped viruses and killing of cells by fatty acids and monoglycerides. *Antimicrob. Agents Chemother.* **31**, 27-31.

## **Chapter 6. New Marine-Derived Inhibitors of HIV cDNA Integration**

**This chapter presents the results of a collaborative effort with the laboratory of Dr. Frederic Bushman at the Salk Institute for Biological Studies. The objective of this collaboration was to discover marine natural products with inhibitory properties against the integrase enzyme of the human immunodeficiency virus (HIV). Integrase is an attractive target for the development of antivirals to treat HIV infection, but clinically useful integrase inhibitors have so far eluded development. Dr. Frederic Bushman is an expert in the field of retroviral integration, and I was very fortunate to have been able to interact with the many intelligent, dedicated, and friendly scientists working under his guidance. I must especially acknowledge the significant efforts of Ms. Denise Rhodes and Dr. Mark Hansen. Ms. Rhodes was responsible for conducting the screening assay used to detect integrase activity in crude extracts and to measure the *in vitro* potencies of pure compounds. Dr. Hansen conducted the advanced biological evaluations with the thalassiolins, the major group of inhibitors discovered in this investigation. A further extension of this study was conducted in collaboration with the laboratory of Dr. J. Andrew McCammon in the Department of Chemistry and Biochemistry at UCSD. Dr. Christoph A. Sotriffer and Dr. Haihong Ni, both post-doctoral researchers in the McCammon lab, conducted molecular modeling studies on potential binding interactions between the thalassiolins and the catalytic core domain of HIV integrase.**

## **6.1 Introduction**

HIV and the associated Acquired Immunodeficiency Syndrome (AIDS) continue to pose one of the greatest human health challenges worldwide. AIDS has led to the death of approximately 20 million people globally, and an estimated 36 million persons are currently infected with HIV. Sub-Saharan Africa is the hardest hit by the pandemic, with approximately 25.3 million people now HIV positive.<sup>1</sup> In the United States, nearly 450,000 persons have reportedly died of AIDS. However, due to the advent of new antiretroviral chemotherapies, the rate of AIDS related deaths in the U.S. has now begun to decline.<sup>2</sup>

The breakthroughs in developing drugs against HIV are a testament to our ability to treat viral disease by chemotherapy. "Cocktails" consisting of protease and reverse transcriptase enzyme inhibitors have proven effective in lowering the viral load in some patients to below detectable levels. Multi-drug therapy is necessary because the HIV genome rapidly mutates and thus quickly develops resistance to any single drug. However, these drugs are not without side effects<sup>3</sup> and most are prohibitively expensive for much of the world's infected population. New drugs are still needed, especially ones with novel modes of action to help prevent the evolution of HIV drug resistance.

Integrase is an essential enzyme in the replication cycle of HIV, and represents an attractive drug target since it shares no functional homology with normal cellular proteins. Integrase catalyzes the processing of the viral cDNA product from reverse transcription and its insertion into a host chromosome (Figure 35A). After binding to

the viral cDNA, integrase mediates endonucleolytic processing to cleave a dinucleotide from each 3' end. Transesterification of the recessed 3'-hydroxyls then occurs with 5'-phosphates on the target DNA. The points of covalent joining are separated by five base pairs. Subsequent melting of these base pairs followed by DNA repair completes the formation of the provirus.<sup>4</sup>

The development of *in vitro* assays based on this model has aided in the identification of small molecule integrase inhibitors. Typically, purified integrase enzyme is used to catalyze the reactions of 3'-processing and strand transfer on oligonucleotides matching one end of the unintegrated HIV cDNA (Figure 35B). Alternatively, preintegration complexes, or PICs, can be partially purified from HIV infected cells and used to perform *in vitro* integration reactions.<sup>5</sup> PICs are assemblies of integrase enzyme bound to viral cDNA, and likely contain additional HIV and cellular proteins. Therefore, PIC assays more closely resemble *in vivo* integration events and represent a more stringent assay system for the identification of inhibitors.

The search for clinically useful integrase inhibitors has yielded few promising leads. Recently, researchers at Merck have reported a series of diketo acids (for example 56-59) that display specific and potent inhibition of purified integrase enzyme and PICs, as well as antiviral activity against HIV in cell culture.<sup>6,7</sup> HIV-1 variants resistant to these compounds consistently contained specific mutations in the integrase-coding region, documenting action against integrase *in vivo*. Other reported integrase inhibitors have either lacked antiviral efficacy, suffered from toxicity problems, or have been proven to block viral replication steps other than cDNA



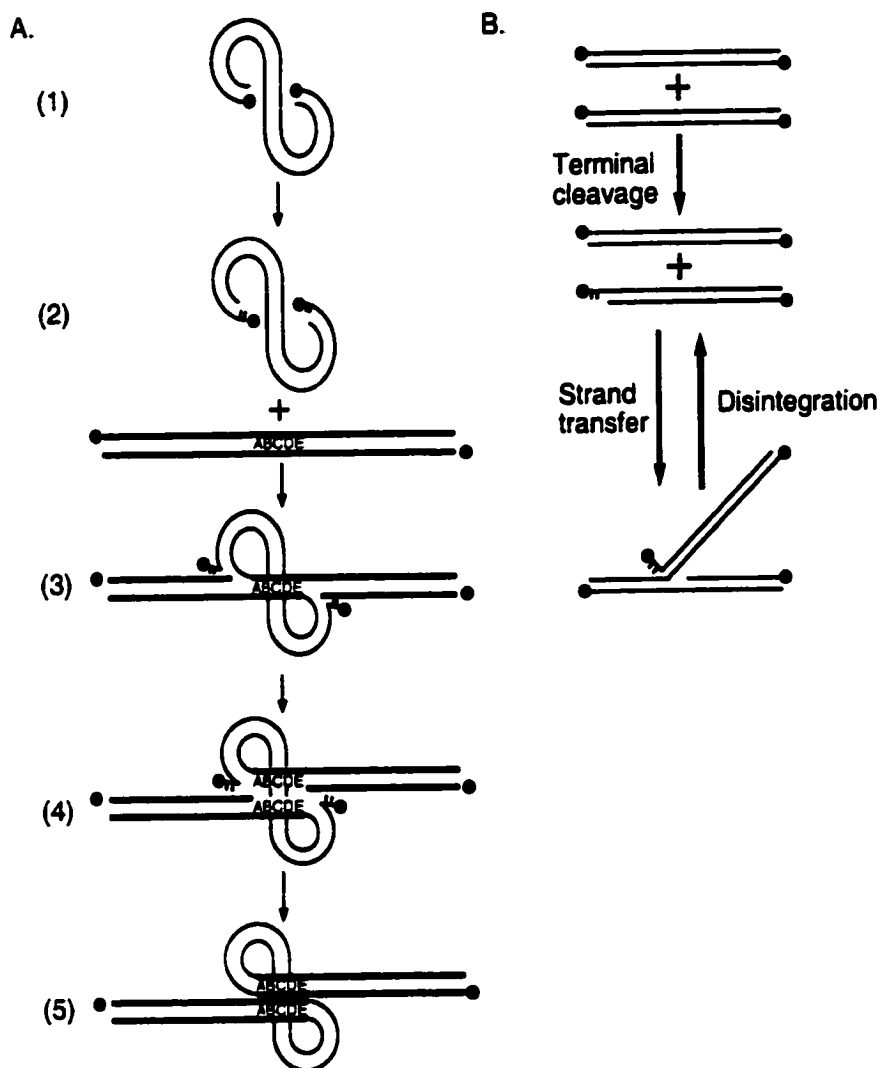
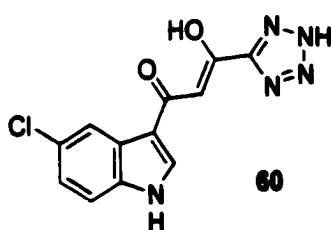
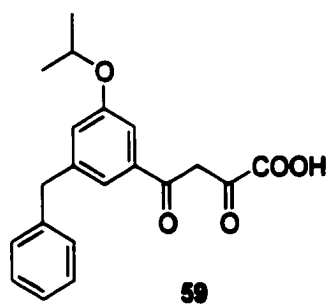
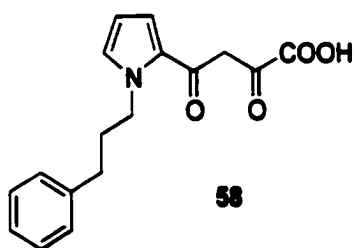
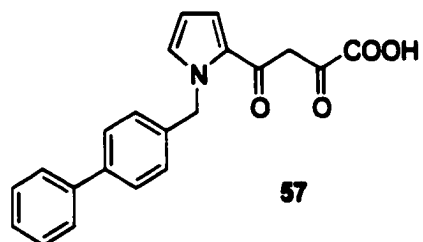
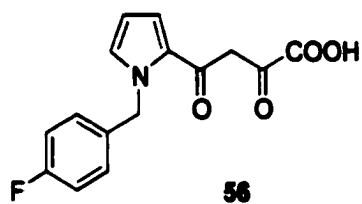


**Figure 35. Integration events catalyzed by HIV integrase. (A)** Viral cDNA from reverse transcription (1) is processed by cleavage of two nucleotides from each 3' end (2). The recessed 3' ends are then joined to protruding 5' strand breaks in the host DNA (3). The points of joining of the two DNA molecules are offset by five base pairs which subsequently melt (4). Filling and sealing of these gaps then yields the integrated provirus (5). **(B)** Assay reactions catalyzed *in vitro* by purified integrase.



integration *in vivo*. Nevertheless, the *in vitro* activities of these clinically non-useful inhibitors add to a growing body of structure-activity relationship data that may prove useful in the future design of an integrase drug. Investigations involving proteolysis and site-directed mutagenesis have identified the catalytic site in the core domain of HIV integrase, and established three critical catalytic residues: Asp-64, Asp-116, and Glu-152.<sup>8,9</sup> Goldgur and coworkers have described a crystal structure of HIV integrase with the inhibitor SCITEP (**60**) complexed in the active site.<sup>10</sup> Molecular modeling techniques have been successful in reproducing the experimental binding mode of this inhibitor, and should therefore be useful in analyzing possible binding modes of other IN-inhibitors as well.<sup>11</sup>

The aim of my collaboration with the Bushman laboratory has been the identification of new small molecule inhibitors of HIV integrase derived from unique marine sources. Several thousand crude extracts and purified compounds, most derived from marine microbial sources, were screened for *in vitro* activity against integrase. A counter assay that tested for activity against MCV topoisomerase, another DNA modifying enzyme, was used to evaluate extracts for selective enzyme inhibition. The top ranked hits were further pursued by chemical investigation to determine the identity of the inhibitors.

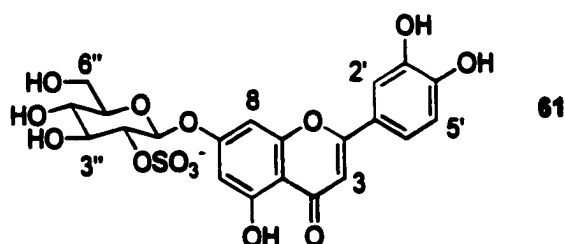
## **6.2 Thalassiolins A-C, Inhibitors of HIV cDNA Integration**

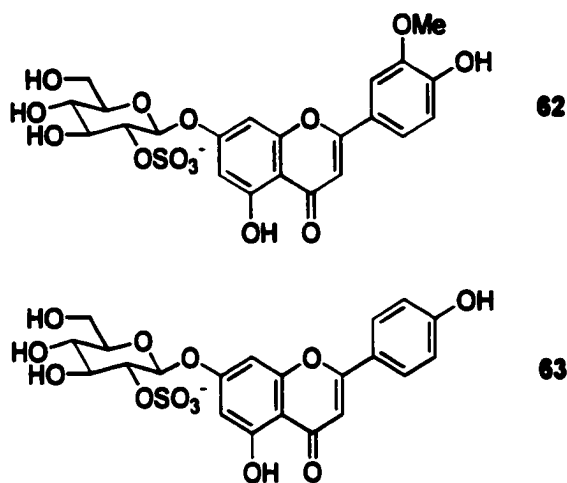
The most promising lead in this project was from an aqueous extract prepared from a collection of the Caribbean sea grass *Thalassia testudinum*. Chemical analysis

revealed that the inhibitory properties were due to the presence of a series of water-soluble flavones named the thalassiolins A-C. Thalassiolin A had been previously described as a chemical defense molecule produced by the sea grass to deter fouling microorganisms.<sup>12</sup> The thalassiolins contain unique functionality in the form of  $\beta$ -D-glucopyranosyl-2''-sulfate, a substituent that imparts increased potency against integrase in biochemical assays versus the parent flavone. Thalassiolin A displays submicromolar *in vitro* activity against the strand transfer reaction, inhibits HIV replication in cell culture, and shows little cytotoxicity.

### 6.2.1 Isolation and Structural Characterization

*Thalassia testudinum* was collected from a shallow lagoon located at Little San Salvador Island in the Bahamas. The sea grass was blended with deionized H<sub>2</sub>O and then filtered through celite to remove particulates. The filtrate was vacuum filtered through C18 silica gel, and the flavonoid components retained on the resin were eluted with 10% MeCN in H<sub>2</sub>O. The lyophilized fraction was further fractionated using LH-20 column chromatography with methanol, and the active compounds separated into three yellow bands. Reversed phase HPLC using a gradient of 5-15% MeCN in H<sub>2</sub>O provided pure thalassiolins A-C (61-63).





Thalassiolin A (**61**) was identified as luteolin 7- $\beta$ -D-glucopyranosyl-2''-sulfate by comparison of  $^1\text{H}$  and  $^{13}\text{C}$  NMR, IR, and mass spectral data with the previously reported compound.<sup>12</sup> Thalassiolin B (**62**) analyzed for the molecular formula  $\text{C}_{22}\text{H}_{21}\text{O}_{14}\text{S}$  by high resolution MALDI FTMS. Analysis of  $^1\text{H}$ ,  $^{13}\text{C}$ , and DEPT NMR spectra, as well as molecular formula considerations, supported the presence of an additional methoxy group that was subsequently placed at the 3' position by HMBC-NMR correlations (Figure 38). The aglycone of thalassiolin B was therefore assigned as chrysoeriol. Thalassiolin C (**63**) analyzed for the molecular formula  $\text{C}_{21}\text{H}_{19}\text{O}_{13}\text{S}$  also by high resolution MALDI FTMS. A para-substituted phenol was easily recognized by symmetry in both the  $^{13}\text{C}$  NMR spectrum and the  $^1\text{H}$  NMR aromatic proton coupling pattern. Hence, substitution of a phenol for a catechol ring accounts for the one fewer oxygen atom than in **61**. The aglycone of **63** therefore corresponds to apigenin. All 2D-NMR data, including COSY, gHMOC, and gHMBC, were consistent with these assignments. Proton and  $^{13}\text{C}$  chemical shift and coupling

Table 10.  $^1\text{H}$  and  $^{13}\text{C}$  NMR Assignments for Thalassiolins A-C in  $\text{DMSO-}d_6$ .

C#	Thalassiolin A (61)		Thalassiolin B (62)		Thalassiolin C (63)	
	$\delta^{13}\text{C}^a$	$\delta^1\text{H}^b$ (m, J (Hz))	$\delta^{13}\text{C}$	$\delta^1\text{H}$ (m, J (Hz))	$\delta^{13}\text{C}$	$\delta^1\text{H}$ (m, J (Hz))
2	164.6		164.3		164.4	
3	102.9	6.75 (s)	103.2	6.96 (s)	102.6	6.82 (s)
4	181.9		182.0		181.9	
5	161.2		161.2		161.2	
6	99.6	6.42 (s)	99.4	6.42 (s)	99.5	6.39 (s)
7	162.7		162.6		162.6	
8	95.0	6.76 (s)	95.3	6.82 (d, 1.8)	95.0	6.78 (d, 1.8)
9	156.9		156.9		156.8	
10	105.4		105.4		105.4	
1'	120.8		120.8		119	
2'	113.3	7.44 (s)	110.1	7.58 (s)	128.7	7.92 (d, 8.7)
3'	146.0		148.2		116.3	6.87 (d, 8.4)
4'	150.7		151		162.6	
5'	116.0	6.89 (d, 8.1)	115.9	6.92 (d, 8.5)	116.3	6.87 (d, 8.4)
6'	119.3	7.46 (dd, 8.1, 1.5)	120.7	7.60 (dd, 8.5, 1.2)	128.7	7.92 (d, 8.7)
1''	97.4	5.30 (d, 7.5)	97.3	5.28 (d, 7.8)	97.2	5.3 (d, 7.8)
2''	78.5	4.04 (dd, 7.8)	78.5	4.03 (dd, 8.1)	78.4	4.02 (dd, 8.4)
3''	75.9	3.62 (dd, 8.7)	75.9	3.61 (dd, 8.7)	75.9	3.60 (dd, 8.4)
4''	69.4	3.28 (dd, 9)	69.5	3.26 (dd, 9)	69.4	3.28 (m)
5''	76.9	3.52 (m)	76.9	3.50 (m)	76.8	3.50 (m)
6''	60.5	3.73 (m)	60.5	3.71 (d, 9.9)	60.4	3.70
OMe		3.49 (dd, 10.2)	56.0	3.49 (m)		3.48 (m)
				3.89 (s)		

a) 100 MHz b) 300 MHz Assignments by DEPT, COSY, HMQC, and HMBC.

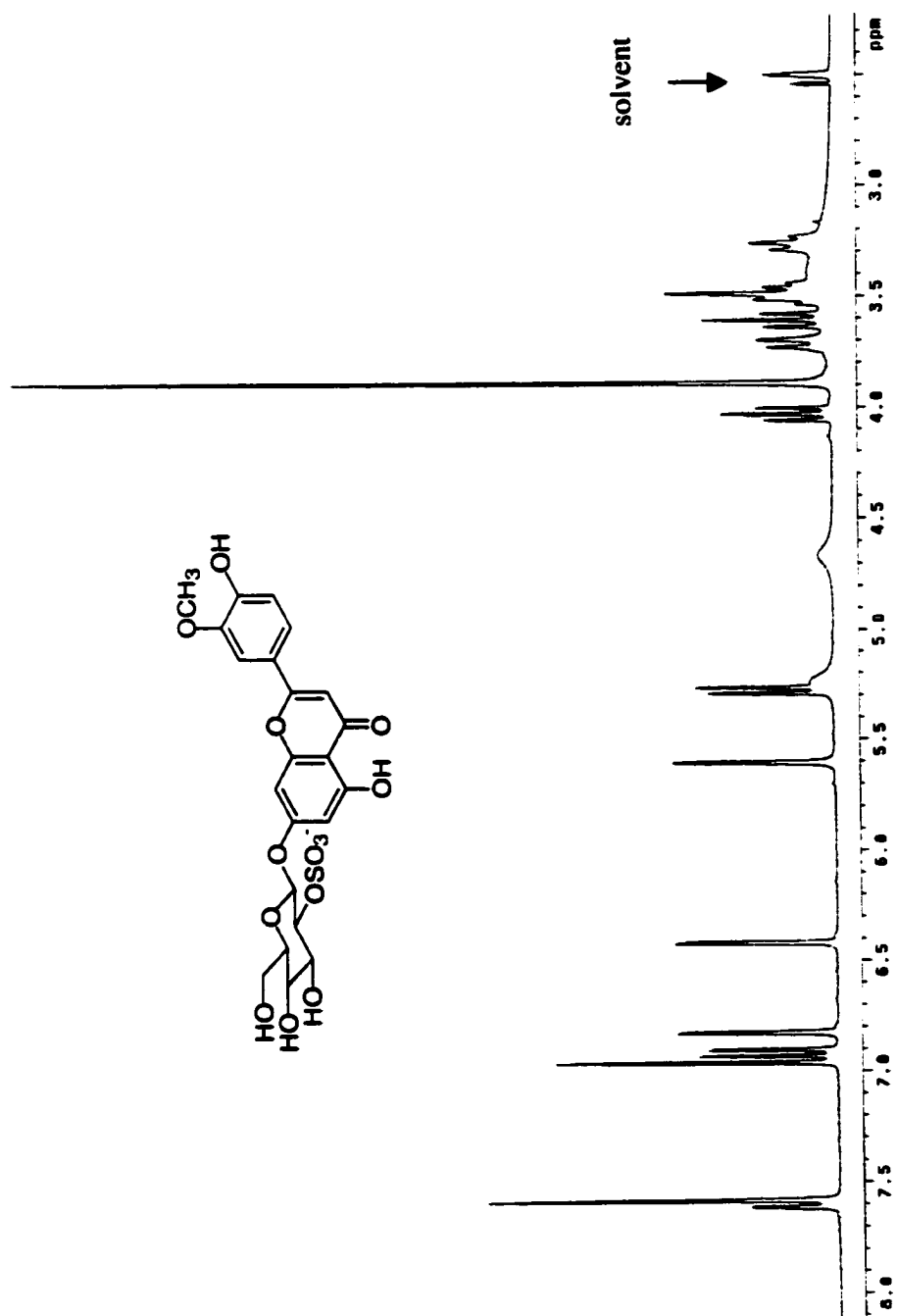


Figure 36. Proton NMR spectrum (300 MHz) of thalassiolin B (62) in DMSO-*d*<sub>6</sub>.

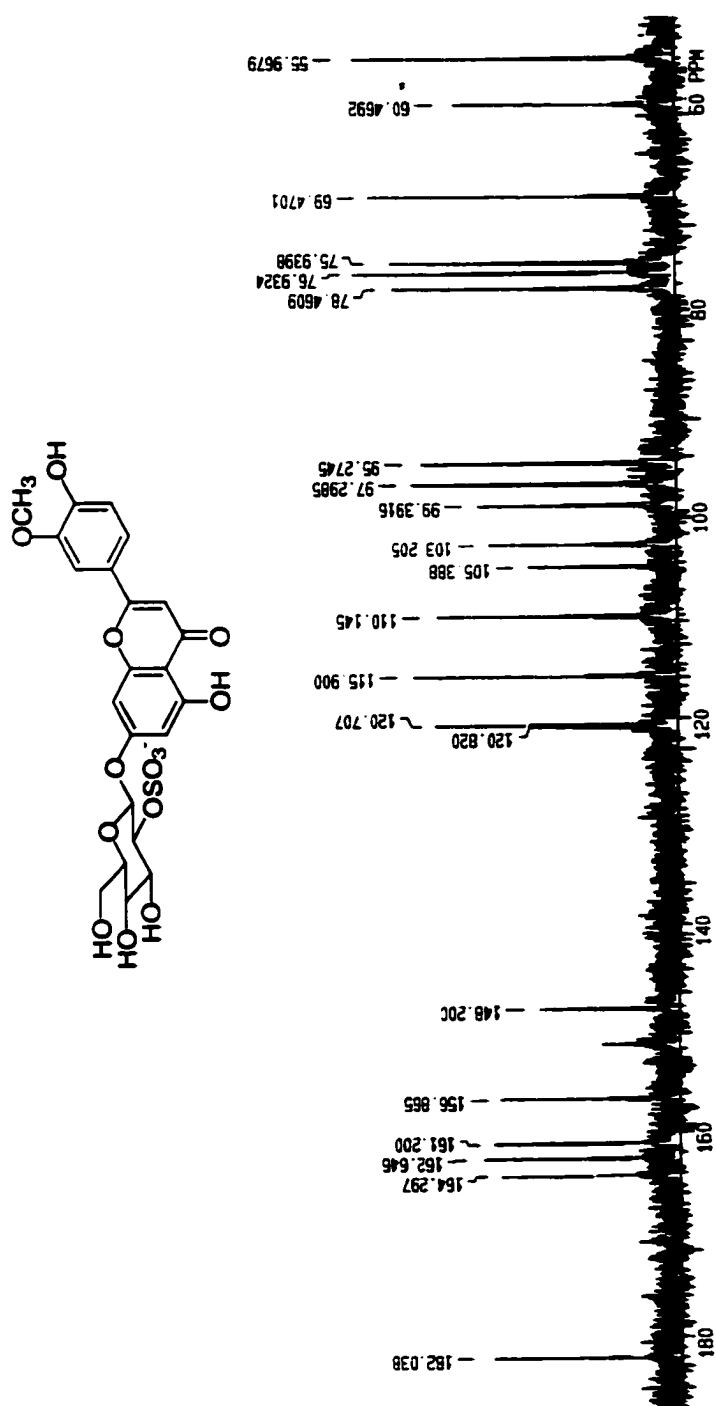


Figure 37. Carbon NMR spectrum (100 MHz) of thalassiolin B (62) in DMSO-*d*<sub>6</sub>.



constant data, as well as IR data, fully supported the sugar moieties of **62** and **63** as matching that of **61** (see Table 10). Compounds **62** and **63** were therefore identified as chrysoeriol 7- $\beta$ -D-glucopyranosyl-2"-sulfate and apigenin 7- $\beta$ -D-glucopyranosyl-2"-sulfate, respectively.

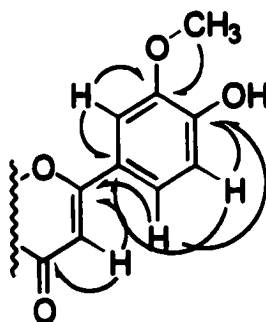
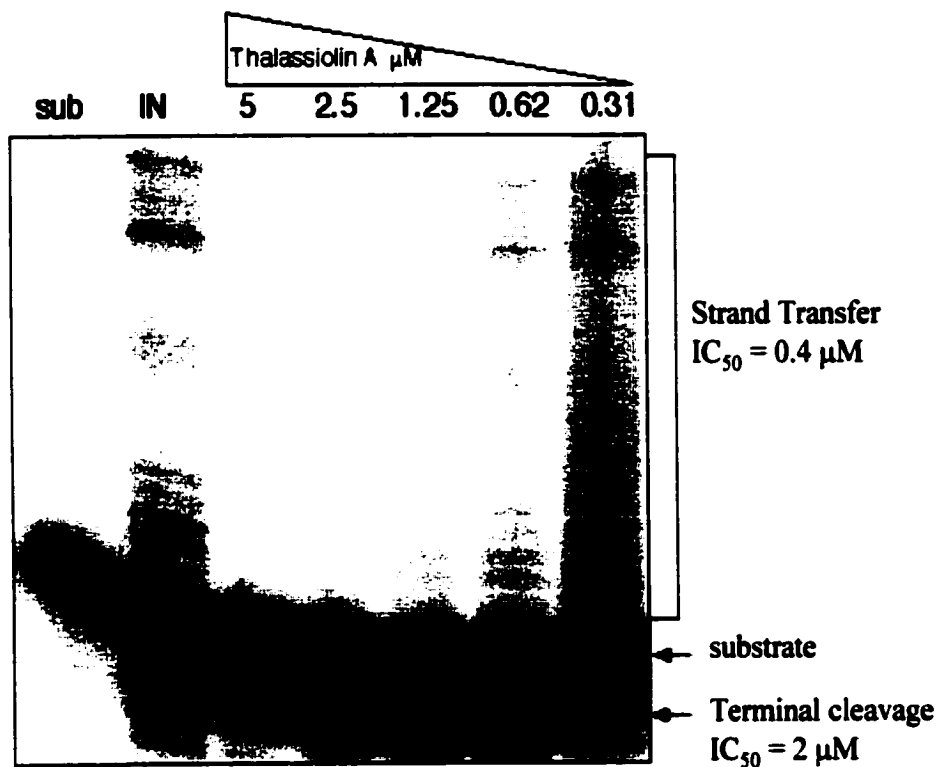


Figure 38. Partial HMBC analysis of thalassiolin B (**62**).

### 6.2.2 Biological Properties

$IC_{50}$  values for inhibition of purified HIV integrase protein were determined using two assays. In the first, purified integrase was incubated with end-labeled DNA substrates and various concentrations of **61-63**. Reaction products were denatured and separated by electrophoresis on denaturing polyacrylamide gels. Reactions were quantitated by phosphorimager analysis of the radioactive products.<sup>13-16</sup> These reactions were carried out in the presence of  $Mn^{+2}$  as the metal cofactor.

Thalassiolin A was most active, inhibiting the integrase terminal cleavage and strand transfer activities with  $IC_{50}$  values of 2.1 and 0.4  $\mu M$ , respectively (Figure 39 and Table 11). Thalassiolins B and C were less potent inhibitors, with  $IC_{50}$  values in the 30-100  $\mu M$  range.



**Figure 39.** Inhibition of integration *in vitro* by thalassiolin A. The figure displays an autoradiogram of reaction products. The lane marked "sub" contained substrate only, the others contained full length HIV-1 integrase. The concentrations of thalassiolin tested are indicated above the lanes. The mobility of the substrate, terminal cleavage, and strand transfer products are marked with arrows.

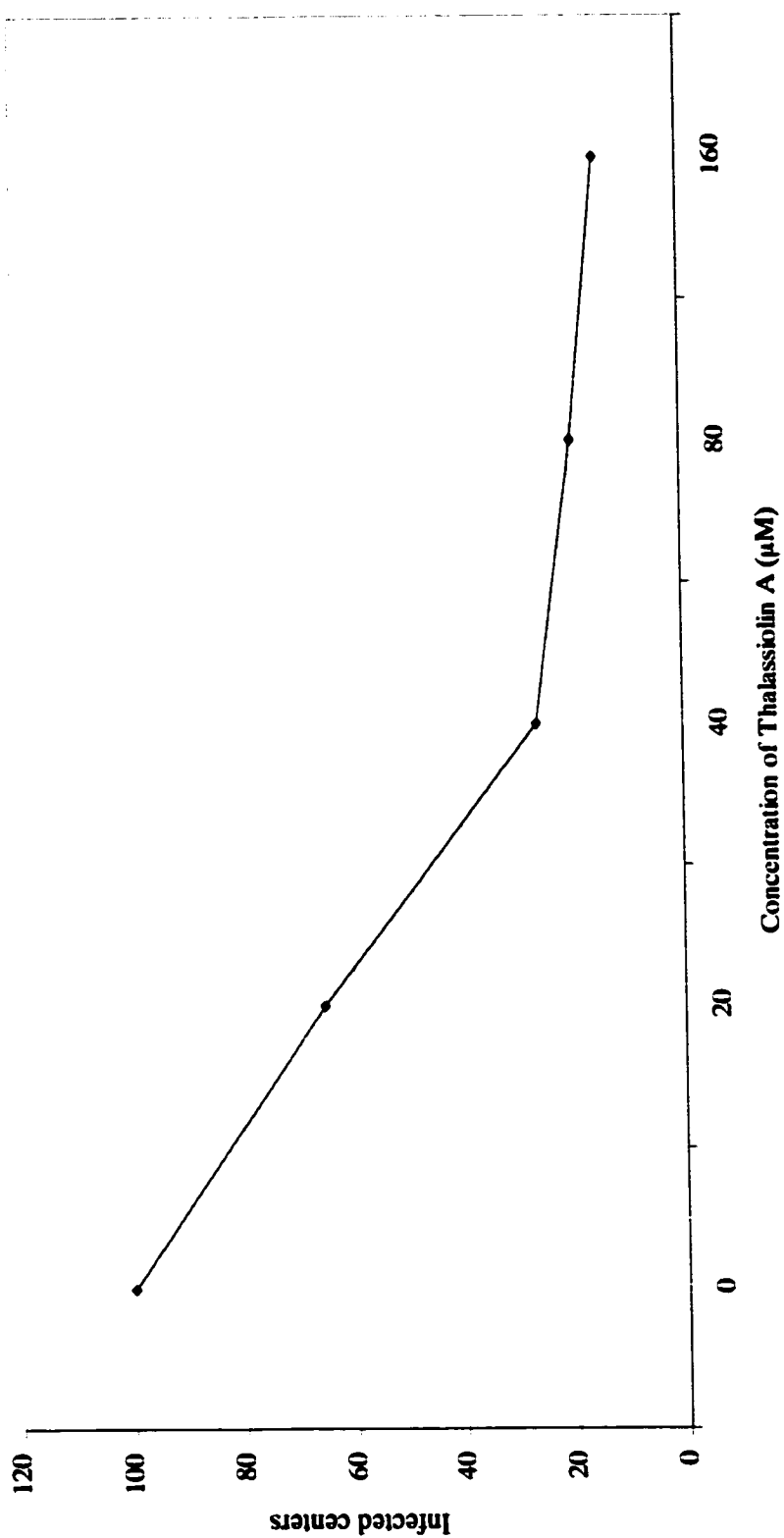


**Figure 40.** Dose dependent antiviral activity of thalassiolin A (**61**) versus HIV-1. P4 cells were infected with HIV-1 treated with increasing concentration of **61**. After 48 hours, cells were fixed and stained to detect  $\beta$ -galactosidase, a reporter for HIV infection. Infectious centers were counted and normalized to the uninfected control (660 infected centers). A background of two infected centers seen in uninfected samples was subtracted from each sample. The concentrations of **61** are 20, 40, 80, 120, and 160  $\mu$ M.

Table 11. IC<sub>50</sub> Inhibitory Activities of the Thalassiolins (μM)

Compound	purified integrase		ELISA <sup>b</sup>	live virus	LD <sub>50</sub> <sup>d</sup>	MCV Topo
	T. Cl. <sup>a</sup>	Str. Tr. <sup>a</sup>				
Thalassiolin A (61)	2.1	0.4	2	27	>800	>200
Thalassiolin B (62)	112	43	>200	ND <sup>c</sup>	>800	>200
Thalassiolin C (63)	67	28	140	ND <sup>c</sup>	>800	>200

a) Mn<sup>2+</sup> metal cofactor

b) Mg<sup>2+</sup> metal cofactor

c) ND = not done

d) Cytotoxicity against MT2 cells

Inhibitory activities against the strand transfer reaction were compared in the presence of  $Mg^{+2}$ , since this is more likely to be the metal cofactor utilized *in vivo*. Integrase was preassembled with viral DNA substrates, thereby mimicking the stably assembled preintegration complexes active *in vivo*. Hazuda and coworkers have reported that screens using such preassembled complexes can yield inhibitors active against HIV in cell culture.<sup>6</sup> Thalassiolin A inhibited the  $Mg^{+2}$  dependent strand transfer reaction with an  $IC_{50}$  of 2  $\mu M$ . Thalassiolins B and C were inactive in this assay.

The antiviral activity of thalassiolin A against HIV replication was determined using the MAGI indicator cell assay in which infected centers score as  $\beta$ -galactosidase positive syncytia.<sup>17</sup> Figure 40 shows that the addition of **61** to infected cultures indeed inhibited infection with an  $IC_{50}$  of about 30  $\mu M$ . Since the MAGI assay requires HIV to complete cell entry, reverse transcription, integration, and gene expression, we can deduce that the step affected by thalassiolin A is one of these.

The effect of **61** on the growth of HIV over multiple cycles of viral replication was also assessed. Cultures were infected with low titers of HIV and viral replication monitored by assaying synthesis of the viral capsid protein p24. HIV overgrew the culture within 10 days, while in the presence of **61** growth was barely detectable. Taken together, these studies document inhibition of HIV replication by thalassiolin A.

As a test of the specificity of inhibition, the effects of **61-63** were tested against the topoisomerase of the pathogenic poxvirus MCV (Table 11). Assays monitored the

strand cleavage and religation activities of this enzyme.<sup>18</sup> The IC<sub>50</sub> values were found to be greater than 200  $\mu$ M, the highest concentration tested.

Cellular toxicity was also monitored. No toxicity was detected against MT2 cells at 800  $\mu$ M, the highest concentration tested. Similarly, no toxicity was observed against HCT-116 cells at 75  $\mu$ M.

### **6.2.3 Possible Binding Sites on Integrase.**

Docking of thalassiolin A to the active site showed that binding close to the catalytic center is possible (Figure 41). For the top-ranked result of the computational search procedure, a free energy binding of -7.2 kcal/mol is calculated. In this energetically preferred binding mode, the sulfated glucose ring is embedded in a shallow pocket surrounded by His 67, Lys 156, and Lys 159. At the bottom of this pocket it interacts with Cys 65, Thr 66, and Asn 155. The 6''-oxygen is coordinated to the Mg<sup>2+</sup> ion, and the sulfate interacts with the two lysine side chains (Lys 156, Lys 159). The benzopyranone ring is placed close to Gln 148 and Glu 152, while the catechol ring extends into the space between Gln 148 and Asp 116, showing additional interactions with Asn 117 and the backbone of Phe 139.

The computer-based docking result also revealed a variant of this possible binding mode. It shows a somewhat less favorable free energy of binding (-7.0 kcal/mol), but needs to be considered as a possible alternative. While the glucose and sulfate are similarly oriented as in the first result, the position of the catechol ring and the orientation of the benzopyranone system are different. The catechol is now found

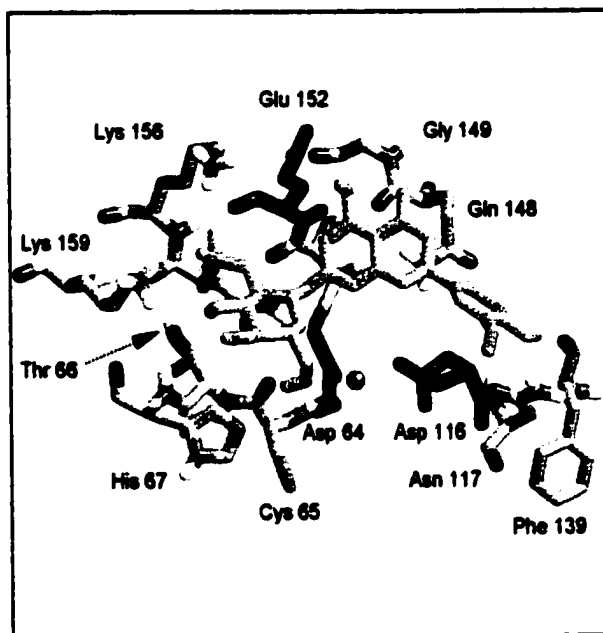


Figure 41. Computer-generated docking of thalassiolin A to the catalytic core domain of HIV-1 integrase. The inhibitor is shown in yellow and the catalytic residues (64, 116, 152) are highlighted in green, while the other amino acids are color coded by atom type; the metal ion is shown in violet. Except for the buried residues Ile 151 and Asn 155, all displayed amino acids are labelled.

in a rather exposed position between Gly 149 and Glu 152. The benzopyranone, instead, occupies exactly the same plane as in the first binding mode, but rotated by 180° such that the hydroxyl group (5-OH) points to Asp 116 instead of Glu 152.

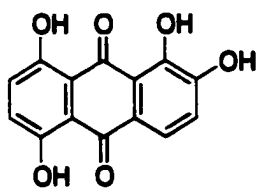
Docking of **62** and **63** to the active site provided essentially the same binding modes as observed for **61**, but with slightly less favorable binding free energy (-6.2 to -6.8 kcal/mol) for the least strained conformations.

#### 6.2.4 Discussion

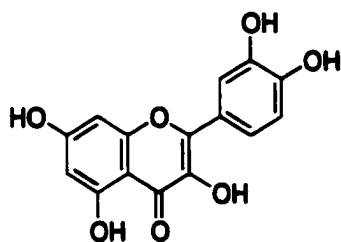
The HIV integrase inhibitory properties of the thalassiolins A-C, a series of sulfated-flavone glycosides isolated from the Caribbean sea grass *Thalassia testudinum*, were identified during a screening effort involving several thousand of marine extracts from diverse sources. The lead compound thalassiolin A (**61**) showed potent inhibition of reactions catalyzed by purified integrase in addition to antiviral activity against HIV in cell culture. The thalassiolins are non-cytotoxic, water soluble, and relatively easy to acquire, making them interesting candidates for further study as anti-HIV agents.

Polyhydroxylated aromatic compounds have been previously identified as inhibitors of HIV integrase. Activity is generally correlated to the presence of at least one pair of vicinal hydroxyl groups on an aromatic ring. Examples include quinalizarin (**64**),<sup>5</sup> flavones such as quercetin (**65**),<sup>19</sup> and the bis-catechols  $\alpha$ -conidendrin (**66**) and hematoxylin (**67**).<sup>20</sup> A shortcoming of these inhibitors is that *in vitro* enzyme inhibition has generally not translated to antiviral activity. An exception

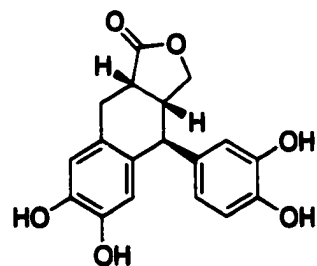




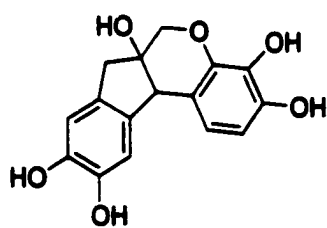
64



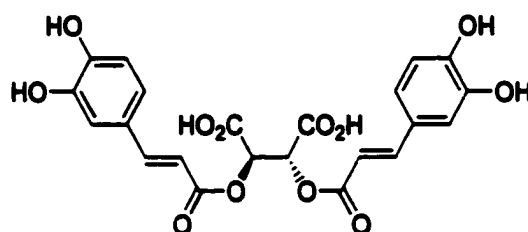
65



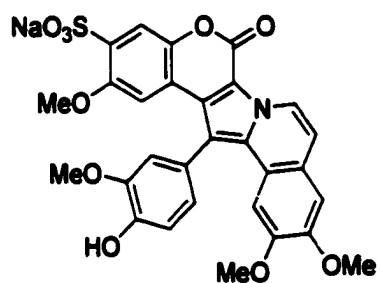
66



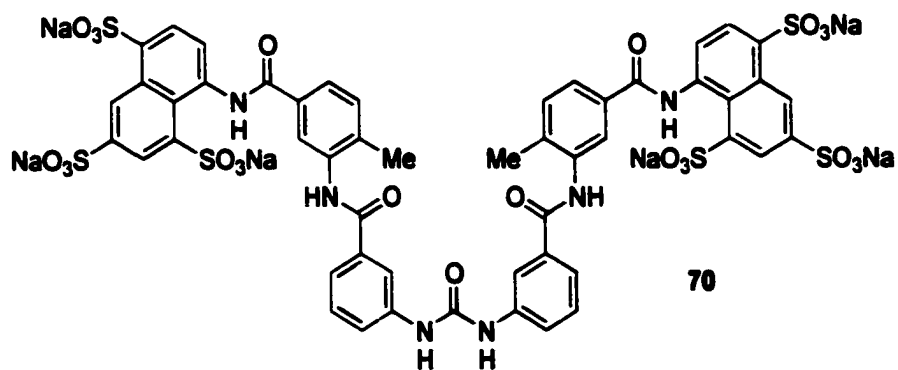
67



68



69



70

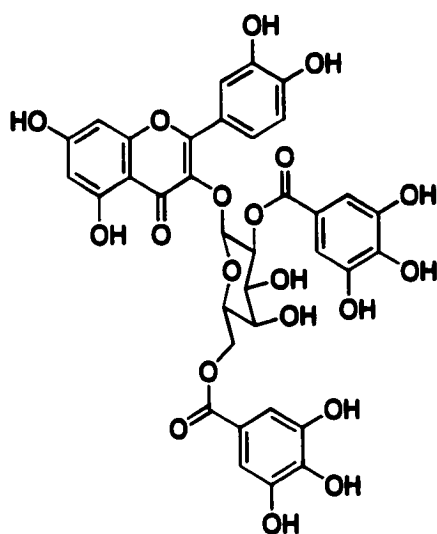
to this trend is L-chicoric acid (68), although this bis-catechol has recently been demonstrated to block viral entry as a primary mode of action.<sup>21</sup>

Sulfated phenols have also been previously reported as *in vitro* inhibitors of HIV integrase. Lamellarin- $\alpha$ -20-sulfate (69) shows moderate activity against purified enzyme and PICs, as well as more potent antiviral activity against HIV.<sup>22</sup> Suramin (70),<sup>23</sup> naphthalenesulfonic acid derivatives,<sup>24</sup> and sulfonated biphenyls<sup>25</sup> are further examples. However, the presence of a sulfated sugar alone is not sufficient to impart *in vitro* inhibitory properties against HIV integrase.<sup>24</sup>

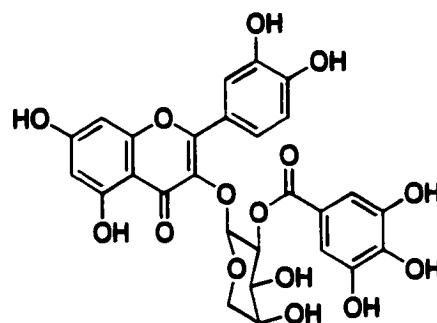
Structure-activity relationships for flavones have indicated that potency against integrase is increased in proportion to the number of ortho-hydroxyl pairs, and the inclusion of methoxy substituents generally reduces activity.<sup>26</sup> The results here are in agreement, since either the omission or methylation of the 3' phenyl hydroxyl group of 61 resulted in significantly less potent inhibitors. Interestingly, the integrase activity was less tolerant to 3' methylation, perhaps indicating the importance of steric effects at the binding site.

In contrast to our results, glycosylation of flavones has been reported to reduce or eliminate integrase activity. In the case of quercetin, substitutions at the 3-position with rhamnose, arabinose, glucose, or rutinose lead to significantly less potent or inactive compounds. Substitution of glucose at position 8 diminished the potency by a factor of 2-3.<sup>26</sup> One apparent exception to the glycosylation trend is the naturally occurring quercetin glycosides (71,72) with either one or two gallate esters appended to a galactose at the flavone 3-position.<sup>27</sup> Gallate esters contain three adjacent phenyl

hydroxyl groups, and are therefore likely to account for a portion of the integrase activity of these glycosylated quercetins. Although these compounds are only approximately as active as the parent flavone, this example suggests the possibility of using sugars as tethers for functionality to improve enzyme inhibition.



71



72

Thalassiolin A is to my knowledge the only glycosylated flavone reported that is more active than the parent aglycone. Although sugar substitution at the 7-position has not been well studied, methylation of quercetin at this site has been shown to decrease integrase activity by approximately 2-fold.<sup>26</sup> Perhaps then it is an appropriately placed sulfate that is responsible for the increased activity of these inhibitors.

Structural information about inhibitor binding to HIV integrase is still very limited, and only a single crystal structure with a ligand complexed to the active site is

currently available.<sup>10</sup> In the absence of experimental data, computational docking studies can help to generate hypotheses about protein-inhibitor interactions. Such an approach has been followed here. The applied docking method has recently been shown to successfully reproduce the experimental binding mode of the IN-inhibitor 5CITEP (**60**) in its crystallographic environment<sup>11</sup> and should therefore be a useful tool for the analysis of other IN-inhibitors as well.

The results suggest that the thalassiolins can be accommodated near the catalytic center. Interestingly, the binding modes overlap entirely with the location of 5CITEP.<sup>10</sup> The tetrazole ring of this inhibitor occupies the same binding position as the sulfated glucose of the thalassiolins, and the orientations of the keto-enol and chloroindole moieties of **60** show similarities with the benzopyranone binding position. The apparent similarities of how these two structurally different molecules can bind to the catalytic center of HIV integrase could be useful in the design of future inhibitors of this target.

The estimated binding free energy of **61** compares well with the expected affinity range based on the IC<sub>50</sub> value. The binding strengths of the weaker inhibitors **62** and **63** may be somewhat overestimated. In both binding modes suggested for **61**, the catechol ring is fairly exposed and the 3'-OH forms a weak hydrogen bond (with the side chains of Asn 117 and Glu 152, respectively). However, the catechol ring is located in a protein region known to be flexible, and it can be assumed that local conformational changes occur which lead not only to a better hydrogen bond geometry, but also to an improved fit of the entire catechol ring. Consequently, the

substitution of the 3'-OH with a methoxy group or a hydrogen atom may have a more dramatic effect on the binding energy than observed in the docking simulations in which the protein is required to be rigid.

In summary, binding to the active site appears to be a plausible way of interaction for the investigated inhibitors. While docking results alone are not sufficient to rule out other possible modes of action, binding to the active site should definitely be considered as one mechanism through which these compounds act as inhibitors of integrase.

The mechanism by which thalassiolin A inhibits replication of HIV in cell culture has not been fully clarified. Inhibition of viral entry or reverse transcription cannot be ruled out. However, the relative level of antiviral activity versus enzyme inhibition of **61** is consistent with what one might expect based on the potency of inhibition against the purified integrase enzyme. Perhaps more importantly, though, the proposed binding similarities of the thalassiolins and 5-CITEP with the catalytic core domain of HIV-1 integrase provide additional framework for the design and development of future inhibitors.

### 6.2.5 Experimental

Thalassiolin B (62): yellow amorphous solid;  $[\alpha]_D = -72^\circ$  ( $c = 0.25$ , MeOH); IR (neat) 3378, 1659, 1602, 1497, 1259, 1073, 1029, 1001, 817; UV (MeOH)  $\lambda_{\max}$  346 ( $\epsilon$  20600), 268 ( $\epsilon$  15900), 251 ( $\epsilon$  16800), 207 ( $\epsilon$  35800); HRMALDI FTMS  $m/z$  541.0636

$[M - H]^+$ , calcd for  $C_{22}H_{21}O_{14}S$ , 541.0657 ( $\Delta = 3.9$  ppm);  $^1H$  and  $^{13}C$  NMR data are shown in Table 10.

**Thalassiolin C (63)**: yellow amorphous solid;  $[\alpha]_D = -54^\circ$  ( $c = 0.25$ , MeOH); IR (neat) 3384, 1653, 1605, 1497, 1244, 1177, 1073, 1000, 835; UV (MeOH)  $\lambda_{max}$  334 ( $\epsilon$  13600), 268 ( $\epsilon$  12300), 207 ( $\epsilon$  23400); HRMALDI FTMS  $m/z$  511.0552  $[M - H]^+$ , calcd for  $C_{21}H_{19}O_{13}S$ , 511.0552 ( $\Delta = 0$  ppm);  $^1H$  and  $^{13}C$  NMR data are shown in Table 10.

**In vitro Assays.** Assays of HIV integrase were either carried out with  $Mn^{2+}$  as the metal cofactor and assayed on gels, or carried out with  $Mg^{2+}$  and assayed in microtiter plates. Assay of purified HIV integrase was carried out essentially as described,<sup>28</sup> except strand transfer products were detected using a digoxigenin label instead of a radioactive label. In assays with Mg, integrase and LTR DNA were preassembled by a brief preincubation at room temperature. Assays with such preassembled complexes have yielded inhibitors with antiviral activity in previous studies (Hazuda *et al.*, 2000). Assays of MCV topoisomerase were carried out using a microtiter assay that monitored religation of oligonucleotide substrates.<sup>29</sup>

**Cell Culture.** MT-2 cells were maintained between  $2 \times 10^5$  and  $1 \times 10^6$  cells in RPMI (BioWhitaker) supplemented with 10% FCS (GIBCO). MT-2 cells producing HIV-1 strain R9 were grown in RPMI supplemented with 20% FCS. P4 Cells<sup>30</sup> were maintained in DMEM (BioWhitaker) supplemented with 10% FCS.

**Infections.**  $10^6$  MT-2 cells were infected at a multiplicity of infection approximately equal to 0.01 (2 ng p24) in a 5 mL culture containing 8  $\mu g/mL$

polybrene (Sigma). Parallel infections were carried out in the absence or presence of 300  $\mu\text{M}$  thalassiolin A. Infected cells were maintained between  $2 \times 10^5$  and  $8 \times 10^5$  cells per mL. Samples were removed, filtered, and assayed for the presence of p24 antigen. P4 cells were plated in 96 well plates at  $10^4$  cells per well. The following day, growth media was aspirated and cells were infected with R9 HIV-1 virus in the absence or presence of varying concentrations of 1. Ten  $\mu\text{L}$  of viral supernatant was diluted to a volume of 100  $\mu\text{L}$  in the presence or absence of thalassiolin A and incubated for five minutes at room temperature. Supernatants were applied to plate wells for three hours at 37 °C. For detection of infected centers, reactions were incubated for 48 hours, fixed with glutaraldehyde and paraformaldehyde for 30 minutes and stained with X-Gal. Infected centers in each well were counted (600 for uninhibited reactions) and plotted as a percentage of the uninhibited reaction.

**P24 Elisa.** Viral supernatants were incubated for two hours in 0.1% empigen (CalBiochem) and TBS (10 mM Tris pH 7.6, 100 mM NaCl) at room temperature. Plates were washed three times with TBS and 100  $\mu\text{L}$  viral samples were added to plate wells for two hours at 37 °C. Samples were washed three times with TBS and 100  $\mu\text{L}$ . Normal mouse serum in TBS was added for 15 minutes at 37 °C. Plate wells were washed three times with TBS. 100  $\mu\text{L}$  of the detection antibody solution was added to each well. This solution contained 2.2  $\mu\text{L}$  monoclonal antibody, 2.2 mL sheep serum, 55  $\mu\text{L}$  10% tween and 8.8 mL TBS. After a one hour incubation at room temperature, wells were washed four times with 0.1% tween 20 in PBS. Wells were rinsed with 1x Tropix assay buffer and 50  $\mu\text{L}$  of Tropix Sapphire solution was added

to each well. After a 30 minute incubation at room temperature, luminescence was detected using a Topcount luminometer. Signal was converted to p24 antigen by comparison to titration of known concentration of recombinant HIV-1 p24.

Modeling of Thalassiolins A-C in the Active Site. Docking was performed with version 3.0 of the program AutoDock using the new empirical free energy function to evaluate binding free energies and the Lamarckian genetic algorithm to search for favorable binding positions.<sup>31</sup> While the protein is required to be rigid, the program allows torsional flexibility in the ligand. A standard AutoDock protocol was applied, with an initial population of 50 randomly placed individuals, a maximum number of  $3.0 \times 10^6$  energy evaluations, a mutation rate of 0.02, a crossover rate of 0.80, and an elitism value of 1. Proportional selection was used, where the average of the worst energy was calculated over a window of the previous 10 generations. For the local search the so-called pseudo-Solis and Wets algorithm was applied using a maximum of 300 iterations per local search. The probability of performing local search on an individual in the population was 0.06, and the maximum number of consecutive successes or failures before doubling or halving the local search step size was four. Fifty independent docking runs were carried out for each ligand using these parameters.

The structures of the ligands were generated with QUANTA® and optimized with the implemented CHARMM® force field (these programs are distributed by Molecular Simulations Incorporated). Atomic charges were assigned using the Gasteiger-Marsili formalism,<sup>32</sup> which is the type of atomic charges used in calibrating



the AutoDock empirical free energy function.<sup>31</sup> Torsional degrees of freedom were defined with the help of AutoTors. A moderate torsion constraint was defined for the bond between the benzopyranone and the substituted phenyl ring in the flavone unit in order to avoid perpendicular conformations [i.e. a torsion angle of 90°; a perpendicular torsional barrier of about 3 kcal/mol has been reported for flavones].<sup>33</sup>

The crystal structure of the IN catalytic core domain obtained by Goldgur *et al.*<sup>10</sup> was used as protein structure. It was set up for docking as previously described.<sup>11</sup> The grid maps defining the search region and representing the protein in the actual docking process were calculated with AutoGrid and had dimensions of 30 Å x 30 Å x 30 Å, with a spacing of 0.375 Å between the grid points.

### References

1. U.S. Department of Health & Human Services. (2001). The Global HIV and AIDS Epidemic, 2001. *M. M. W. R.* **50**, 434-439.
2. U.S. Department of Health & Human Services. (2001). HIV and AIDS - United States, 1981-2000. *M. M. W. R.* **50**, 430-434.
3. Sahai, J. (1996). Risks and synergies from drug interactions. *AIDS* **10**, S21-S25.
4. Hansen, M., Carreau, S., Hoffman, C., Li, L. & Bushman, F. (1998). Retroviral cDNA integration: mechanism, applications and inhibition. *In Genetic Engineering*. Vol. 20. J.K. Setlow, editor. Plenum Press, New York. 41-61.
5. Farnet, C.M., Wang, B.B., Lipford, J.R. & Bushman, F.D. (1996). Differential inhibition of HIV-1 preintegration complexes and purified integrase protein by small molecules. *Proc. Nat. Acad. Sci. USA* **93**, 9742-9747.
6. Hazuda, D.J., Felock, P., Witmer, M., Wolfe, A., Stillmock, K., Grobler, J.A., Espeseth, A., Gabryelski, L., Schleif, W., Blau, C. & Miller, M.D. (2000). Inhibitors of strand transfer that prevent integration and inhibit HIV-1 replication in cells. *Science* **287**, 646-650.

7. Wai, J.S., Egbertson, M.S., Payne, L.S., Fisher, T.E., Embrey, M.W., Tran, L.O., Melamed, J.Y., Langford, H.M., Guare, J.P., Zhuang, L., Grey, V.E., Vacca, J.P., Holloway, M.K., Naylor-Olsen, A.M., Hazuda, D.J., Felock, P.J., Wolfe, A.L., Stillmock, K.A., Schleif, W.A., Gabryelski, L.J. & Young, S.D. (2000). 4-Aryl-2,4-dioxobutanoic acid inhibitors of HIV-1 integrase and viral replication in cells. *J. Med. Chem.* **43**, 4923-4926.
8. Engelman, A. & Craigie, R. (1992). Identification of conserved amino acid residues critical for human immunodeficiency virus type-1 integrase function in vitro. *J. Virol.* **66**, 6361-6369.
9. Kulkosky, J., Jones, K.S., Katz, R.A., Mack, J.P.G. & Skalka, A.M. (1992). Residues critical for retroviral integrative recombination in a region that is highly conserved among retroviral retrotransposon integrases and bacterial insertion sequence transposases. *Mol. Cell Biol.* **12**, 2331-2338.
10. Goldgur, Y., Craigie, R., Cohen, G.H., Fujiwara, T., Yoshinaga, T., Fujishita, T., Sugimoto, H., Endo, T., Murai, H. & Davies, D.R. (1999). Structure of the HIV-1 integrase catalytic domain complexed with an inhibitor: A platform for antiviral drug design. *Proc. Nat. Acad. Sci. USA* **96**, 13040-13043.
11. Sotriffer, C.A., Ni, H. & McCammon, J.A. (2000). HIV-1 integrase inhibitor interactions at the active site: prediction of binding modes unaffected by crystal packing. *J. Am. Chem. Soc.* **122**, 6136-6137.
12. Jensen, P.R., Jenkins, K.M., Porter, D. & Fenical, W. (1998). Evidence that a new antibiotic flavone glycoside chemically defends the sea grass *Thalassia testudinum* against zoosporic fungi. *Appl. Environ. Microbiol.* **64**, 1490-1496.
13. Bushman, F.D. & Craigie, R. (1991). Activities of human immunodeficiency virus (HIV) integration protein *in vitro* - Specific cleavage and integration of HIV DNA. *Proc. Nat. Acad. Sci. USA* **88**, 1339-1343.
14. Craigie, R., Fujiwara, T. & Bushman, F. (1990). The IN protein of moloney murine leukemia virus processes the viral DNA ends and accomplishes their integration *in vitro*. *Cell* **62**, 829-837.
15. Katz, R.A., Merkel, G., Kulkosky, J., Leis, J. & Skalka, A.M. (1990). The avian retroviral IN protein is both necessary and sufficient for integrative recombination *in vitro*. *Cell* **63**, 87-95.
16. Katzman, M., Katz, R.A., Skalka, A.M. & Leis, J. (1989). The avian retroviral integration protein cleaves the terminal sequences of linear viral DNA at the *in vivo* sites of integration. *J. Virol.* **63**, 5319-5327.

17. Kimpton, J. & Emerman, M. (1992). Detection of replication-competent and pseudotyped human immunodeficiency virus with a sensitive cell line on the basis of activation of an integrated beta-galactosidase gene. *J. Virol.* **66**, 2232-2239.
18. Hwang, Y., Park, M., Fischer, W.H., Burgin, A. & Bushman, F. (1999). DNA contacts by protein domains of the molluscum contagiosum virus type-1B topoisomerase. *Virology* **262**, 479-491.
19. Fesen, M.R., Kohn, K.W., Leteurtre, F. & Pommier, Y. (1993). Inhibitors of human immunodeficiency virus integrase. *Proc. Nat. Acad. Sci. USA* **90**, 2399-2403.
20. Lafemina, R.L., Graham, P.L., Legrow, K., Hastings, J.C., Wolfe, A., Young, S.D., Emini, E.A. & Hazuda, D.J. (1995). Inhibition of human immunodeficiency virus integrase by bis-catechols. *Antimicrob. Agents Chemother.* **39**, 320-324.
21. Pluymers, W., Neamati, N., Pannecouque, C., Fikkert, V., Marchand, C., Burke, T.R., Pommier, Y., Schols, D., De Clercq, E., Debyser, Z. & Witvrouw, M. (2000). Viral entry as the primary target for the anti-HIV activity of chicoric acid and its tetra-acetyl esters. *Mol. Pharm.* **58**, 641-648.
22. Reddy, M.V.R., Rao, M.R., Rhodes, D., Hansen, M.S.T., Rubins, K., Bushman, F.D., Venkateswarlu, Y. & Faulkner, D.J. (1999). Lamellarin alpha 20-sulfate, an inhibitor of HIV-1 integrase active against HIV-1 virus in cell culture. *J. Med. Chem.* **42**, 1901-1907.
23. Carteau, S., Mouscadet, J.F., Goulaouic, H., Subra, F. & Auclair, C. (1993). Inhibitory effect of the polyanionic drug suramin on the in vitro HIV DNA integration reaction. *Arch. Biochem. Biophys.* **305**, 606-610.
24. Nicklaus, M.C., Neamati, N., Hong, H.X., Mazumder, A., Sunder, S., Chen, J., Milne, G.W.A. & Pommier, Y. (1997). HIV-1 integrase pharmacophore: Discovery of inhibitors through three-dimensional database searching. *J. Med. Chem.* **40**, 920-929.
25. Hazuda, D., Felock, P., Hastings, J., Pramanik, B., Wolfe, A., Goodarzi, G., Vora, A., Brackmann, K. & Grandgenett, D. (1997). Equivalent inhibition of half-site and full-site retroviral strand transfer reactions by structurally diverse compounds. *J. Virol.* **71**, 807-811.
26. Fesen, M.R., Pommier, Y., Leteurtre, F., Hiroguchi, S., Yung, J. & Kohn, K.W. (1994). Inhibition of HIV-1 integrase by flavones, caffeic acid phenethyl ester (CAPE) and related compounds. *Biochem. Pharmacol.* **48**, 595-608.

27. Kim, H.J., Woo, E.R., Shin, C.G. & Park, H. (1998). A new flavonol glycoside gallate ester from *Acer okamotoanum* and its inhibitory activity against human immunodeficiency virus-1 (HIV-1) integrase. *J. Nat. Prod.* **61**, 145-148.
28. Craigie, R., Mizuuchi, K., Bushman, F.D. & Engelman, A. (1991). A rapid *in vitro* assay for HIV DNA integration. *Nucleic Acid Res.* **19**, 2729-2734.
29. Hwang, Y., Rowley, D., Rhodes, D., Gertsch, J., Fenical, W. & Bushman, F. (1999). Mechanism of inhibition of a poxvirus topoisomerase by the marine natural product sansalvamide A. *Mol. Pharm.* **55**, 1049-1053.
30. Charneau, P. & Clavel, F. (1991). A single-stranded gap in human immunodeficiency virus unintegrated linear DNA defined by a central copy of the polypurine tract. *J. Virol.* **65**, 2415-2421.
31. Morris, G.M., Goodsell, D.S., Halliday, R.S., Huey, R., Hart, W.E., Belew, R.K. & Olson, A.J. (1998). Automated docking using a Lamarckian genetic algorithm and an empirical binding free energy function. *J. Comput. Chem.* **19**, 1639-1662.
32. Gasteiger, J. & Marsili, M. (1980). Iterative partial equilization of orbital electronegativity - a rapid access to atomic charges. *Tetrahedron* **36**, 3219-3228.
33. Meyer, M. (2000). Ab initio study of flavonoids. *Int. J. Quantum Chem.* **76**, 724-732.

## **Chapter 7. Discovery of Marine-Derived Inhibitors of Molluscum Contagiosum**

### **Virus Topoisomerase**

An extended focus of my collaboration with the laboratory of Dr. Frederic Bushman at the Salk Institute for Biological Studies was a program designed to identify marine natural product inhibitors of the molluscum contagiosum virus (MCV) topoisomerase enzyme. Molluscum contagiosum is a poxvirus that causes persistent skin lesions in children and AIDS patients, and the topoisomerase enzyme represents a novel target for the discovery of antiviral agents to treat these infections. The strategy for this investigation was to screen crude extracts and purified compounds derived from marine microbial fermentations in an *in vitro* enzyme-based assay. Ms. Denise Rhodes and Mr. Jeff Gertsch provided expert technical support in the operation of the basic screening assay used to identify enzyme inhibitory activities. Dr. Young Hwang, a postdoctoral researcher, conducted the mechanism of action studies involving sansalvamide A, a cyclic depsipeptide inhibitor of MCV topoisomerase. The discovery of sansalvamide A as a novel inhibitor of this enzyme was the most significant accomplishment of this investigation, and an account of that project is included here as a reprint of the original article published in *Molecular Pharmacology*.

#### **7.1 Introduction**

DNA topoisomerases catalyze the relaxation or winding of coiled DNA via the breaking and rejoining of phosphodiester bonds.<sup>1</sup> There are two distinct classes of topoisomerases. Type I enzymes bind to double-stranded DNA, transiently nick one

strand, allow passage of a segment of DNA through the break, and then reseal the DNA at the initial site of cleavage (see figure in section 7.2). Type II topoisomerases, which include DNA gyrases, effect topological changes by cleaving both strands of DNA. Inhibitors of DNA topoisomerases have been identified as therapeutic agents for the treatments of cancer and bacterial infections.<sup>2</sup>

Poxviruses are large, double-stranded DNA viruses. Because poxvirus replication occurs entirely in the cytoplasm, they encode a large number of proteins, including type 1B topoisomerases. The vaccinia virus topoisomerase, the most well studied of the group, is highly sequence specific, binding to the DNA segment 5'-(T/C)CCTT-3' and cleaving just 3' of the last base pair.<sup>3</sup> The vaccinia enzyme has unusual pharmacological properties. It is sensitive to the coumarin drugs coumermycin and novobiocin, compounds that are classic inhibitors of DNA gyrase.<sup>4,5</sup> Further, it is resistant to camptothecin, a type I topoisomerase poison.<sup>6</sup>

The Bushman laboratory was the first to characterize the *in vitro* properties of MCV topoisomerase.<sup>7</sup> The gene for MCV topoisomerase had been successfully cloned from viral DNA obtained from infected human lesions, and the protein overexpressed and purified. MCV topoisomerase is 54% identical to that of vaccinia virus. Analysis of the topoisomerase cleavage sites on plasmid and oligonucleotide substrates indicated that it also cleaves just 3' of the sequence 5'-(T/C)CCTT-3'.<sup>7</sup> Base pairs flanking this sequence are selectively important for covalent binding between the enzyme and substrate DNA.<sup>8,9</sup> MCV topoisomerase is also sensitive to coumermycin A1 (IC<sub>50</sub> = 32 μM), and resistant to other inhibitors of type-I and II topoisomerases including camptothecin, etoposide, ellipticine, novobiocin, and nalidixic acid at

concentrations less than 100  $\mu\text{M}$ .<sup>7</sup> This selective response raised the possibility that MCV infections might be successfully treated with a topoisomerase inhibitor non-toxic to human cells.

Crude extracts and purified compounds derived from the fermentation of marine microorganisms were screened in an *in vitro* enzyme assay to identify inhibitory activity against MCV topoisomerase (see section 7.2 for a description of the assay). The initial assay concentration was 100  $\mu\text{g}/\text{mL}$ . Each extract was also tested in the HIV integrase assay (chapter 6), and extracts with non-selective inhibition were eliminated from further consideration. HIV integrase is an appropriate enzyme for counterscreening since it also binds and cleaves DNA. Eight crude extracts were selected for further consideration, and one-liter regrows of the producing organisms were undertaken. In two cases the subsequent fermentations did not reproduce the desired activity. Bioassay-guided fractionations were pursued on the crude extracts of the other six fermentations. Unfortunately, these efforts led to the discovery of free fatty acids, both saturated and unsaturated, as the active components of these extracts. These compounds were deemed to be nuisance compounds and were not further studied.

## **7.2 Sansalvamide A, a novel inhibitor of MCV topoisomerase**

The screening of purified compounds led to the discovery of sansalvamide A, a cyclic depsipeptide of marine fungal origin, as an inhibitor of MCV topoisomerase. The results of the study were published in the journal *Molecular Pharmacology*, and are included here as a reprint of the original article.

*Molecular Pharmacology*, **55**:1049-1053 (1999).

Reprinted with permission of the American Society for Pharmacology and Experimental Therapeutics. All rights reserved.

## Mechanism of Inhibition of a Poxvirus Topoisomerase by the Marine Natural Product Sansalvamide A

YOUNG HWANG, DAVID ROWLEY, DENISE RHODES, JEFF GERTSCH, WILLIAM FENICAL, and FREDERIC BUSHMAN

*Infectious Disease Laboratory, The Salk Institute (Y.H., D.R., J.G., F.B.); and Center for Marine Biotechnology and Biomedicine, Scripps Institution of Oceanography, University of California-San Diego (D.R., W.F.), La Jolla, California*

Received December 22, 1998; accepted March 17, 1999

### ABSTRACT

At present no antiviral agents are available for treatment of infection by the pathogenic poxvirus molluscum contagiosum virus (MCV). Here we report the identification and characterization of an inhibitor active against the virus-encoded type-1 topoisomerase, an enzyme likely to be required for MCV replication. We screened a library of marine extracts and natural products from microorganisms using MCV topoisomerase assays *in vitro*. The cyclic depsipeptide sansalvamide A was found to inhibit topoisomerase-catalyzed DNA relaxation. Sansalvamide A was inactive against two other DNA-modifying

enzymes tested as a counterscreen. Assays of discrete steps in the topoisomerase reaction cycle revealed that sansalvamide A inhibited DNA binding and thereby covalent complex formation, but not resealing of a DNA nick in a preformed covalent complex. Sansalvamide A also inhibits DNA binding by the isolated catalytic domain, thereby specifying the part of the protein sensitive to sansalvamide A. These data specify the mechanism by which sansalvamide A inhibits MCV topoisomerase. Cyclic depsipeptides related to sansalvamide A represent a potentially promising chemical family for development of anti-MCV agents.

Here we present a study of a marine fungal product, sansalvamide A, which inhibits the topoisomerase enzyme of the pathogenic poxvirus molluscum contagiosum virus (MCV). MCV infection in healthy people causes only small papules that are easily treated. In AIDS patients, however, MCV causes severe lesions that are essentially untreatable. Cells near the surface of lesions become many times larger than normal, forming papules that become filled with a granular mass called "molluscum bodies". Untreated papules in healthy people usually disappear spontaneously within several months, but in AIDS patients dense crops can persist, disfiguring infected patients. In HIV-infected people, rates of infection may be as high as 5 to 18% and as many as 33% of AIDS patients with CD4+ counts of less than 100 cells/mm<sup>3</sup> may be infected (Petersen and Gerstoft, 1992; Porter et al., 1992; Schwartz and Myskowski, 1992; Gottlieb and Myskowski, 1994).

Among the MCV genes identified in the recently completed primary sequence was one encoding a putative type I topoisomerase (Senkevich et al., 1996). Type I topoisomerases catalyze the formation of transient nicks in DNA that permit DNA relaxation (Gupta et al., 1995). MCV and the other poxviruses all encode topoisomerases, and in the case of vaccinia, it has been shown that replication requires topoisomerase function (Shuman et al., 1989).

MCV topoisomerase, like that of other poxviruses, is highly sequence-specific (Hwang et al., 1998; Y.H., A. Burgin and F.B., in press). Poxvirus topoisomerases bind to the sequence 5'-(C/T)CCTT-3' and cleave DNA just 3' of the last T, forming a covalent phosphotyrosine linkage. After DNA relaxation, the single strand DNA break is resealed by transesterification with the adjacent 5' hydroxyl, releasing the enzyme from the relaxed DNA product. Topoisomerase activity has been implicated as important for DNA replication, repair, transcription, and other biological processes (Wang, 1996).

We have carried out a survey of crude extracts and purified secondary metabolites from marine bacteria and fungi in an effort to identify useful inhibitors of MCV topoisomerase (Jensen and Fenical, 1994; Davidson, 1995). Here we report that sansalvamide A, a cyclic depsipeptide produced by a marine fungus *Fusarium* species, inhibits MCV topoisomerase *in vitro*. Assays of different steps in the topoisomerase catalytic cycle reveal that sansalvamide A inhibits DNA binding, but not strand religation. Sansalvamide A also inhibited the activity of the enzyme catalytic domain, beginning to specify the inhibitor site of action. This represents the first identification of a new inhibitor isolated by primary screening against MCV topoisomerase *in vitro*.

### Materials and Methods

**Purification of MCV Topoisomerase.** MCV topoisomerase (MCV-TOP) was purified using nickel-chelating sepharose as described (Hwang et al., 1998). MCV-TOP (82-323), the catalytic do-

This work was supported by Grant R97-SAL-088 from the University of California University-wide AIDS Research Program (F.D.B.) and a grant from the Pendleton Foundation for imaging facilities, and by the National Institutes of Health National Cancer Institute Grant CA 44846 (W.F.). F.D.B. is a scholar of the Leukemia Society of America.

**ABBREVIATIONS:** MCV, molluscum contagiosum virus; sub a, oligonucleotide substrate a; MCV-TOP, MCV topoisomerase.



main, was purified using chromatography on nickel-chelating sepharose and carboxy-methyl-sepharose (Y.H., M. Park, W. Fisher and F.D.B., submitted).

**MCV Topoisomerase Activity Assays.** Standard conditions for assaying relaxation, DNA binding, covalent complex formation, and religation activities were 200 mM potassium glutamate, 20 mM Tris-Cl (pH 8.0), 1 mM dithiothreitol, 0.1% Triton X-100, and 1 mM EDTA. To test inhibition of MCV topoisomerase, sansalvamide A was added to the enzyme and preincubated for 5 min and then the reaction was started with the addition of substrate. The reaction mixtures contained a 10% (v/v) final concentration of dimethyl sulfoxide.

Relaxation assays using pUC19 DNA were carried out as described (Hwang et al., 1998). For the DNA binding assays, oligonucleotide substrate (sub a) was 5'-end labeled with  $^{32}$ P, added to MCV topoisomerase enzyme previously incubated with sansalvamide A, and incubated for 5 min at 37°C. The reaction mixtures were separated on 5% polyacrylamide gels, visualized by autoradiography, and the radioactivity was quantitated by a PhosphorImager. Sub a was a duplex DNA of 5'-TCCGTGTCGCCCTTATTCCTTTTTCGGCATTTTGCCT-3' and 5'-GAGGCAAAATGCCGAAAAAGGGAATAAGGGCGACACGG-3'. The covalent complex formation assay using sub a was carried out as described (Hwang et al., 1998).

For religation assays, a suicide substrate derived from sub a DNA was used. In this substrate (sequence 5'-TCCGTGTCGCCCTTATTCCT-3' and 5'-GAGGCAAAATGCCGAAAAAGGGAATAAGGGCGACACGG-3'), the short duplex extension 3' of the 5'-CCCTT-3' sequence can be dissociated upon covalent complex formation, trapping the covalent complex but permitting religation to an added complementary DNA strand. Covalent complex formation was followed by religation induced by addition of 50-fold excess of a 15-mer single strand DNA (5'-ATTCCCTTTTTCGGG-3'). Covalent complex reaction mixtures were transferred to individual tubes, followed by addition of sansalvamide A, incubated for 5 min at room temperature, and then religation reaction was started by addition of a 15-mer single strand DNA to generate a product containing a 29-mer DNA. After incubation at 37°C for 5 min, formamide was added to 50% (v/v), the samples were denatured for 5 min at 95°C, and then the aliquots of samples were analyzed on DNA sequencing type gels. The extent of inhibition of religation was visualized by autoradiography and quantitated by PhosphorImager.

**Sansalvamide A.** Purification and structure determination for sansalvamide A (Fig. 1), produced by a marine fungus *Fusarium* species collected off the Bahamas, is described in (G. Belofsky and W. Fenical, submitted). The compound was assayed using NMR and thin-layer chromatography methods.

## Results

**Screening Compounds from Marine Sources for Inhibitory Activity.** To identify inhibitors of MCV topoisom-

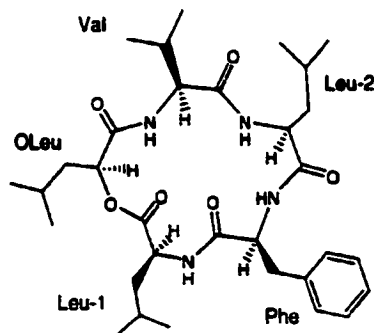


Fig. 1. Structure of sansalvamide A.

erase, 460 candidate extracts and purified compounds from marine microorganisms were screened. The investigation focused on secondary metabolites from marine fungi and bacteria, because compounds of interest could be readily obtained as needed by culturing the appropriate microorganisms (Jensen and Fenical, 1994). Assays *in vitro* were carried out initially in the presence of high concentrations of compound or extract in an effort to identify potential inhibitors. Extracts or compounds that selectively inhibited MCV topoisomerase were then titrated to determine the concentration sufficient for 50 percent inhibition ( $IC_{50}$ ).

**Inhibition of DNA Relaxation by Sansalvamide A.** Type I topoisomerases carry out relaxation of DNA by first binding to duplex DNA, cleaving one strand to generate a enzyme-DNA covalent complex, relaxing the DNA, and subsequently resealing the nick by religation of the cleaved strand (Fig. 2).

To test the effect of sansalvamide A on DNA relaxation by MCV topoisomerase, the enzyme was incubated with supercoiled plasmid substrate, reaction mixtures were separated on agarose gels by electrophoresis, and DNA was visualized by staining with ethidium bromide. DNA relaxation results in a reduction in mobility of the relaxed DNA because the relaxed DNA form is less compact than the supercoil. Conversion of the supercoiled plasmid substrate DNA to relaxed circular DNA was measured after 5 min of incubation at 37°C in the presence of different concentrations of sansalvamide A. As shown in Fig. 3, sansalvamide A inhibited DNA relaxation by MCV topoisomerase in a concentration-dependent fashion. Quantitation of multiple tests yielded an  $IC_{50}$  of 124  $\mu$ M.

**Specificity of Inhibition by Sansalvamide A.** As a counterscreen, inhibition of HIV-1 integrase was tested. HIV-1 integrase directs the cleavage of the termini of the HIV-1 cDNA and the subsequent covalent integration of the cleaved DNA ends into target DNA (for review, see Hansen et al., 1998). No inhibition of integrase was detectable ( $IC_{50} > 850 \mu$ M, data not shown).

In another counterscreen, inhibition of DNA cleavage by the restriction enzyme *Hind*III was tested. The  $IC_{50}$  was determined to be  $>400 \mu$ M (data not shown).

**Effect of Sansalvamide A on DNA Binding.** To investigate the mechanism of inhibition of MCV topoisomerase by sansalvamide A, we assayed inhibition of DNA binding, covalent complex formation, and religation separately.

To test the effect of sansalvamide A on DNA binding, 39-mer duplex DNA matching the highly active sub a sequence was used as substrate. MCV topoisomerase binds and produces a covalent complex at sites containing the sequence 5'-(CT)CCTT-3'. The sub a substrate used for these tests contains the 5'-CCCTT-3' embedded in optimal flanking sequences (Hwang et al., 1998; Y.H., A. Burgin and F.B., *in press*). MCV topoisomerase was mixed with end-labeled sub

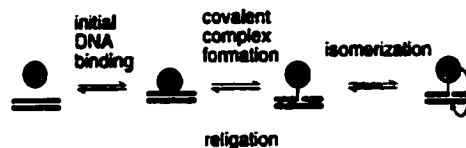


Fig. 2. Diagram of the mechanism of type I topoisomerases such as that encoded by MCV. Rotation as drawn in the "isomerization" step is hypothetical.

a DNA and the reaction mixture was separated by electrophoresis on native polyacrylamide gels. Protein-DNA complexes were visualized as slower migrating bands. Exposure of topoisomerase to sansalvamide A before addition of sub a caused a concentration-dependent decrease in the extent of complex formation (Fig. 4 lanes 3-7). The  $IC_{50}$  for inhibition of DNA binding was approximately 80  $\mu$ M.

**Effect of Sansalvamide A on Covalent Complex Formation.** The effect of sansalvamide A on covalent complex formation was tested using sub a as substrate. Sub a was end-labeled on the 5'-end of the scissile DNA strand, then mixed with MCV topoisomerase and incubated at 37°C for 5 min. Covalent protein-DNA complex formation was assayed by SDS-polyacrylamide gel electrophoresis and autoradiography. The covalent complex was visualized as a labeled species migrating more slowly than the substrate DNA that exhibited the molecular weight expected of the topoisomerase linked to the covalently bound DNA. Exposure of topoisomerase to sansalvamide A before addition of the sub a substrate caused a concentration-dependent decrease in the extent of covalent complex formation (Fig. 5, lanes 3-7) with an  $IC_{50}$  of approximately 110  $\mu$ M.

**Effect of Sansalvamide A on Religation of the Covalent Complex.** The effect of sansalvamide A on the religation activity of MCV topoisomerase was also tested. The covalent complex was trapped using a suicide substrate, which contains a short (5 base pairs) DNA segment 3' of the 5'-CCCTT-3' sequence. Upon covalent complex formation, the resulting 5-base strand will be released and lost by diffusion (Fig. 6A). To monitor religation, a labeled 15-base sequence was added that is complementary to the single stranded DNA in the covalent complex. Religation of the labeled input DNA was detected by the formation of a radioactive 29-mer product (Fig. 6B).

Religation product was detected after addition of the labeled 15-mer single strand DNA to the covalent complex (arrow marked \*29\*, Fig. 6B, lane 3). Quantitative measurement showed that 70% of the suicide substrate was

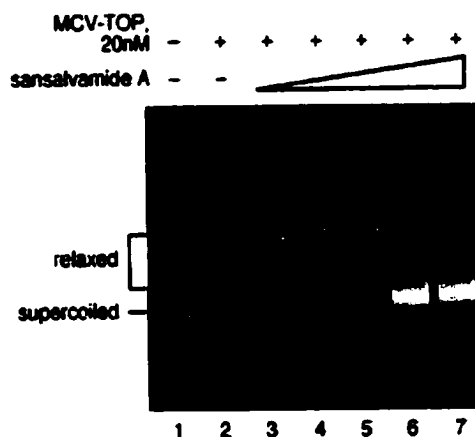


Fig. 3. Inhibition of DNA relaxation by sansalvamide A. Control reactions were performed without enzyme (lane 1) or without sansalvamide A (lane 2). Concentrations of sansalvamide A added were 10  $\mu$ M (lane 3), 30  $\mu$ M (lane 4), 100  $\mu$ M (lane 5), 200  $\mu$ M (lane 6), and 300  $\mu$ M (lane 7).

converted into covalent complex (compare Fig. 6B, lanes 1-2 and data not shown). Exposure of topoisomerase-DNA covalent complex to sansalvamide A before addition of the 15-mer single stranded DNA had no effect on the accumula-

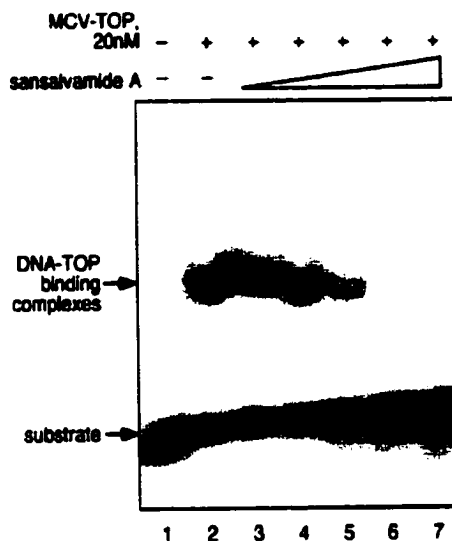


Fig. 4. Inhibition of DNA binding by sansalvamide A. Control reactions were performed without enzyme (lane 1) or without sansalvamide A (lane 2). Concentrations of sansalvamide A added were 10  $\mu$ M (lane 3), 30  $\mu$ M (lane 4), 100  $\mu$ M (lane 5), 200  $\mu$ M (lane 6), and 300  $\mu$ M (lane 7). Enzyme-DNA complexes are indicated by the arrow.

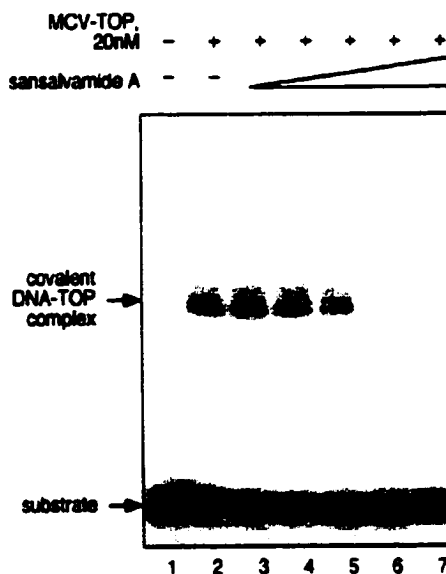
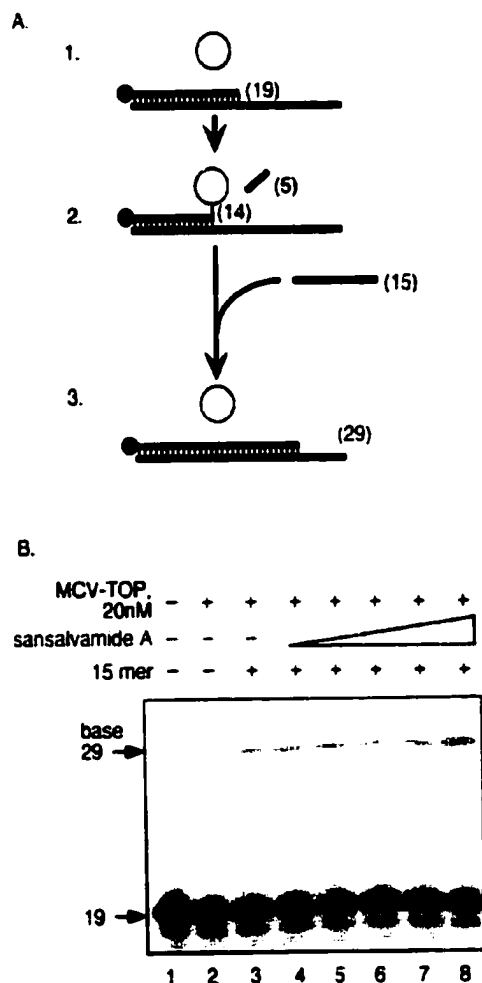


Fig. 5. Inhibition of covalent complex formation by sansalvamide A. Control reactions were performed without enzyme (lane 1) or without sansalvamide A (lane 2). Concentrations of sansalvamide A added were 10  $\mu$ M (lane 3), 30  $\mu$ M (lane 4), 100  $\mu$ M (lane 5), 200  $\mu$ M (lane 6), and 300  $\mu$ M (lane 7).

tion of religated products over the concentration range tested (Fig. 6B, lanes 4–7).

**Inhibition of DNA Binding by the Catalytic Domain of MCV Topoisomerase.** Residues 82 to 323 of MCV topoisomerase comprise a flexible linker and the carboxyl terminal catalytic domain of the enzyme (Y.H., M. Park, W. Fisher

and F.D.B., submitted). To examine the part of the enzyme affected by sansalvamide A, MCV-TOP (82–323), the purified linker and catalytic domain, was tested in reactions containing sansalvamide A. Titration of sansalvamide A into reactions containing 100 nM MCV-TOP (82–323) and labeled sub a DNA revealed inhibition of DNA binding (Fig. 7). The  $IC_{50}$  was indistinguishable from that seen with the full length enzyme. Note that covalent complex formation by MCV-TOP (82–323) is slower than with the full enzyme, so most of the complex seen in this experiment is the noncovalently bound form. Separate analysis of inhibition of covalent complex formation revealed inhibition paralleling the inhibition of DNA binding (data not shown). Evidently sansalvamide A is also capable of inhibiting function of the catalytic domain by blocking DNA binding, specifying the site of action of the compound.



**Fig. 6.** Effect of sansalvamide A on DNA strand religation. A, diagram of the religation reaction. The suicide substrate labeled on 5' end of the top strand (indicated by the ball) was incubated with MCV topoisomerase (step 1). Covalent complex formation resulted in releasing the short duplex extension 3' of the 5'-CCCTT-3' sequence (step 2), thereby trapping the covalent complex. This allowed the religation reaction to be carried out after addition of the 15-mer donor DNA to covalently linked topoisomerase. Religation generates a product containing a radiolabeled 29-mer DNA strand (step 3). MCV topoisomerase protein is indicated by the shaded circle. The number of bases in single stranded DNAs are indicated in parentheses. B, lack of inhibition of DNA strand religation by sansalvamide A. Control religation reactions were performed without enzyme (lane 1), with enzyme (lane 2), or with enzyme and 15-mer single strand DNA (lane 3). Concentrations of sansalvamide A added were 10  $\mu$ M (lane 4), 30  $\mu$ M (lane 5), 100  $\mu$ M (lane 6), 200  $\mu$ M (lane 7), and 300  $\mu$ M (lane 8).

## Discussion

Here we describe the identification of the marine depsipeptide sansalvamide A as an inhibitor of MCV topoisomerase. Sansalvamide A inhibited the initial DNA binding by MCV topoisomerase and, consequently, formation of covalent protein-DNA complexes, but did not inhibit religation by the covalent protein-DNA intermediate. This work provides a starting point for possible development of depsipeptide inhibitors for treating MCV infection.

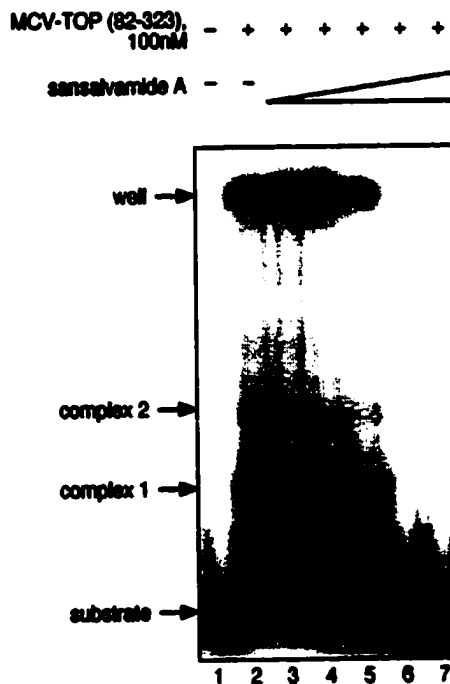


**Fig. 7.** Inhibition of DNA binding of the catalytic domain (MCV-TOP 32–323) by sansalvamide A. Control reactions were performed without enzyme (lane 1) or without sansalvamide A (lane 2). Concentrations of sansalvamide A added were 10  $\mu$ M (lane 3), 30  $\mu$ M (lane 4), 100  $\mu$ M (lane 5), 200  $\mu$ M (lane 6), and 300  $\mu$ M (lane 7). DNA binding complexes are indicated by the arrows.

Cyclic peptides such as sansalvamide A are a potent class of naturally occurring bioactive molecules. The immunosuppressant drug cyclosporin is a cyclic peptide secondary metabolite produced by the fungus *Cylindrocarpum lucidum* (Borel et al., 1976). Bacitracin and polymyxin, also cyclic peptides of microbial origin, are in use as topical antibiotic agents (Strohl, 1997). Marine invertebrates are also prolific producers of bioactive cyclic peptides, including the antiviral and cytotoxic molecule didemnin B (Rinehart et al., 1988), the thrombin inhibitor cyclotheonamide A (Fusetani et al., 1990), and patellamide and lissoclinamide cytotoxins (Ireland et al., 1982). Recently, several potent bioactive molecules have also been isolated from combinatorial libraries of cyclic peptides (Eichler et al., 1995; Giebel et al., 1995).

Cyclic decapeptides have several advantages as inhibitors. Cyclic decapeptides by definition contain one or more amino acids replaced by a hydroxy acid, forming at least one ester bond in the core ring structure. These compounds lack charges at the peptide amino and carboxyl termini and lacking zwitterionic character are more lipophilic and membrane-permeable. Oral bioavailability is increased by faster membrane absorption in the digestive tract (Amidon and Lee, 1994) and cyclic peptides have greater half-lives in vivo than the cognate linear peptides (Blackburn and Van Breemen, 1993; Pauletti et al., 1996). The cyclic nature of these compounds also restricts bond rotation, creating more rigid three dimensional structures. This conformational constraint can result in greater binding affinity and selectivity for protein ligands (Giebel et al., 1995). Even slight changes in the core ring structure of molecules such as cyclosporin and didemnin B can greatly reduce their biological activities, emphasizing the specificity of binding (Wenger, 1986; Sakai et al., 1996).

The mechanism by which sansalvamide A inhibits DNA binding has not been fully clarified. It seems unlikely that sansalvamide A binds indiscriminately to the substrate DNA, because it did not inhibit HIV-1 integrase or *HindIII*. Sansalvamide A did inhibit catalysis by an isolated domain of MCV topoisomerase containing the catalytic center, implying action at least in part against this protein domain and potentially the active site. It has not been possible to study the target of sansalvamide A in vivo due to the toxicity of the compound to cells. If more potent or less toxic derivatives of sansalvamide A can be identified, it may be possible to isolate a poxvirus insensitive to sansalvamide A and map the target of action by identifying the location of viral drug escape mutants.

#### Acknowledgments

We thank members of the Fenical and Bushman laboratories for suggestions and comments and Allison Bocksrucker for artwork.

#### References

- Amidon GL and Lee HJ (1994) Absorption of peptide and peptidomimetic drugs. *Annu Rev Pharmacol Toxicol* 34:321-341.
- Blackburn RK and Van Breemen RB (1993) Application of an immobilized digestive enzyme assay to measure chemical and enzymatic hydrolysis of the cyclic peptide antibiotic lysobactin. *Drug Metab Dispos* 21:573-579.
- Borel JF, Feurer C, Gubler HU and Stahelin H (1976) Biological effects of cyclosporin A: A new antilymphocytic agent. *Agents Actions* 6:468-475.
- Davidson BS (1995) New dimensions in natural product research: Cultured marine microorganisms. *Curr Opin Biotechnol* 6:284-291.
- Eichleray, Lucká AW, Pinilla C and Houghten RA (1995) Novel alpha-glucosidase inhibitors identified using multiple cyclic peptide combinatorial libraries. *Mol Divers* 1:233-240.
- Fusetani N, Matsunaga S, Matsumoto H and Takabayashi Y (1990) Cyclotheonamides, potent thrombin inhibitors, from a marine sponge *Theonella* sp. *J Am Chem Soc* 112:7053-7054.
- Giebel LB, Case RT, Milligan DL, Young DC, Arza R and Johnson CR (1995) Screening of cyclic peptide phage libraries identifies ligands that bind streptavidin with high affinities. *Biochemistry* 34:15430-15435.
- Gottlieb SL and Myskowski PL (1994) Molluscum contagiosum. *Int J Dermatol* 33:453-461.
- Gupta M, Fujimori A and Pommery Y (1985) Eukaryotic DNA topoisomerases I. *Bio Biophys Acta* 198:91-114.
- Hansen MST, Carteau S, Hoffmann C, Li L and Bushman P (1996) Retroviral cDNA integration: Mechanism, applications and inhibition. in *Genetic Engineering, Principles and Methods* (Setlow JK ed) pp 41-62. Plenum Press, New York.
- Hwang Y, Wang B and Bushman PD (1996) Molluscum contagiosum virus topoisomerase Purification, activities and response to inhibitors. *J Virol* 70:3401-3406.
- Ireland CM, Durso AR, Newman RA and Hacker MP (1982) Antineoplastic cyclic peptides from the marine tunicate *Lissoclinum patella*. *J Org Chem* 47:1807-1811.
- Jensen PR and Fenical W (1994) Strategies for the discovery of secondary metabolites from marine bacteria: Ecological perspectives. *Annu Rev Microbiol* 48:559-584.
- Pauletti GM, Gangwar S, Okumu FW, Sibaana TJ, Stella VJ and Borchardt RT (1996) Esterase-sensitive cyclic prodrugs of peptides: Evaluation of an acyloxyalkoxy promoiety in a model heptapeptide. *Pharm Res* (NY) 13:1615-1623.
- Petersen CS and Gerstoft J (1992) Molluscum contagiosum in HIV-infected patients. *Dermatology* 184:19-21.
- Porter CD, Blake NW, Cream JJ and Archard LC (1992) Molluscum contagiosum virus, in *Molecular and Cell Biology of Sexually Transmitted Diseases* (D. J. A. Wright L., ed) pp 223-257. Chapman and Hall, London.
- Rinehart KL, Kishore V, Bible KC, Sakai R, Sullins DW and Li KM (1988) Didemnins and tuniclorin: Novel natural products from the marine tunicate *Trididemnum nudum*. *J Nat Prod* 51:1-21.
- Sakai R, Rinehart KL, Kishore V, Kundu B, Farciot G, Gluer JB, Carnay JR, Namikoshi M, Sun P, Hughes RG, Gravalos DG, Quesada TG, Wilson GR and Heul RM (1996) Structure-activity relationships of the didemnins. *J Med Chem* 39: 2819-2834.
- Schwartz JJ and Myskowski PL (1992) Molluscum contagiosum in patients with human immunodeficiency virus infection. *J Am Acad Dermatol* 27:583-588.
- Senkevich TG, Bugert JJ, Sialer JR, Koonin EV, Darat G and Moss B (1996) Genome sequence of a human tumorigenic poxvirus: Prediction of specific host response- evasion genes. *Science* (Wash DC) 273:813-816.
- Shuman S, Golder M and Moss B (1989) Inertional mutagenesis of the vaccinia virus gene encoding a type I DNA topoisomerase: Evidence that the gene is essential for virus growth. *Virology* 170:302-306.
- Strohl WH (1997) *Biotechnology of Antibiotics*. Marcel Dekker, Inc., New York.
- Wang JC (1996) DNA topoisomerases. *Annu Rev Biochem* 65:635-692.
- Wenger RM (1986) Synthesis of cyclosporin and analogues: Structural and conformational requirements for immunosuppressive activity. *Prog Allergy* 38:46-64.

Send reprint requests to: Dr Frederic Bushman, Infectious Disease Laboratory, The Salk Institute, 10010 North Torrey Pines Rd., La Jolla, CA 92037. E-mail: bushman@salk.edu

This chapter, in part, is a reprint of material as it appears in *Molecular Pharmacology*, 1999, 55, 1049-1053. The dissertation author was a secondary author and the co-authors listed in this publication directed and supervised the research which forms the basis for this chapter.

### References

1. Wang, J.C. (1996). DNA topoisomerases. *Annu. Rev. Biochem.* **65**, 635-692.
2. Liu, L.F. (1989). DNA topoisomerase poisons as antitumor drugs. *Annu. Rev. Biochem.* **58**, 351-375.
3. Shuman, S. & Prescott, J. (1990). Specific DNA cleavage and binding by vaccinia virus DNA topoisomerase I. *J. Biol. Chem.* **265**, 17826-17836.
4. Shaffer, R. & Traktman, P. (1987). Vaccinia virus encapsidates a novel topoisomerase with the properties of a eukaryotic type I enzyme. *J. Biol. Chem.* **262**, 9309-9315.
5. Sekiguchi, J., Stivers, J.T., Mildvan, A.S. & Shuman, S. (1996). Mechanism of inhibition of vaccinia DNA topoisomerase by novobiocin and coumermycin. *J. Biol. Chem.* **271**, 2313-2322.
6. Shuman, S., Golder, M. & Moss, B. (1988). Characterization of vaccinia virus DNA topoisomerase I expressed in *Escherichia coli*. *J. Biol. Chem.* **263**, 16401-16407.
7. Hwang, Y., Wang, B. & Bushman, F.D. (1998). Molluscum contagiosum virus topoisomerase: Purification, activities, and response to inhibitors. *J. Virol.* **72**, 3401-3406.
8. Hwang, Y., Burgin, A. & Bushman, F. (1999). DNA contacts stimulate catalysis by a poxvirus topoisomerase. *J. Biol. Chem.* **274**, 9160-9168.
9. Hwang, Y., Park, M., Fischer, W.H., Burgin, A. & Bushman, F. (1999). DNA contacts by protein domains of the molluscum contagiosum virus type-1B topoisomerase. *Virology* **262**, 479-491.